AN EVALUATION OF THE PERFORMANCE OF AN OPTICAL MEASUREMENT SYSTEM FOR THE THREE-DIMENSIONAL CAPTURE OF THE SHAPE AND DIMENSIONS OF THE HUMAN BODY

by

Claire Nicola Orwin BSc (Hons)

A thesis submitted in partial
fulfilment of the requirements
for the degree of
Doctor of Philosophy

Department of Textile Design and Production
De Montfort University
Leicester, United Kingdom

June 2000

ABSTRACT

As the clothing industry moves away from traditional models of mass production there has been increased interest towards customised clothing. The technology to produce cost effective customised clothing is already in place however the prerequisite to customised clothing is accurate body dimensional data. In response, image capture systems have been developed which are capable of recording a three-dimensional image of the body, from which measurements and shape information may be extracted. The use of these systems for customised clothing has, to date, been limited due to issues of inaccuracy, cost and portability.

To address the issue of inaccuracy a diagnostic procedure has been developed through the performance evaluation of an image capture system. By systematically evaluating physical and instrumental parameters the more relevant sources of potential error were identified and quantified and subsequently corrected to form a 'closed loop' experimental procedure. A systematic test procedure is therefore presented which may be universally applied to image capture systems working on the same principle.

The methodology was based upon the isolation and subsequent testing of variables that were thought to be potential sources of error. The process therefore included altering the physical parameters of the target object in relation to the image capture system and amending the configuration and calibration settings within the system. From the evaluation the most relevant sources of error were identified as the cosine effect, measurement point displacement, the dimensional differences between views and the influence of the operator in measurement.

The test procedure proved to be effective in both evaluating the performance of the system under investigation and in enabling the quantification of errors. Both random and systematic errors were noted which may be quantified or corrected to enable improved accuracy in the measured results. Recommendations have been made for the improvement of the performance of the current image capture system these include the integration of a cosine effect correction algorithm and suggestions for the automation of the image alignment process.

The limitations of the system such as its reliance on manual intervention for both the measurement and stitching processes, are discussed, as is its suitability for providing dimensional information for bespoke clothing production. Recommendations are also made for the creation of an automated test procedure for testing the performance of alternative image capture systems, which involves evaluating the accuracy of object replication both for multiple and single image capture units using calibration objects which combine a range of surfaces.

AN EVALUATION OF THE PERFORMANCE OF AN OPTICAL MEASUREMENT SYSTEM FOR THE THREE-DIMENSIONAL CAPTURE OF THE SHAPE AND DIMENSIONS OF THE HUMAN BODY

CONTENTS

LIST OF FIGURES

LIST OF TABLES

ACKNOWLEDGEMENTS

I wish to thank the following people for their help, advice and encouragement during this work:

At De Montfort University:

Professor Ray Harwood, my first supervisor, for the opportunity to study for a PhD, his supervision and for providing thought provoking discussion throughout;

Dr Jane Wyatt, my second supervisor, for her supervision and support and encouragement throughout my programme of research;

Dr Nick Longford & Dr Sergei Grishanov for their kind advice on statistical methods.

Wicks & Wilson Ltd for providing the image capture systems and thus creating the opportunity to study this topic and for their permission to reproduce illustrations relating to their system. In particular I wish to thank Mr Bob Brash, Mr Tony Wicks and Mr Richard Smale of Wicks & Wilson Ltd. for their help and advice throughout this investigation.

The Draper's Consolidated Charity, London for awarding the Draper's Company Postgraduate Textile Research Award and hence generously funding this work, without whose support this PhD would not be possible.

Open University Press for permission to reproduce the illustration on page 14.

To my family, especially my parents for all their encouragement and unwavering faith in my abilities, especially my Dad for the initial idea of returning to study and his constant badgering, which didn't always fall on deaf ears. Last but by no means least my husband, Austin, for allowing me to give up work, keeping me sane and generally looking after me, you really are a star.

ACKNOWLEDGEMENTS

I wish to thank the following people for their help, advice and encouragement during this work:

At De Montfort University:

Professor Ray Harwood, my first supervisor, for the opportunity to study for a PhD, his supervision and for providing thought provoking discussion throughout;

Dr Jane Wyatt, my second supervisor, for her supervision and support and encouragement throughout my programme of research;

Dr Nick Longford & Dr Sergei Grishanov for their kind advice on statistical methods.

Wicks & Wilson Ltd for providing the image capture systems and thus creating the opportunity to study this topic and for their permission to reproduce illustrations relating to their system. In particular I wish to thank Mr Bob Brash, Mr Tony Wicks and Mr Richard Smale of Wicks & Wilson Ltd. for their help and advice throughout this investigation.

The Draper's Consolidated Charity, London for awarding the Draper's Company Postgraduate Textile Research Award and hence generously funding this work, without whose support this PhD would not be possible.

Open University Press for permission to reproduce the illustration on page 14.

To my family, especially my parents for all their encouragement and unwavering faith in my abilities, especially my Dad for the initial idea of returning to study and his constant badgering, which didn't always fall on deaf ears. Last but by no means least my husband, Austin, for allowing me to give up work, keeping me sane and generally looking after me, you really are a star.

CHAPTER 1

INTRODUCTION

1.1. Overview

Within the clothing industry the body is traditionally measured by manual means. However this method is subject to inconsistency and inaccuracy and can typically be time consuming. In response to this, automated human body capture systems have been developed, the main advantages being both speed and the vast amount of data collected without the use of skilled operatives. In addition to capturing body dimension data, information relating to shape and postural characteristics can also be acquired. The use of such systems has as yet, been limited, due to issues of inaccuracy, cost and portability. Therefore the use of such systems for bespoke clothing manufacture has been minimal. Consequently the primary use has been for body dimension surveys where the measured results are open to a lesser degree of scrutiny.

The primary objective of the research contained within this thesis is to evaluate the performance of an optical system for the measurement of the shape and dimensions of the human body required by the clothing industry. The performance of the system was therefore evaluated according to the accuracy requirements of bespoke manufacture which necessitates a greater degree of precision than body dimension surveys as, for good fit, it is imperative that these measured dimensions are accurate. For the purpose of this investigation the method has been restricted to a single optical measurement system, which is based upon a variation of the Moiré Fringe technique, for the location of a 3D object in space. The system under consideration was still in its development stages. Errors were identified, quantified and subsequently corrected to form a 'closed loop' experimental procedure, thus ensuring the root cause of any error

was correctly identified. By using objects of simple shapes that reflect those found within the human form, the effect of surface and planar differences were also identified.

1.2. Background to the Research

The study was formulated as a progression of an original idea based upon the characterisation of body shapes and dimensions of women with specific disabilities, namely, Downs Syndrome, Achondroplasia, and Scoliosis. It was originally proposed to investigate the development of pattern translation algorithms whereby 'standard' sized basic garment patterns could be converted to fit those of an equivalent size for each of the three conditions. At this stage the research focussed on a manual body measurement survey as no previous study had collated the range of measurements required on all of these groups. However, the practicalities of undertaking such a survey as a single researcher proved problematic in terms of the time and expense related to travelling and on the dependence on other colleagues to assist in the process.

During this time a prototype human body image capture system was offered on loan to the Department of Textile Design and Production of the University by Wicks and Wilson Ltd, with a view to the progression of the system through the feedback from research use. Initially it was thought that this development offered the potential to concentrate on a single more complex condition, namely Scoliosis, with a view to characterising the torso shape for pattern translation algorithms. However, following an initial trial, it became clear that the image capture system, at that stage, was not accurate enough to conduct a detailed human body capture survey as certain dimensions were producing errors as high as 5cm. The complexity of the system, in terms of the number of potential sources of error, was examined and found to be both challenging and extremely interesting, hence the programme of research was redirected towards an

evaluation of the image capture system. The findings of the research to be supplied to Wicks and Wilson Ltd. to aid further system development.

1.3. Research Problem

The research presented here is based upon determining whether the image capture system under investigation is suitable for providing measurement information to a satisfactory standard for bespoke clothing manufacture. In doing so an original test procedure has been devised to isolate the potential sources of error for such a system, and evaluate their impact on the accuracy of the system. Whilst the investigation focuses on a single image capture system, the methodology employed should provide a universal approach to performance assessment of structured light systems for capturing the shape and dimensions of the human body. The methodology has the potential to be incorporated into an automated evaluation and error detection procedure for image capture systems.

1.4. Justification for the Research

As the consumer becomes more sophisticated and demanding the need to have individually customised clothing will intensify. Thus the introduction of bespoke or mass-customised clothing production will be consumer led. Whilst the manufacturing technology exists to provide cost effective bespoke manufacturing, the issue of obtaining accurate body measurement data and its interface with pattern construction systems has yet to be resolved. Also the lack of a widespread sizing standard makes the correct size selection problematic, an issue which will become more difficult with the onset of e-commerce. To enable true representation of a garment on a model of the consumer's body accurate 3D data will be required to allow virtual dressing for consumers prior to ordering bespoke garments to ensure the product is suitable for their requirements. In both cases efficient, reliable body scanning systems are the pre-requisite to the

widespread introduction of these new technologies and thus the need to improve the output from such systems is of paramount importance.

The body capture systems currently available are not in widespread commercial use. Whilst a number have been used for body dimension surveys, the use of such systems for bespoke clothing manufacture has been extremely limited. The primary reason for this is the failure of systems to meet the accuracy requirements imposed by retailers/manufacturers. Even when used for body measurement surveys, questions of inaccuracies arise. For example, in the instance of Cyberware, one of the longest established capture systems, manual measurements are still collected alongside automated measurements when conducting surveys, raising questions over the confidence by which they rely on their automated measurements.

Further work is therefore required in order to improve the accuracy of image capture systems. By determining the sources of error within the system and quantifying their effect on measured values, allowances may be built into the 3D point estimation algorithms to account for any discrepancies, thus improving the accuracy of the 3D point solution. Therefore there is a need for a comprehensive test procedure capable of isolating potential error sources and quantifying their impact on measured values.

Whilst the literature shows investigations have been undertaken to evaluate the accuracy of some of the available scanning systems, the depth of analysis is extremely limited. No single study has been found which fully characterises all the potential sources of error and their effects on measured values. No evidence exists within the published literature of a methodology to evaluate a structured light system in terms of all potential sources of error, when the end application is bespoke clothing manufacture.

1.5. Introductory Overview of the Methodology

To establish the performance of the image capture system, procedures were devised to test the system, which allowed each potential source of error to be isolated. The complexity of the system is such that errors can be generated from a wide range of sources, such as optical errors, measurement errors, geometric errors, etc. Within this investigation numerous sources of potential error were identified.

Using the human body for image capture is not the ideal reference object from which to determine these errors. The malleable nature of the body, plus the movements related to breathing, coupled with the dimensional changes due to food and fluid intake make repeat measurements subject to short and long term random variation. The only method by which to test the accuracy of the recorded dimensions is by direct comparison with manual measurements (the errors of which are well documented). Therefore the target objects were limited to basic shapes, namely a 2D board and curved surfaces providing both concave and convex surfaces in each plane, to reflect the types of surfaces found in combination on the human body. Each object was marked with a grid of predetermined dimensions to negate the need to manually measure the object for comparison with the imaged dimensions. The grid was designed on a computer based drawing package to ensure its exact dimensions and was subsequently printed and adhered to the captured object.

By isolating each variable in the system that may potentially cause an error, the effects of altering each variable may be quantified and compared to the measurement readings of a control set up, thus enabling any significant factors to be determined. To test the significance of any deviation in measurement readings, basic statistics were employed as was hypothesis testing and Total

Difference comparisons, which quantified the difference between the readings of the control set up with each change in key variables.

1.6. Errors in Measurement

Three factors are of prime concern in anthropometric measurement; standardisation of the measurement procedure, the reliability that repeat measurements will provide the same result, and the validity that we are measuring what we want (Sanderson [No date]).

To assess the validity of any measurement results it is necessary to make judgements on their accuracy and precision (Eckschlager 1969). Results may be regarded as accurate if the difference between the true and measured values is small and precise if the results equally agree with one another.

1.6.1. Sources of Error

The primary reasons for the occurrence of errors may be summarised in Table 1.1 (Pentz & Shott 1988).

Table 1.1. Causes of Error

Errors	Description
Mistakes	Blunders as opposed to human errors. Generally recognisable, especially where repeat measurements are taken.
Human error	Errors generally related to the skill of the experimenter.
Instrumental limitations	The specified measurement accuracy by the manufacturer. Includes the conditions under which the instrument was calibrated, the fineness of the scale divisions and any sources of imperfection due to a feature of the equipment.
Errors caused by the act of observation	A subject may behave differently when they know they are under observation.
Errors caused by extraneous influences	Which need to be minimised e.g. humidity.
Errors due to statistical fluctuations	As we are not able to measure the whole population, the mean of each sample is therefore subject to some error. The error in the mean estimate will reduce with increased sample size.
Errors due to unrepresentative samples	Where the sample is not typical of the whole population & maybe subject to some bias.

1.6.2. Classification of Errors

Errors may be classified into three categories, random, systematic and gross errors (Eckschlager 1969). Random errors are generally small and form an irregular pattern (Eckschlager 1969). The term relates to chance occurrences that occur in measurement. If the result is not repeatable, then it is likely that it is subject to some random variation (Pentz & Shott 1988). With random errors, positive errors are just as likely to occur as negative errors, with similar magnitudes in each case. In the long run therefore it is likely that these errors will cancel each other out (Carmines & Zeller 1979).

Non-random error produces a systematic bias on measurement instruments (Carmines & Zeller 1979). Systematic error forms a constant pattern and is generally a result of instrument imprecision or through incorrect use of an instrument (Eckschlager 1969). Systematic errors are difficult to assess as they cause a distinct shift in the measurements away from the true value (as shown in Figure 1.1), therefore repeat measurements do not indicate systematic errors and, unlike random errors, their effects, may not be reduced by averaging (Pentz & Shott 1988). Where the source of the systematic error may be found it may be possible to remove it or to make allowances to remove its effects (Eckschlager 1969).

Random & systematic errors often occur together in the same measurement, (an illustration of the effects of this scenario may be seen in Figure 1.1).

Figure 1.1. Random and Systematic Errors (Pentz & Shott 1988)

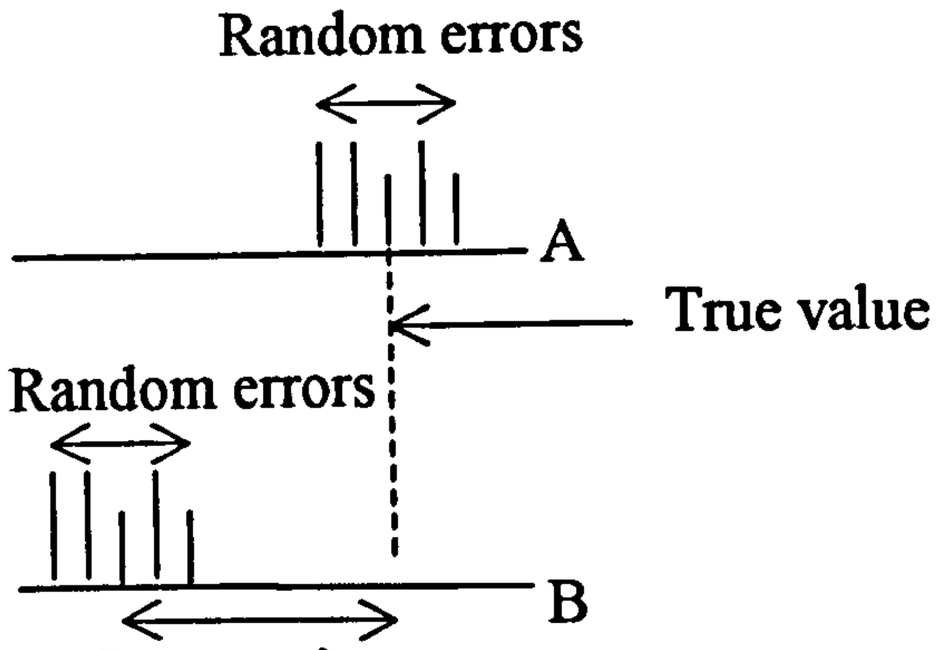

A Random errors indicating the spread of measurements around the true value.

B Systematic errors displace measurements. Where random errors are present, the measurements are not spread around the true value, but rather move with the systematic bias in the measurement.

Gross errors differ from random and systematic errors as they generally arise from mistakes in procedure, incorrect methodology or numerical errors in calculation (Eckschlager 1969). These blunders may be identified by comparison between the measured values and an acceptable range of values (Healy 1989), thereby facilitating their omission from the main results.

1.6.3. Absolute and Relative Errors

Absolute error generally refers to the difference between the measured value and the true value (Eckschlager 1969). The absolute error is referred to in the same units as the result. The value of the absolute error must be considered alongside the true value if any assessment of the impact of its magnitude is to be made. Whereas the relative error is an expression of the accuracy of the result and is derived from the absolute error divided by the true value.

1.7. Outline of the Thesis

The thesis is presented in a traditional format initially covering the author's aims and objectives and a review of relevant literature. The thesis subsequently goes on to discuss the methodology employed, the results obtained and the findings of the investigation. However, as the image capture system was in its prototype stage numerous developments occurred which made an impact on the continuity of the investigation. As the image capture system has evolved, so too have the methodology and the results. The preliminary research undertaken during these developments is summarised in Chapter 4, with the full description of the tests employed and the relevant results presented in Appendices A, B and C. The main body of the thesis therefore focuses on the latest single camera system, which is now offered as a commercial image capture system.

Appendices A, B and C contain accounts of the various stages within the preliminary investigation. They are designed to cover all the necessary information to detail the initial research and thus may be used independently. A glossary of terms for the reader's reference is also included at the end of the thesis.

CHAPTER 2

AIMS AND OBJECTIVES

2.1. Overall Aim

The aim of this investigation is to establish test procedures for the determination of errors in a 3D optical measurement system. Whilst the methodology will be established using a single optical measurement system the overall aim is to produce a complete test procedure which may be applied to other optical measurement systems working on the same principle.

2.2. Objectives

The following objectives form the necessary steps for the creation of a systematic test procedure:

1. To isolate the potential sources of error associated with one optical measurement system.

2. To quantify the magnitude of error associated with each tested variable and establish the effect on measured values.

3. To identify the corrective action required, and retest following the correction of errors within the system.

4. To evaluate the suitability of the system for providing detailed dimensional information on the human body for bespoke clothing production.

5. To document the individual tests undertaken to evaluate the potential for error when altering defined variables.

6. To provide recommendations for the automation of the manual test procedure presented in this thesis.

CHAPTER 3

REVIEW OF THE LITERATURE

3.1. Clothing Sizing Standards

Up to the introduction of ready-to-wear clothing in the twentieth century bespoke clothing production had been commonplace (Tamburrino 1992). The ready-to-wear clothing trend necessitated the need for the population to be split into convenient sizing intervals. The objective of these intervals is to fit the majority, however with every majority there is also a minority whose dimensions do not conform to this norm who are excluded from obtaining well fitting mass produced clothing, reported to be as much as 35% of the population (TecMath [No date]b).

During the twentieth century sizing systems were developed based on blocks of grade rules. These sizing systems were developed through a process of trial and error by each individual manufacturer to suit their particular market, hence the size intervals offered were not consistent between sources of supply (Tamburrino 1992). An attempt to eradicate this inconsistency took place in America in 1939/41(O'Brien & Shelton 1941) and subsequently in the UK in 1951 (Joint Clothing Council Ltd. 1957), with the first major surveys of body dimensions of women. The prime objective, being the provision of measurements to improve the fit of women's patterns and garments (O'Brien & Shelton 1941). However, the attempts to standardise these sizing systems were unsuccessful.

Manufacturers resisted changing their policies in fear of alienating their customers by altering their own proven sizing system (Tamburrino 1992).

The inconsistency between sizing policies still exists today (Tamburrino 1992). A number of reasons have been cited for the opposition towards strict sizing

systems. Firstly, the target market for each garment manufacturer can be different, varying by lifestyle, income and body dimensions/shape. Secondly, the psychological aspect of size identification means a woman generally feels better when the size required makes her feel slim. Thirdly, sizing standards can date very quickly, due to variations in diet, exercise and migration and therefore only have a limited application.

Variations both in size specifications and in size labelling lead to confusion and general dissatisfaction for the clothing consumer (Tamburrino 1992a). Multiple garments need to be tried on for fit by consumers, as there is no continuity between retailer's sizes, making shopping a time-consuming process and mail order shopping problematic. As a result of this there are increased costs for the manufacturer including high returns, higher mark-downs and lower turnover (Tamburrino 1992a). This is due to consumers purchasing incorrect sizes or multiple garments to ensure at least one may fit.

Variations in sizing exist between garment types, and also within garment types, between countries and also within the same country (Tamburrino 1992). The consumer therefore must establish the most suitable size by trying on garments, repeating the same process for each style and manufacturer (DeLong et al. 1993). To further complicate the matter the female body in terms of shape and proportion may also vary considerably even though they still fall within the same size interval (Vouyouka & Vouyouka 1997).

A study undertaken by Tamburrino (1992a) concluded that the sizing system for women in the US was not reliable. By fitting a selection of size 8 garments from a range of manufacturers onto a size 8 standard Wolf form manikin the probability of a garment not fitting was calculated at 80%. Hence only 20% actually fitted the accepted manikin size correctly, with 78% of garments being at least one size too large. However, this was only based on a small sample of

manufacturers and thus may not be taken as representative of the US clothing market as a whole.

Body dimensions are not a static phenomenon, hence neither should sizing be a static process. Over the last forty years women's bodies have changed significantly not only in size but in shape, with women becoming taller and heavier (Finch 1994; Oliver & Hendrie 1996). Additional factors also impact the suitability of sizing standards, such as ageing and the inevitable exclusion of people whose figures do not conform to the norm. A number of the leading consumer countries have an ageing population (Byrne 1995). Studies on women have highlighted the effects that ageing has on the body in terms of both shape and dimensional alterations, with both Goldsberry et. al. (1996) and Maggs (1998) illustrating how this contrasts with younger age groups. In terms of those with 'non-standard' figures, such as those with physical disabilities, the lack of available suitably fitting clothing further stigmatises this group by restricting them to specialist clothing which often lacks the aesthetic appeal that the average consumer has come to accept (Wyatt 1999).

3.2. Anthropometric Measurement

A lack of reliable data exists on body shape (Byrne 1995). The majority of anthropometric data continues to be outdated and often only covers specific groups within the population. Obtaining accurate body measurement data can be problematic. The ISO standard 8559 (1989) suggests an accuracy of ±1% or ±5mm whichever is the smaller, whilst anthropometric surveys of military populations have determined acceptable errors of between 2mm and 24mm dependent on the dimension being measured (Gordon et al 1989).

Variation in the value of body dimension measurements can be found between

successive measurements on the same person, due to postural changes and varying tape tensions and by successive measurements by different measurers, due to differences in technique and location of key points (Pfister & Pfister 1991). Manual measurement techniques can therefore be inaccurate, inconsistent and the time to collect the measurements can be lengthy (Early [No date]). In illustration, Vincourek (1990) noted differences of up to ±4cm when measuring the arm by different traditional methods used by department store buyers.

The errors related to anthropometric measurement are well documented (Himes 1989; Jamison & Zegura 1974; Marks et.al. 1989; Wilmore et.al. 1997). Two main types of error exist, instrumental error and observer error which refers to inconsistency in measurement methodology (Gordon & Bradtmiller 1992). Instrumental error may be easily quantified whereas observer error forms a more difficult problem. Observer error is not necessarily random and may be systematic in the sense that consistent differences can exist in the techniques utilised by different measurers.

Horn and Gurel (1981) rate visual proportion of greater importance than tape measurements. Variation in length and depth dimensions means individuals with the same bust, waist and hip measurements can appear distinctly different in size, even though they may still fall into the same size interval.

Standardisation of body posture for measurement is required so any variance in measurement is related to body form as opposed to movement (Croney 1980). The measurements are taken from or between landmarks on the body; these may be either bony prominence or markers placed on the skin to identify the location of the measuring points. For the purpose of manual measurement all measurers must be trained, with the accuracy in measurement being dependent on experience of the body form. The difficulties related to identifying landmarks and maintaining a constant posture mean an accuracy of better than 5mm is

virtually impossible (Pheasant 1986), both being common problems for both manual and automated measurement.

The handedness of a subject is known to influence certain anthropometric dimensions (Martorell et. al. 1988). The dominant side may return values significantly greater than the non-dominant side, particularly dimensions of the arm. However, the measurement bias between sides is less than the measurement error, therefore Martorell et al. suggest the choice of side should be left to the discretion of the investigator.

A number of factors determine the number of measurements required to successfully produce a garment (Tamburrino 1992b). The design, the desired quality, the method of pattern construction and the skill of the tailor. Those measurements displaying a high degree of variation often need to be measured directly, as they do not have a consistent relationship with other measurements and hence cannot be predicted with any accuracy. Those with a low degree of variation however can often be derived on the basis of related measurements.

3.3. Body Characterisation

There are several alternative methods of body measurement that depart from the traditional methodology used for pattern construction. Hutchinson (1977) measured 44 women of various ages both by tape measure and by a specially constructed measuring frame. The shape of the back was determined by measuring the displacement from the horizontal and vertical planes at various points. Following this he devised an original method of assessing body shape based upon moulding polyethylene foam sheeting around the subject's torso. The moulded shapes were cut in specific places to enable the form to be used as a template for pattern construction. The patterns constructed from the moulding method were found to provide a better fit than a conventional block pattern.

Visual somatometry was developed as a method of body classification by Douty (1968) based on the work of Sheldon (1940) on somatotyping (a system of body typing). Douty (1968) utilised silhouette photography to create a "somato-graph". Rear views of the subject allow body characteristic measurement and the categorising of figure types, whilst profile views (posture graphs) enable an examination of stance. A derived form of this system (graphic somatometry) has been utilised for altering and generating clothing patterns (Heisey et. al. 1986; Farrell-Beck & Pouliot 1983; Shen & Huck 1993).

3.4. Shape Measurement

Shape measurement may be achieved through contact or non-contact methods (Ward et. al. 1996). Often contact methods are cheaper, but can be more intrusive and thus may deform the area being measured. They include, casting or moulding techniques, kyphometers and rod matrices, which rely on the movement of pins when the surface is pressed against the body and derivatives of the vector stereograph, where a probe is passed over the surface, whilst the spatial co-ordinates of the probe tip are recorded. Non contact methods include airborne ultrasound, moiré fringe topography, stereographic methods, raster stereography and laser light, (discussed further in section 3.5). The primary applications of these technologies are the detection and evaluation of conditions like Scoliosis and the design of orthotic and prosthetic appliances.

Direct methods of measurement such as the use of probes require the subject to remain very still with the accuracy of measurement dependent on the skill of the operator (as a consistent application must be maintained for accurate measurement) (Turner-Smith & Harris 1985). Indirect methods such as moiré fringe topography and raster stereography have the advantages of being both quicker and non-contact methods of obtaining shape information. Both methods have been employed for the detection of Scoliosis. However, moiré fringe

topography illustrates both the subjects posture and condition and hence requires the subjects posture to be maintained if comparisons are to be made. The results of moiré topography are also difficult to quantitatively assess. Raster stereography conversely enables the quantification of any asymmetry thus the technique may be used more reliably for the assessment of such conditions as Scoliosis (Docter & Ensink 1985).

Researchers at Nottingham Trent University are investigating body dimension information with body shape data, to attempt to generate an alternative criterion for garment selection (Gray 1996). However, the shape investigation is based on a 2D silhouette generated by the Telmat 2D automated body measurement system (Conner 1995) as opposed to full true 3D, thereby providing only limited information on the contours of the body.

3.5. Body Scanning

According to Early ([No date]), automated body measurement systems are capable of providing a more efficient and consistent method of body measurement data collection when compared to manual methods. The systems may be used to produce clothing designs, to conduct large-scale surveys or to assist in mannequin design and manufacture. Three-dimensional body measurement for customised apparel has been envisaged since the 1980's (Gerber 1983), however as yet there are still relatively few systems in commercial use.

The primary automated body measurement systems include the LASS system, (Loughborough Anthropometric Shadow Scanner); (Bell 1987; Brooke-Wavell et. al. 1994; Jones et. al. 1993; Jones et. al. 1995; Kee 1993; Li & Jones 1994; West 1987), the TELMAT systems (Conner 1995; Rennesson 1998; Telmat 1999; Telmat 1999a; World Clothing Manufacturer 1999), the Cyberware WB-4

whole body scanner (Addleman 1997; Burnsides 1997; Cyberware 1998; Daanen et. al. 1997; Kreibich 1994; SAE 1997), the $[TC]^2$ system (Textile/Clothing Technology Corporation) (Bruner 1999; Demers 1997; Holusha 1996), the Hamamatsu 3D BodyLine scanner (Dekker & Buxton 1998; Hamamatsu 1997; Ody 1998; Treleaven & Dekker 1998), and the TecMath/Vitronic scanners (TecMath [No date]; TecMath [No date]a; Vitronic 1999). Several other organisations are also working in this area, however these are too numerous to be included in the scope of this review.

3.5.1 LASS

The LASS system (Loughborough Anthropometric Shadow Scanner) is based upon analysing shadows to determine size and shape to an accuracy of a approximately one millimetre (Bell 1987). The subject stands on a turntable, wearing only underwear, whilst it is rotated through 360 degrees in 5 degree intervals. Four strips of light are projected onto the body at an angle and are subsequently measured by cameras (Jones et. al. 1993). The radius on the body determines the deviation of the light at each point. At that point the radius may subsequently be calculated by trigonometry. The system is able to define numerous points on the body by generating thousands of measurements (Kee 1993). The whole process taking approximately 3 minutes. From an initial data collection of 315,000 raw data points, these are then reduced down to approximately 30,000 data points, based on a person of average height (Jones et. al. 1995). The resultant data may be interrogated to extract linear, surface distance or tape measure distances in any plane. Information on surface area, segment volumes and cross-sections is also available (Jones et. al. 1993).

Queens University has developed software to translate the points obtained by the LASS system into curvilinear co-ordinates (Bell 1987). This allows the

formation of a dummy on-screen on to which a garment design can be developed. Ultimately enabling the formation of a set of garment patterns.

Another product of the output of the Loughborough Anthropometric Shadow Scanner is a reference body created to provide a surface model for applications that include garment design (Li & Jones 1994). This may then be modified using anthropometric data to remodel the shape and dimensions of the torso. The concept being to bridge the gap in design houses, which do not require or cannot afford a 3D body scanner, but which do need a reference model which may be manipulated to their required dimensions. The difficulty with this current method is that it only covers the torso, without arms, and thus has limited application in replacing the live model.

During the development of the LASS system an exercise in the determination of errors was undertaken to identify the source of distortion noted in test measurement results (West 1987). This covered basic tests to determine the source of any errors, including a lens test, and a camera tube test. No measurable error was identified in the lens and there was no significant non-linearity in the camera tube. This forms a very basic error test procedure, which is by no means comprehensive; hence the source of the distortion error remained unidentified and the issue was never resolved within his thesis.

An investigation was also undertaken comparing the reliability and repeatability of LASS measurements to anthropometry (Brooke-Wavell et. al. 1994). Whilst the measurements were generally similar, some significant differences did exist in taking horizontal tape measurements and differences in locating measurements through LASS due to difficulties with the landmark markers. Intra-observer errors were greater for anthropometry than LASS, whereas inter-observer errors were generally similar. The repeatability of the measurement procedure was found to be no better for LASS than for anthropometry. Whilst this study used a

range of measurements covering different planes it was only based on a limited number of measurements and therefore does not provide a full analysis of the reliability and repeatability of the system for body characterisation.

3.5.2 Telmat

Telmat produces two automated body measurement systems based on a light projection technique (Rennesson 1998). A 2D body outlining system designed for mass customisation and a 3D body capture system for bespoke clothing production. Both systems require the subject to stand within a measuring booth, in their underwear. The 2D system takes front and profile images, taking approximately 30 seconds (Conner 1995). The images are then manipulated to generate a data bank of predefined measurements. The measurements in this case are not calculated on a real body, but rather a model adapted to a 2D outline (Rennesson 1998). The measurements being extracted, once the landmarks are detected on the 2D outline.

The image capture process for the Telmat Turbo Flash/3D system takes $1/25^{th}$ of a second (Telmat 1999). The system uses a method of automatic calibration, with a reported precision of 0.8 mm on a point and 2 mm in a circumference measurement (Rennesson, 1998). Measurements may be generated automatically by the 3D system, with the dimensions being calculated on a real 3D body, in contrast to the approach used on the 2D system. The automatic detection of the anthropometrical points used for measurement is carried out according to the standard ISO 8559 (1989), with postural information such body figuration quantification also now being included (Telmat 1999a). The individual measurements created by the system may then be sent to a specialised CAD system for made to measure pattern construction. Telmat is undertaking a partnership with Eastman Machine Company and Scanvec Garment Systems to

provide an automated bespoke apparel production facility (World Clothing Manufacturer 1999).

3.5.3. Cyberware

The WB-4 whole body scanner by Cyberware uses four scanning units mounted on vertical towers, to enable a vertical traverse to scan the body in one sweep, taking only 17 seconds to complete (Daanen et al. 1997). The system is based upon laser light, which is projected on to the body, the light is then viewed by cameras to digitise the subject, thus providing a complete 3D image of the subject (SAE 1997). During the scanning process both 3D data and colour information is generated to give a 3D-geometry scan, Red/Blue/Green (RGB) values being stored for each digitised point on the surface of the body (Burnsides 1997).

The WB4 scanner has a capture volume of 200cm in height x 120cm in diameter. For larger subjects who exceed this limit 'zippering software' is available to join multiple scans into a complete model (Cyberware 1998). The scanning instruments consist of laser diodes to project the light onto the subject and a CCD (charge-coupled device) to view the interaction of the light on the subject (Addleman 1997). The data may be presented in wireframe, point cloud, profile or surface formats (Burnsides 1997). Whilst the surface of the model may be presented as true-colour, shaded or colour-coded to indicate curvatures, clearances, stress or pressure. Measurement functions include surface & straight line measurements, circumferences, arcs, true diameters, surface area and volume measurements.

On the CARD Lab's system, landmarks may be selected by manual point picking, semi-automatically by selecting a group of points then extending that mathematically and automatically by a process of automated landmark

provide an automated bespoke apparel production facility (World Clothing Manufacturer 1999).

3.5.3. Cyberware

The WB-4 whole body scanner by Cyberware uses four scanning units mounted on vertical towers, to enable a vertical traverse to scan the body in one sweep, taking only 17 seconds to complete (Daanen et al. 1997). The system is based upon laser light, which is projected on to the body, the light is then viewed by cameras to digitise the subject, thus providing a complete 3D image of the subject (SAE 1997). During the scanning process both 3D data and colour information is generated to give a 3D-geometry scan, Red/Blue/Green (RGB) values being stored for each digitised point on the surface of the body (Burnsides 1997).

The WB4 scanner has a capture volume of 200cm in height x 120cm in diameter. For larger subjects who exceed this limit 'zippering software' is available to join multiple scans into a complete model (Cyberware 1998). The scanning instruments consist of laser diodes to project the light onto the subject and a CCD (charge-coupled device) to view the interaction of the light on the subject (Addleman 1997). The data may be presented in wireframe, point cloud, profile or surface formats (Burnsides 1997). Whilst the surface of the model may be presented as true-colour, shaded or colour-coded to indicate curvatures, clearances, stress or pressure. Measurement functions include surface & straight line measurements, circumferences, arcs, true diameters, surface area and volume measurements.

On the CARD Lab's system, landmarks may be selected by manual point picking, semi-automatically by selecting a group of points then extending that mathematically and automatically by a process of automated landmark

recognition (Burnsides 1997). Shape information may also be extracted to enable further analysis or direct manufacture of bespoke products.

An investigation into the accuracy of the Cyberware WB4 scanner was undertaken by Daanen et al (1997), by comparing the known dimensions of a calibration object with those measurements generated from the scanning system. The calibration device was sited in 9 unique locations and at 5 unique heights in order to test the measurement error within the capture area. The results of the investigation indicated that the position of the calibration object was not a source of systematic error. Measurement errors, however, were noted which formed random errors due to resolution and human fallibility. The errors in the vertical direction were less than those in the horizontal direction, due to the resolution. (The camera has a resolution of, 5mm in the row direction and 2mm in height, and 0.5mm in depth).

When selecting landmarks the detected point may be 2.06mm away from that selected by the operator (Daanen et. al. 1997). Therefore when determining distance measurements this error could become as much as 4.12mm. Whilst this error is within the ISO 8559 specification (1989) of ±5mm, it refers purely to point picking hence any other errors present in the 3D data or measurement process would further increase the error in measurement which could then exceed the ±5mm specification. The investigation presented forms a simplistic error analysis, which essentially only covers the placement of the object to be scanned, and the random errors associated with point picking. In addition the landmarks were identified by washers with an inner diameter of 10mm and an outer diameter of 21mm, which must introduce significant errors by virtue of their size.

A number of limitations are reported in reference to the cyber head scanner (which works on a similar principle to the whole body scanner). The scanner does not handle glasses or hair very well (Kreibich 1994). Glasses cause

problems with the tracking laser and the colour camera image, whereas with hair the laser beam tends to scatter. One other issue is that the scanner does not always capture the top of the head, which means for visual effect the image then has to be altered using 'toupee' commands. For applications requiring a good physical likeness to the scanned person, such as virtual reality dressing, these issues could create some significant problems.

3.5.4. $[TC]^2$

The Textile/Clothing Technology Corporation, ($[TC]^2$), have a three-dimensional body measurement system based upon the structured light method using white light (Demers 1997). The system requires the subject to stand in either their underwear or a body suit, in a booth in front of a banded light source (Holusha 1996). Six stationary projectors are used containing a two-dimensional patterned grating that is projected onto the body; these projectors are combined with six CCD cameras which read the projected patterns of light from different angles (Demers 1997). The system provides automated extraction of a predetermined list of body measurements. The software also has the flexibility to add new measurements, for example, 4cm underbust, plus the capability to customise existing measurements (Bruner 1999). For example, to measure the waist at an angle for a gentleman who may wear their trousers lower at the front than the back.

The capture volume is 2 metres high, 1.1 metres wide and 1 metre thick, with four front views (two upper and two lower views) being taken 60 degrees apart and two back views (one upper and one lower view) (Demers 1997). The system utilises sinusoidal patterns using fine grating with a period of 1mm and coarse grating projections with a period of 5mm. A total of 48 images are captured in an image capture procedure comprising of four images per sensor for the 1mm grating and four images per sensor for the 5mm grating. For each sensor the

phase information from the collected images is used to calculate the 3D point cloud.

An investigation into system measurement errors is presented for the phase measurement and 3D point solution (Demers 1997). Sources included in the investigation were the effect of image noise on phase measurement accuracy, and phase measurement error on point position.

In order to combine the sectional views from each of the six sensor heads into one whole image, the orientation of each view in respect to its partners must be determined by calibration (Demers 1997). The views are matched by a minimisation routine, and once the orientation of each sensor is known a transformation matrix changes the data into global co-ordinates. However, the object used to illustrate the 3D composite data set was a manikin, which due to the complexity of its surface features, can hide any discrepancies in the matching routine.

3.5.5. Hamamatsu

The 3D BodyLine scanner from Hamamatsu Photonics works on the infra red principle (Treleaven & Dekker 1998). Each scan takes 10 seconds and generates 300,000 body points. The scanning heads vertically traverse the body in one downward sweep whilst the person to be scanned stands in their underwear (Ody 1998). The whole process from scan to data output is complete within one minute (Hamamatsu 1997). The capture volume covers 1850/2000mm in height, 500mm in thickness and 900mm in width, with a vertical measurement interval of 5mm.

Researchers from University College London are developing the 3D BodyLine Scanner (Ody 1998). Current work is based on automated measurement

extraction. From a point cloud, artificial intelligence is used to obtain body measurements (Ody 1998), with feature recognition employed for the automatic location of landmarks (Dekker & Buxton 1998). The Hamamatsu hardware is accurate to +/- 1mm, however, the issue of the accuracy of extracting landmarks is based upon software (Treleaven & Dekker 1998). Fifty linear measurements are available (Dekker & Buxton 1998), however, in a more recent article Treleavan is reported as saying that seventy measurements are required by the clothing industry, of which 50% are currently available (Ody 1998). Tests over a primary set of 15 measurements gives a mean error of 12mm (3% error), over the full 50 measurements this figure rises to 20mm (6% error) (Dekker & Buxton 1998).

Treleaven and Dekker (1998) suggest the challenge of data capture comprises of

- Shadow in the inner legs, arms etc.
- Sway - front, back, sideways
- Breathing - sensitivity to body position
- Accurate identification of the correct landmarks for measurement over a wide range of body types and builds (to ensure the location of a dimension remains constant regardless of subject).

3.5.6. TecMath/Vitronic

TecMath/Vitronic produce two scanning systems, the 2D Contour system and the 3D Vitus system (TecMath [No date]). The Contour system is based upon photogrammetry and whilst the system creates a 2D outline, the creation of a 3D model is also possible. From the scan data an automated body measurement extraction process is undertaken with a view to providing selection of the most appropriate size interval (TecMath [No date]a), much like the Telmat 2D system.

The Vitus 3D body scanner utilises the laser stripe method for data capture, providing a capture volume of 1.2metres by 0.8metres and 2.1metres in height (Vitronic 1999). The scan takes approximately 10 to 20 seconds, providing a resolution of between 1 and 2 millimetres. Colour data for each 3D point is also available by the inclusion of four colour cameras.

3.6. Structured Light Systems

Structured light is an image capture method, utilised for a number of body scanners, including the image capture system under investigation in this study. Structured light systems consist of a projector and a camera (Valkenburg & McIvor 1998). Patterns of white light are projected onto the target object and the CCD camera records the distortion of the light as it is meets the object (Kaufmann 1997). The displacement generates data on the distance between the target object and the camera, software may then be used to generate a three-dimensional image from the distance data. For each point there will be a stripe value and pixel co-ordinate (Valkenburg & McIvor 1998). The stripe value defines the plane, whereas the pixel co-ordinate defines a ray in space. The combinations of the two form the 3D location in space.

3.6.1. Errors and Calibration

As the lenses for the projector and camera are subject to distortion, uncertainty in the 3D location exists. The distortion present being relative to the quality of the lens. The projected line is subject to distortion by the lens, which results in a slightly curved surface, whereas the camera lens distortion results in a displacement of the ray in space from its nominal location (Valkenburg & McIvor 1998).

An analysis of errors in 3D shape construction using structured light was presented by Yang and Wang (1996). The objective was to identify potential sources of error and evaluate the impact of these errors on computing surface properties. The research identified three categories of error sources, those being, image processing, system modelling and experimental error. The image processing error comprises of error due to the quantization process, and error due to incorrect location of features in the image plane. The quantization process requires the location of the image pixels to be restricted to an integer grid, which makes the potential error as much as half a pixel in the x and y directions. The mislocation of features is suggested to be a more critical error, as where the light stripes are wider than a pixel, a greater number of potential locations may be available, if an incorrect selection is made the stripe will be misplaced, resulting in a error when locating image features. Practically this would result in inaccuracies in the 3D point solution and hence in the imaged representation of the captured object.

Yang and Wang (1996) suggest the image processing error may be minimised by ensuring the width of the stripes on the projector slide are thin and/or the projector direction is kept near to the normal direction of the imaged surface. The system modelling error was considered in terms of the error introduced by the difference between the ideal projection model, which assumes all projection rays are parallel and the actual reality, where projected rays are at an angle to the optical axis.

According to Weng et. al. (1992) when attempting to obtain dimensional measurements in 3D it is crucial that the cameras used are accurately calibrated. It is more important that the actual positioning of points in an image plane is correct rather than the image quality. The quality of the image may be poor, but the image position of a point may still be accurately located. Weng et al. consider three different types of distortion, which affect the image points in the

image plane. Radial distortion, which is a result of imperfect lens shape, decentering distortion and thin prism distortion which are a result of problems in the camera and lens assembly, resulting in radial and tangential errors. The paper, however, only addresses camera distortion, and by no way provides a complete analysis of all possible types of distortion present in a structured light system.

For camera calibration, Godhwani et al. (1994) use the comparison between analytically projected co-ordinates of the calibration object and the co-ordinates in the image plane of the calibration object to establish the error in observation. This may then be minimised by using statistical estimation methods. For projector calibration, again the known physical values are compared to the projected co-ordinates, determined by least-squares fit, to establish the observation error, which may then by minimised using statistical estimation methods. However, the error in this case is only minimised and therefore still exists as a residual error that will impact on any measurements taken; the accuracy of digitisation in this case being approximately 0.25mm.

3.7. Body Scanning Applications

A number of commercial surveys have been undertaken using 3D body measurement systems. Gray of Nottingham Trent University's clothing centre has been involved in measuring women for the Burton Group (Leonard 1997) and Marks and Spencer (Nuki 1999).

The CAESAR project is undertaking the collection of body measurements from 8,000 US and 6,800 European civilians, male and female aged 18-65 (Stokes 1997). The project will use the Cyberware scanner to collect a total of 64 univariate measurements (36 scan measurements and 28 traditional measurements) for the US measurements and the TNO Human Factors Research

Institute will use the Vitus whole body scanner for the European data collection (NedScan 1999). The data will be used for apparel sizing amongst other uses such as workstation and equipment design, with an international database of the body measurements collected due in the year 2000.

A number of projects are investigating the feasibility of custom clothing. A £3.4 million award has been granted under the Foresight Link programme (Cookson 1998) to establish a centre for 3D electronic commerce (Treleaven et. al. 1999). The consortium consists of members from education, manufacturing, retailing, electronics and information technology (Cookson 1998). The research will be split into three distinct areas, national sizing survey, the development of prototype customised clothing services and a virtual clothes shopping service (Russell 1999). A European Centre of Individual Production is being established in Germany to investigate the issues relating to producing individual products, covering clothing, footwear, and transportation (TecMath 1998). Also based in Germany is the Production 2000 project, whose objective is to establish an integrated custom clothing system (TecMath [No date]b). Partners include TecMath, the Hohenstein Institute for Clothing Physiology, Expert Systemtchnik and G.M. Pfaff. Two European Union funded research projects also relate to customised clothing. The EASYTEX project has been investigating custom clothing for elderly and disabled people (Russell 1999); this project includes the evaluation of the use of body scanning and pattern adaptation for those with 'non-standard' figure types (Wyatt 1999). Whilst the e-Tailor project is concerned with integrating 3D body measurement, CAD and e-commerce technologies for the clothing industry (ATC 2000).

The use of body scanners in retail outlets has as yet been limited. The Hamamatsu BodyLine scanner is being used for ladies foundation garments in the Far East (Bruner 1999a), and the Tecmath system is being used in five stores in Holland, Slovenia and Germany (Russell 1999). Whilst the Levi's Union

Square store in San Francisco, are using a [TC]2 scanner to measure customers for their custom fit jeans programme (Bruner, 1999a).

Only two cases of garments being made-to-measure from data points of a body scan are noted in the literature. Interactive Custom Clothes Company have demonstrated the application on custom jeans (www.ic3d.com 1999) facilitated by means of a genetically engineered neural network, whereas Tom and Linda Platt demonstrated the application on an evening gown (Bruner 1999a).

3.8. Mass Customisation and Bespoke Manufacturing

The predominant manufacturing model of mass production has more recently been challenged by new technology, changing consumer requirements and instability in the economic climate (Anderson et. al. 1998). The recent interest in bespoke manufacture and mass customisation has been pushed to the forefront by the marketing opportunities available over the Internet (Gerber 1998).

Mass customisation can be seen as a compromise between bespoke manufacturing and mass production (Gerber 1998). It may be defined as the process by which mass-market goods are individualised at an affordable cost based upon a defined customer requirement (Gerber [No date]a). In contrast to made-to-measure which is based upon full customisation, where the garment is made entirely to the consumers specifications. Both mass customisation and bespoke production provide a number of advantages, such as a reduction in inventories, returns and necessary floor space. It also strengthens customer relations by improved service levels and identifying customer preferences and buying habits. Levi's has demonstrated the viability and consumer acceptance of custom apparel with their bespoke jeans service (Ross 1996). A reported increase of 300% in terms of sales has been achieved in those areas where the service was introduced.

A study undertaken by Caldwell and Workman (1991) investigated the retailer's perceptions of consumer interest towards customised patterns against a set of predefined factors, namely anatomical structure, pattern design and fabric. Results indicated a specific market for customised patterns based upon women with irregular anatomical structures, using complex patterns designs and/or complex fabrics. Perceived interest decreased as the complexity of the structure, design and fabric decreased. A similar investigation based upon focus groups of consumers highlighted similar findings with suits/jackets, evening/formal wear, and dresses identified as the apparel categories where customised fit was preferred (Anderson et. al. 1998). However, 56.5% of the sample already owned customised apparel, which primarily was contained within the apparel categories stated, therefore the sample was biased to some extent by their previous experiences.

Knight and Cassill (1994) undertook an investigation into the acceptance of body scanning and found that based on a sample of 97 females 76% found the concept of body scanning appealing. The size and age of the respondent was not shown to be a significant factor in their views towards body scanning. However the sample was drawn from University staff and whilst the occupational range appears varied, it is highly likely that the majority of the respondents were from the Department of Clothing and Textiles which would introduce a considerable bias into the results.

For an initial scan 36.1% of respondents were willing to pay $5, and 20.6 were willing to pay up to $10, with 44.3% willing to spend $5 on an updated scan and 3.1% were willing to pay $10 (Knight & Cassill 1994). However, there is no indication of the views of the remaining percentage respondents in each case, which may suggest they are not willing to pay.

Whilst Anderson et. al. (1998) indicated a greater preference for more evening/formal wear, Knight and Cassill (1994) reports the primary interest areas for customised clothing to be jeans and trousers, swimwear and blouses/shirts. This indicates a deviation in the results of the investigations. However it is not clear whether the choices of garment types were restricted to those imposed by the author, which would account for such a discrepancy.

3.9. Applications of Three Dimensional Data to Clothing

3.9.1. Pattern Construction

A number of research projects are being undertaken in the area of converting the three dimensional bodyform to a two dimensional form for patterns for clothing construction. Heisey et. al. (1990) have presented an algorithm for drafting patterns by computer from three-dimensional data. However, this works on the principle that the fabric remains in constant contact with the surface and restricts the application by being dependent on the physical characteristics of the fabric. In the second part of the paper (Heisey et. al. 1990a) the concept is extended to the individual drafting of fitted garments by computer from three-dimensional data. This is based on modelling the garment draping process. A pattern for a basic straight skirt is used to demonstrate the algorithm, however no functional ease was included in the garment, thereby limiting its application.

The problems are also being addressed by Hinds et. al. (1992) who present a CAD system, which allows the creation and presentation of garments as three-dimensional models, utilising data, obtained from the LASS system.

The difficulties associated with implementation of three dimensional modelling for garment pattern design has been investigated by Ng et. al. (1993). The difficulties were found to be the lack of a mathematical model to describe the

human body, the relationship between the three-dimensional human body and two-dimensional patterns, the difficulties associated with predicting fabric behaviour and the absence of a mathematical model to accommodate the variation in fashion styling. Following a review of previous literature, the authors conclude that when ease is taken into account the previously established methods may either fail or require further work. A research team from WIRA and the Computer Aided Design Centre mirrored this view (Manufacturing Clothier 1983), highlighting the impact of fabric characteristics on the allowances required for such factors as fullness, ease or drape. Hence they believed the problem could not be simplified to a mathematical model.

3.9.2. Garment Representation

CDI Technologies Inc. (Byrne 1995) have developed a system to design and represent garments in three dimensions. They are also working on simulating drape on computer generated images. Draping algorithms are also being developed in conjunction with the North Carolina State College of Textiles based upon interpreting fabric properties measured by the Kawabata Evaluation system.

The ability already exists to capture fabric texture and 'warp' the image in order to provide a representation of the fabric in garment form (Hinds et. al. 1992). Images of garments may be produced which provide near photographic quality. Hinds et al present a CAD system which enables the creation and presentation of garments as 3D models which allows the images to be viewed from any direction and distance. However for garment representation on a moving form, the issue becomes more complex.

The introduction of E-business for clothing raises a number of issues in terms of correct order selection. To ensure the garment both suits the individual and to ensure that it is the right size the customer generally tries on most garments

before purchase. For E-business therefore correct order selection is important to ensure customer satisfaction and to minimise returns.

Clarity Fit Technologies (1999) offer a solution based upon the generation of a suitable 3-D body model based upon body scan data of those matching the subjects parameters for a virtual try on, coupled with a size matching technique to offer the closest size. (A custom pattern generation system is also offered by Clarity Fit). The body model may also be created by using a standard size, by matching existing body models to the customer's own dimensions or by using the customers own scan data, if available. The virtual try-on allows the customer to view the dressed model to determine whether the appearance is acceptable and whilst the paper does make reference to the quality of fit, it does not mention whether drape is taken into consideration in the virtual try-on. Cyberdressforms are also working in this area, producing dress forms from body scan data (Bruner 1999a). Also the CAD company PAD system provide a virtual manikin in their software which may be adapted to the customers measurements, a recent trial with [TC]2 has also successfully used scan data to provide a virtual manikin form (Bruner 1999).

3.10. Main Conclusions from the Review

1. There is a significant level of variation between sizing policies of manufacturers and retailers, leading to dissatisfaction for the consumer and high costs for the manufacturer or retailer.

2. Manual body measurement is subject to variation between successive measurements and inaccuracy due to variations in measurement techniques and postural differences in subjects. The limited data provided following general practice provides measurements which alone do not characterise the body, therefore any postural or shape information which

may be important for pattern construction is not necessarily recorded. This is in contrast to the tailor's approach, generally used for bespoke suiting which is based upon a series of figurations in addition to body measurements.

3. Body scanning systems show the potential to provide postural, shape and dimensional data, in a timely, cost effective manner, which is acceptable to the consumer.

4. Questions arise over the accuracy of the dimensional data obtained from body scanning systems. Those that provide automated measurement extraction are not as yet proven to be as accurate as manual anthropometric measurement. Whilst those which utilise manual point picking are subject to both observer and instrumental error, which suggests the accuracy will also be questionable.

5. Efficient, reliable body scanning systems are the pre-requisite to the widespread introduction of mass customisation and bespoke manufacturing. Manufacturing technology exists to provide cost effective bespoke manufacturing, however, the issue of obtaining accurate body measurement data and its interface with pattern construction systems has yet to be resolved.

6. The use of virtual reality as a selling medium on the Internet will require accurate 3D data for its models. The combination of the three-dimensional body image with garment representation will allow virtual dressing for consumers prior to ordering bespoke garments. However, for this to become a reality, realistic garment simulation models will have to be devised.

7. Whilst investigations have been undertaken on the accuracy of some of the scanning systems presented here, the depth of analysis is extremely limited and only covers a restricted number of error sources. No single study has been found which fully characterises all the potential sources of error and their effects on measured values.

8. The analysis already undertaken on structured light measurement systems has focussed on calibration, in terms of matching known points in space with those points in the imaged object and error analysis in terms of projector and camera lens distortion and in computing the imaged surface. The error sources covered include lens distortion, image processing and system modelling errors. Experimental errors were not included in either of the investigations. No evidence exists within the literature review of a methodology to evaluate a structured light system in terms of all potential sources of error, particularly when the end application is bespoke clothing manufacture.

CHAPTER 4

PRELIMINARY RESEARCH

4.1. Introduction

For the purpose of this investigation the tests have been restricted to a single image capture system, still in its prototype stage. Due to the nature of this investigation the image capture system has been modified by the manufacturer throughout this piece of work as the test findings have been realised. Therefore this chapter will focus on the original prototype two-camera system supplied at the start of the investigation. The system was modified during its use and finally a more advanced, single camera system was introduced, which will be detailed in Chapter 5.

The preliminary research on which the main investigation was based comprised of three phases of testing through which the methodology for the evaluation of the single camera system was determined. The results of the preliminary research are presented in summarised form to illustrate the development of the methodology and the evolution of the investigation. The complete detailed information on the preliminary research is contained in Appendices A, B and C as are the full results from each test.

4.2. The TriForm™ Two-Camera 3D Image Capture System

The TriForm™ 3D image capture system was developed following the construction of a prototype designed to record facial features before and after surgery. The system used for this investigation was also a prototype model based upon the same principle but with a larger capture volume. An illustration of the system is shown in Figure 4.1.

Figure 4.1. The TriForm™ Two-Camera 3D Image Capture System (Wicks & Wilson Ltd. 1999)

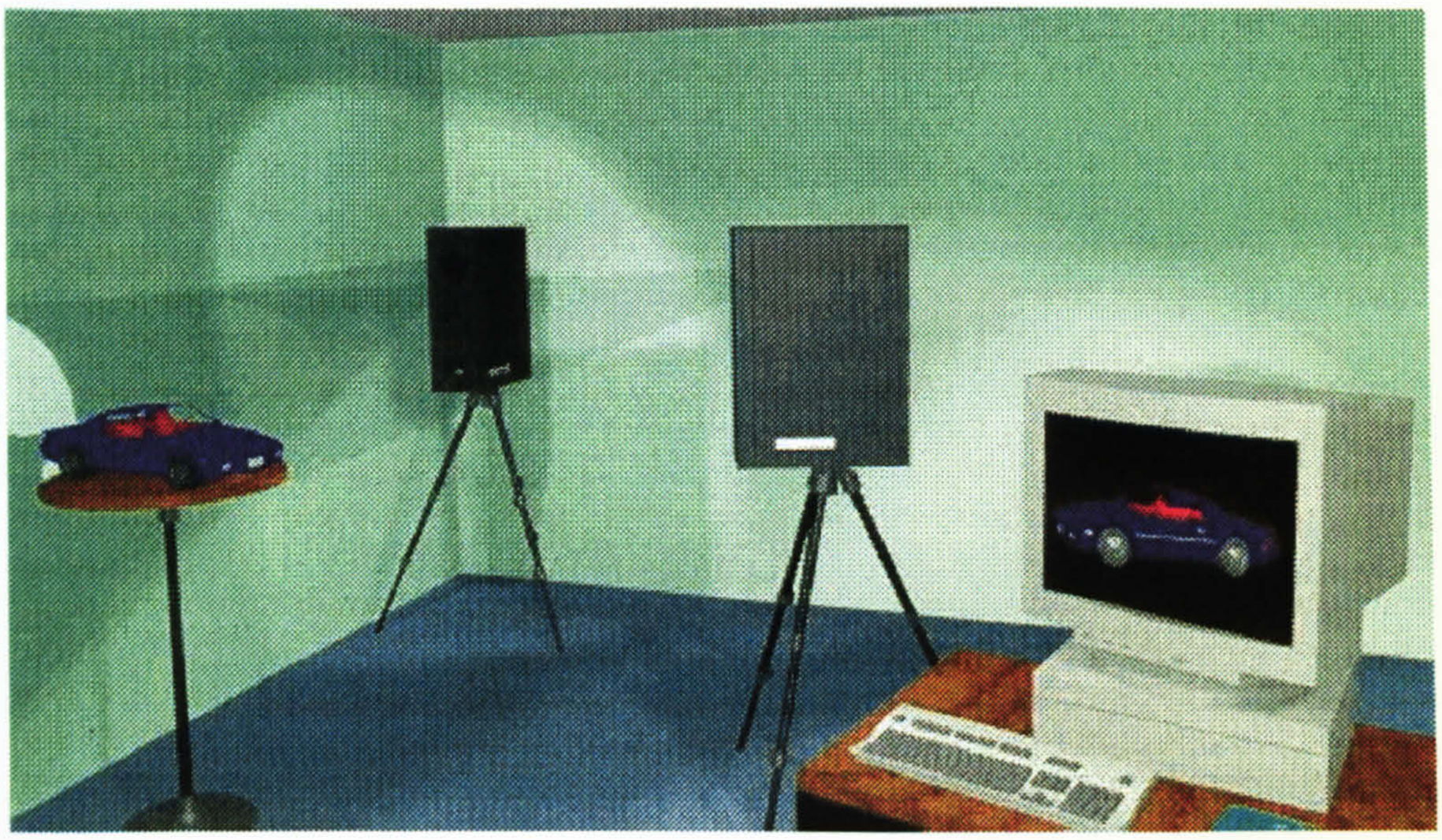

The system employs a variation of the Moiré fringe technique to capture the shape and appearance of an object in three dimensions. The Moiré fringe technique is based upon the projection of a grid onto the target object, which is then viewed through a further grid by a camera (Lewis & Sopwith 1986). The pattern is distorted where the projection meets the object, according to the topography of the surface, producing a contour line image of the object that may be interpreted to provide three-dimensional information (Batouche et al. 1996).

The system employed in this investigation is based upon the principle of structured light, a variation of the Moiré fringe technique, which in this case, utilises a sequence of projected stripes of light. A series of structured light patterns are projected on to the scene, which are viewed simultaneously by a CCD colour camera. The original system was based upon two Capture Units, each consisting of a LCD projector mounted above a CCD camera each being fixed relative to one another.

The projector produces a two-dimensional pattern, which is projected onto the target object. The pattern forms a series of light stripes that are produced by the projection of light through a series of grating patterns used within the projector Unit. The sequence includes both coarse and fine gratings (an example of the projection from each is illustrated in Figure 4.2), plus a reference pattern, based on a combination of both fine & coarse gratings, which defines the centre of the image and a white projection to obtain the colour data. Both the fine and coarse gratings are each projected four times, each time the fringes are projected ninety degrees out of phase with each other. The resultant image produced after the capture process is therefore a combination of the ten images captured by the frame grabber during the gratings projection sequence.

Figure 4.2. Projector Gratings

Fine Gratings Pattern

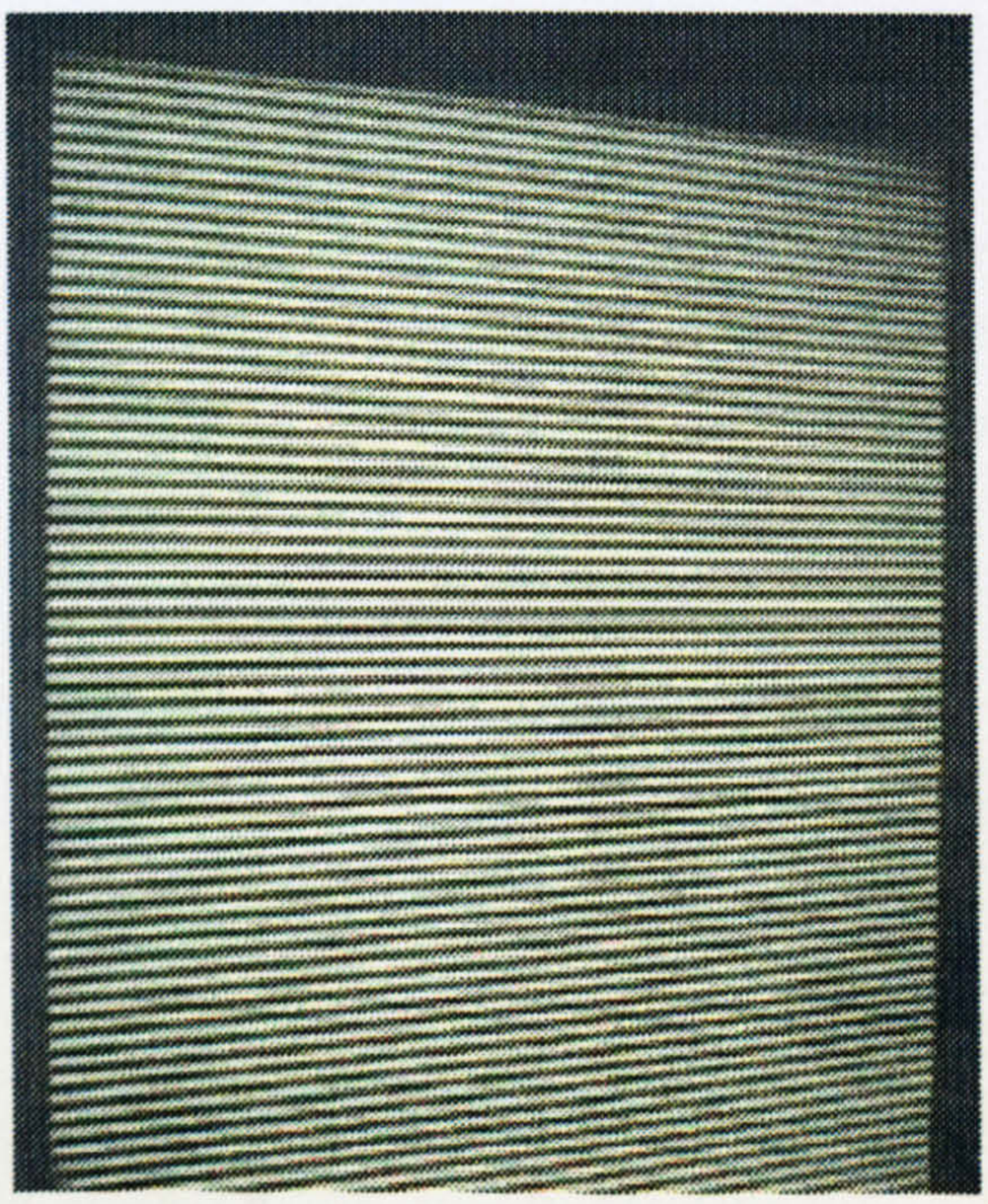

Coarse Gratings Pattern

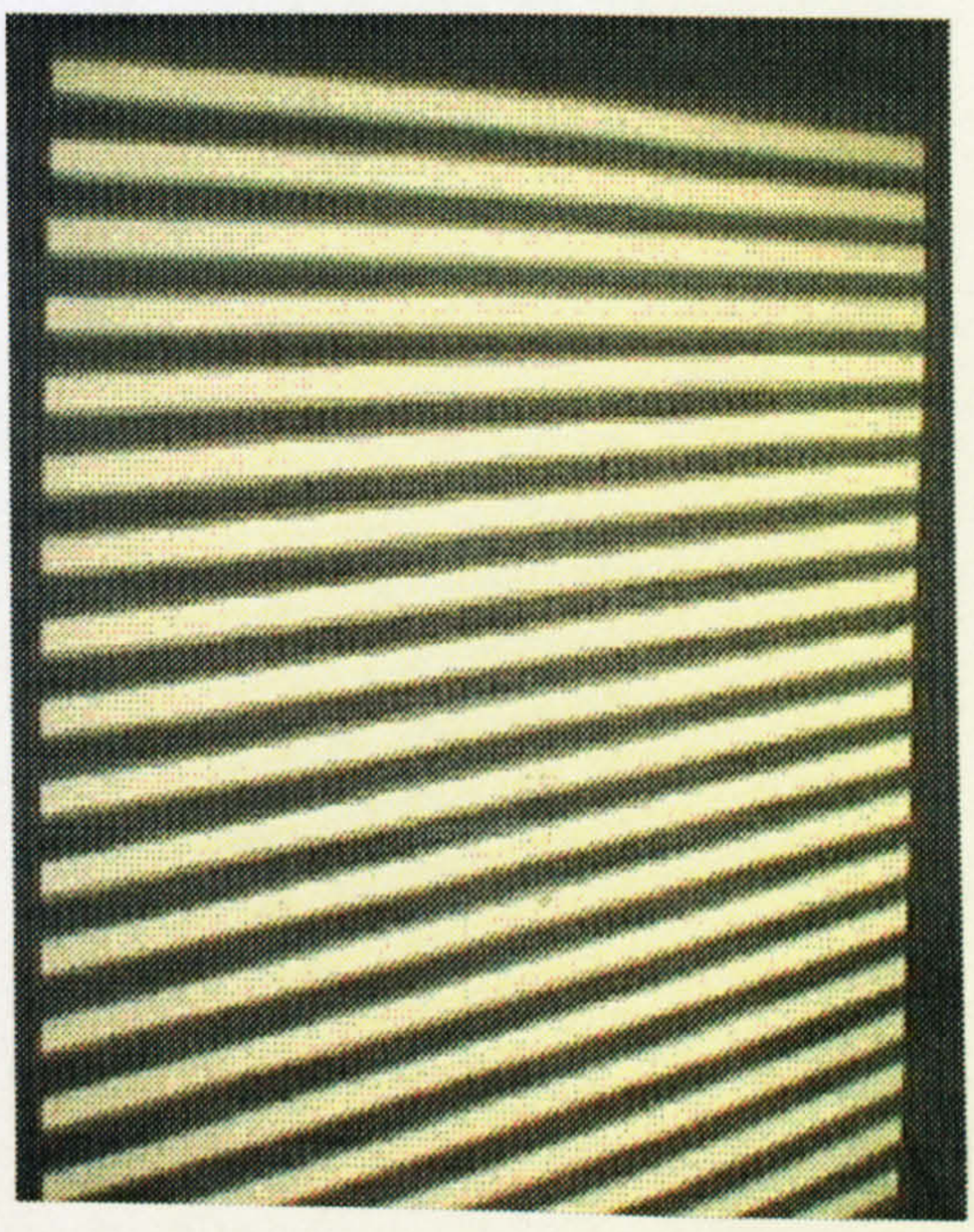

Both fine and coarse gratings are projected to enable the accurate measurement in the z plane. The fine gratings being used to provide the required distinction in depth between data points, whereas the coarse gratings are used to check the

depth information to avoid any errors arising from equivocal data produced by the fine grating. The deformation of the stripes is used to calculate the distance from the subject to the camera. This distance information may be analysed by software to yield the three-dimensional shape information relative to the object, as the depth may be inferred by triangulation based upon the known camera and projector geometry.

Three-dimensional data is computed for each pixel, from the co-ordinates in space by analysing the distortion in the patterns of light when they meet the object. This is achieved by the interaction of the 2D projection onto the target object, which creates a 3D distribution of the projected pattern. The projected stripes define a plane in 3D space whereas the pixel location on the CCD array defines a unique ray in space. The point of intersection between the plane and ray defines a unique location in 3D space. A simplified illustration of this process may be viewed in Figure 4.3. The procedure follows for the complete set of three-dimensional co-ordinates for the surface of the captured object. These result in a point cloud containing up to 300,000 sets of 3D co-ordinates and associated colour data. However this refers to the full capture volume, and as the target object generally occupies less than the whole capture volume, the number of points in the image is generally less than the maximum.

Figure 4.3 Three Dimensional Point Estimation

Key: x = horizontal dimension y = vertical dimension z = depth dimension

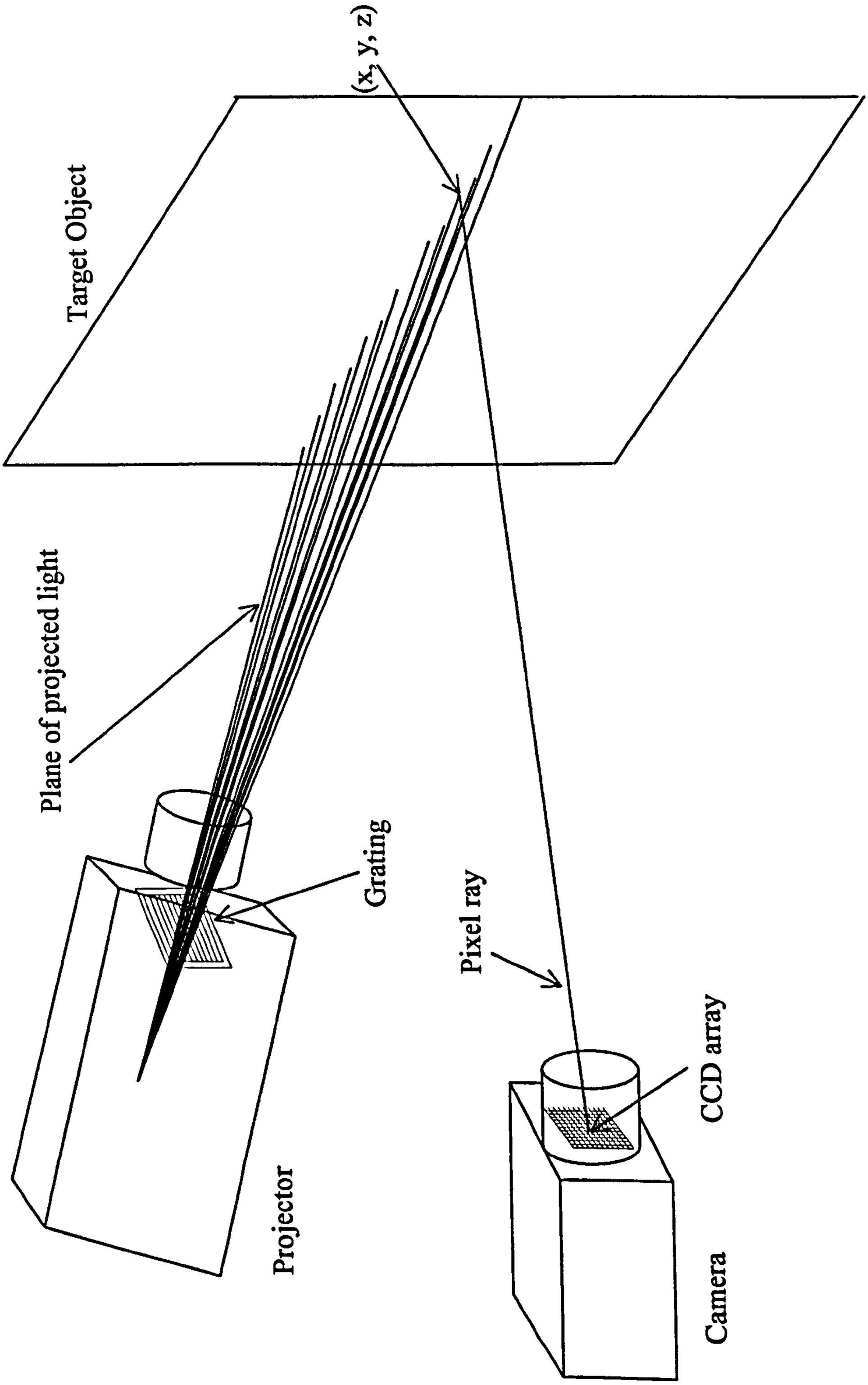

As the projector and the camera view the scene from an angle, corrections need to be employed to cover the variation arising from the cosine effect. As the Capture Unit views the target object from an angle, the distance from the Capture Unit to the target is variable across its length and thus this needs to be incorporated into the software to ensure the cosine effect does not impact on measured values, illustrated in Figure 4.4. Correction in the z plane needs to be made for the variation in Fringe Spacing for the projector, whilst correction in both the x and y planes are required for the variation in pixel spacing for the camera. Correction algorithms to cover the effects of the cosine effect are included in the software for the TriForm™ system. Correction factors such as K1 and K2 also exist for incorporating errors arising from projector and camera lens distortion.

Figure 4.4. Cosine Effect

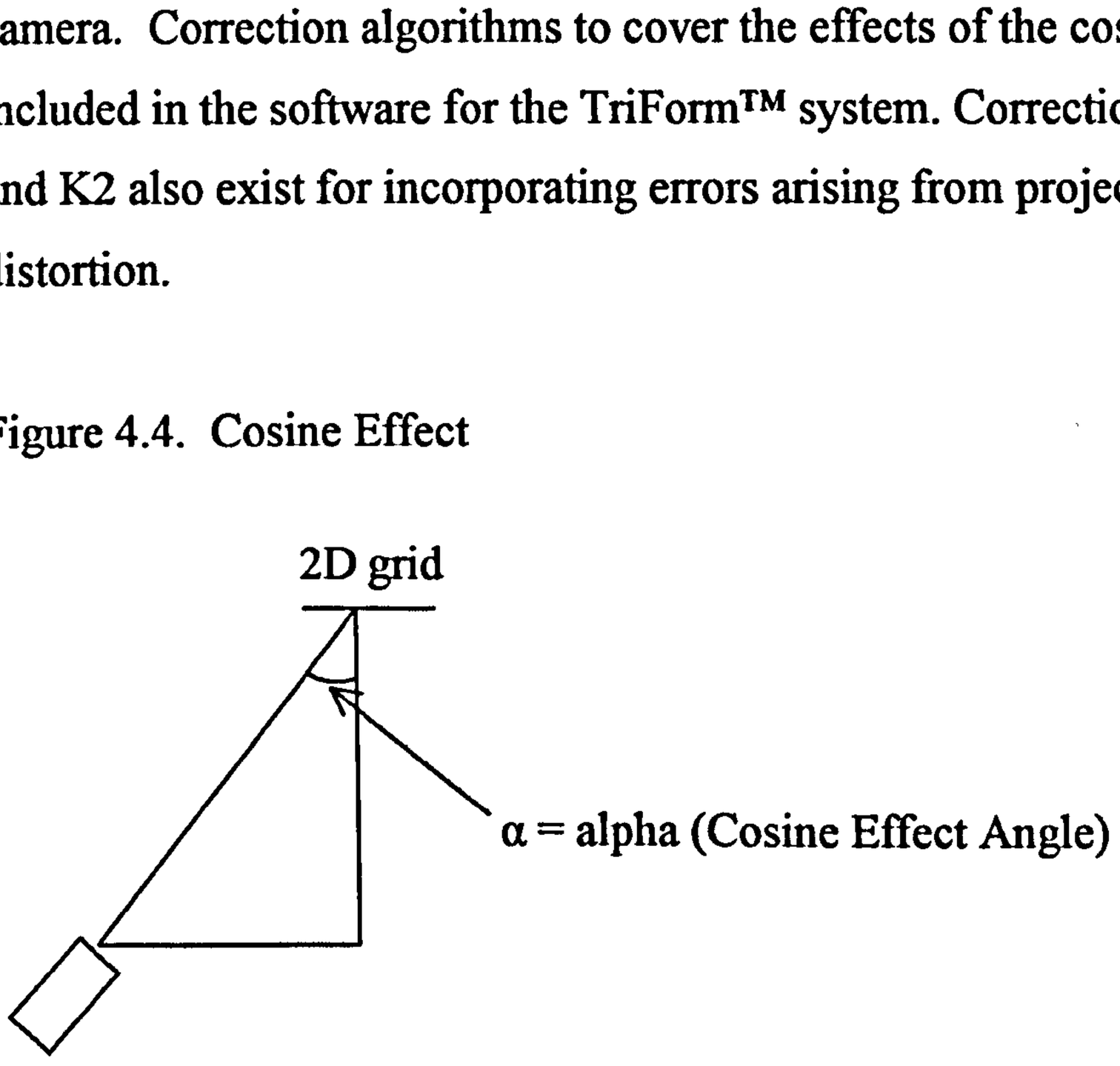

The export formats are currently limited to TFM (Wicks and Wilson's own proprietary format) and ASCII, with an average file size in of 2MB in TFM format, with 3 bytes of colour per point. However plans to provide file export in DXF, STL and VRML are in place.

4.2.1. Capture Units

The original system was based upon two Capture Units, each consisting of an LCD projector mounted above a CCD camera. The capture area of a single Unit is a maximum of 120° in a single capture process, with a deterioration in image quality towards the extremes of the available capture area. The current capture volume has been restricted to a vertical cylinder of 700mm in diameter and 700mm in height, although the system initially had the capability to capture 2000mm in height. This parameter was restricted before the start of the investigation to improve the image quality without costly lens upgrades.

Each Capture Unit provides a separate point cloud/view. These two images may then be 'stitched' together to provide a seamless view semi-automatically, resulting in a complete 180 degree view when a human body is captured.

4.2.2. Specifications:

Capture time 1 second

Process time 10 seconds

Co-ordinate spacing: 1.5mm

Accuracy +/-2mm

24 bit colour

Measuring in units of 0.1mm.

All specifications courtesy of Wicks and Wilson Ltd.

4.2.3. Image Capture Environment

The area behind the object being captured should be covered in light absorbing material as a backdrop, (in this case, black pile fabric). During image capture low level lighting is required to avoid any interference with the structured light projections.

4.2.4. System Configuration

Each Capture Unit is mounted on a tripod. Each should be of equal height and set up in such a way that the Capture Unit is level in both the vertical and horizontal plane. The configuration of the Capture Units should be such that they form a triangle with the object to be captured (see Figure 4.5.). The distance between each Capture Unit and from each Unit to the object being observed is determined during the calibration procedure. Image A refers to the right hand image (from Unit A), whereas image B refers to the left hand image (from Unit B).

The Units are controlled by a Pentium II 300 computer with 128Mb-memory. The Monitor used for the investigation was a 21" (20" viewable) Hitachi CM802ET set at a resolution of 1152 x 864.

Figure 4.5.

The TriForm™ Two-Camera 3D Image Capture System Configuration

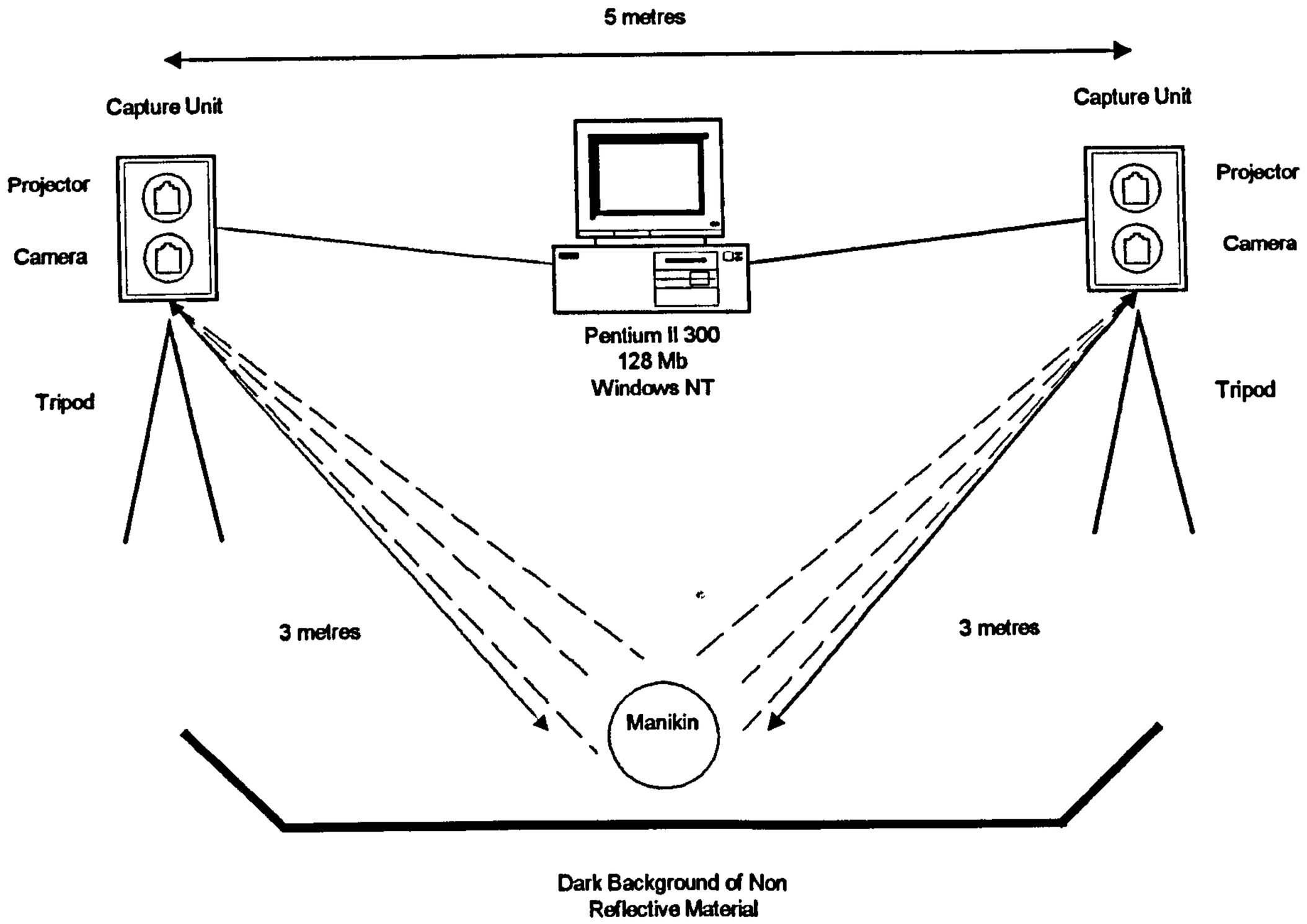

4.2.5. Hardware Calibration

The height and levelness of each Capture Unit must be equalised with the object to be captured which should appear central within the Unit's Field of View. Cross hairs are visible on-screen which indicate whether the object is level and central. The captured object (in this case a computer generated grid mounted on

a white board) was positioned perpendicular to the front of each individual Unit whilst the procedures detailed in the following paragraphs were undertaken to find the optimum calibration for each Unit.

For the purpose of calibration and for setting up each test, the projector & camera may be operated to provide a live view on-screen. In this mode gratings may also be projected onto the object to be captured.

Projector	The focus of the projector may be checked when the gratings are projected onto the target object (see Figure 4.2). This may be viewed on the target object and also as a live image on-screen. Ideally the black lines should be sharp with a slight band of grey edging, with the coarse grating (thick black line) falling on the target object.

Camera	The front ring on the lens controls the focusing, whereas the back ring controls the aperture. The focus should be set to provide a clear, sharp image of the captured object. The aperture should be adjusted to provide the correct level of light saturation, on the captured image. To test the aperture the object must be captured and viewed prior to processing. In this mode the object appears as a green image on a blue background. If the aperture is too great the background will begin to be picked up by the system. Conversely when the aperture is too small parts of the object to be capture will not be fully recognised and begin to break up, for example the darker areas towards the edge of the Field of View. The ideal is to have the object to be captured clearly represented with the least amount of 'speckle' from background interference.

A fine tuning sensitivity control is also available within the software for on-screen adjustment. This however does not alter the physical aperture on the camera, but alters the threshold limit by which information is included or excluded.

4.2.6. Calibration Parameters

The camera angle in the configuration parameters is set once the geometry of the target object to the Capture Units is known. The value reflects the angle at the target object from two projecting Units. The principle is illustrated in Figure 4.6.

Figure 4.6. Angle Determination

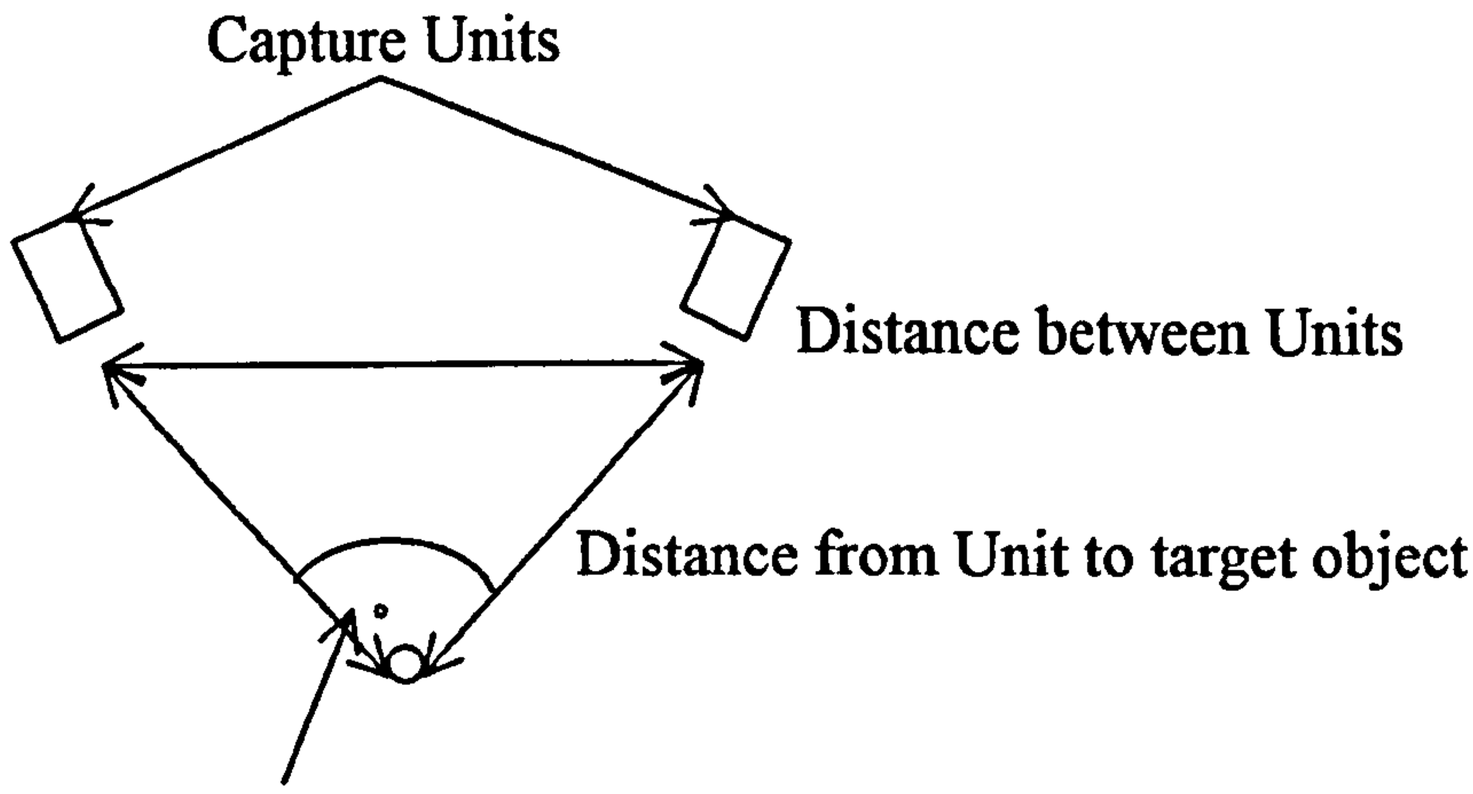

The following parameters may be adjusted to facilitate calibration. Note that these variables are adjusted using the software in contrast to the physical calibration of the hardware, discussed in section 4.2.5.

Fringe Spacing	The Fringe Spacing setting is initially based on a manual measurement by quantifying the difference between fringes on a flat surface. However the variable may also be used to adjust the vertical orientation of the captured object. Changes in Fringe Spacing are noted during the capture process. If the target object is leaning forwards the Fringe Spacing decreases whereas if the target object is leaning backwards the converse will be true. By increasing the Fringe Spacing setting, the target object tilts backwards, whereas decreasing the spacing results in the object tilting forwards. This is achieved by comparison of the actual projected fringes compared to the spacing originally set at calibration.

Field of View	Initially set by measurement, this setting is then primarily used to adjust the x and y values, however as it affects the scaling in the x, y and z-axis. Any adjustment made to the Field of View should be followed by the same percentage adjustment to the Fringe Spacing to reduce the interdependence between parameters. A fine trim to the Fringe Spacing is then required to ensure the target is exactly vertical when viewed on-screen.
Camera to Projector Height	Initially set by measurement, the Camera to Projector Height is then attuned in the software to adjust the z scaling, the physical orientation of the camera to projector being fixed within the Capture Unit. Any adjustments affect the scaling in all three axes, however the impact on z is greatest. An increase in the Camera to Projector Height value will decrease the z scaling and vice versa.
Camera to Projector Depth	To be set by measurement, however it may be used to alter the z scaling in relation to x and y by adjustments in the value within the software. The z scaling may be increased using a negative value for the parameter, although following any change to the Camera to Projector Depth the Fringe Spacing should be adjusted to ensure the target remains vertical. However when altering the Camera to Projector Depth it is not known whether the effect will be linear.

Camera to System Centre	To be set by measurement. It is not imperative that this value is correct, provided the calibration procedure has been undertaken with the same Camera to System Centre value. The System Centre is defined as the centre of the target object.
Capture Frame Delay	This is a hardware variable, designed to alter the speed of pattern change according to the performance of the processor. No change is required for calibration once the initial value has been selected; hence the value remains as a constant.
Resolution	The resolution refers to the way in which the data is stored therefore no adjustment is needed once the initial value is set; hence the value remains as a constant.
Distortion Correction K1	The K1 value is initially set to zero, prior to calibration of the system. During calibration the value is used to correct any vertical convex or concave distortion in the image. This is achieved by checking for any distortion in the image, in the case of a 2D grid this may be identified by checking the profile view of the captured grid on-screen. Ideally the image should show a perfectly vertical line, however distortion may result in a deviation from this vertical line. By increasing the positive value of K1 the image may be made more convex, whereas a negative value will make the image more concave. Therefore by altering the setting the

distortion may be minimised by a process of trial and error until the visual representation is nearest to a perfect vertical line.

Distortion Correction K2

As described for Distortion Correction K1, the K2 value is set to zero prior to the calibration of the system. During calibration the value is used to correct any 'S' shaped distortion in the image, which remains after K1 is optimised. The process for determining the value is much the same as for K1. By a process of trial and error the value is altered until the visual representation of the target object is at its optimum.

4.2.7. System Software

The software consists of four individual modules:

Capture

The capture module facilitates the set-up, calibration and operation of the 3D Capture Units.

Viewer

A 3D viewer package enables the image to be rotated through 360° in all directions to enable viewing from various angles.

Editor

The editor mode enables the manipulation of an image or multiple images. Multiple images may be stitched together into one seamless image and sections of the image may be removed or merged. This module also facilitates the saving of stitched images & also individual views from each Capture Unit.

Analysis — The analysis mode enables the analysis of the 3D surface by providing various measurement facilities and profiling tools.

The process by which images are captured and subsequently analysed is detailed in Figure 4.7. To illustrate this process further screen captures have been included (Figures 4.8 – 4.16) to provide a visual reference for each stage of the capture process these should be consulted with reference to Figure 4.7.

Figure 4.7. Image Capture and Interrogation Procedure

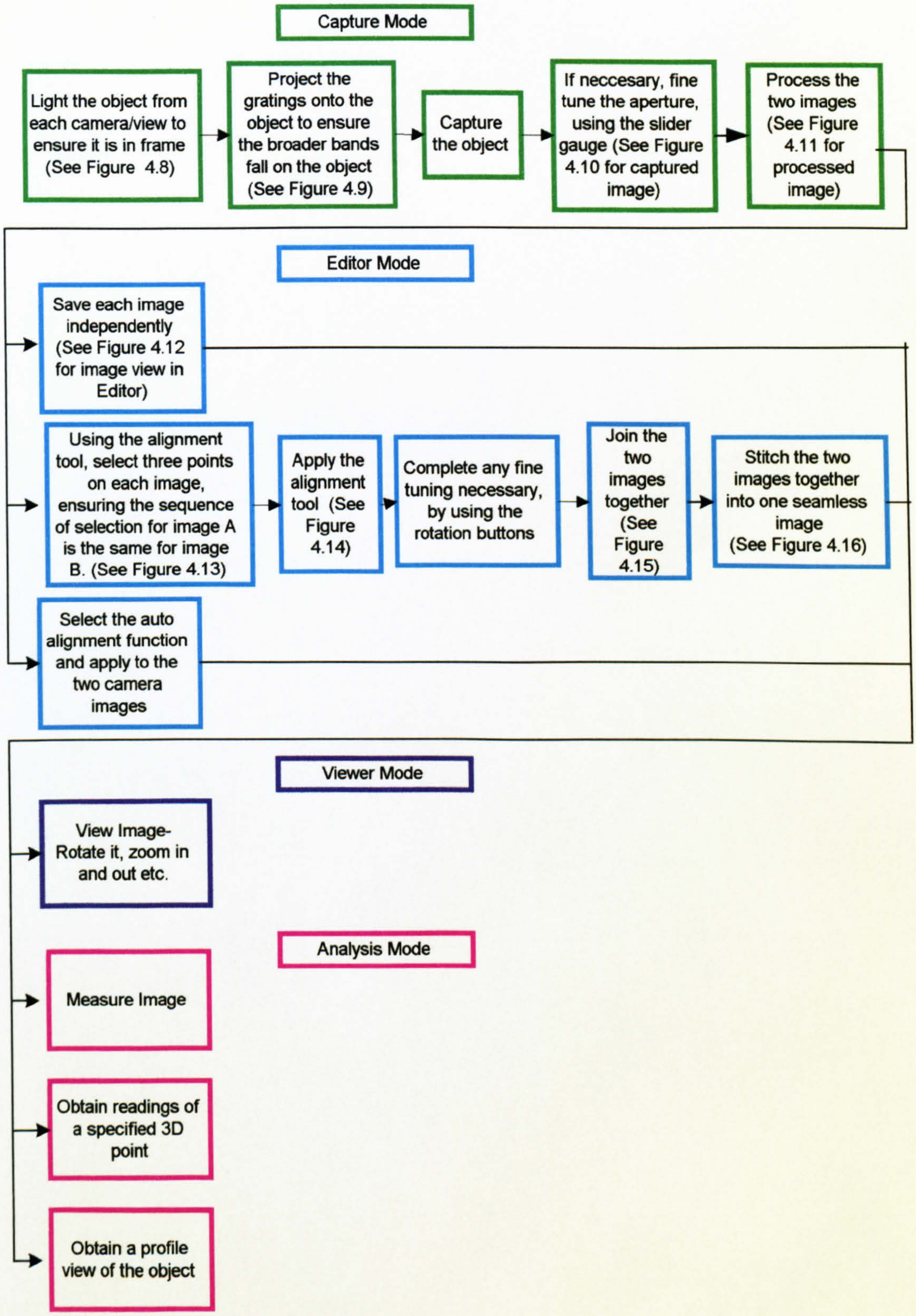

Figure 4.8. Live Image of the Target Object

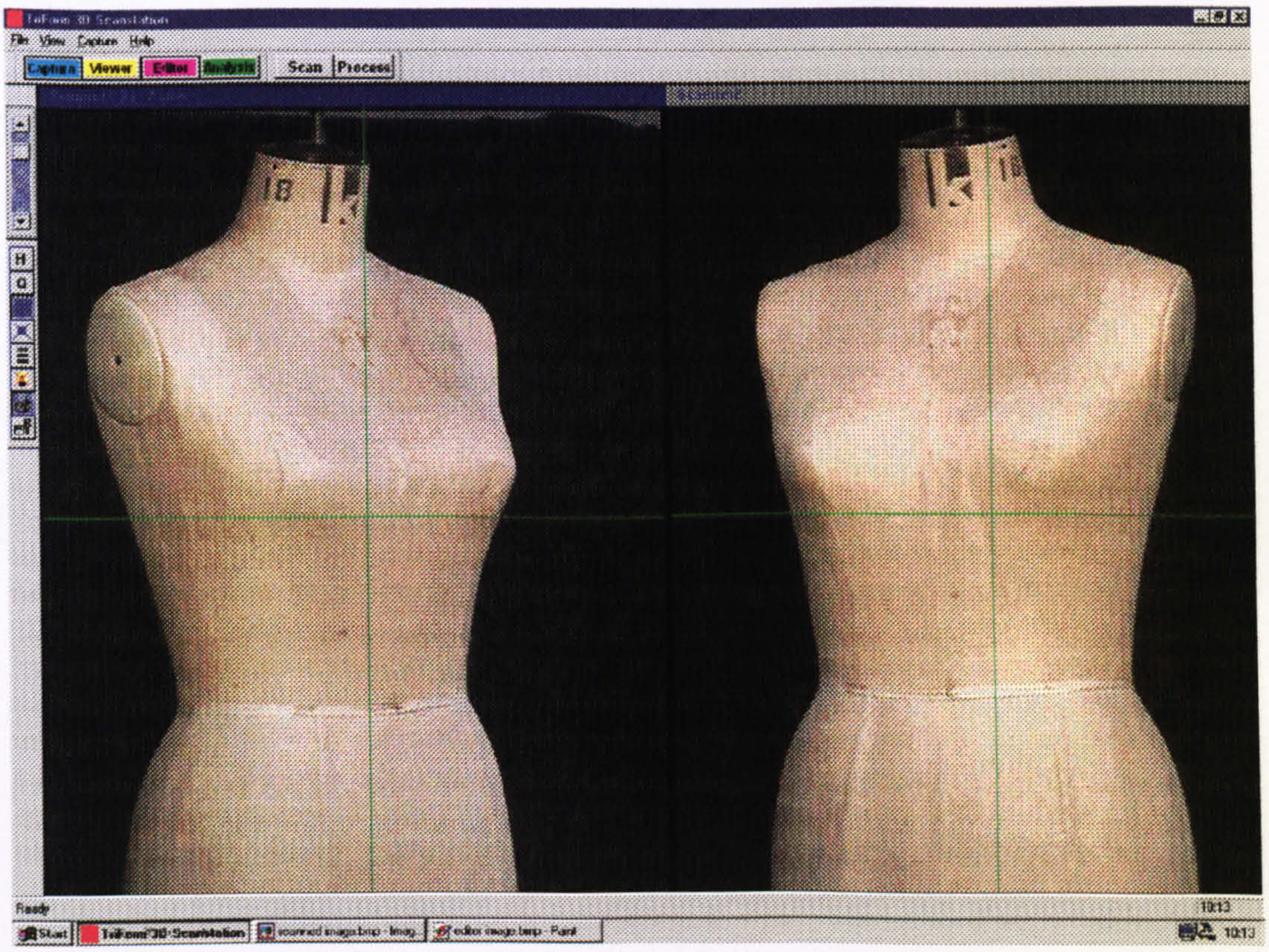

Figure 4.9. Reference Gratings Pattern Projection onto Target Object

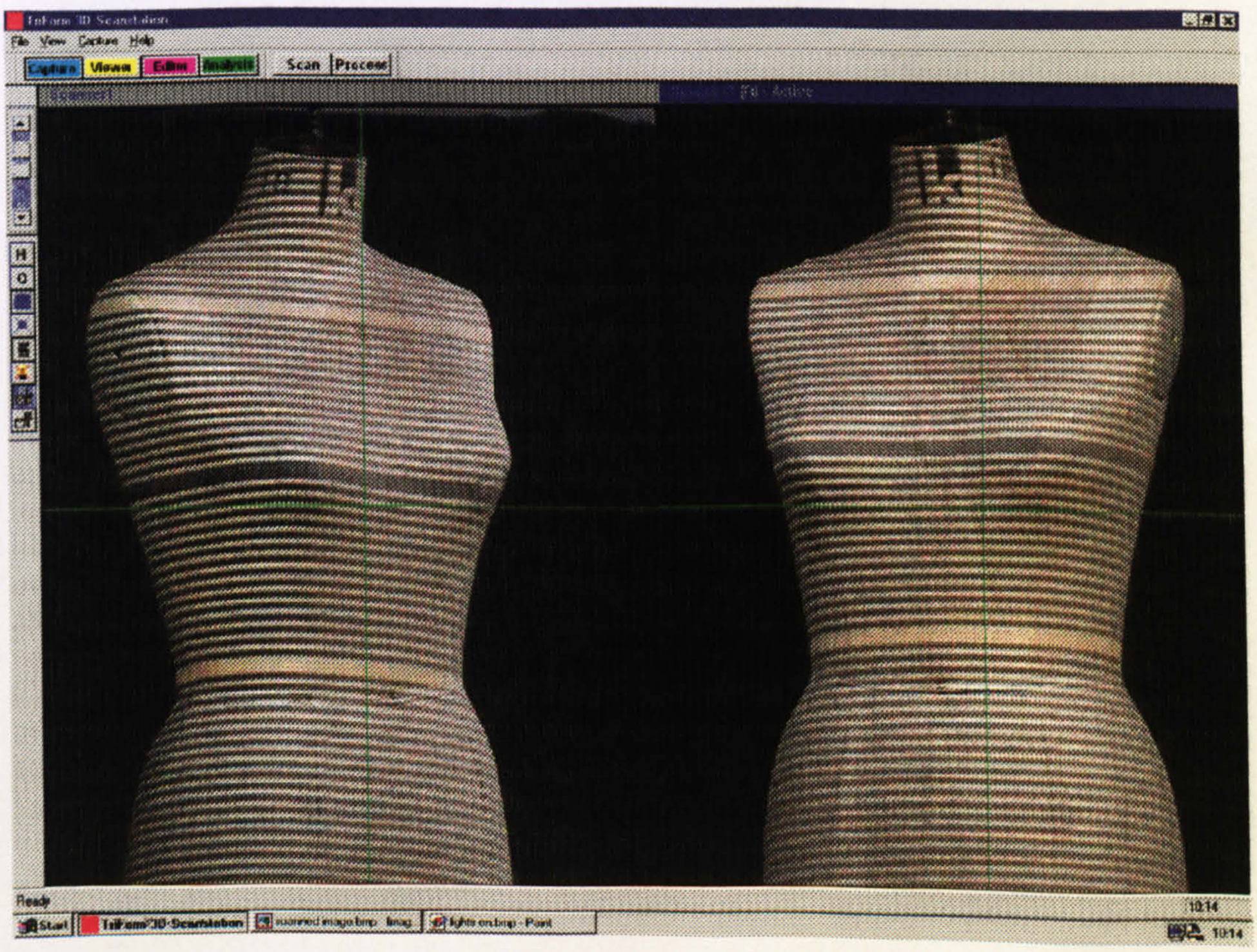

Figure 4.10. Captured Image Based on Raw 3D Data

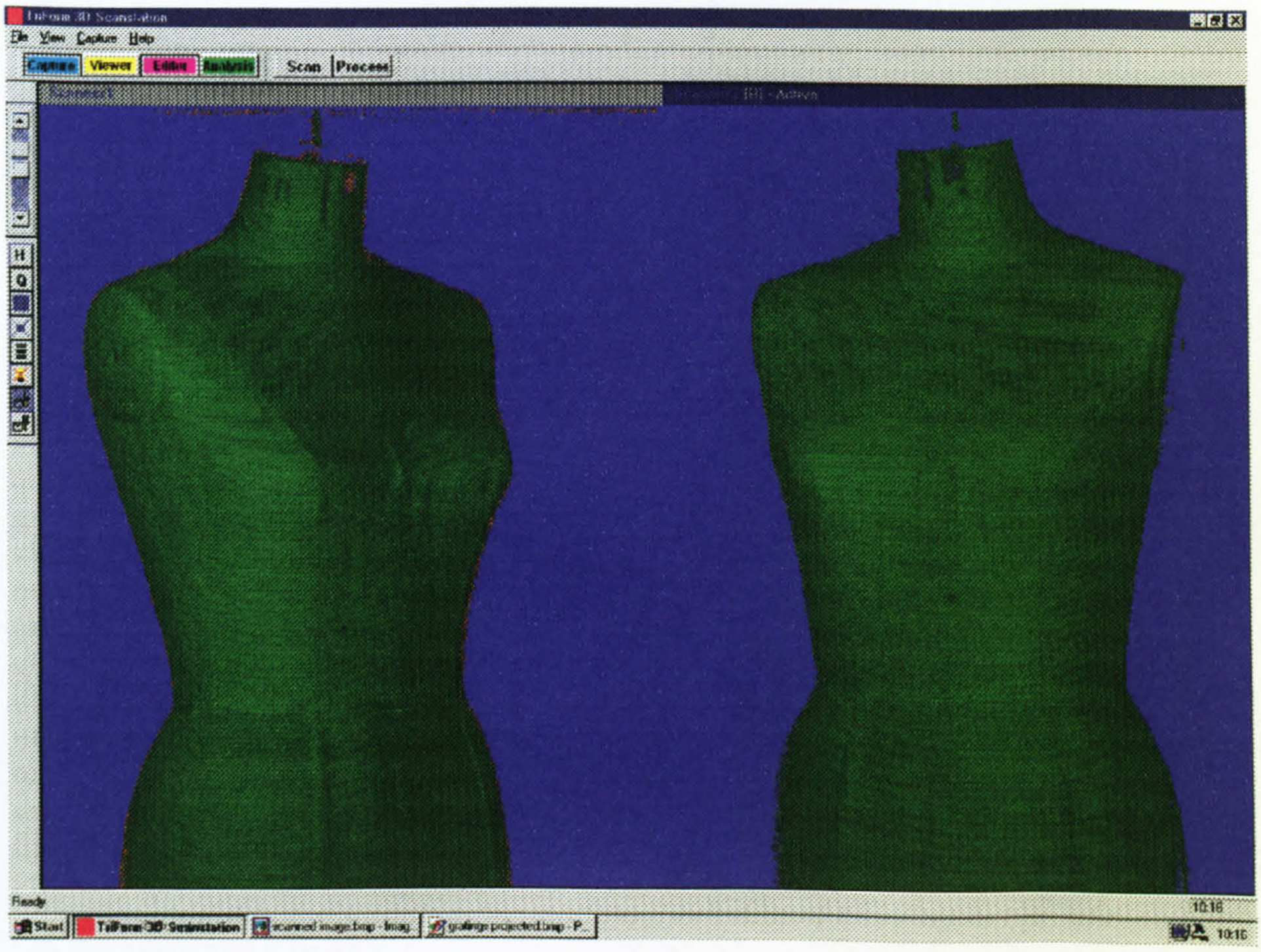

Figure 4.11. Processed Image

Figure 4.12. Captured Object as Seen When Using the Editor Mode of the Software

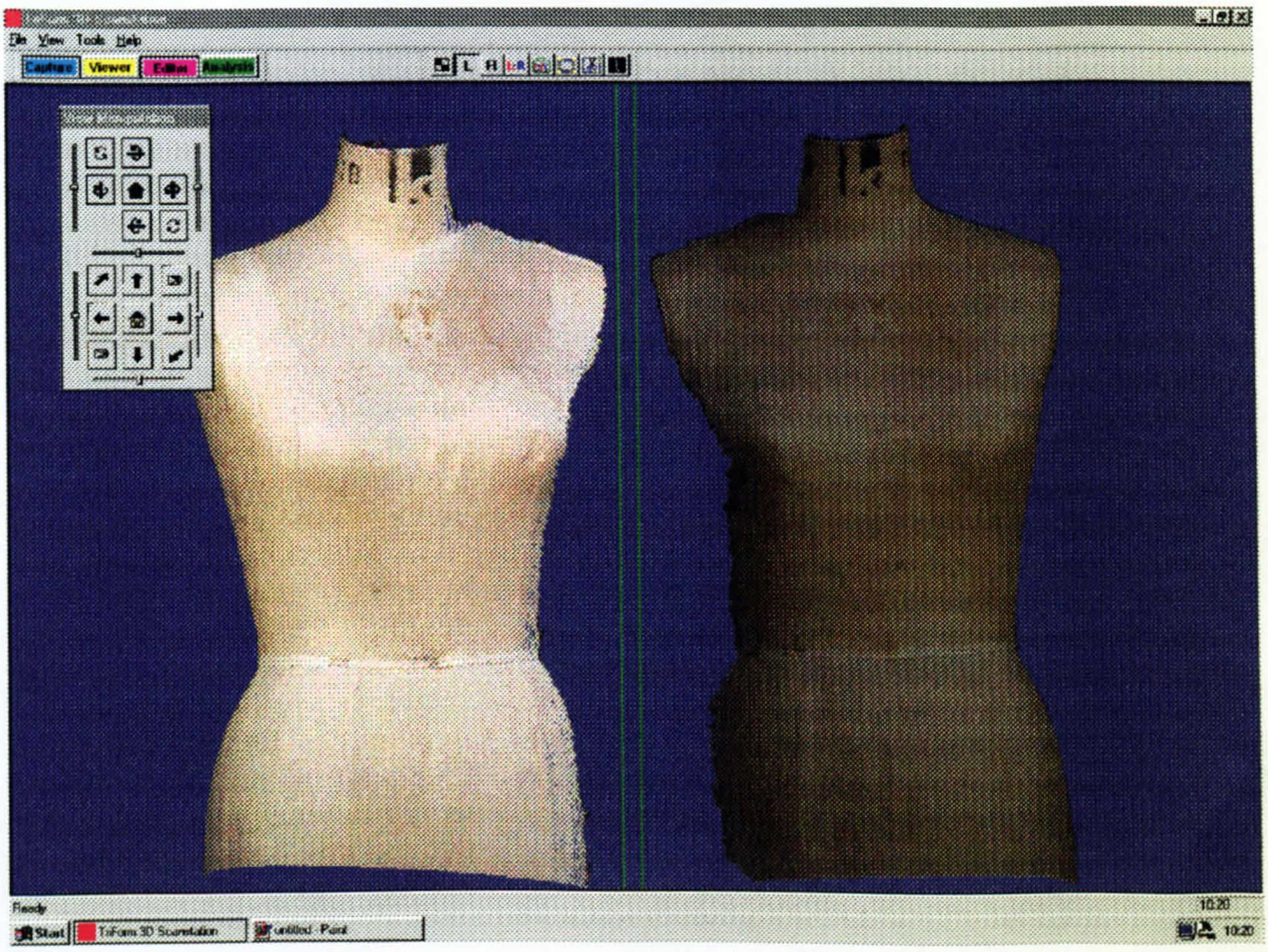

Figure 4.13. Selection of Alignment Points

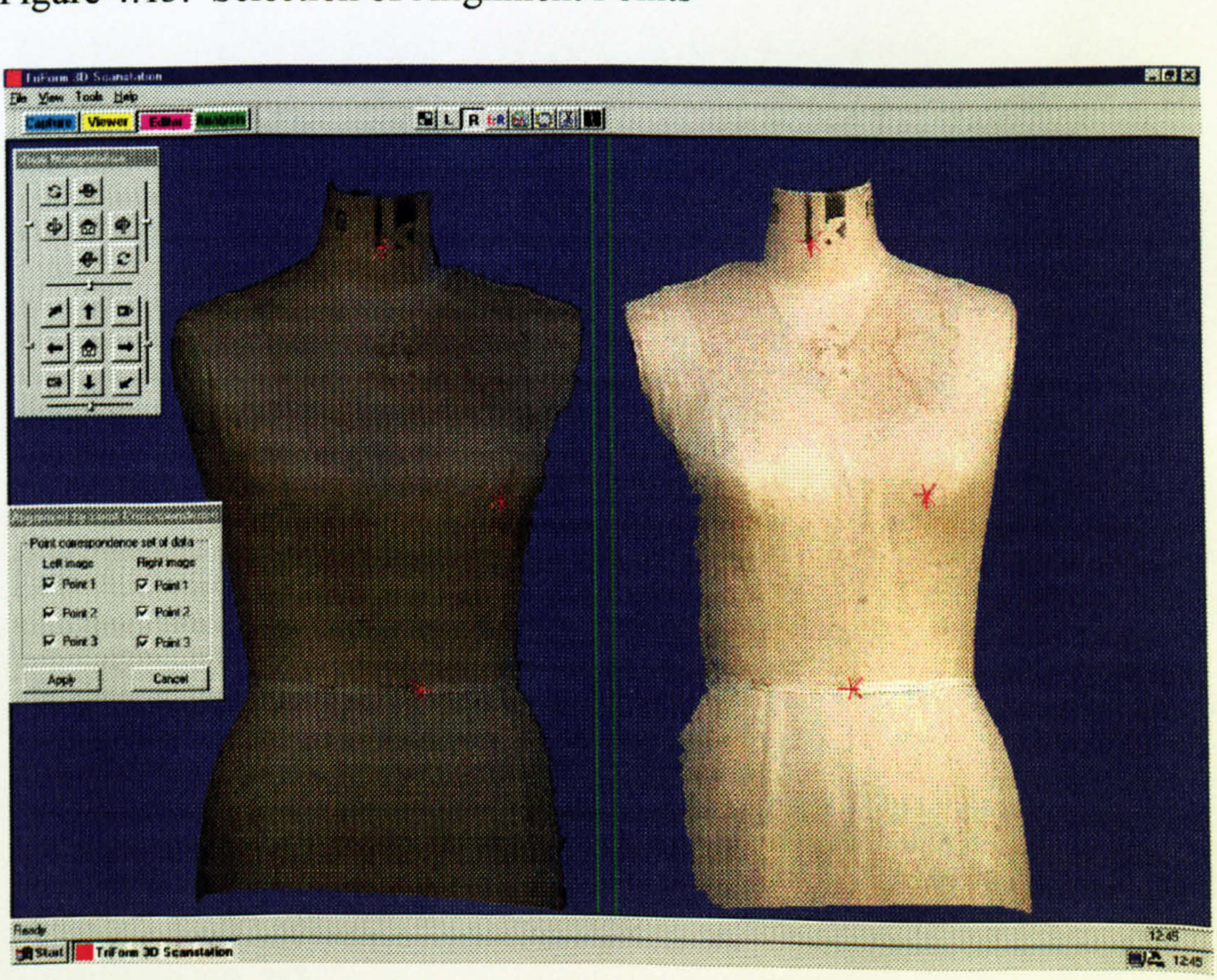

Figure 4.14. The Aligned Image Produced by the Matching of the Selected Alignment Points

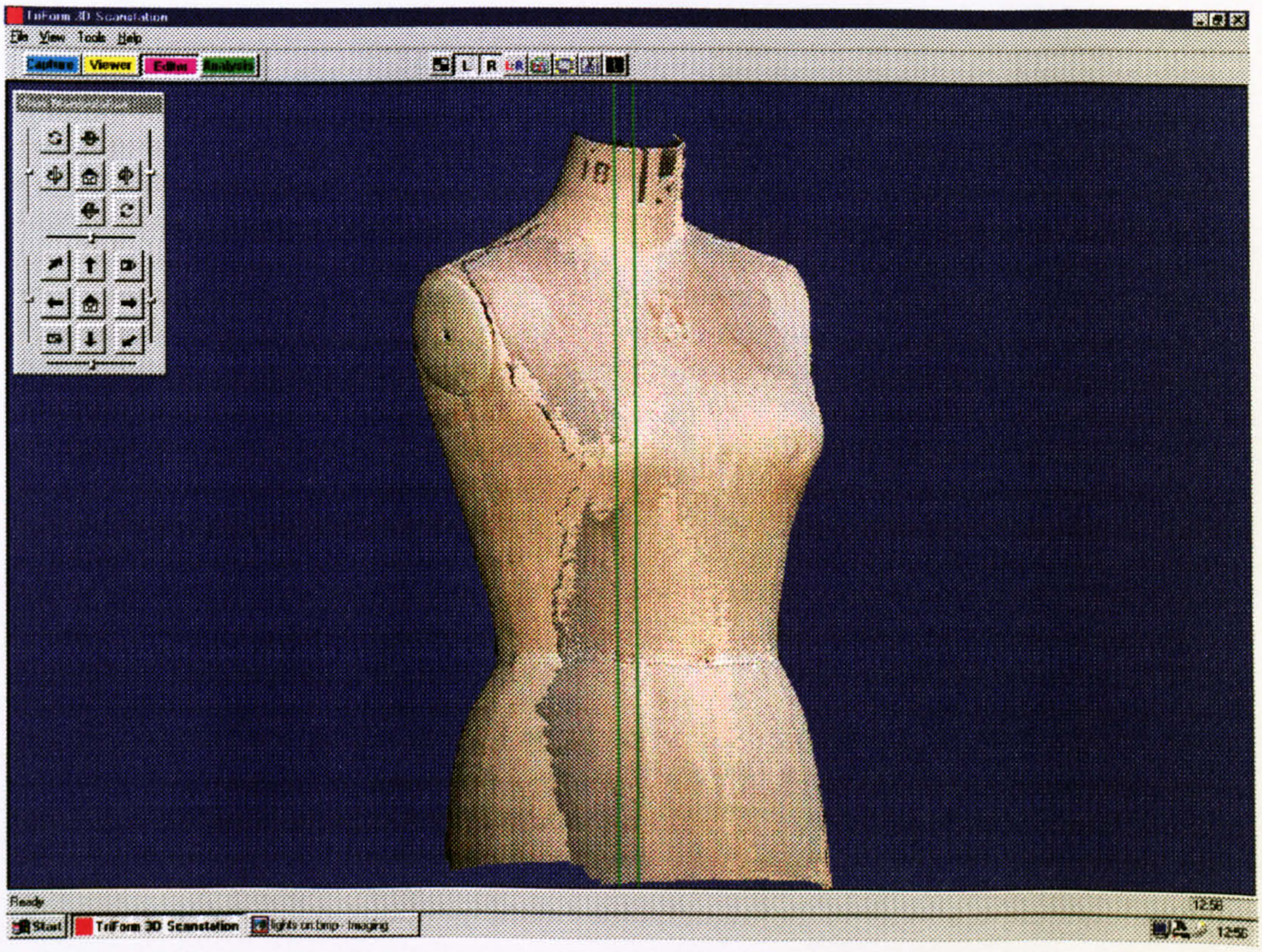

Figure 4.15. Joined Image (Removal of Any Overlap of the Point Clouds)

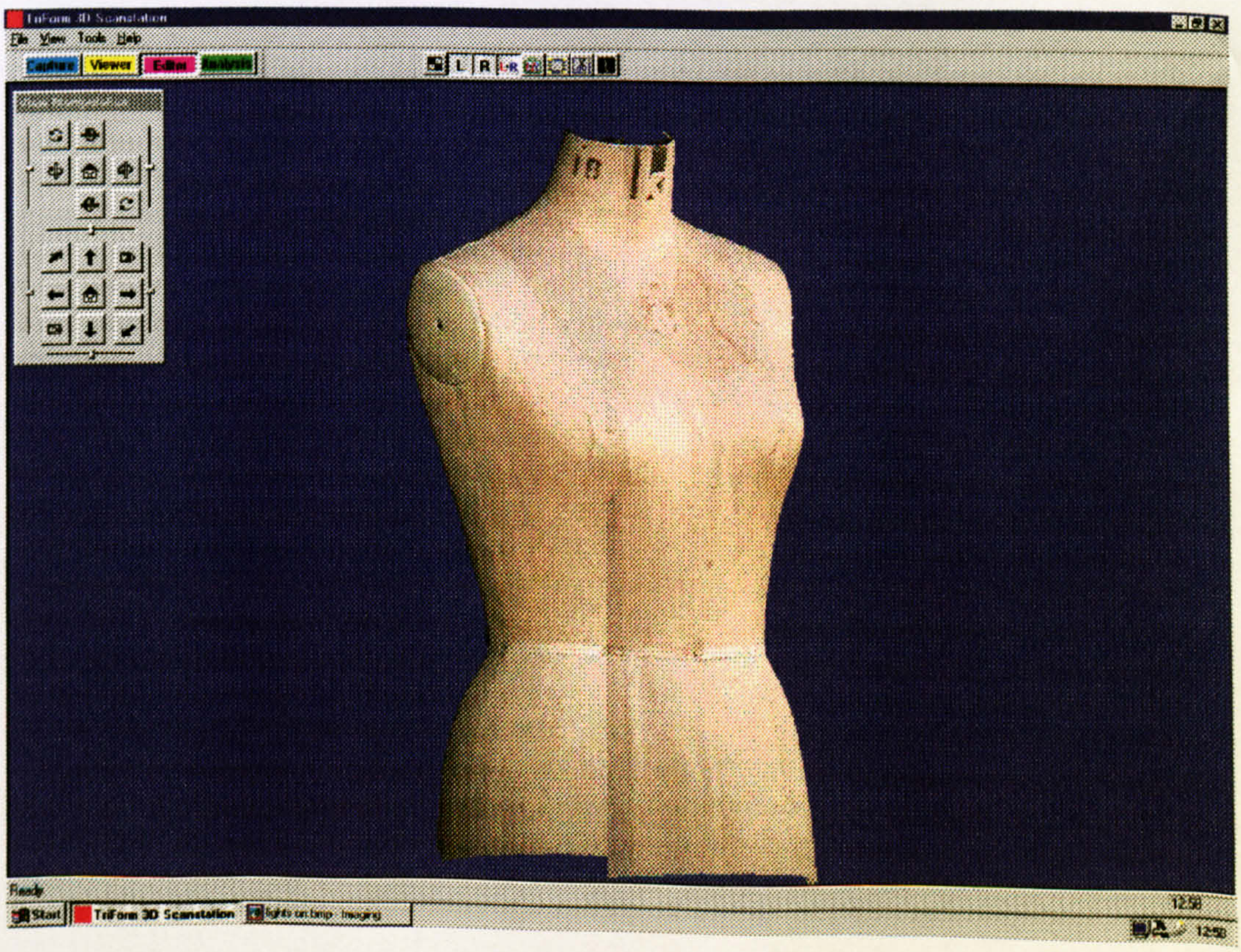

Figure 4.16. Stitched Image

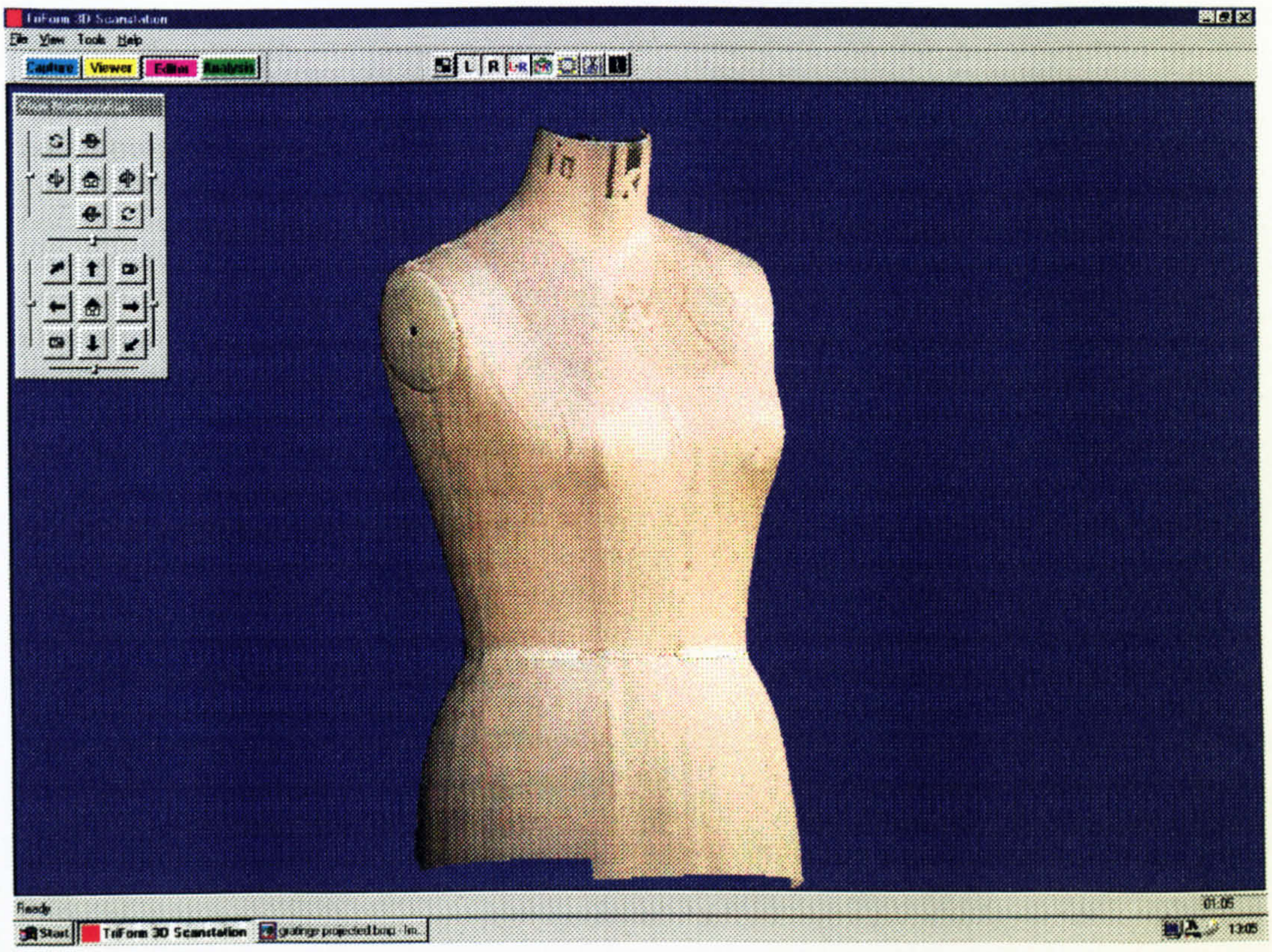

4.2.8. Three Point Alignment

Two separate camera images (or point clouds) may be stitched together (as long as sufficient overlap exists) to form a single unified image. The first stage is the selection of three stitching points, which must be selected at identical spots on each of the point clouds (or images). Three points are used, as it is essentially a three-stage process, enabling the two images to be orientated in three dimensions. Figure 4.17 illustrates the alignment process.

Figure 4.17. Point Cloud Alignment: Stage 1 (Wicks & Wilson Ltd. 1999)

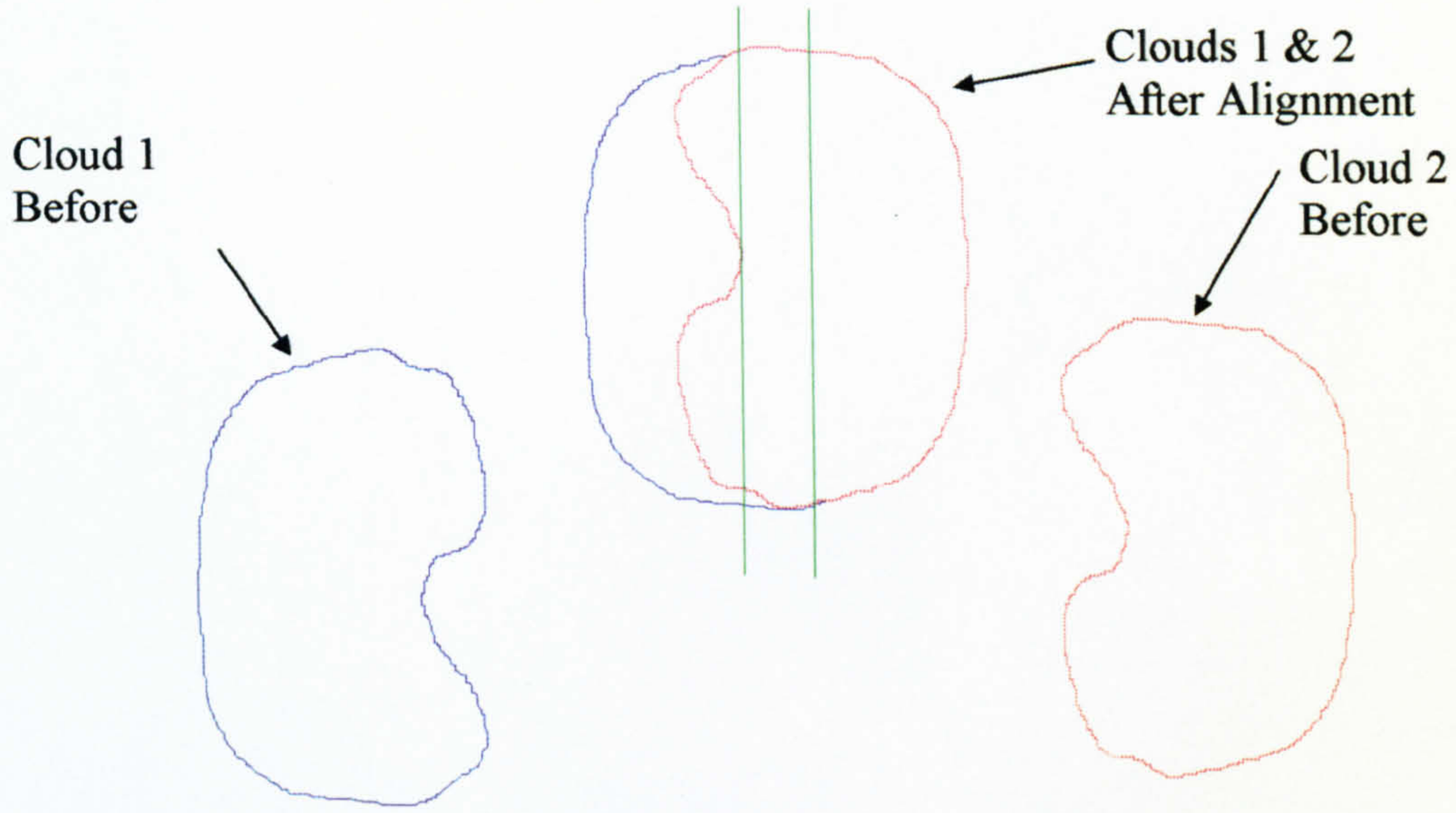

The first stitching point is the most important. It aligns the two point clouds in the x, y and z dimensions, therefore it is of paramount importance that the selection of this point in both point clouds is identical. Any error in the selection of this first point will impact on the whole alignment process as the remaining alignment points are all referenced from this point.

At the first point the two point clouds are pinned together at that point only and can pivot around this point in the x, y and z axes.

Figure 4.18. Point Cloud Alignment: Stage 2 (Wicks & Wilson Ltd. 1999)

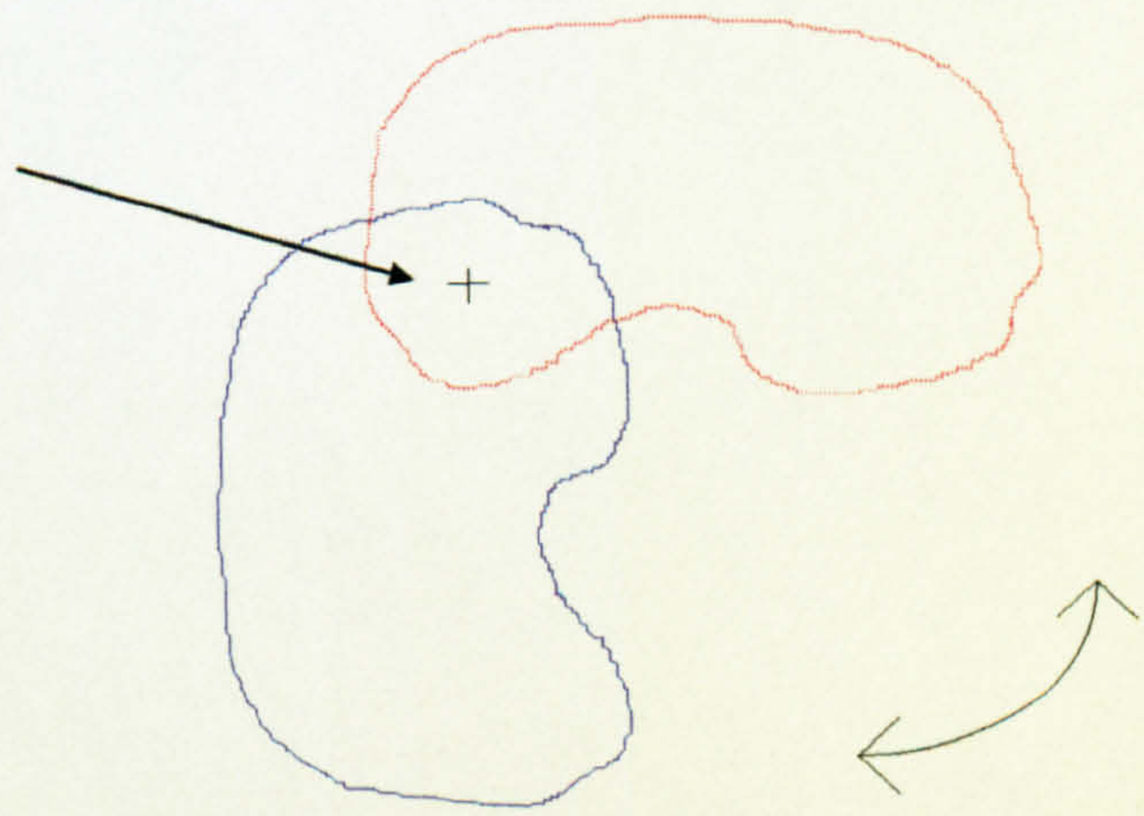

The second point is the next most important in aligning the two point clouds. This should be selected as far away from point 1 as possible, but in line with it. As the two points lie within the same plane this forms an axis on which the two point clouds can rotate (not unlike a hinge).

Figure 4.19. Point Cloud Alignment: Stage 3 (Wicks & Wilson Ltd. 1999)

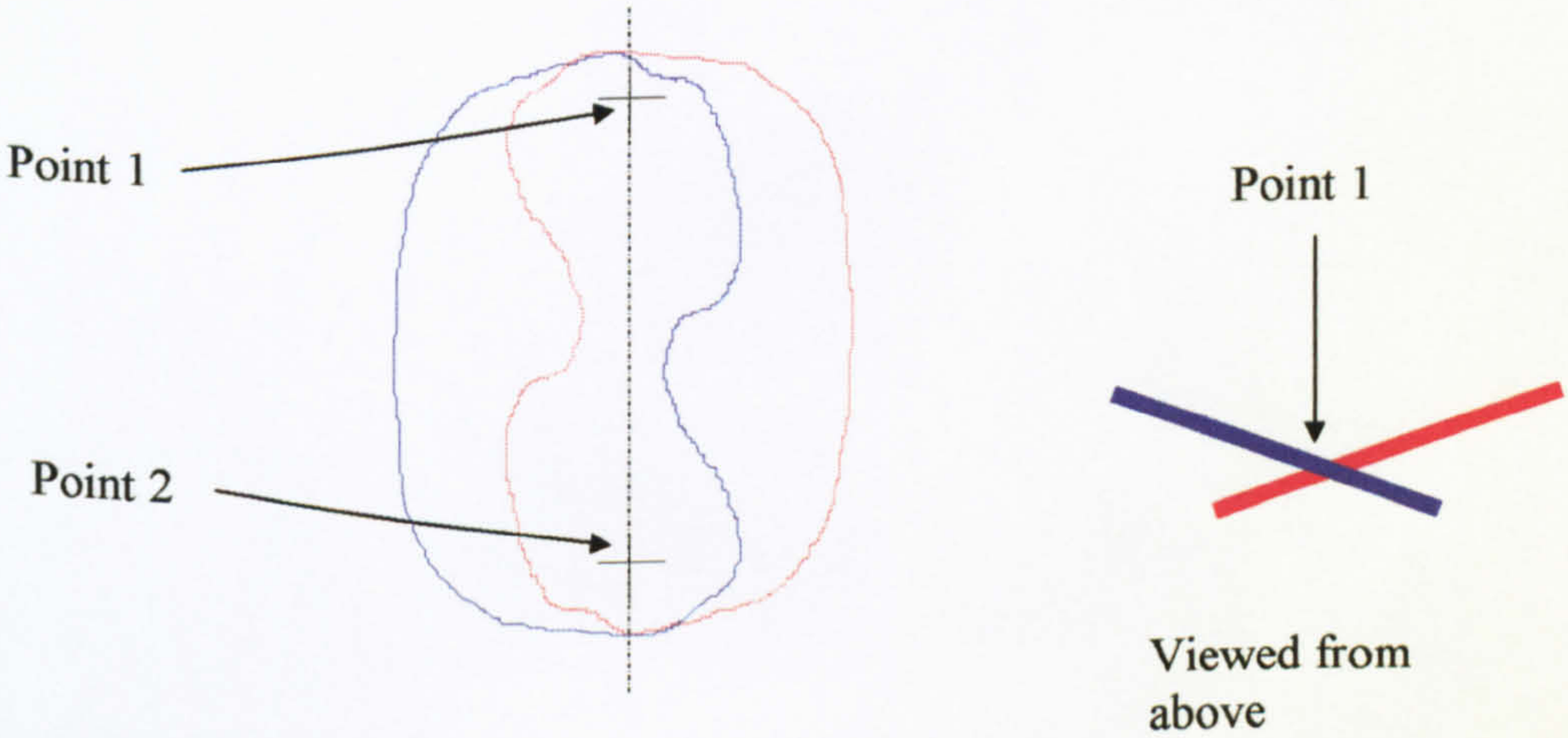

The third point forms the final step of the alignment. It should be placed at a right angle to the axis formed by points one and two, as far away as possible

Figure 4.20. Point Cloud Alignment: Viewed from Above (Wicks & Wilson Ltd. 1999)

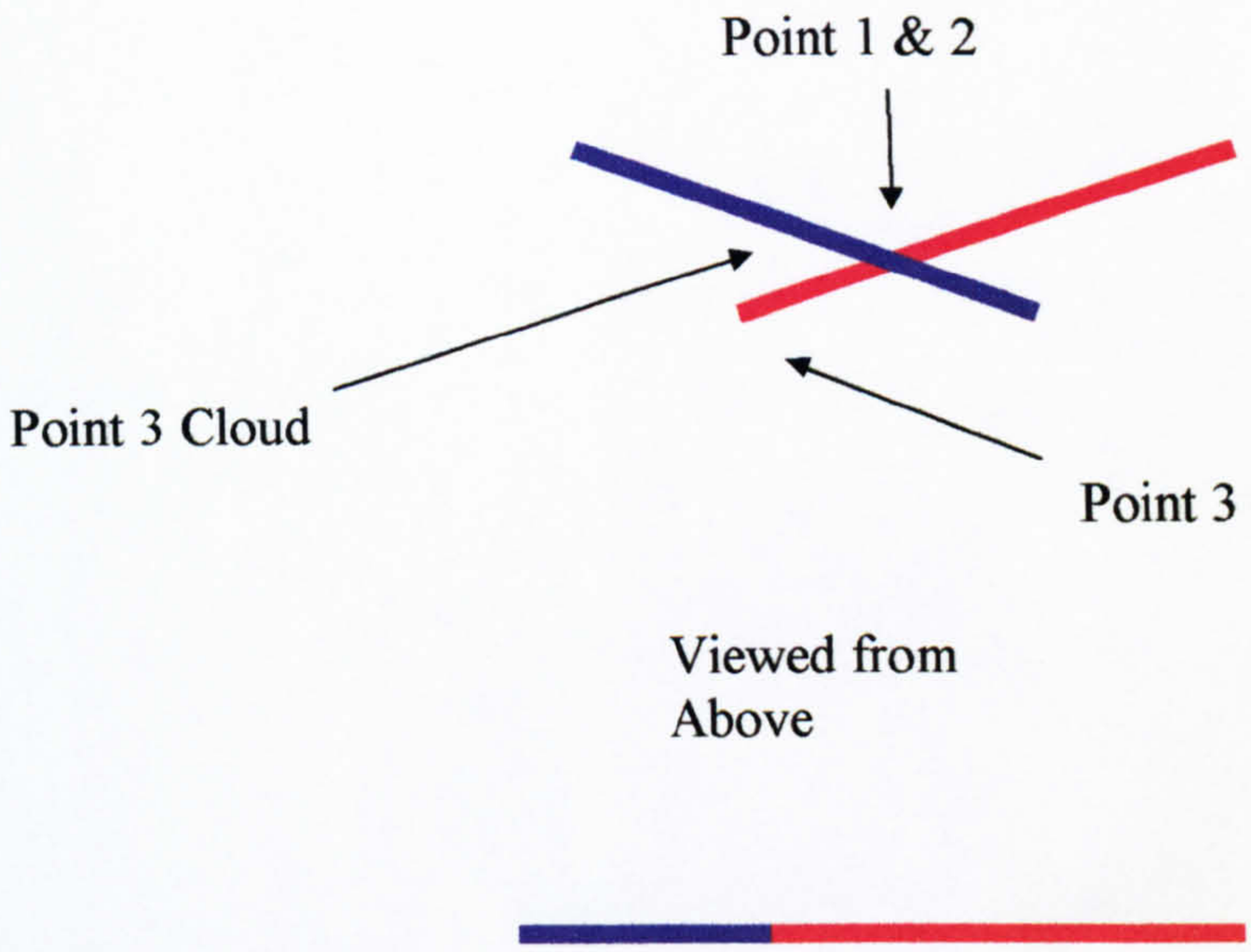

Any errors in the selecting the correct location of points for stitching on each cloud may result in the stitching points not being precisely coincident with each other. This may also occur where scaling errors are present. However the lines joining Point 1 and Point 2 will always be coincident, as shown in Figure 4.20 above. After the alignment of point 3 all of the points will always lie in one plane, regardless of whether all the points are coincident.

The order of selection of each of the stitching points must remain the same for each image so the two images are stitched in the correct order relative to each other. Once the points are selected the point clouds may be aligned by selecting the 'Align' button from the three point alignment tool. The align process then takes place which requires no further operator intervention.

4.2.9. Analysis Features

Figure 4.21 illustrates the on-screen analysis tools.

Figure 4.21. On-screen Analysis Tools

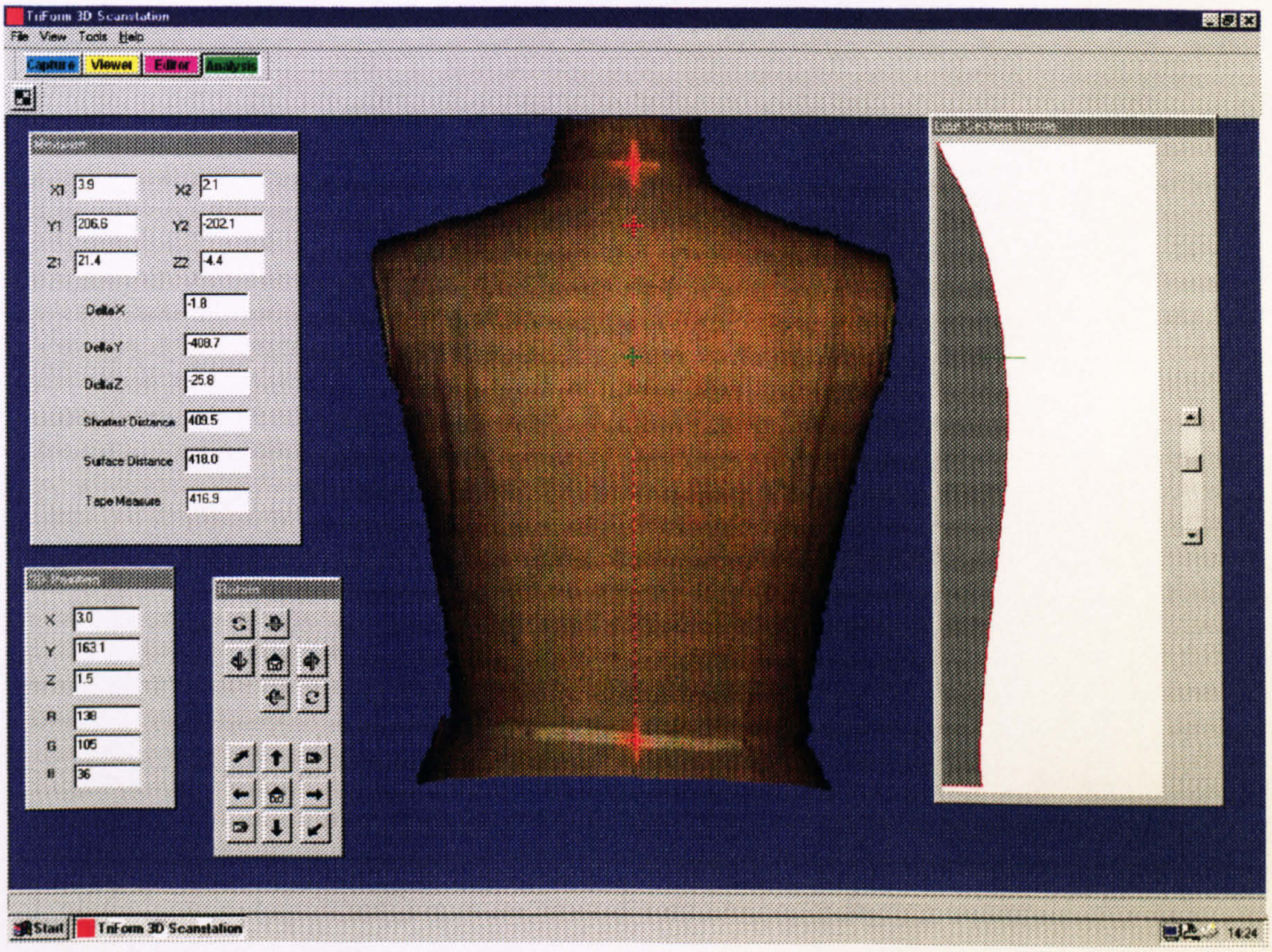

The rotation tools enable the movement of the image on-screen. The image may be rotated through 360 degrees through either the horizontal or vertical plane. The image may also be moved to the left or right or up and down. It is also possible to zoom in and out of the image (this tool is also available in the Viewer and Editor modes).

For any given point, selected by the mouse, the reference point tool provides the details of the x, y, and z co-ordinates and the RGB values for that particular point.

The profiling tool enables the viewing of the profile of an image on-screen. By taking a straight line across the image at any point the profile for that particular area may be viewed.

The measurement tools may be used to measure between any two points on the image, to a reported precision of 0.1mm. This provides the shortest, surface and tape measure distances and also gives the co-ordinates of that point in space. The shortest distance measure is the shortest distance between the selected points regardless of surface features, whereas the surface distance gives the measurement between the two points following the contour of the surface of the image. The tape measure distance is designed to replicate the use of a tailor's tape measure on the body, in the sense that it follows the protruding contours of the image, but not the receding contours. The path taken by all three measurements is illustrated in Figure 4.22.

Figure 4.22. Measurement Routes

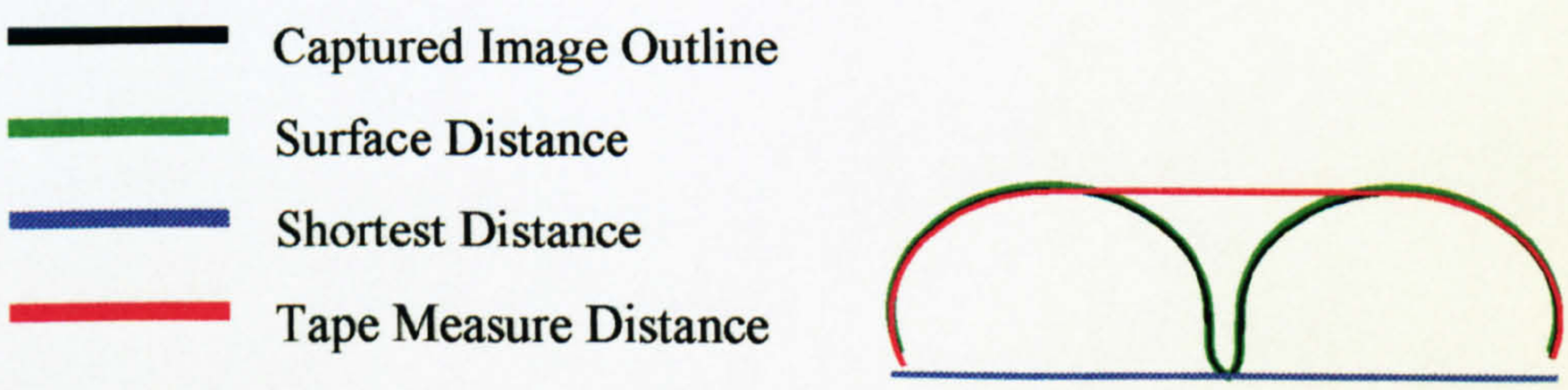

When measurements are taken the x, y, z delta values are also displayed for the two points from which the measurement is taken, these values may be positive or negative dependent on their orientation on each axis, the principle is illustrated in Figure 4.23.

Figure 4.23. Axis Orientation

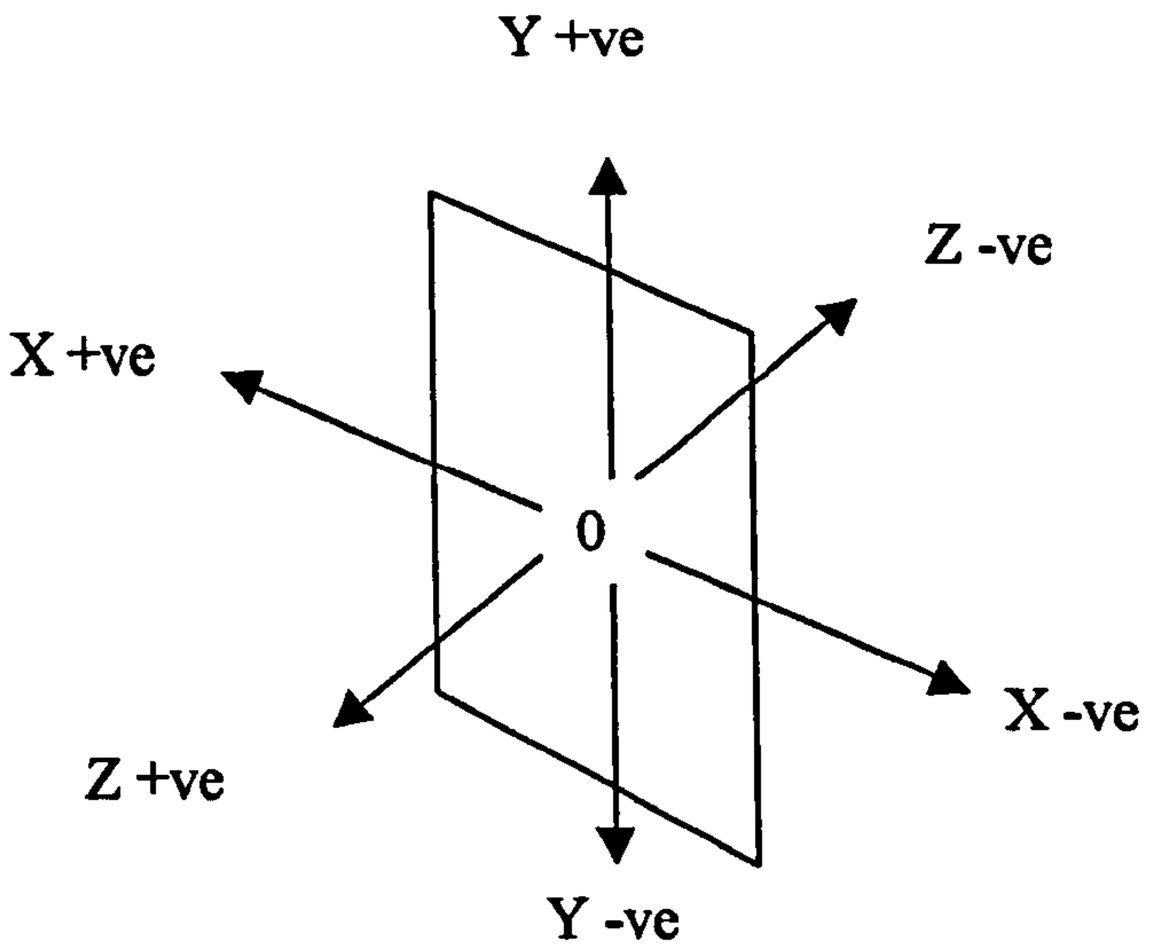

Note that the operator selects the points used as the boundaries for the measurement by placing markers, generated by the software, by use of a mouse. The measurement process on-screen is therefore a manual action that is subject to variability.

4.3. Error Determination

Any measurement taken with the TriForm™ system is subject to a certain degree of error. The point cloud produced by the system and the overall colour data matching is subject to errors, as is the actual closeness by which a point may be selected and a distance measured. Any measurement is based upon the operator's skill at selecting the correct points to measure between and to the extent by which that process may be accurately repeated. The accuracy specification for the TriForm™ system is stated as ±1.5mm in the x axis and ±2.0mm in the y and z axis. After discussions with the systems manufacturer the specification was found to be based upon the likely error which would be generated from a point pitch of 2.0mm and 3.0mm respectively for the x, y and z axis. The point pitch refers to the spacing of the points within the point cloud

and hence the operator may select a location that does not fall on a point within the cloud. As the software is designed to select the nearest point an associated error will be included within the measurement, the likely error therefore has been estimated by the manufacturers as ±1.5mm in the x axis and ±2.0mm in the y and z axis.

One additional source of error cited previously was the potential for a slight error in the z dimension. This is thought (by the manufacturers) to be extremely small and would primarily affect the surface and tape measure distances whose measurements follow the surface to some degree. An error in the z dimension would cause the displacement of points, which may result in the surface or tape measure distance taking a slightly longer route. However, it is thought that it may also influence the shortest distance measurement although its contribution would be small. Presuming the error caused a deviation that was random in nature it would be likely that over a reasonable distance this error would cancel itself out and therefore not affect measured readings. It is the very short distances therefore which would be most susceptible to its influence.

The manufacturers have also raised a potential colour data matching error, which primarily relates to the visual image on-screen as opposed to the determination of the physical point cloud. Colour data is collected during the image capture process by the cameras and is mapped onto the physical point cloud to provide a realistic surface to the image. However there is a possibility of slight mis-matching between the two and hence a marker locating a certain feature on a subject's body may be fractionally misplaced. Whilst this would not affect the spacing of the points it would affect the operator's selection of points used for measurement.

In the current investigation the points selected for measurement are based upon cross-sections of lines within a grid. If the colour matching was not correct it is

highly likely that the points selected would not reflect the area which was selected for measurement after reference to the target object. The impact of this error should in theory be minimal, as the colour matching error is likely to be linear. The actual measured distance therefore should remain the same and should also be situated in very close proximity to the desired points. An examination of the colour matching error was not included within the evaluation procedure as the facility to view images without the colour data was not available at the time of the investigation.

One would also think that the resolution of the monitor and mouse would to some extent dictate the ability to view and select points on-screen for measurement. However, provided the resolution is such that the captured object may be clearly represented on-screen, its impact, in terms of its contribution to errors, is thought to be minimal. This is because the captured image on-screen is based upon 3D data which is a series of unconnected points in space. Therefore provided the points required for measurement may be accurately selected the resolution by which it is viewed and by which points are selected, is of limited importance.

As the measurements taken on the TriForm™ system are still essentially manual measurements the influence of the operator must also be taken into account when determining the accuracy by which an individual measurement may be taken. Within the operator error the size of the marker used on the object to denote the location for the measurement would be taken into account, as it affects the repeatability of the selecting the same area for measurement. In the manikin test the markers were approximately 3mm wide, hence at any measuring point the error could be as much as ±1.5mm. However, later in the tests based on the 2D grid the marker size was reduced to 1.5mm and hence the associated error was ±0.75mm. The impact of the operator's influence on error is discussed further in Chapter 5.

4.4. Manikin Test

The initial focus of the investigation was to ascertain the performance of the system in terms of its capability to accurately capture the shape and dimensions of the human body, with a view to using the system to characterise the torso area for ladies with Scoliosis, as discussed in section 1.2. To evaluate the performance of the system a test was devised based on measuring areas of the torso of a female manikin to ascertain how closely the measurements generated by the image capture system compared to those taken by anthropometric measurement. The summarised methodology and results are detailed below, with a full detailed account of the methodology and results available in Appendix A.

The test was based on measuring a standard size 18 female tailor's manikin, (without arms). A total of 27 measurements were taken which covered several planes, utilising the different types of measurement offered by the TriForm™ system. Both the capture system and anthropometric measurement readings were recorded for each dimension for comparative purposes. The tests were undertaken by two observers each taking the 27 measurements. This measurement process was then repeated by each observer, both with the TriForm™ system and by anthropometric means to provide information on intra- and inter-observer variability.

The anthropometric measurements were taken using a Harpenden Anthropometer (Holtain Ltd, Dyfed), and a Rabone Chesterman Miniflex steel anatomical tape (Cranlea & Company, Birmingham). All dimensions were measured except one tape measure and five surface distances, due to impracticalities in taking accurate measurements. The TriForm™ measurements were taken from the following images, four images (front, right side, back and left side views) were captured using a single Capture Unit system, and two images (front and back view) were

captured on a two-camera system. This was to allow both single image and stitched image measurements to be taken.

The results were evaluated by determining the mean, standard error of the mean, mean difference and inter and intra-observer variability. Table 4.1 details the range of difference between the TriForm™ and anthropometric measurements.

Table 4.1. Range of Difference Between TriForm™ and Anthropometry

		Total Number of Measurements (*n*)	Range of Difference (mm) (Triform™ - Anthropometry)	% Range of Difference
Single Camera System	Shortest Distance	*n*=108	-17.70 – 49.70	-9.39 – 31.86
	Surface Distance	*n*= 88	-27.43 – 36.65	-6.22 – 27.00
	Tape Measure Distance	*n*=104	-46.58 – 3.07	-11.63 – 1.44
Two-Camera System	Shortest Distance	*n*=108	-27.50 – 47.28	-10.54 – 30.30
	Surface Distance	*n*= 88	-33.03 – 4.95	-11.58 – 3.65
	Tape Measure Distance	*n*=104	-49.45 – -2.90	-1.64 – -11.74

n = individual measurements measured four times.

The range of difference between TriForm™ and anthropometric measurements remains high for across all measurement types and techniques, with differences as high as 49.70mm and 47.28mm for the single and two-camera systems respectively. Whilst this may be the case for specific measurements, the majority of differences for each measurement are under 10mm for the single camera

system, however, for the two-camera system less than half the measurements were under 10mm difference.

The variability between observers and successive measurements is generally below 10mm for TriForm™ and anthropometric measurements, the exceptions being the irregular surface measure results which were prevalent using the TriForm™ system and certain specific measurements, which are more difficult to take on-screen. The TriForm™ shortest distance measurements however, have proved to be more repeatable than the anthropometric shortest distance measurements.

The majority of measurements (both locations and types) display an increase in difference between the anthropometric and TriForm™ results when changing from a single to a two-camera system. However, the overall range of difference remains similar regardless of the system. One potential reason is the introduction of additional errors following the stitching process, which may have affected individual measurements.

The system (at that time a prototype) proved to be unsatisfactory in its current form, due to issues of inaccuracy. Whilst the manikin test highlighted some of the issues applicable to automated measurement, it became clear that a more simplistic surface was required for further evaluation to determine the nature and sources of error to enable further development work to be undertaken.

The human body comprises of a series of complex concave and convex surfaces, which makes the identification of any source of error and the magnification associated with it unfeasible. The individual areas of the body that are constant in curvature are so small it is difficult to identify whether errors are the result of surface curvature, or a product of the operator or the image capture system. Some areas may be subject to errors more than others, for example, concave

areas where the lighting of the object may be below optimum. The lack of surface continuity also makes the assessment of any image distortion near impossible, as the surface does not provide a critical enough base upon which to examine such issues. The manikin test therefore highlighted the limitations of undertaking performance evaluations of image capture systems on body forms. The surface is too complex to enable the errors involved to be independently quantified, hence evaluations based on similar methodologies, undertaken by other researchers such as Brooke-Wavell et al. (1994) can also be regarded as having limited diagnostic sensitivity.

4.5. Image Capture System Evaluation: Methodology Justification

To attempt to identify any possible reasons for the problems noted during the manikin test a more simplistic surface was used. Namely a two-dimensional board marked with a grid of predetermined dimensions. The theory being the lack of curvature may assist in clearer identification and quantification of errors. Full details of the test procedure and results may be found in Appendix B.

A large white flat board was marked with a grid of square cells. The grid was produced by computer with each cell measuring 20mm x 20mm. The lines were drawn in red on a white background so as to be clearly visible on-screen after image capture, a line thickness of 1.5mm was chosen for ease of viewing on-screen. The grid was situated so as to form a triangle with the two Capture Units, as shown in Figure 4.24. Its position was assured by measuring the exact distances between the Units and the target object.

Figure 4.24. System Configuration

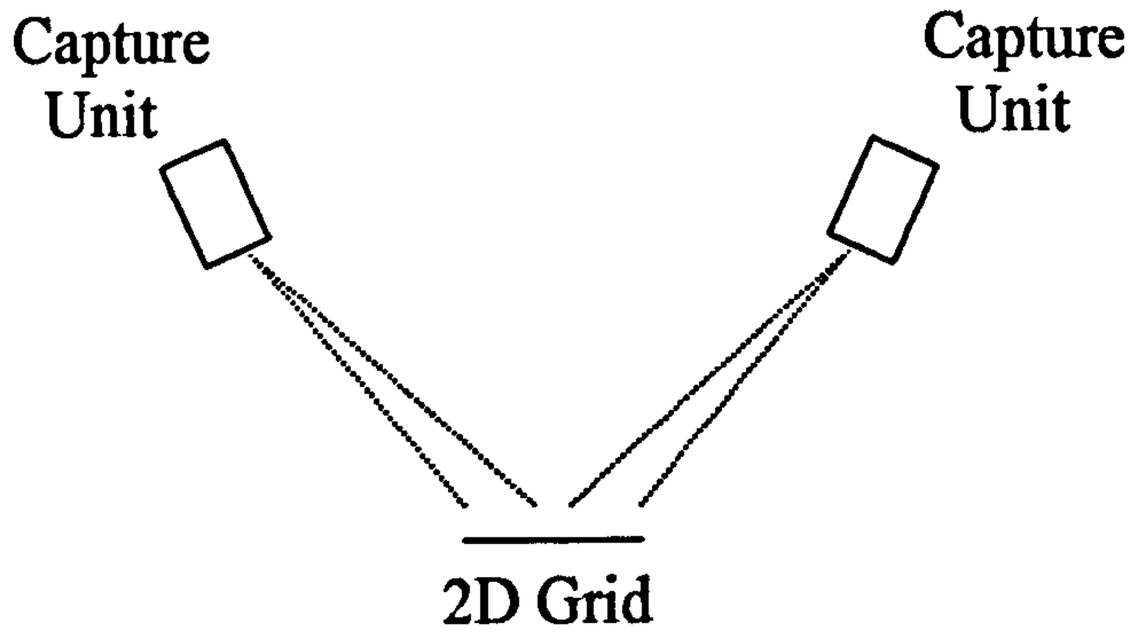

Angle formed at the target object
(based upon the relative distances
between the Capture Units and the
target object)

Both Units in the two-camera system were used to capture the target object from which 3 variations were measured:

1. The image from Unit A
2. The image from Unit B.
3. The stitched image

A single set of measurements were taken, initially over 2 cells (40 mm), then subsequently over 4 cells, 6 cells, 8 cells and so on, the process being repeated in both the horizontal and vertical direction. The TriForm™ measurements were then compared to the known measurements of the computer generated grid. The test proved the value of using a simple object such as a 2D grid, as a systematic error was clearly identified within the system once the measured readings obtained from the TriForm™ system were plotted against the true value of 40mm, (illustrated by Figures B1 – B6 in Appendix B). A systematic error for both Units was apparent in both the horizontal and vertical directions, the TriForm™ readings being consistently less than the actual grid measurements.

The error in the horizontal direction displayed the greatest magnitude on average reaching approximately 6%, whereas the error in the vertical direction was approximately 2.5%. Both of these errors are position dependent, the maximum error being approximately 10%.

A degree of 'S' type distortion was also noted within the images, which was made clear by the inclusion of such a fine grid. This distortion results in images that are not accurate representations of the physical object, which must, in turn, impact upon the measurements taken on-screen.

The two-dimensional grid proved to be a useful tool for identifying errors in a three-dimensional image capture system. The grid enabled sources of error to be identified which were not apparent during the manikin test. The absence of surface curvature enabled the deviation in the TriForm™ system measurements to be clearly quantified against the actual distances marked on the grid. The simplicity of the object has also illustrated the distortion present during image capture. Neither of these problems could be clearly identified using the manikin as a test object. The simplicity of its surface and the inclusion of a relatively fine grid provided both quantitative and visual information to assist in identifying the areas that could be improved upon through calibration, justifying its use as the primary target object used for this investigation.

The investigation evolved to focus on the evaluation of the performance of the optical measurement system under investigation. The system at that stage was not suited to fulfilling the functions of accurately capturing the human body. Therefore the aim of the investigation shifted towards the determination and evaluation of the errors inherent within the system. This was achieved by the creation of a test procedure that could isolate these sources and enable the quantification of their impact upon measurement readings.

Following the results of the initial grid test modifications were made to the image capture system configuration and the calibration settings. The objective was to improve the current performance of the prototype system, to enable the full evaluation to be undertaken with the system performing at its optimum level. The full details of the next phase in the investigation are covered in Appendix C.

A 2D (20mm x 20mm) grid was used similar to that used in the preliminary investigation. The only exception being that the overall size was altered to fit onto A2 paper to improve ease by which the grid could be printed. The squares, in this instance were measured in 80mm blocks, as opposed to 40mm blocks to reduce the likelihood of operator fatigue affecting the measurement results. The reason for the continued inclusion of such a fine grid was to help to the visual perception of any deformity in the grid which could have easily been overlooked on a larger grid. The grids in each case were measured both in the horizontal and vertical directions, unless specified otherwise.

For the purpose of calibration investigators have used various target objects such as spheres (Bruner 1999), cylinders and boxes (Daanen et al. 1997) which provide various surface representations which are mirrored to some degree in the human form. Whilst these test procedures are acknowledged, their application to the methodology being created by the author remains limited. For calibration, the manufacturers of the image capture equipment often have known tolerances within which their particular system needs to operate, therefore the object is merely a medium by which the required performance may be checked.

The use of objects such as spheres and cylinders are particularly relevant to 360° multiple Capture Unit systems, as a single object can provide a calibration reference for multiple Units. However, the objective of this particular investigation is to create a test methodology to evaluate the performance of an image capture system, which then may be universally applied to other capture

systems working on the same principle. Thus the investigation is primarily based upon the performance of a single Capture Unit, as the methodology may then be applied to alternative systems with differing numbers of Capture Units. By evaluating the errors in a single Unit the individual errors present within a system may be identified without the interference of joining together multiple views, which in its own right can introduce further errors. Further test procedures may then be developed to test the performance of combining multiple views for each system.

A two-dimensional board provides a more critical surface for the determination of individual errors than a curved surface. By using a 2D surface, a curved surface may still be simulated by varying the physical geometry of the object. Viewing a 2D surface, as shown against the cylinder in Figure 4.25, illustrates that by the movement of the 2D surface in terms of angle and distance a curved surface may also be simulated.

Figure 4.25. Curved Surface Simulation

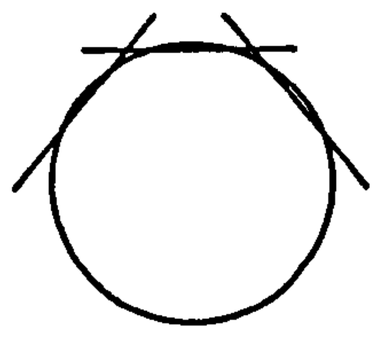

The use of a two-dimensional board is preferable when the aim of each test within the methodology is to keep all variables constant with the exception of the one under investigation. With a 2D surface the System Centre and hence the distance may be kept constant for any point across the board, whereas for a curved surface the distance and angle of various points does not remain constant across the surface. Thus increasing the number of known variables that could be responsible for the source of error.

As the capture volume of each Unit is limited to a vertical cylinder of 700mm in diameter, with a maximum view of 120°, the size of sphere or cylinder that could be used is limited. A curved surface differs across the horizontal plane in terms of the angle and distance. Therefore when evaluating distances over the horizontal direction within the system it is not feasible to compare areas within the capture volume for continuity of results, such as checking for any lens distortion towards the outer areas of the capture volume. A two-dimensional surface however provides a far clearer representation of any distortion that may be present, as the surface itself is not subject to any curvature and the grid area may be constructed to cover the majority of the capture volume. This is an important issue as the number of variables present within the image capture procedure and the combination of these additional factors make the identification and evaluation of errors difficult. Any additional variability which may be introduced by the target object selection could result in the misidentification of the source of error or the incorrect proportioning of each individual variables contribution to total error. The added variability associated with a curved surface also makes the evaluation of operator error as an individual entity subject to outside influences and thus open to error. However, to ensure the application of the findings to curved surfaces, (as the human body is subject to a high degree of curvature), a curved surface was used for a limited range of testing. This is discussed further in section 5.8.8.

4.6. Design of the Investigation

A list of the sources of potential error for the image capture system were determined. These broadly fell into three categories, optical, measurement and geometric. The design of the study was based around identification of possible sources of error and the creation of test procedures to isolate each variable and determine the magnitude of its impact upon the error of the system as a whole. The test procedures were divided into categories according to whether either the

physical set up or the configuration/calibration settings needed adjustment. A summary table of potential sources of error and test procedures is shown in Table 4.2. The primary reason for this restriction is to maintain continuity through like test procedures so that no additional variation is introduced which could impede the isolation of each single factor under investigation.

Table 4.2. Potential Sources of Error

Error Type	Potential sources of error	Required Action
System	The repeatability of measurements following software reboot	No movement in set up, no changes in software settings
System	The repeatability of the capture process over timed intervals	
System	The consistency of results throughout the capture area	
System	Effects of rotation	
System	Effects of enlarging the image	
System	The error related to the stitching algorithm	
System	Positioning of the stitching points	
System	The comparative performance of each Unit	
System (Measurement)	The accuracy of the measurement tool itself	
System (Measurement)	The different types of measurements and the way they work	
Operator	The operator error present during measurement	
Operator	Any operator bias in measuring in a specified direction	
System	The relationship between measured values and the calibration variables	No movement in set up required, changes in software settings
System	The effect of changing the angle setting in the software	
Object	The error related to the size of the marker	Movement in set up required, no changes in software settings
Object	Planar differences (2D vs. 3D objects)	
Object	The angle of the target object to the Unit	
Object	The distance between the target object & the Unit	Movement in set up required, and changes in software settings

The following variables were tested.

Software Reboot Test	To identify whether the software is subject to any changes after rebooting.
Camera Timed Test	To test whether the Units were subject to any thermal effect.
Distance Test	To ascertain the effect of distance on measured values. To evaluate the influence of the angle setting in the configuration settings.
Horizontal Grid Angle Position Test	To test the effect of altering the angle of the target object in respect to the camera axis.
Capture Unit Comparison Test	To test for any difference between the images produced by the two Units.

For each test, both camera images were measured, in both the horizontal and vertical directions, (unless otherwise stated). The images from each camera were compared separately, to provide a check for each camera, as were the two directions. For each test the mean, standard deviation and standard error of the mean were calculated for each measurement type. Full details of the methodology and results may be found in Appendix C.

z or *t* tests for matched samples were also undertaken for hypothesis testing to ascertain whether any significant difference existed between the test results. *z* tests were employed for all the hypothesis testing with the exception of the distance test, where *t* tests were employed due to a smaller available sample size.

z and *t* tests for matched samples test for differences between population means. The null hypothesis of 'no difference' was tested to determine whether the source of potential error under investigation is a factor that impacts on measured values. This was achieved by comparing an original captured image with that captured following a change in a specified variable, relative to each particular test.

4.7. Summarised Findings

Table 4.3 summarises the basic statistics, for the shortest distance, showing the range for the mean.

Table 4.3. Mean Range by Measurement Type

Unit/ Direction	*n*	Shortest Distance (mm)	Surface Distance (mm)	Tape Measure Distance (mm)	Difference Surface – shortest (mm)	Difference tape measure – shortest (mm)
Unit A/ Horizontal	623	75.07-79.43	80.12-87.06	75.16-79.67	5.05- 7.63	0.09-0.24
Unit B/ Horizontal	610	80.44-81.93	86.18-91.78	80.67-82.10	5.74- 9.85	0.03-0.17
Unit A/ Vertical	454	80.64-81.93	83.41-91.84	80.67-82.07	2.77- 9.91	0.03-0.14
Unit B/ Vertical	444	82.08-83.46	85.89-94.02	82.13-83.62	3.81-10.56	0.05-0.16

n = the total number of measurements taken per grid multiplied by the number of variants in each test.

By examination of Table 4.3 a large discrepancy can be clearly seen between the surface and shortest measurement results. A discrepancy may also be noted between the tape measure and shortest distance results, although this is to a far lesser degree. The object being measured is a flat surface, hence each measurement type should give the same or at least very similar results as opposed to the notable difference recorded in Table 4.3. By analysing the range of the mean it is clear that regardless of Unit, the vertical measurement results are

higher than those recorded for the horizontal direction. A clear discrepancy also exists between the measured values for the two images. The mean range, for all the tests, being 75.07-79.43mm and 80.44-81.93mm for the horizontal direction for Unit's A and B respectively and 80.64-81.93mm and 82.08-83.46mm for the vertical direction (shortest distance only).

Table 4.4. Shortest Distance Test Statistics

Unit/ Direction	Test	Variant	*n*	Mean (mm)	Standard Deviation (mm)	Standard Error of the Mean (mm)
Unit A/ Horizontal	Reboot Test	Before	40	78.07	1.27	0.20
		After	40	78.09	1.15	0.18
	Capture Unit Timed Test	0 mins.	40	77.77	1.04	0.16
		60 mins.	40	78.07	1.27	0.20
	Distance Test	Image 1	40	78.18	1.23	0.19
		Image 2	26	78.60	1.20	0.24
		Image 3	29	78.59	1.18	0.22
		Image 4	12	78.11	1.09	0.31
		Image 5	12	78.68	0.97	0.28
		Image 6	40	78.75	1.41	0.22
		Image 7	40	78.82	1.27	0.20
		Image 8	32	78.54	1.44	0.25
		Image 9	32	78.26	1.47	0.26
	Horizontal Grid Angle Position Test	Image 1	40	77.11	1.44	0.23
		Image 2	40	76.12	1.38	0.22
		Image 3	40	75.07	1.43	0.23
		Image 4	40	78.34	1.18	0.19
		Image 5	40	79.43	1.09	0.17
Unit B/ Horizontal	Reboot Test	Before	40	81.45	1.18	0.19
		After	40	81.49	1.19	0.19
	Capture Unit Timed Test	0 mins.	40	81.40	1.04	0.16
		60 mins.	40	81.45	1.18	0.19
	Distance Test	Image 1	40	81.05	1.01	0.16
		Image 2	21	81.03	1.38	0.30
		Image 3	21	81.29	1.03	0.22
		Image 4	12	80.85	0.88	0.25
		Image 5	12	81.01	0.99	0.29
		Image 6	40	81.33	1.31	0.21
		Image 7	40	81.27	1.49	0.24
		Image 8	32	81.90	1.41	0.25
		Image 9	32	81.93	1.68	0.30
	Horizontal Grid Angle Position Test	Image 1	40	81.24	1.23	0.19

n = the total number of measurements taken for each variant.

Table 4.4. Shortest Distance Test Statistics (continued)

Unit/ Direction	Test	Variant	*n*	Mean (mm)	Standard Deviation (mm)	Standard Error of the Mean (mm)
Unit B/ Horizontal	Horizontal Grid Angle Position Test	Image 2	40	81.10	1.28	0.20
		Image 3	40	81.32	1.21	0.19
		Image 4	40	81.48	1.20	0.19
		Image 5	40	80.44	1.49	0.24
Unit A/ Vertical	Reboot Test	Before	40	80.88	1.32	0.20
		After	40	81.34	1.46	0.23
	Capture Unit Timed Test	0 mins.	40	80.96	1.54	0.24
		60 mins.	40	80.88	1.32	0.20
	Distance Test	Image 1	42	81.15	1.43	0.22
		Image 2	29	80.64	1.22	0.23
		Image 3	31	81.36	1.30	0.23
		Image 4	15	81.19	1.06	0.27
		Image 5	15	80.74	0.84	0.22
		Image 6	42	81.52	1.12	0.17
		Image 7	42	81.81	1.35	0.21
		Image 8	35	81.91	1.41	0.24
		Image 9	35	81.93	1.38	0.23
Unit B/ Vertical	Reboot Test	Before	40	82.47	1.52	0.23
		After	40	82.82	1.45	0.22
	Capture Unit Timed Test	0 mins.	40	82.24	1.22	0.19
		60 mins.	40	82.47	1.52	0.23
	Distance Test	Image 1	42	82.24	1.22	0.19
		Image 2	25	82.08	1.13	0.23
		Image 3	25	82.54	1.33	0.27
		Image 4	15	82.15	0.86	0.22
		Image 5	15	82.09	1.37	0.35
		Image 6	42	82.96	1.20	0.19
		Image 7	42	82.59	1.13	0.17
		Image 8	35	83.13	1.18	0.20
		Image 9	35	83.46	1.47	0.25

n = the total number of measurements taken for each variant.

On examination of the basic statistics presented in Table 4.4 it is clear that the results for the reboot test, Capture Unit timed test and distance test, the mean,

standard deviation and standard error of the mean are generally consistent with one another for both units.

For the grid angle position test, (which was only concerned with the horizontal direction) a clear pattern may be noted in the results for Unit A. The mean decreases as the target object was turned in the clockwise direction (images 2 and 3) and increases as the object was turned towards the anti-clockwise direction (images 4 and 5). The results, however, for Unit B, do not follow this trend, indicating a difference between the images produced by each Unit.

The hypothesis testing at 95% indicated no difference for the reboot test, camera timed test and distance test hence the null hypothesis was not rejected. For the horizontal grid angle position test however the null hypothesis was rejected for all angle comparisons for the Unit A image. Whilst the null hypothesis was not rejected for images 1-2, 1-3 and 1-4, the image comparisons 1-5 and 3-5 were rejected as these compare the extremes of each angle direction. Therefore a significant difference is reported between the images produced after rotating the target object, especially for Unit A.

The two Capture Units were compared in both directions to see whether the discrepancies in the horizontal direction and vertical direction, shown by the results were significant enough to reject the null hypothesis of no difference at the 95% confidence interval. When comparing the results from each Unit in the horizontal and vertical directions the null hypothesis is rejected at the 95% confidence interval. Therefore a significant difference can be reported between the Unit A image and the Unit B image, indicating the importance of evaluating the impact of changes in variables independently on each Unit.

The measured values from each Unit image were plotted against the true value of 80mm per cell for the whole grid to enable a visual comparison of the results. These can be seen in Figures 4.26 and 4.27 for Units A and B respectively.

Figure 4.26. Measured Values Vs. True Values - Unit A

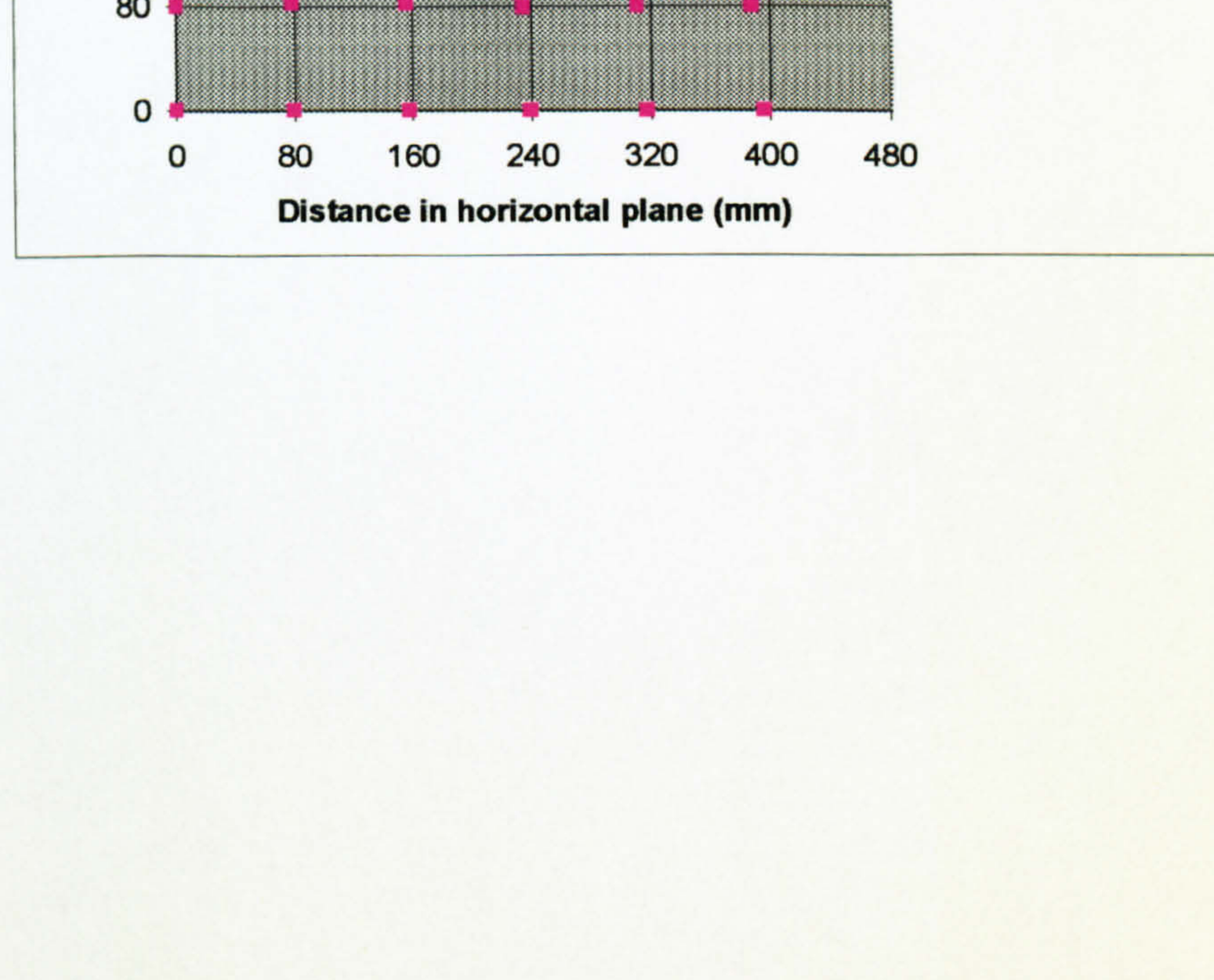

Figure 4.27. Measured Values vs. True Values - Unit B

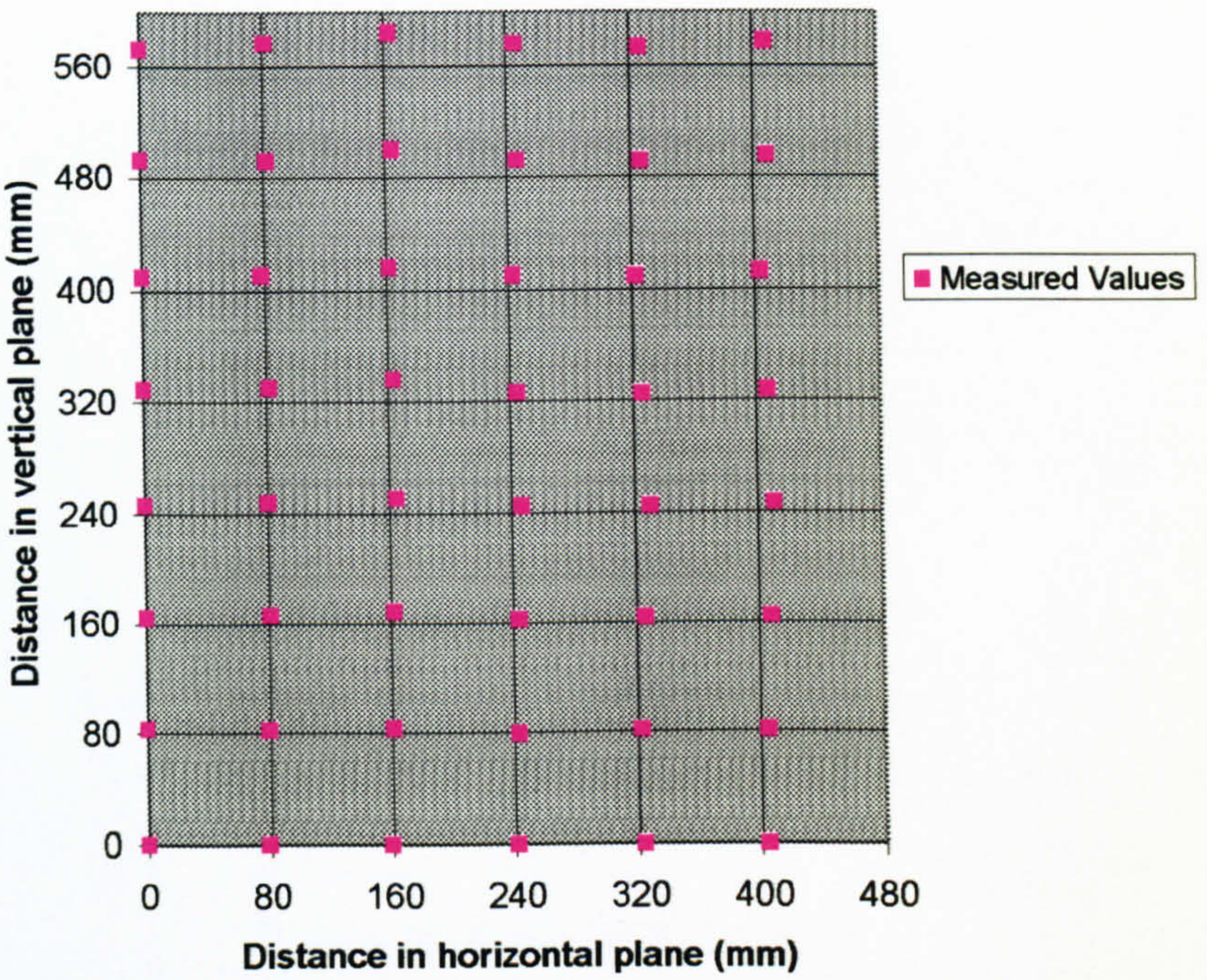

The Capture Unit comparison test which was undertaken following the results of the horizontal grid angle position test, proved the distinct difference between Units A and B which was suggested in the basic statistics and brought to light primarily by the horizontal grid angle position test.

The results from Unit A indicate a problem with the Unit where the accuracy of the measured results appears to be angle dependent. Whilst inherent errors exist in the image generation and the measuring procedure the pattern of results noted during the horizontal grid angle position test relates directly to the angle of the target object, suggesting a linear relationship between the target object angle and the error in measured values. Following subsequent testing a potential mis-alignment in the LCD in the projector of the Capture Unit was identified, which was thought to be the cause of the results noted for Unit A.

4.8. Research Outcomes

The methodology employed during the preliminary research has illustrated the rationale for the design of the main investigation and also the process by which the investigation developed. Only limited conclusions may be drawn at this stage in the investigation, as the sources of error that have been evaluated are limited. However, a number of general conclusions can be formed on the performance of the system. The measurement readings from the horizontal and vertical directions for each Unit are inconsistent with one another and the opportunity to equalise the two is not available under the calibration settings. This is not of paramount importance for comparative testing however, it does not assist in the objective of obtaining more accurate measurement results. At present the discrepancies result in a systematic error for each direction.

Whilst it is known that the results gained from either Unit are not consistently in keeping with the true value of 80mm, it must be noted that discrepancies are bound to exist between the true value and the measured value, however good the calibration. The lines on the grid are 1.5mm thick and therefore the markers used for measurement on-screen could be incorrectly placed. The accuracy of the point cloud and associated colour data must be taken into account, as discussed in section 4.3, with the accuracy in the x dimension being specified by the manufacturer as ±1.5mm and ±2.0mm in the y and z dimensions. Also the measurements are all undertaken by the operator and hence are subject to some operator error, although one would assume that the error related to the marker size and point pitch would be included within any operator variability. It is unlikely therefore that one would ever get absolute agreement with the true value.

One would expect that these error factors would impact on the various distances to the same extent. Whilst a slight error in the z dimension would affect the

surface (and tape measure) distances to a greater extent, it is highly unlikely that it would explain the deviation noted in the results. The deviation in the shortest distance measurement however could be accounted for by taking into account the previously stated sources of error, which would impact on every measurement taken. However the deviation exhibited in the horizontal grid angle position test cannot be explained in this manner and therefore must be subject to an additional source of error, identified as an error in the mounting of the LCD.

The differences between the two Capture Units when used independently are manageable, however when stitching multiple views together, the problem would lead to scaling errors between the two images, which would result in an inaccurate stitching process. The problem highlighted with Unit A means that corrective work will need to be undertaken upon the Unit to improve the LCD mounting and thus the results obtainable. It is clear from the measurement results that the shortest and tape measure distances are the only reliable measurement indicators, the surface distance proving to be both inaccurate and inconsistent. Whilst the shortest distance only is being used for comparisons, this issue is of no great importance, however, for three-dimensional objects, the surface distance is a measure of paramount importance in replicating anthropometric measurement.

Following the feedback given to the system manufacturers from the research carried out on the two-camera system the software was revised. The new software update included a modified method of generating the surface distance measurement, by using more reference points along the length of the measurement and restricting the spread of points so that only those directly in the path of the measurement would be included. The remaining modifications related to the user interface and primarily consisted of changes in the Analysis mode. The update provided the same capabilities as the previous version, but with the additional capabilities of being able to measure from one point on, for

example, the side of the body over to the opposite side. This is achieved by being able to select a start point for a measurement, then being able to rotate the object before selecting the end measurement point.

A test was designed to provide a comparison between the performance of the new measurement software against that used previously with the two-camera system. This used an image that had been previously measured in the old software and comprised of re-measuring it in the latest software and comparing the results to identify whether any improvements in the measurement accuracy were apparent.

Table 4.5. Basic Statistics: Software Comparison Test

Unit/ Direction	*n*	Mean Shortest Distance (mm)		Mean Surface Distance (mm)		Mean Tape Measure Distance (mm)	
		Old Software	New Software	Old Software	New Software	Old Software	New Software
Unit A/ Horizontal	40	78.07	78.26	84.31	79.02	78.18	78.71
Unit A/ Vertical	42	80.88	80.67	90.27	81.69	81.01	81.37
Unit B/ Horizontal	40	81.45	81.47	88.77	82.30	81.70	82.03
Unit B/ Vertical	42	82.47	81.92	94.02	83.21	82.60	82.98

n = the total number of measurements taken per grid.

The most significant difference may be noted in the surface distance, which highlights the improvements made in the calculation of surface distance.

Comparing the horizontal and vertical directions, the horizontal direction has mean values which are closer to the true values compared to the vertical direction, suggesting the horizontal direction was, and remains, the more accurate measurement direction.

CHAPTER 5

THE TRIFORM™ SINGLE CAMERA 3D IMAGE CAPTURE SYSTEM

5.1. Introduction

Following the findings of the two-camera system performance tests it became clear that the system would have to be modified in some way to rectify the LCD mounting problem. The manufacturer therefore provided an amended system with a new LCD mounting, which was used for the remainder of the investigation.

5.2. System Configuration

At this time Wicks and Wilson Ltd., the suppliers of the image capture system, developed a whole body capture system based upon a combination of Capture Units and mirrors. By using four Capture Units essentially the same as those used in the two-camera test, combined with mirrors, an eight view system was developed capable of 360 degree capture. The modifications to the Units included an improvement in the mechanical alignment of the lens, projector, camera and ultimately the two views produced, plus a more robust LCD mounting. The whole body capture system was configured to have two Units directly in front of the person, one capturing the upper portion of the body and one capturing the lower, with the further two Units being placed directly behind the person, in the same vertical configuration. A motorised rotating mirror just in front of the Units, projects the light onto the outer mirrors, this is then reflected onto the person to enable a full 360 degree view to be achieved.

Whilst the use of a whole body image capture system would enable an evaluation of a full 360 degree system, it was decided to not use the system due to the stage

already reached in the investigation. By using an eight view system, the testing would become more time consuming as the potential for the introduction of additional errors by stitching eight views together would undoubtedly make it difficult to identify any source of error. Plus the application of the methodology employed would have more limited application to alternative image capture systems.

Further investigation of the original two-camera system was thought to be of limited application, as the technology had already advanced from this type of approach, therefore a torso image capture system was provided as the replacement to the two-camera system. The torso system was based upon exactly the same principle as the whole body system, but in essence was a quarter of the system. The torso system provided the same capture area as the previous two-camera configuration, but was based on a single Capture Unit with a series of mirrors to provide the corresponding two views. This system in its own right is now marketed as a commercial image capture device. An illustration of the system is shown in Figure 5.1 and a drawing of the configuration is shown in Figure 5.2.

Figure 5.1. The TriForm™ Single Camera 3D Image Capture System (Wicks & Wilson Ltd. 1999)

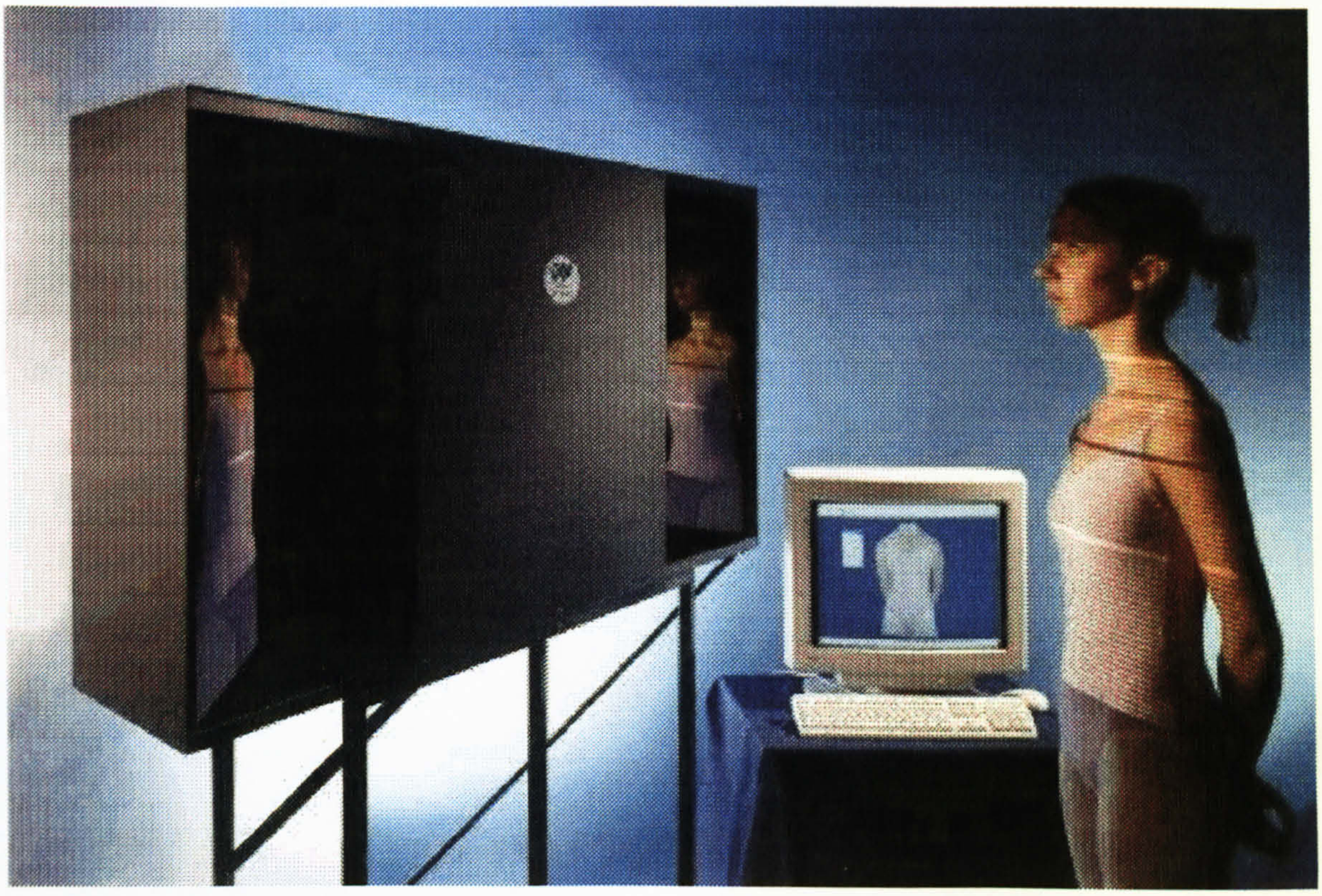

Figure 5.2. The TriForm™ Single Camera 3D Image Capture System Configuration (adapted from, Wicks & Wilson Ltd. 2000)

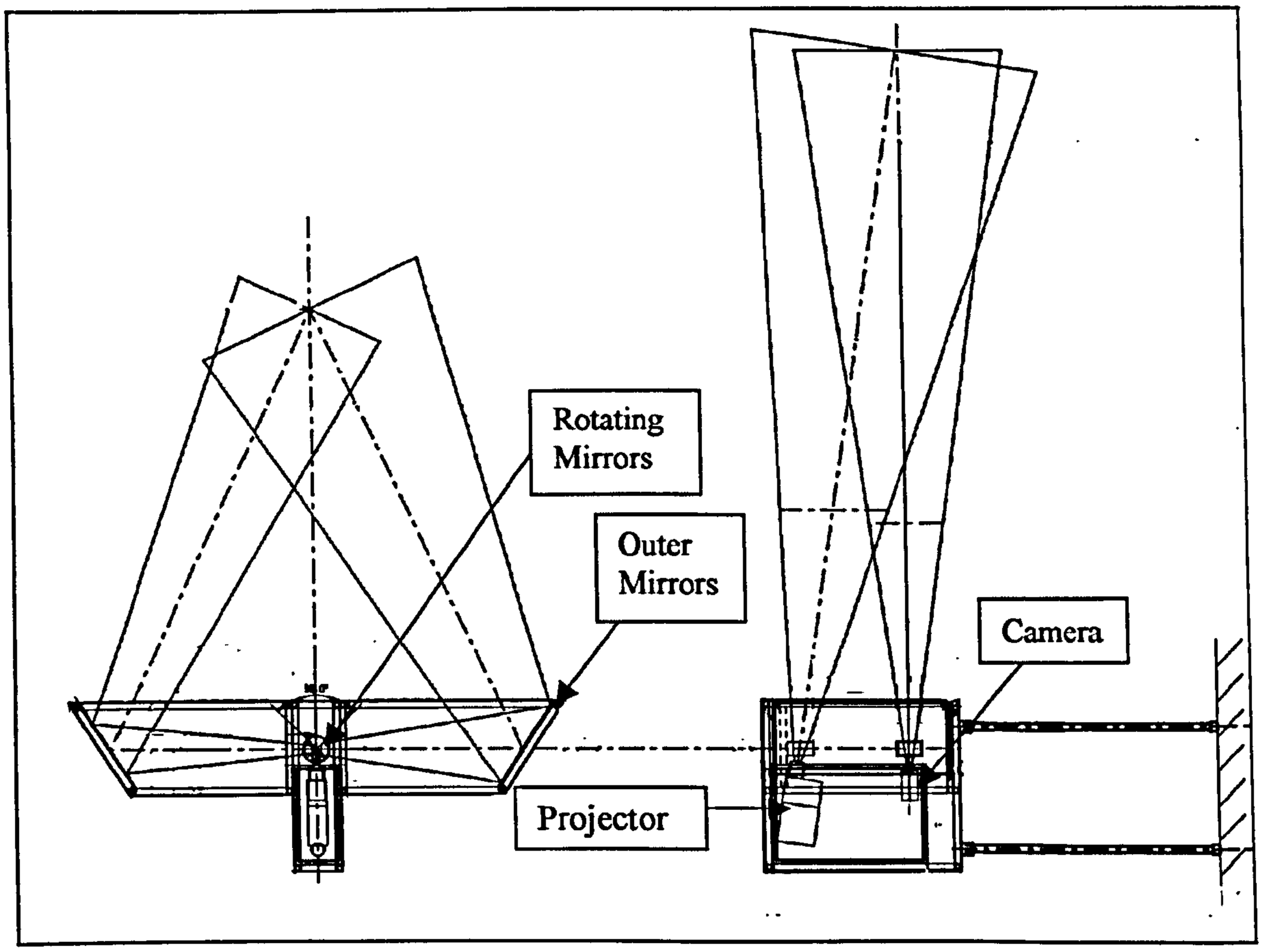

Due to the revised housing for the single camera system, the Unit was made more robust with no potential to upset the levelness, height or angle of the camera or mirrors in respect to the object to be captured. By using the torso system the current methodology may still be employed based on the tests undertaken previously. The relevance of the operation of the torso system in comparison with the whole body system makes any findings applicable to both systems, as the tests may also be adapted to relate to the whole body system.

The advantage of using a capture system based on mirrors is the removal of variability in the hardware. The lens for the projector and camera are the same for both views, hence theoretically the impact of any lens distortion will also be equal for each view. The mirrors and the mounting of those mirrors are therefore

the only hardware elements that could result in a discrepancy between views. The calibration built into the software is used to remove the effects of any such differences, hence the calibration settings may be different for each view. Because the hardware is constant it is therefore possible to identify more clearly the impact of the hardware and software independently, which was not previously possible when using the two individual Capture Units.

Please note the same computer and monitor configuration was used throughout the investigation. This was described fully in section 4.2.4.

5.3. Specifications:

Total scan time <4 seconds

Process time <60 seconds

Scanned circumference 180 degrees

Scanned height 1050mm

Point pitch – azimuth and elevation 1.5mm approximately

Accuracy +/- 2mm

Total footprint 2.5 x 2.5 metres

All specifications courtesy of Wicks and Wilson Ltd.

5.4. Calibration

Whilst the new system is based upon a single Capture Unit, each view still needs to be calibrated individually as any slight differences in the mirrors will affect the measured results and hence the settings required. The system was calibrated prior to delivery using much the same method as described in Chapter 5. Each view was calibrated in turn, with the 2D grid facing directly onto each individual projection from the mirror in turn to check the calibration settings for each view.

5.5. Error Determination

As discussed in section 4.3 any measurement taken with the TriForm™ system is subject a certain amount of error, based upon the point cloud generation, colour data matching and the operator error concerned with selecting the area to measure. The accuracy of the TriForm™ system is specified, by the manufacturer, as ±2.0mm for a measurement, on the basis of the point pitch, plus any slight error arising from a discrepancy in the colour data matching, and any slight z error which may be present.

To attempt to find the true theoretical accuracy of the system the point pitch was calculated based on the current system configuration. The theoretical accuracy therefore may be determined by the physical view dimension divided by the camera resolution, as this will specify the spacing of points within the point cloud (i.e. the point pitch). The physical view width was determined by measuring the available captured area from each Unit. This is approximated by physical measurement of the lit area on the target object that may be viewed on screen. The measurement is taken for each view with the target object facing the mirror in each case. This angle however may only be approximated and hence the measured view width is subject to changes in dimension due to the angle. The approximate physical view of 695mm in height and 680mm in width was determined. As the resolution of the camera is specified as 768 (height) x 576 (width), the point pitch may be estimated as follows:

Point pitch in the x axis = Physical view width/Actual horizontal resolution

= 680/576

= 1.18mm

Point pitch in the y axis = Physical view height/Actual vertical resolution

= 695/768

= 0.90mm

To check the estimated point pitch the spacing of the individual points in the point cloud were measured as these form the actual point pitch which is generated during image capture. A series of previously captured images were enlarged until the individual points of the point cloud became visible. By selecting specific points and measuring between them a point pitch of 1mm in x and 0.9mm in y was determined. Thus the point pitch for the y axis was corroborated, whereas the pitch for the x axis was reduced from 1.18mm to 1mm. As the captured image provides the clearest indicator of actual point pitch, the revised pitch for the x dimension was accepted at 1mm.

During this test it became apparent that regardless of location when a point was selected the markers generated by the computer (used to denoted the extremities of the measurement) were displaced by one point i.e. 1/0.9mm, which could be as much as 1.3mm when the displacement was diagonal. The magnitude by which points were displaced remained constant however the route taken appeared to be random. Both points, however, always moved in the same direction and thus the measurement remained the same even though the location may be displaced by as much as 1.3mm. The phenomenon was checked on several files, using both left and right view images and the results remained the same. Where a start or finish location was selected which fell between points the marker did not select the nearest point, but instead moved to the adjacent point which resulted in the measurement being displaced by as much as 1 1/2 point pitches.

Additional sources of instrumental error namely the potential for a slight error in the z dimension and the influence of a colour data matching error, were discussed fully in section 4.3. Both were thought (by the manufacturers) to be extremely

small. The z error is random in nature and therefore is expected to cancel out over any reasonable distance, whilst the colour matching error is likely to be linear. Any slight mis-matching would therefore result in the fractional displacement of measurement points and hence the actual measured distance should remain the same.

The stated sources of error which are a product of the system will henceforth be termed as the instrumental error, which may be quantified as the influence of the point pitch and the displacement of points from their selected position. The points are spaced by 1mm in the x dimension and 0.9mm in the y dimension, therefore if a position was selected between points the error could be as much as 0.5mm in the x dimension and 0.45 in the y dimension. Therefore the error in selecting the nearest point is a maximum of ±0.5/±0.45 on any measurement.

The displacement of the measurement can be as much as 1.3mm if the displacement is diagonal regardless of whether the measurement is taken in the x or y dimension, providing the location for the measurement lands on a point within the cloud. Failing this the displacement could be as much as 1.35mm (1.3mm + 0.5mm). The displacement however appears to be in a constant direction hence its influence cannot be quantified at this stage, as its impact would be relative to the intricacies of the surface being measured, therefore its presence must just be noted within the findings of the tests.

The influence of the operator must also be taken into account when determining the errors inherent in an individual measurement. Due to the nature of point selection for measurement any errors relating to the size of the markers (i.e. the thickness of the lines for the grid) and the point pitch will be included with the error introduced by the operator. Both errors will naturally occur during any measurement and thus their effects will be included when assessing the repeatability of measurement. Sections 5.8.1. and 5.8.2. therefore detail test

procedures to quantify the impact of operators influence which will be discussed further in the results in Chapter 6.

5.6. Measurement Objects

The same 2D grid was employed as used in the previous investigation, as essentially the investigation is a continuation in methodology from the two-camera tests. For the purpose of testing whether any differences did exist between the measured values from a 2D grid when compared to a 3D grid, a curved object was also used. This comprised of a section of exhibition equipment, onto which the printed grid was carefully mounted. The orientation of the object is discussed further in the planar test procedure in section 5.8.8.

5.7. Design of the Investigation

As this part of the investigation is a continuation from the work that had been undertaken in the two-camera test the remainder of the investigation concentrates on those sources of error which had not been investigated previously. Whilst a change in system had taken place it was not necessary to repeat all the tests taken with the two-camera system. Hence, the reboot test and the Capture Unit timed test were not repeated, as the findings of these tests were still valid for the new configuration. Only those affected by this change in configuration were repeated, namely the distance test and grid angle position test. Again the test procedures were divided into categories according to whether either the physical set up or the configuration/calibration settings needed adjustment. A summary table of potential sources of error & test procedures investigated for the single camera system is shown in Table 5.1.

Table 5.1. Potential Sources of Error

Error Type	Potential sources of error	Required Action
System	The consistency of results throughout the capture area	No movement in set up, no changes in software settings
System	Effects of rotation	
System	Effects of enlarging the image	
System	The error related to the stitching algorithm	
System	Positioning of the stitching points	
System	The comparative performance of each view	
System	The performance of the single camera system v. the two-camera system	
System (Measurement)	The accuracy of the measurement tool itself	
System (Measurement)	The different types of measurements and the way they work	
Operator	The operator error present during measurement	
Operator	Any operator bias in measuring in a specified direction	
System	The relationship between measured values and the calibration variables	No movement in set up required, changes in software settings
System	The effect of changing the angle setting in the software	
Object	The error related to the size of the marker	Movement in set up required, no changes in software settings
Object	Planar differences (2D vs. 3D objects)	
Object	The angle of the target object to the Unit	
Object	The distance between the target object & the Unit	

5.8. Evaluation Procedure

For each test, both camera images were measured, over intervals of 80mm, in both the horizontal and vertical directions, (unless otherwise stated). The images from each view were compared separately, to provide a check for each view, as were the two directions. Initially the mean, standard deviation and standard error of the mean were calculated for each measurement type. The Total Difference (TD) was also recorded where appropriate by comparing the known true value of the dimensions of the grid (80mm) with the measured value obtained from the image capture system. Note that Total Difference is a measure that has been designed purely for this investigation.

Total Difference (TD) = $\sum$ |Absolute error for each cell|

where, Absolute Error = True Value – Measured Value

The Total Difference is based upon the calculation of the absolute error for each cell. The absolute error is calculated independently for each measurement taken within the grid. Thus the difference between the true value of 80mm and the measured value for each of the forty measurements taken in the horizontal direction and each of the forty-two in the vertical direction is calculated. To avoid negative differences cancelling the effect of positive differences, the absolute error values were squared to remove the effect of negative values. The square root of each was then calculated to provide the absolute error without the sign. The value of these differences was then totalled to provide the Total Difference. Each direction was totalled independently to identify whether the deviation primarily exists in the horizontal or vertical direction. The Total Difference for the entire grid is also calculated by summing the TD for the horizontal and vertical directions.

The Total Difference was used as opposed to hypothesis testing to provide a measure that would enable comparisons between results, by providing more detailed information on the magnitude of differences between sample data sets. The measure provides the total absolute error for the grid in millimetres, the same units as the measurement. Hypothesis testing provides a result of a 'rejected' or 'not rejected' null hypothesis. It is only by the analysis of confidence intervals that any further measure may be gained. In contrast the measure of Total Difference enables a comparison of results by providing information on the magnitude of difference between sample data sets. However one limitation of this measure is that comparisons may only be drawn between results of equal sample size.

Note only the shortest distance results were considered in the Total Difference tests, to provide a consistency between the results from the two-camera system evaluation. The only exception to this is for the 3D tests where the surface distance was used to measure the curved surfaces of the test object.

As an additional tool graphical representations of the measured values against the original grid were also plotted, where relevant, to provide a visual impression of the deviation between true and measured values. These are included with the results from each test in Chapter 6.

5.8.1. Operator Error Test

To ascertain the impact of any error resulting from the operators influence a number of repeat measurements were taken on previously measured images to determine the variability associated with the operator undertaking the measurement process. Each of the images used were based on the original settings and therefore should not be subject to additional variability introduced

by changing the image capture system settings. The images re-measured are detailed below in Table 5.2.

Table 5.2. Images Used for the Operator Error Test

Image Reference	Image Description	No. of individual repeat measurements
Image A	Base left grid from distance test	246
Image B	Base right grid from distance test	82
Image C	Base left grid from angle in computer test	82
Image D	Base right grid from angle in computer test	82
Image E	Base left grid from stitch test	82

Image A was measured in its entirety three times, whereas Images B to E were measured once to compare with the results gained during measurement for an alternative test. Image A was measured repeatedly to provide a consistent basis for comparison however during the test it was thought that bias may occur if the operator became familiar with the measurement being taken, hence a number alternative images were also re-measured to ensure no bias was present.

As the grids used throughout the investigation are based on cells of known dimensions (80mm x 80mm), a further test was undertaken to check the effect of the operators influence on measured readings by having prior knowledge of the true values. A grid was therefore produced of varying dimensions that were unknown to the operator. The grid was captured and measured then the measured values were compared with the true values of the grid to determine whether the variance was comparable to that generated whilst using the 80mm x 80mm grid.

5.8.2. Directional Bias Test

As each grid has always been measured left to right in the horizontal and top to bottom in the vertical, a test was devised to determine whether any bias existed by constantly measuring in only one direction. Hence in this test a previously measured grid (image 1 set at 50 degrees, angle in computer test) was re-measured but in the opposite direction. The results of the two were then compared.

5.8.3. View Comparison Test

Whilst the capture system is based on a single Capture Unit, it is still imperative to establish whether there is any significant difference between the views. Differences in these circumstances would be most likely due to slight differences in the mirrors and also in the calibration of the system. To test the continuity between captured images, both the left and right hand images were measured in the horizontal and vertical directions on the same capture to check whether the two views were providing comparable results. Previously captured images from the angle in computer test (detailed in section 5.8.5) were used as a basis for the test, as it reflected the original set up used for comparisons in all tests. The images used were from the one camera system evaluation, with the angle set at 50 degrees.

5.8.4. Distance Test

To ascertain the effect of distance on measured values three images were captured, each at various distances.

Image 1 145cm from target to Unit

Image 2 100cm from target to Unit

Image 3 171cm from target to Unit.

(For each distance the angle in the configuration settings was left at 50 degrees)

The distances were chosen on the basis of providing extreme distances that could still be adequately captured as moving the target object any nearer or further away from the Unit would result in an image which was only barely in view. The number of cells available to measure however, are reduced by altering the distance from the target to the Unit. As the view width of the unit is fixed the grid at certain distances is no longer captured in its entirety. Hence when comparing like for like cells between the left and right views only a limited number of cells may be used for comparison against one another.

5.8.5. Angle in Computer Test

The value of the camera angle in the configuration parameters reflects the angle at the target object from two projecting Units, as illustrated in Figure 5.3.

Figure 5.3. Angle Determination

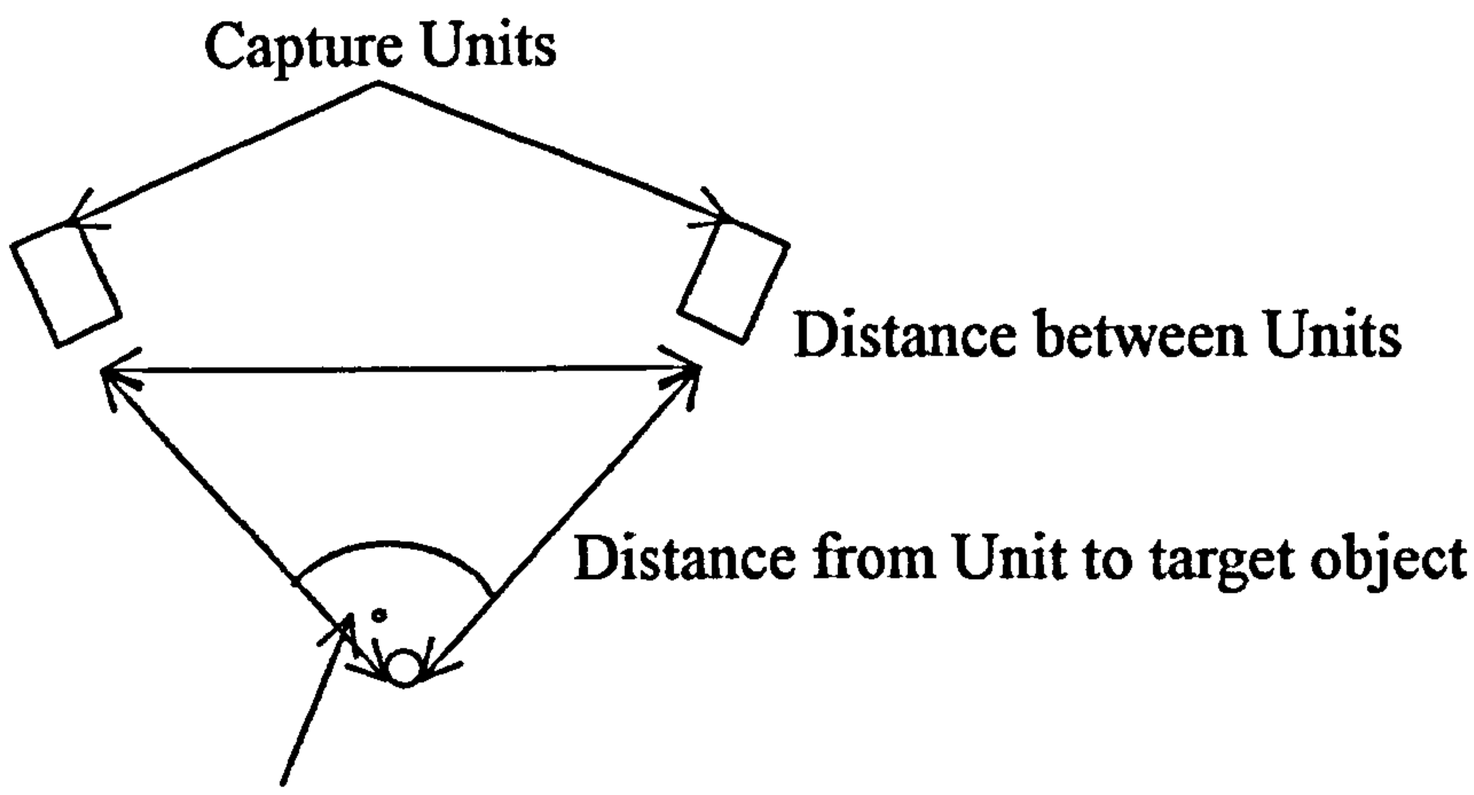

To test whether the value of the setting would effect measured values three images, using the 2D grid, were taken each with a different angle set in the configuration settings.

Image 1 50 degrees

Image 2 100 degrees

Image 3 0 degrees.

All images were taken with the target object facing parallel to the front of the Unit, at a distance of 145cm from the target to the Unit.

5.8.6. Image Enlargement Test

To check whether enlarging the image on screen made any impact on measured values a 2D grid was measured as it appears after the image capture process. The image was then re-measured after it was enlarged by 200 single depressions of

the enlargement button, which equates to an increase in size of 25%, (the magnification ratio per step being 1:1.00125). The test was not repeated for a reduction in the size of the image, as this would never be used as it results in an image that is too small to precisely measure. The image used for the test was based on the distance test control grid at 145cm.

5.8.7. Rotation Test

When measuring angled surfaces it is often necessary to rotate the on-screen image to enable clear viewing of the area to be measured, hence the rotation test was devised to evaluate whether rotating the image on screen has any significant impact on the measured results. A previously measured grid (distance test control grid at 145cm), therefore was re-measured after being rotated in various directions. These being,

60 depressions of the clockwise rotation button (15 degrees)
60 depressions of the anti-clockwise rotation button (15 degrees)
60 depressions of the forwards rotation button (15 degrees)
60 depressions of the backwards rotation button (15 degrees)

(The fixed step value for a single depression being 0.25degrees/step).

The distance to rotate the object was determined by the ease of viewing on screen. Any more rotation would have made it difficult to select the correct measuring points. As the rotation in the clockwise and anti-clockwise directions only affects the horizontal plane that was the only dimension considered, the same applies to the forwards and backwards rotations, only this time for the vertical direction.

5.8.8. Planar Differences Test

As the majority of tests have been undertaken using a 2D grid, it is imperative to ensure there is no significant difference between the measured results from a 2D grid when compared to a 3D grid, especially as the human body is a 3D object. For the purpose of testing any differences a curved object comprising of a section of exhibition equipment was used, onto which the printed grid was carefully mounted. Figure 5.4 provides an illustration of the object.

Figure 5.4. 3D Measurement Object

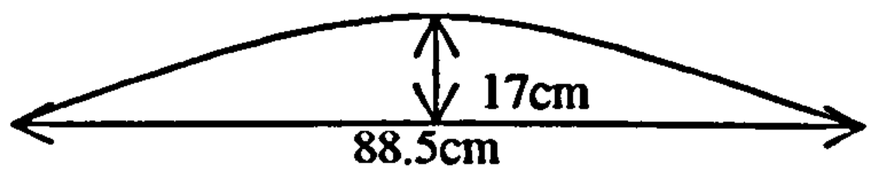

The object provided a smooth surface that could be used to provide a concave or a convex surface in either the horizontal or vertical direction. Thus enabling the separate evaluation of the effects in both directions, in both the horizontal and vertical plane.

The 3D object was captured in the following positions shown in Figures 5.5 – 5.8. Note that these illustrate the support system for the grid, identifiable as the brown curved object in the foreground of the picture.

Figure 5.5. 3D Object: Concave in the Horizontal Direction, Vertical Normal

View From Above

Curved Support System for Grid in Position

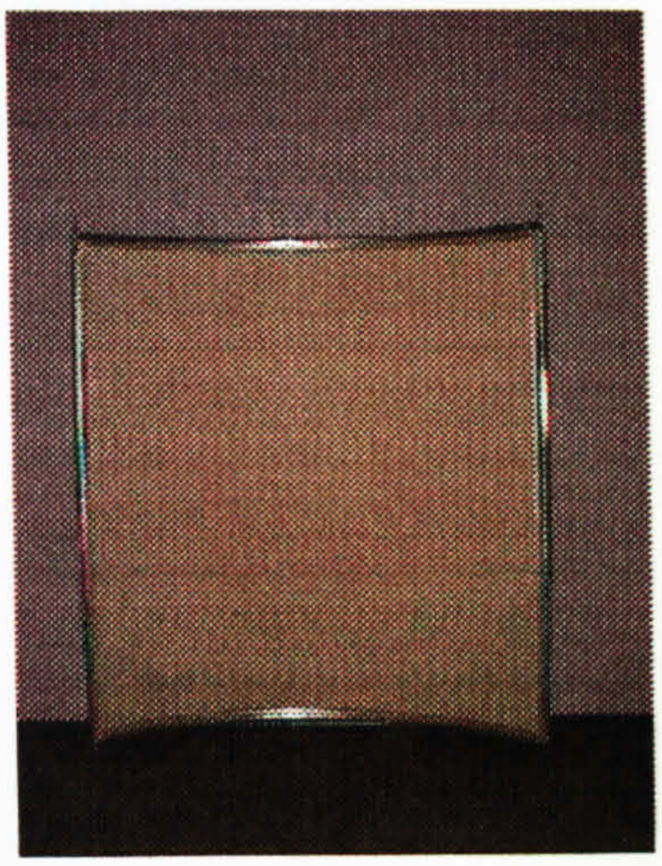

Figure 5.6. 3D Object: Concave in the Vertical Direction, Horizontal Normal

View From Left Side

Curved Support System for Grid in Position

Figure 5.7. 3D Object: Convex in the Horizontal Direction, Vertical Normal

View From Above

Curved Support System for Grid in Position

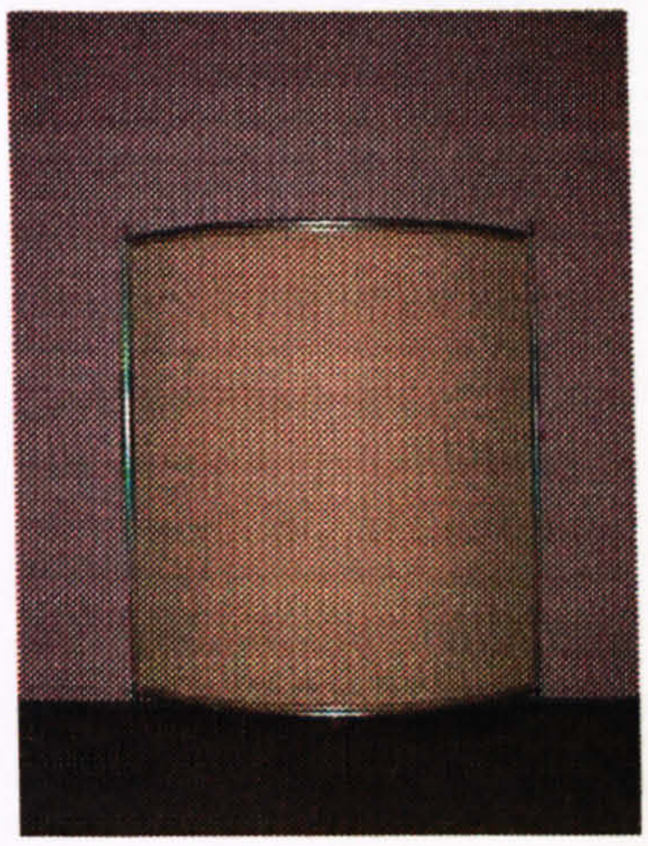

Figure 5.8. 3D Object: Convex in the Vertical Direction, Horizontal Normal

View Left Side

Curved Support System for Grid in Position

These 3D images were compared to a reference 2D grid image based on the control grid for the 2D stitching test.

5.8.9. Stitching Test

To test the accuracy of the stitching algorithm and the effect of the placement of the stitching points a series of images were used, both as originals and as test stitching files. A list of the images measured is as follows.

Image 1	A Original left view image B Original right view image
Image 2	Live stitch of the right & left images using point 1 at the centre of the top line, point 2 at the centre of the bottom line and point 3 on the centre row at the furthest line to the right.
Image 3	A repeat of image 2 to check the repeatability of the operator performing the selection of stitching points.
Image 4	Live stitch of the right & left images each point placed as for image 3 with the exception of point 3 which was placed on the centre row at the furthest line to the left.
Image 5	A repeat of image 4 to check the repeatability of the operator performing the selection of stitching points.
Image 6	Auto-align on a fresh image capture (align saved from Image 5 stitch)
Image 7	A repeat of image 6 to check the repeatability of the auto-align process.

To ensure an optimum stitch the capture system manufacturers recommend the stitching points to be located in the configuration described above. (I.e. placing point 1 at the top of the centre of the image, point 2 at the bottom of the centre of the image and point 3 at the centre but either to the extreme left or right of the image). This suggested configuration of points is due to the way in which the stitching process is undertaken (detailed further in Section 4.2.8). The variation in location of stitching points, therefore, relates only to whether a left or right placement makes any significant difference to the performance of the stitch.

5.8.10. Calibration Settings Test

To ascertain the effects of altering the calibration settings a number of tests were devised. These were based on increasing/decreasing two interdependent parameters at a time, to establish their effect on measured values. The choice of parameters and the intervals used were based upon knowledge acquired from one of the technical representatives at Wicks and Wilson Ltd. The intervals were designed to be such that they would provide a difference in the image capture process. Table 5.3 details the settings for each image undertaken. A base image was also taken for reference using the original settings, set during calibration, so that it may be used for comparative purposes.

Table 5.3. Calibration Values Used for the Setting Test

Settings	Original Value From Calibration	Amended Value For Test Purposes
Fringe Spacing (pixels) Field of View (mm) Image 1	10 608	10.04 618
Fringe Spacing (pixels) Field of View (mm) Image 2	10 608	9.96 598
Camera to Projector Height (mm) Fringe Spacing (pixels) Image 1	415 10	435 10.04
Camera to Projector Height (mm) Fringe Spacing (pixels) Image 2	415 10	395 9.96
Camera to Projector Depth (mm) Fringe Spacing (pixels) Image 1	0 10	30 10.06
Camera to Projector Depth (mm) Fringe Spacing (pixels) Image 2	0 10	-30 9.94
Camera to Projector Depth (mm) K1 (no units) Image 1	0 -0.05	30 0
Camera to Projector Depth (mm) K1 (no units) Image 2	0 -0.05	-30 -0.12
Camera to Projector Depth (mm) K2 (no units)	0 0.16	30 0.22
Camera to Projector Depth (mm) K2 (no units) Image 1	0 0.16	-30 0.10
Camera to System Centre (mm) K1 (no units)	2870 -0.05	2950 0
Camera to System Centre (mm) K1 Image 2 (no units)	2870 -0.05	2800 -0.10
Camera to System Centre (mm) K2 (no units)	2870 0.16	2950 0.21
Camera to System Centre (mm) K2 (no units)	2870 0.16	2800 0.11

(See section 4.2.6 for further information on the definitions of the calibration parameters).

Note that only the right view was considered in this test.

5.8.11. Vertical Grid Angle Position Test

This test was based upon changing the physical vertical angle of the target in respect to the Capture Unit. The test was undertaken at a distance of 145cm from the centre of the target to the Capture Unit. The 2D grid was used and the angle in the configuration setting remained at its original 50 degrees.

Image 1 10 degrees backwards

Image 2 20 degrees backwards

Image 3 30 degrees backwards

Image 4 10 degrees forwards

Image 5 20 degrees forwards

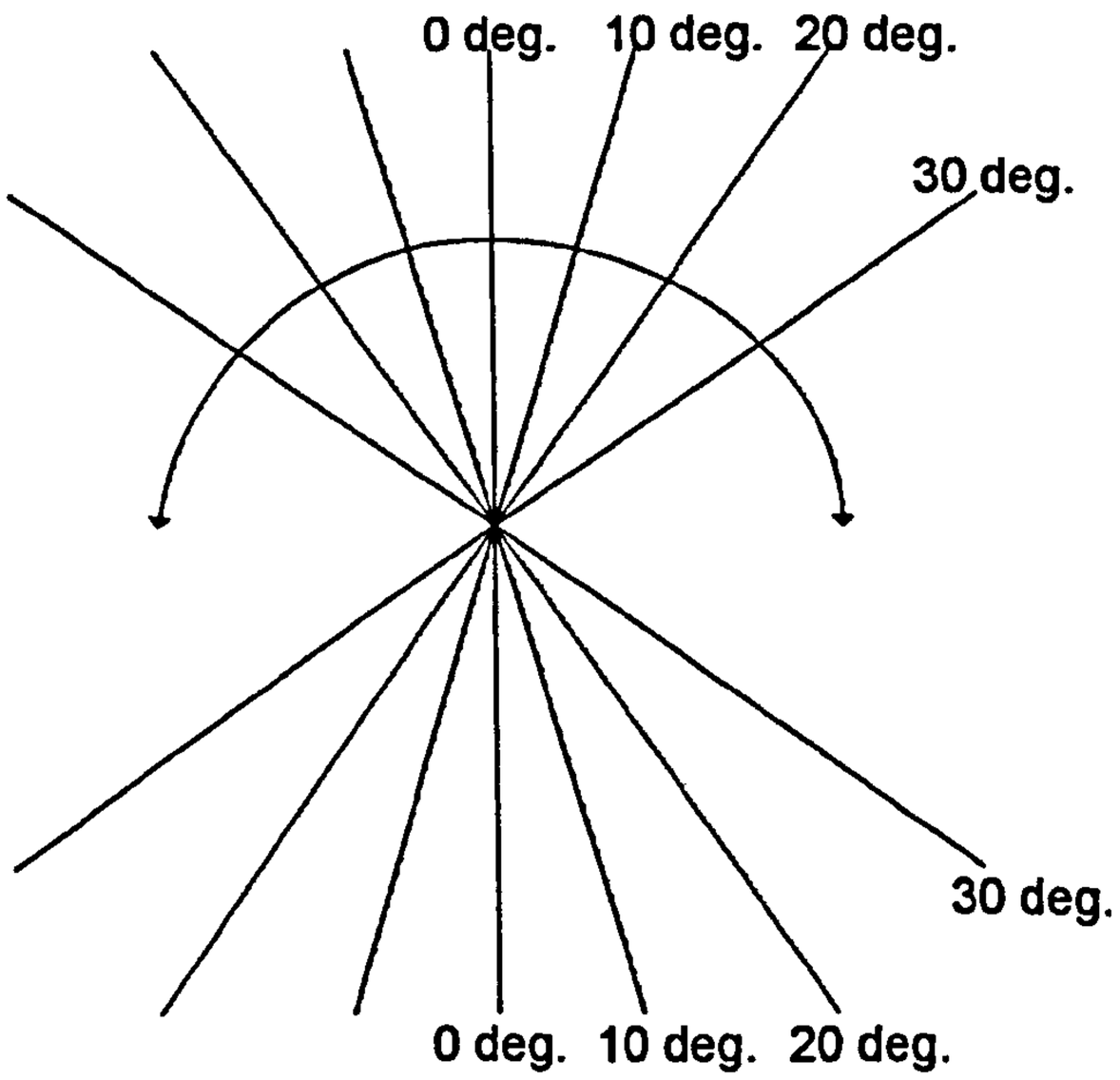

A control image was also taken with the grid directly facing the Unit, i.e. at 0 degrees. The same base image was also used for the angle in computer test (image 1 set at 50 degrees). The objective of the test was to establish whether the angle of the target object would affect the measured results.

5.8.12. Horizontal Grid Angle Position Test

As in the previous test the evaluation was based upon changing the physical angle of the target in respect to the Capture Unit, however in this instance the target object was rotated left to right as opposed to forwards and backwards. Again the test was undertaken at a distance of 145cm using the 2D grid. The following images were captured:

Image 1	10 degrees anti-clockwise
Image 2	20 degrees anti-clockwise
Image 3	30 degrees anti-clockwise
Image 4	10 degrees clockwise
Image 5	20 degrees clockwise
Image 6	30 degrees clockwise

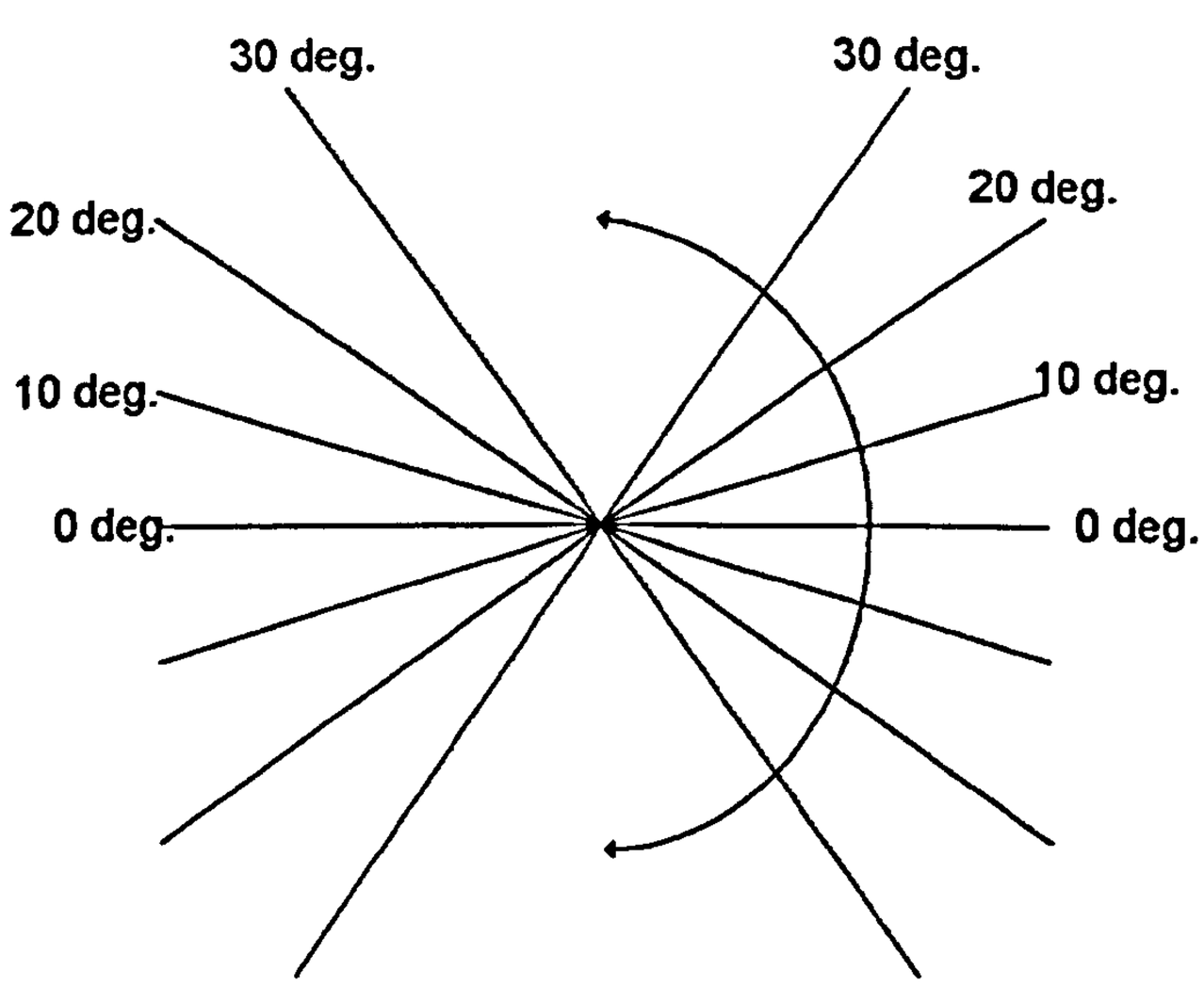

The same control image was used for both the vertical and horizontal grid angle position tests. The objective of the test was to establish whether the angle of the target object would affect the measured results and thus test the rigour of the cosine effect correction algorithms.

CHAPTER 6

THE PERFORMANCE OF THE SINGLE CAMERA TRIFORM™ SYSTEM

6.1. Results

A substantial number of results were generated by the test procedures. The results of primary importance have been selected for discussion, and appear in sections 6.1.1. - 6.1.13. The full results appear in complete form in Appendix D.

6.1.1. Operator Error Test

Table 6.1. Basic Statistics: Operator Error Test

View/ Direction	Measurement Type	Variant (Measurement of the image)	*n*	Mean (mm)	Standard Deviation (mm)	Standard Error of mean (mm)
Left/ Horizontal	Shortest	Base Grid	40	80.19	0.85	0.13
		Re-measure 1A	40	80.33	0.80	0.13
		Re-measure 2A	40	80.35	0.93	0.15
		Re-measure 3A	40	80.17	1.02	0.16
		Base Grid	40	80.23	0.86	0.14
		Re-measure 1C	40	80.38	0.78	0.12
		Base Grid	40	80.62	0.86	0.14
		Re-measure 1E	40	80.51	0.88	0.14
Left/ Vertical	Shortest	Base Grid	42	79.90	0.91	0.14
		Re-measure 1A	42	79.91	0.82	0.13
		Re-measure 2A	42	79.92	0.89	0.14
		Re-measure 3A	42	79.82	0.74	0.11
		Base Grid	42	79.80	0.82	0.13
		Re-measure 1C	42	79.85	0.77	0.12
		Base Grid	42	80.06	0.69	0.11
		Re-measure 1E	42	80.00	0.51	0.08
Right/ Horizontal	Shortest	Base Grid	40	78.26	1.08	0.17
		Re-measure 1B	40	78.32	0.76	0.12
		Base Grid	40	78.64	1.02	0.16
		Re-measure 1D	40	78.94	0.80	0.13
Right/ Vertical	Shortest	Base Grid	42	79.14	0.92	0.14
		Re-measure 1B	42	79.45	0.82	0.13
		Base Grid	42	79.85	0.82	0.13
		Re-measure 1D	42	79.75	0.65	0.10

n = the total number of measurements taken on each grid.

(See page 160 for the definition of each variant).

By analysis of the mean measurement results in Table 6.1 the repeat measurements of each grid, (regardless of direction or Unit) are very close to those recorded originally. The degree of variability noted by the standard deviation and standard error of the mean also appears to be very close for both the original and repeat measurements.

Table 6.2. Total Difference: Operator Error Test

Variant	Image				
Measurement of the image	Left Horizontal (mm) *n*=40	Left Vertical (mm) *n*=42	Right Horizontal (mm) *n*=40	Right Vertical (mm) *n*=42	Sum (mm)
Base Grid	28.0	30.9			58.9
Re-measure 1A	28.1	29.6			57.7
Re-measure 2A	32.5	30.9			63.4
Re-measure 3A	33.8	24.5			58.3
Base Grid			69.6	41.8	111.4
Re-measure 1B			67.4	33.1	100.5
Base Grid	29.6	27.7			57.3
Re-measure 1C	28.2	27.4			55.6
Base Grid			60.6	28.0	88.6
Re-measure 1D			44.3	23.5	67.8
Base Grid	32.1	24.5			56.6
Re-measure 1E	29.4	17.5			46.9

n = the total number of measurements taken on each grid.

To evaluate the repeatability of measurement by the operator the TD value for the base grid was compared with the TD value for the re-measure. The differences in TD values range from 0.6-9.7 for the left view and 10.9-20.8 for the right. The values for the left view are consistent between repeat measurements taken on the same image, however the results for the right view are relatively high by comparison. This suggests a further source of error is present, probably related to the measurement process for the right view as opposed to the image capture process, as the file remains the same in both instances. Whilst the errors related to the displacement of measurement points could have some bearing on the results it is unlikely that they would be manifested purely in the right view. A possible cause could therefore be a z error.

To identify and quantify the maximum operator error, re-measures 1A to 3A were compared against the original measurement readings for that grid to determine the maximum error at any one cell, shown in Table 6.3. (Note that this

is based on a left view image). The sign of the differences is shown in the table to indicate whether the difference was positive or negative (shown in brackets).

Table 6.3. Operator Error Differences by Measured Cell

		Horizontal					Vertical						
		0-4 cells	4-8 cells	8-12 cells	12-16 cells	16-20 cells	0-4 cells	4-8 cells	8-12 cells	12-16 cells	16-20 cells	20-24 cells	24-28 cells
1st line	Diff Orig v 1 (mm)	(-) 0 8	(-) 1	(-) 0.8	0 2	0	0	0.9	1 8	0	(-) 0.9	(-) 0 9	0.1
	Diff Orig v 2 (mm)	0	(-) 1.2	(-) 0 7	0 2	0	0 9	0.9	0 9	0	(-) 1.8	(-) 0 9	(-) 1
	Diff Orig v 3 (mm)	(-) 0 8	0.2	0.2	(-) 1.4	0	0 9	0 8	0.1	0	0.9	0	0
5th line	Diff Orig v 1 (mm)	(-) 0.4	(-) 0.7	0	(-) 0 9	(-) 0 9	1	(-) 0.9	(-) 0 9	0.9	0	1	(-) 0 8
	Diff Orig v 2 (mm)	(-) 0.1	(-) 1 8	0 9	(-) 1 9	0.1	1.1	(-) 1.1	(-) 1.7	0.9	0	1	(-) 2 9
	Diff Orig v 3 (mm)	0.8	(-) 0.7	(-) 0.1	(-) 1.1	(-) 0 9	0.1	0.8	(-) 0 8	0.9	0	1	(-) 2.9
9th line	Diff Orig v 1 (mm)	(-) 1.4	(-) 0.8	(-) 1.1	(-) 0.2	1.3	(-) 0 6	0 8	(-) 1	(-) 2 2	0.1	0	1 6
	Diff Orig v 2 (mm)	(-) 0 2	0 3	(-) 0 8	(-) 0.2	0.2	0.4	(-) 0.2	(-) 1	0.1	0.1	(-) 1.2	2 6
	Diff Orig v 3 (mm)	(-) 1.2	0.3	0.2	(-) 0.1	0.1	1.2	(-) 0.2	(-) 1	(-) 0.8	0.1	(-) 0.1	1 6
13th line	Diff Orig v 1 (mm)	0	0.2	(-) 0.2	0.1	0 9	(-) 0 9	1	0	0	1 8	(-) 1 8	(-) 0.6
	Diff Orig v 2 (mm)	0	0 2	(-) 1.1	1.1	(-) 0.1	(-) 0.9	(-) 1	1.9	1.9	1 8	(-) 0.9	0 2
	Diff Orig v 3 (mm)	0	0.2	(-) 0 2	0.1	(-) 0 2	0	1	0	0	1 8	(-) 0 9	(-) 0.9
17th line	Diff Orig v 1 (mm)	0	(-) 0.1	0 4	(-) 0 1	1.2	1.7	(-) 0 8	0.9	0 1	0	(-) 0 9	1
	Diff Orig v 2 (mm)	0	(-) 0.1	1.1	(-) 1.1	0 1	1.7	0	0.9	0.1	(-) 1.9	0 9	0.1
	Diff Orig v 3 (mm)	2	(-) 0.2	0.1	(-) 1.1	(-) 0 1	0.7	0.1	0	(-) 0.9	(-) 1	1	(-) 1
21st line	Diff Orig v 1 (mm)	2	0	(-) 1	0.9	(-) 1.1	(-) 0.2	(-) 0.9	0 9	0.1	(-) 1.1	0	(-) 1
	Diff Orig v 2 (mm)	2 2	0 3	0.1	1.7	(-) 2 2	(-) 1.1	(-) 0.8	0.9	0.1	(-) 1 9	0	(-) 0 1
	Diff Orig v 3 (mm)	2 2	0 3	(-) 1	0.7	(-) 1.1	(-) 0.2	1	0 9	0.1	(-) 2	1	(-) 0.1
25th line	Diff Orig v 1 (mm)	0	0	0 1	(-) 2	(-) 0.9							
	Diff Orig v 2 (mm)	0	0.1	0	(-) 0 9	(-) 1							
	Diff Orig v 3 (mm)	0	0 8	(-) 0 8	(-) 0 9	1 2							
29th line	Diff Orig v 1 (mm)	0 8	(-) 0 8	(-) 0.9	1.1	1 2							
	Diff Orig v 2 (mm)	1.8	(-) 0.6	(-) 1	0.2	(-) 2.3							
	Diff Orig v 3 (mm)	2.8	(-) 0.8	(-) 1	1	1 1							
Mean Absolute Error (mm)	0 69						0 80						
(regardless of sign)													
Std Dev. Overall	0 64						0 66						
Std. Error (mm)	0.06						0 06						
		Min	Max					Min	Max				
Range	Diff Orig v 1 (mm)	-2 00	2 00				Diff Orig v 1 (mm)	-2 20	1.80				
	Diff Orig v 2 (mm)	-2.30	2 20				Diff Orig v 2 (mm)	-1.90	1.90				
	Diff Orig v 3 (mm)	-1.40	2 80				Diff Orig v 3 (mm)	-2 00	1.80				
Mean TD based on 40 cells (mm)		27 5					Mean TD based on 42 cells (m		33 6				

N.B: The sign of the differences is shown to indicate negative and positive differences.

The results in Table 6.3 indicate maximum errors in the range of –2.30mm to +2.80mm for the horizontal direction and –2.20mm to +1.90mm for the vertical direction, however it is highly unlikely that the maximum error will occur to any significant degree as the error is shown to be random. Therefore the mean absolute error may be used. The mean absolute error was calculated by establishing the mean Total Difference divided by the number of measurements. The mean Total Difference was calculated by squaring, then square rooting the difference for each cell measurement, then summing these values. The product was then divided by three to provide the mean Total Difference, found to be 27.5mm in the horizontal direction and 33.6mm in the vertical direction. The mean absolute error was then calculated by dividing the mean Total Difference by the number of measurements within the grid.

The mean operator error was calculated to be 0.69mm in the horizontal direction and 0.80mm in the vertical direction, based on a measurement of 80mm. By evaluating the standard error of the mean these figures may be revised to 0.69±0.06mm for the horizontal direction and 0.80±0.06mm for the vertical direction. This is based upon quoting the standard error at full value, although according to Pentz & Shott (1988) the uncertainty should be quoted as 2/3rd's of the variability to reduce the likely over-estimation of the likely uncertainty. However even at 2/3rd's the error in the mean value is still over-estimated. Therefore the error may be revised with the mean quoted with 2/3rds of the variability of the uncertainty, to read 0.69±0.04mm and 0.80±0.04mm for the horizontal and vertical directions respectively, based on measurements taken over 80mm intervals.

The mean Total Difference for the operator error may be used as a basis for evaluating the TD results in other tests. The TD for the operator test refers directly to a comparison of a measured grid, which is then re-measured, and the results compared. For all other TD calculations the Total Difference is calculated

by comparing the true value to the measured value. Hence in this case the TD refers to the Total Difference from the true value and the contribution to the TD may be summarised as follows:

Total Difference from the true value = Instrumental error + Operator error

This approach assumes the operator error is random and the instrumental error is systematic. Within the operator error the point pitch error and the error related to the thickness of the lines on the grid will both be incorporated, as discussed in section 5.5. Any residual TD left once the operator error is accounted for may be regarded as instrumental error.

Table 6.4. Total Difference: Varying Dimensions Grid Test

Variant			
Grid size	Left Horizontal (mm) n=40	Left Vertical (mm) n=42	Sum (mm)
Varying Dimensions Grid	22.6	24.6	47.2

n = the total number of measurements taken on each grid.

When examining the results of the varying dimensions grid it may be seen that the Total Difference results are comparable to those found using a 80mm x 80mm sized grid. By comparing the TD results for the horizontal and vertical direction with those from the operator test both values were found to be within the limits of operator error. The issue of prior knowledge of the grid's dimensions in this investigation therefore are not identified as a factor in the influence introduced by the operator.

6.1.2. Directional Bias Test

Table 6.5. Basic Statistics: Directional Bias Test

View/Direction	Measurement Type	Variant (Measurement of the image)	*n*	Mean (mm)	Standard Deviation (mm)	Standard Error of mean (mm)
Left/Horizontal	Shortest	Base grid	40	80.23	0.86	0.14
Left/Horizontal	Shortest	Re-measure in opposite direction	40	80.11	0.80	0.13
Left/Vertical	Shortest	Base grid	42	79.80	0.82	0.13
Left/Vertical	Shortest	Re-measure in opposite direction	42	79.69	0.58	0.09

n = the total number of measurements taken on each grid.

Table 6.6. Total Difference: Directional Bias Test

Variant	Image		
Measurement of the image	Left Horizontal (mm) *n*=40	Left Vertical (mm) *n*=42	Sum (mm)
Base grid	29.6	27.7	57.3
Re-measure in opposite direction	25.8	20.9	46.7

n = the total number of measurements taken on each grid.

The impact of the direction in which each grid is measured was tested by the directional bias test. The results of this test indicate a good level of agreement in the basic statistics. The Total Difference readings are also comparable. Whilst there is a deviation in the Total Difference measurement readings it is not of any practical significance as the TD values are comparable to those of the operator error test. Hence the direction of measurement can not be seen as a factor which has any additional bearing on the influence of the operator.

6.1.3. View Comparison Test

Table 6.7. Basic Statistics: View Comparison Test

View/Direction	Measurement Type	*n*	Mean (mm)	Standard Deviation (mm)	Standard Error of mean (mm)
Left/Horizontal	Shortest	40	80.23	0.86	0.14
Right/Horizontal		40	78.64	1.02	0.16
Left/Vertical		42	79.80	0.82	0.13
Right/Vertical		42	79.85	0.82	0.13
Left/Horizontal	Surface	40	80.73	0.90	0.14
Right/Horizontal		40	79.01	0.99	0.16
Left/Vertical		42	80.75	0.95	0.15
Right/Vertical		42	80.56	0.88	0.14
Left/Horizontal	Tape Measure	40	80.54	0.87	0.14
Right/Horizontal		40	78.83	1.01	0.16
Left/Vertical		42	80.47	0.96	0.15
Right/Vertical		42	80.36	0.88	0.14

n = the total number of measurements taken on each grid.

As two views have been measured for the majority of the tests undertaken, it allows conclusions to be drawn and checked under a number of circumstances. The image used for the comparison was taken from the angle in computer test (50 degrees) to provide data on a base level without any alteration in the configuration parameters. The results indicate very close agreement in the vertical direction. However in the horizontal direction the left view measures in excess of the true value of 80mm whereas the right view measures smaller than the true value. The left view on average deviates by +0.23mm, +0.73mm and +0.54mm respectively, whereas the right view deviates by –1.36mm, -0.99mm and –1.17mm respectively, a trend mirrored in all results. Whilst the impact of any random error is reduced by averaging, the mean operator error of ±0.69mm would account for a sizeable proportion of the deviations, especially for the left view.

Table 6.8. Total Distance: View Comparison Test

Variant	Image		
	Horizontal *n*=40	Vertical *n*=42	Sum
Left View	29.6	27.7	57.3
Right View	60.6	28.0	88.6

Upon examination of the TD, the horizontal value for the right image is notably larger (at 60.6) than that for the vertical directions of both images (27.7 for the left image and 28.0 for the right) and the horizontal direction (at 29.6) for the left image. Whilst the TD results for both views in the vertical direction and the horizontal direction for the right view are comparable to the results of the operator error test, the TD results for the horizontal direction in the right view exceeds the 27.5mm which may be attributed to operator error. The residual TD that is left once the operator error is accounted for has been calculated as 33.1mm this residual may be attributed to instrumental error.

Figures 6.1 and 6.2 clearly illustrate the difference between the two views. Whilst the left view appears to have very good agreement with the true value, the right image has good agreement in the vertical direction but relatively poor agreement in the horizontal. On each image s-shaped distortion is apparent, however the distortion is distinctly more pronounced in the right image, which may to some degree account for the poor results in the horizontal direction.

Figure 6.1. True vs. Measured Values: View Comparison Test - Left View

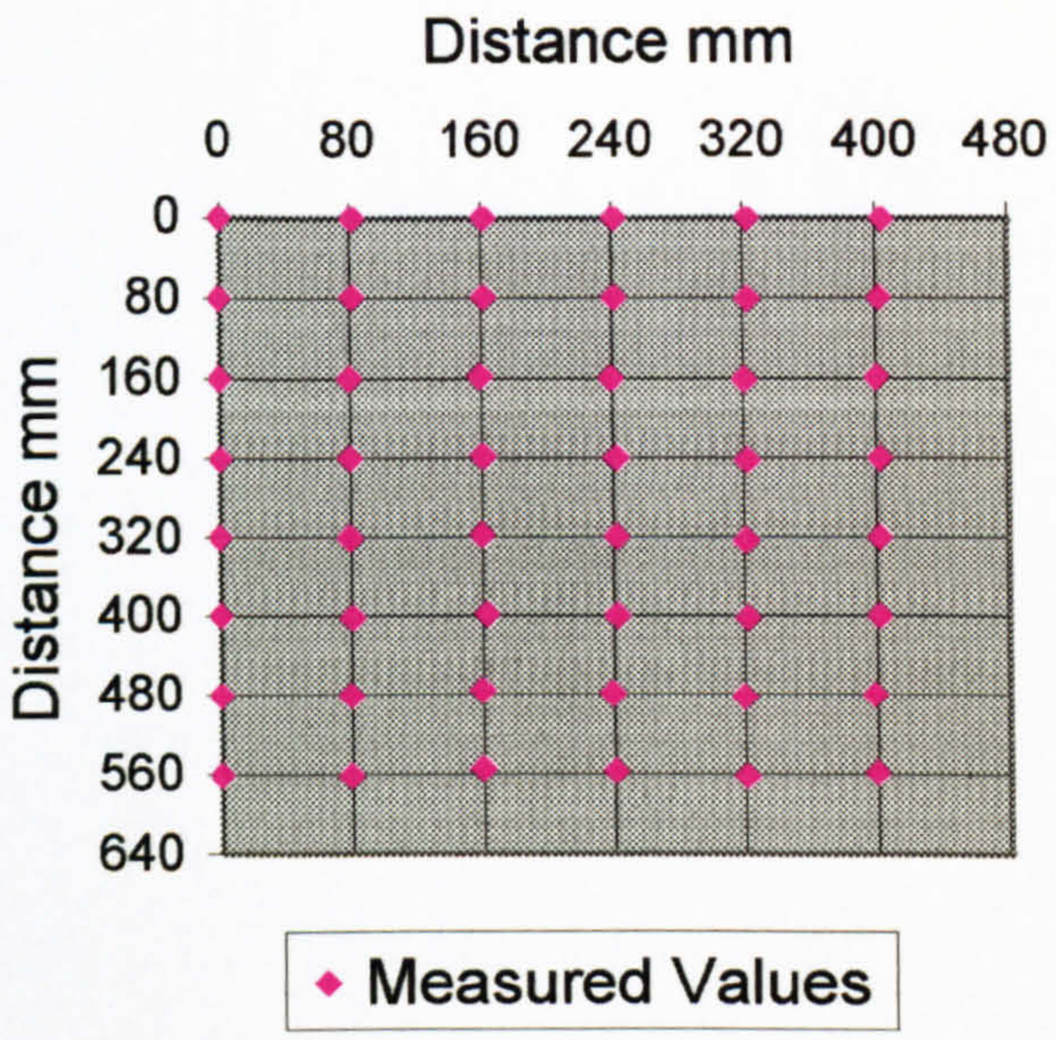

Figure 6.2. True vs. Measured Values: View Comparison Test - Right View

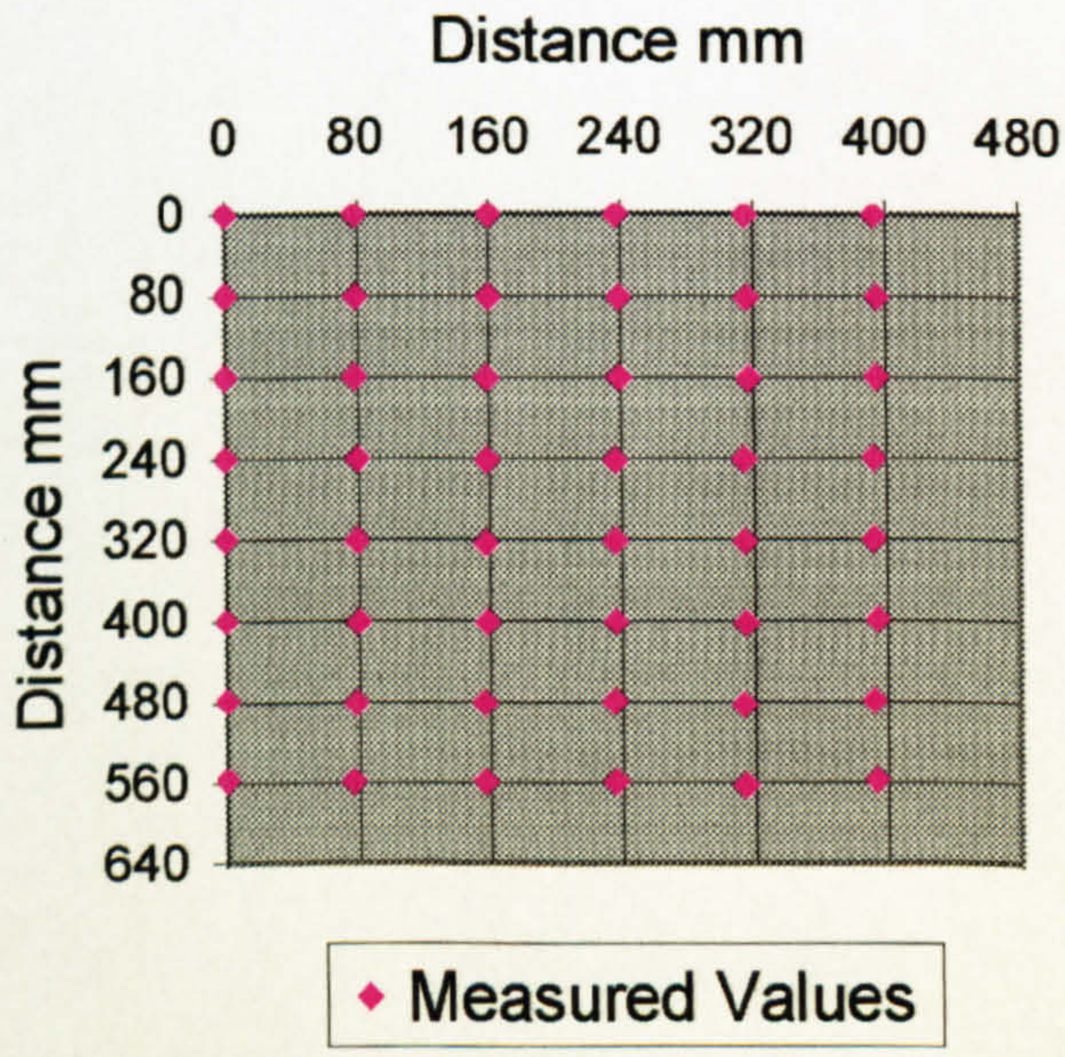

6.1.4. Distance Test

Table 6.9. Basic Statistics: Distance Test

View/ Direction	Measurement Type	Variant (Distance from Capture Unit, cm)	*n*	Mean (mm)	Standard Deviation (mm)	Standard Error of mean (mm)
Left/ Horizontal	Shortest	171cm	32	80.12	0.96	0.17
		145cm (base grid)	40	80.19	0.85	0.13
		100cm	14	80.96	0.92	0.25
Left/ Vertical	Shortest	171cm	35	79.86	1.02	0.17
		145cm (base grid)	42	79.90	0.91	0.14
		100cm	18	80.18	0.57	0.13
Right/ Horizontal	Shortest	171cm	40	79.10	0.74	0.12
		145cm (base grid)	40	78.26	1.08	0.17
		100cm	14	78.32	0.57	0.15
Right/ Vertical	Shortest	171cm	42	80.04	1.13	0.17
		145cm (base grid)	42	79.14	0.92	0.14
		100cm	18	79.04	0.85	0.20

n = the total number of measurements taken on each grid.

The basis statistics at each distance provide similar results when each view is compared independently; hence distance was not found to be a significant factor in the accuracy of measured values. The variability in the standard deviation and standard error of the mean is most likely due to the varying number of results used for the calculation of the statistics.

6.1.5. Angle in Computer Test

Table 6.10. Basic Statistics: Angle in Computer Test

View/Direction	Measurement Type	Variant (Angle setting, degrees)	*n*	Mean (mm)	Standard Deviation (mm)	Standard Error of mean (mm)
Left/Horizontal	Shortest	0°	40	80.51	1.09	0.17
		50° (base grid)	40	80.23	0.86	0.14
		100°	40	80.70	0.83	0.13
Left/Vertical	Shortest	0°	42	80.32	0.95	0.15
		50° (base grid)	42	79.80	0.82	0.13
		100°	42	79.83	0.93	0.14
Right/Horizontal	Shortest	0°	40	78.90	0.90	0.14
		50° (base grid)	40	78.64	1.02	0.16
		100°	40	78.71	1.14	0.18
Right/Vertical	Shortest	0°	42	79.74	1.34	0.21
		50° (base grid)	42	79.85	0.82	0.13
		100°	42	79.82	0.89	0.14

n = the total number of measurements taken on each grid.

No notable difference is apparent between the basic statistics following each angle change, with the mean, standard deviation and standard error of the mean remaining consistent regardless of the angle set in the configuration parameters.

Table 6.11. Total Difference: Angle in Computer Test

Variant	Image				
Angle setting (degrees)	Left Horizontal (mm) *n*=40	Left Vertical (mm) *n*=42	Right Horizontal (mm) *n*=40	Right Vertical (mm) *n*=42	Sum (mm)
0°	40.8	33.3			74.1
50° (base grid)	29.6	27.7			57.3
100°	35.0	32.8			67.8
0°			47.2	31.2	78.4
50° (base grid)			60.6	28.0	88.6
100°			56.4	29.5	85.9

n = the total number of measurements taken on each grid.

For the vertical direction in both the left and right views the Total Difference results are not notably affected by the change in angle setting, as the value of the TD may be accounted for by the anticipated operator error. For the horizontal direction in the right view changing the angle setting appears to improve the agreement with the true value from 60.6 at 50 degrees to 47.2 at 0 degrees and 56.4 at 100 degrees. Conversely for the left view in the horizontal direction the TD increases from 29.6 at 50 degrees to 40.8 at 0 degrees and 35.0 at 100 degrees, indicating an instrumental error which is related to the angle setting.

6.1.6. Image Enlargement Test

Table 6.12. Basic Statistics: Image Enlargement Test

View/Direction	Measurement Type	Variant (%magnification)	*n*	Mean (mm)	Standard Deviation (mm)	Standard Error of mean (mm)
Left/Horizontal	Shortest	0% (base grid)	40	80.19	0.85	0.13
Left/Vertical	Shortest	0% (base grid)	42	79.90	0.91	0.14
Left/Horizontal	Shortest	25%	40	80.28	0.59	0.09
Left/Vertical	Shortest	25%	42	79.97	0.55	0.08

n = the total number of measurements taken on each grid.

Table 6.13. Total Difference: Image Enlargement Test

Variant	Image		
% magnification	Left Horizontal (mm) *n*=40	Left Vertical (mm) *n*=42	Sum (mm)
0% (base grid)	28.0	30.9	58.9
25%	20.3	19.0	39.3

n = the total number of measurements taken on each grid.

Enlarging the image for ease of measurement does not appear to have any detrimental affect on measured values. The basic statistics display a reduction in both the standard deviation and standard error of the mean indicating greater agreement between measured results. These findings reflect those shown in the

Total Difference calculations which suggests enlarging the image improves measurement consistency.

6.1.7. Rotation Test

Table 6.14. Basic Statistics: Rotation Test

View/Direction	Measurement Type	Variant (Rotation, degrees)	*n*	Mean (mm)	Standard Deviation (mm)	Standard Error of mean (mm)
Left/Horizontal	Shortest	0° (base grid)	40	80.19	0.85	0.13
		15°clockwise	40	80.31	0.66	0.10
		15° anti-clockwise	40	80.37	0.71	0.11
Left/Vertical	Shortest	0° (base grid)	42	79.90	0.91	0.14
		15° forwards	42	79.96	0.60	0.09
		15° backwards	42	80.07	0.60	0.09

n = the total number of measurements taken on each grid.

By rotating the images either clockwise, anti-clockwise, forwards or backwards no notable change may be noted in the measurements between those taken at the original position and those taken at each of the four new positions.

Table 6.15. Total Difference: Rotation Test

Variant	Image	
Rotation (degrees)	Left Horizontal (mm) *n*=40	Left Vertical (mm) *n*=42
0° (base grid)	28.0	30.9
15° clockwise	23.6	
15° anti-clockwise	26.3	
15° forwards		20.1
15° backwards		21.5

n = the total number of measurements taken on each grid.

The TD results appear consistent for the rotations made in the clockwise and anti-clockwise directions, with an apparent decrease in the TD for both the

forwards and backwards rotations. Indicating that rotating the image has no particular detrimental affect on measured values.

6.1.8. Planar Differences Test

Table 6.16. Basic Statistics: Planar Differences Test

View/ Direction	Measurement Type	Variant (Surface)	*n*	Mean (mm)	Standard Deviation (mm)	Standard Error of mean (mm)
Left/ Horizontal	Surface	2D (base grid)	40	81.16	0.86	0.14
		Concave Horizontal	36	80.70	0.80	0.13
		Concave Vertical	40	80.64	0.85	0.13
		Convex Horizontal.	36	80.88	0.70	0.12
		Convex Vertical.	40	80.31	0.37	0.06
Left/ Vertical	Surface	2D (base grid)	42	80.95	0.96	0.15
		Concave Horizontal	35	81.14	0.84	0.14
		Concave Vertical	42	80.60	0.84	0.13
		Convex Horizontal.	28	80.81	0.70	0.13
		Convex Vertical.	42	80.41	0.65	0.10
Right/ Horizontal	Surface	2D (base grid)	40	79.36	0.88	0.14
		Concave Horizontal	36	79.35	1.04	0.17
		Concave Vertical	40	79.12	0.71	0.11
		Convex Horizontal.	36	79.12	0.73	0.12
		Convex Vertical.	40	79.68	0.45	0.07
Right/ Vertical	Surface	2D (base grid)	42	80.72	0.63	0.10
		Concave Horizontal	35	80.83	0.94	0.16
		Concave Vertical	42	80.15	0.73	0.11
		Convex Horizontal.	36	80.12	0.52	0.09
		Convex Vertical.	42	80.52	0.65	0.10

n = the total number of measurements taken on each grid.

Upon examination of the basic statistics, the results for the planar differences test display no distinct difference between the 2D and 3D results. Only slight differences exist, such as the convex vertical when measured in the horizontal direction, which displays a lower standard deviation (0.37 and 0.45) and

therefore a lower standard error of the mean (0.06 and 0.07) for the left and right views respectively.

Table 6.17. Total Difference: Planar Differences Test

Variant	Image				
Surface	Left Horizontal (mm) *n*=24	Left Vertical (mm) *n*=30	Right Horizontal (mm) *n*=24	Right Vertical (mm) *n*=30	Sum (mm)
2D (base grid)	25.3	35.9			61.2
Concave Horizontal	27.1	25.9			53.0
Concave Vertical	20.9	25.7			46.6
Convex Horizontal	21.1	22.2			43.3
Convex Vertical	8.6	20.1			28.7
2D (base grid)			22.5	25.2	47.7
Concave Horizontal			21.2	22.6	43.8
Concave Vertical			23.0	19.5	42.5
Convex Horizontal			11.4	28.3	39.7
Convex Vertical			9.7	23.5	33.2

n = the total number of measurements taken on each grid.

Note the TD is calculated using surface distance measurements.

The TD results mirror those found within the basic statistics in that, the overall TD's between the left and right views are comparable. The Total Difference results indicate improved agreement with the true value when changing from a 2D to a 3D object. By comparing the surfaces, the performance for both views can be rated as the 2D surface showing the greatest deviation from the true value, followed by the concave horizontal, concave vertical and convex horizontal, with the convex vertical surface having the least deviation from the true value.

6.1.9. Stitching Test

Table 6.18. Basic Statistics: Stitching Test

View/ Direction	Measurement Type	Variant (Image)	*n*	Mean (mm)	Standard Deviation (mm)	Standard Error of mean (mm)
Left/ Horizontal	Shortest	Base grid Image 1 A	40	80.62	0.86	0.14
Left/ Vertical	Shortest	Base grid Image 1 A	42	80.06	0.69	0.11
Right/ Horizontal	Shortest	Base grid Image 1 B	40	78.85	0.85	0.13
Right/ Vertical	Shortest	Base grid Image 1 B	42	79.93	0.63	0.10
N/A	Shortest	Live stitch Image 2	40	79.68	1.01	0.16
		Live stitch Image 3	40	79.60	1.26	0.20
		Live stitch Image 4	40	80.02	0.97	0.15
		Live stitch Image 5	40	80.13	0.71	0.11
		Auto align Image 6	40	79.34	1.43	0.23
		Auto align Image 7	40	80.23	1.26	0.20

n = the total number of measurements taken on each grid.

(See pages 158-159 for the definition of each variant).

Upon examination of the basic statistics the mean values of each image are consistent with one another, with the stitched image mean values being very similar to those for the original images. The standard deviation and standard error of the mean for the stitched images however are generally higher than the original left and right view images. It is quite likely that this is due to variability occurring in measurements taken around the stitching line of the image and hence it is disguised by averaging, but is illustrated by the measures of variability. In addition to this, the impact of stitching together two views which are dimensionally different (illustrated by comparing the left and right base grid statistics) will undoubtedly have an effect on the variability of measured values.

Table 6.19. Total Difference: Stitching Test

Variant	View		
Image	Horizontal (mm) *n*=40	Vertical (mm) *n*=42	Sum (mm)
Base grid left	32.1	24.5	56.6
Base grid right	46.6	25.1	71.7
Live stitch Image 2	34.5	16.9	51.4
Live stitch Image 3	36.4	19.4	55.8
Live stitch Image 4	33.6	19.3	52.9
Live stitch Image 5	22.2	18.6	40.8
Auto align Image 6	43.7	18.2	61.9
Auto align Image 7	34.7	17.4	52.1

n = the total number of measurements taken on each grid.

From the Total Difference results the greatest variability is generally shown in the horizontal direction. As the single images (base grid left and right) show the greatest difference in the horizontal direction it is logical that this would be carried forward into the stitched image. Whilst the TD in the vertical direction may be accounted for by the operator error, the TD in the horizontal direction exceeds that which may be accounted for by the operators influence, indicating the presence of an instrumental error. The TD results for each of the stitched images are comparable to those shown for the single images, indicating that the stitching process has no notable effect on measured values. Any apparent differences in the TD could be due to stitching together two views that are dimensionally different or the repeatability of the stitching process. In this case it is highly likely that the operator's influence in the reselection of alignment points is also responsible for the difference.

When comparing images 2 and 4, which were aligned using differently placed points, no notable difference in the TD results may be identified. Thus the position of the points may be also be discounted as a potential source of error, on the basis that the positioning follows the specific set of rules, set out in section 4.2.8

6.1.10. Calibration Settings Test

Table 6.20. Basic Statistics: Settings Test

View/Direction	Measurement Type	Variant (Calibration settings)	*n*	Mean (mm)	Standard Deviation (mm)	Standard Error of mean (mm)
Right/ Horizontal	Shortest	Base Grid (no change in any settings)	40	78.91	0.76	0.12
		Fr Sp-Fld View Image 1	40	80.10	0.99	0.16
		Fr Sp-Fld View Image 2	40	77.80	0.73	0.12
		Cam to Prj Ht-Fr Sp Image 1	40	78.88	0.72	0.11
		Cam to Prj Ht-Fr Sp Image 2	40	79.01	0.84	0.13
		Cam to Prj Dp-Fr Sp Image 1	40	79.01	1.59	0.25
		Cam to Prj Dp-Fr Sp Image 2	40	79.02	0.86	0.14
		Cam to Prj Dp-K1 Image 1	40	78.83	0.82	0.13
		Cam to Prj Dp-K1 Image 2	40	78.88	0.76	0.12
		Cam to Prj Dp-K2 Image 1	40	78.62	0.95	0.15
		Cam to Prj Dp-K2 Image 2	40	79.17	0.77	0.12
		Cam to Sys C-K1 Image 1	40	79.41	0.75	0.12
		Cam to Sys C-K1 Image 2	40	78.66	0.70	0.11
		Cam to Sys C-K2 Image 1	40	79.68	0.62	0.10
		Cam to Sys C-K2 Image 2	40	78.72	0.85	0.13

n = the total number of measurements taken on each grid.

Basic Statistics (cont.)

View/Direction	Measurement Type	Variant (Calibration settings)	*n*	Mean (mm)	Standard Deviation (mm)	Standard Error of mean (mm)
Right/ Vertical	Shortest	Base Grid	42	79.84	0.83	0.13
		Fr Sp-Fld View Image 1	42	80.87	1.07	0.17
		Fr Sp-Fld View Image 2	42	78.89	0.54	0.08
		Cam to Prj Ht-Fr Sp Image 1	42	80.41	0.75	0.12
		Cam to Prj Ht-Fr Sp Image 2	42	79.41	0.59	0.09
		Cam to Prj Dp-Fr Sp Image 1	42	83.53	3.15	0.49
		Cam to Prj Dp-Fr Sp Image 2	42	80.10	1.16	0.18
		Cam to Prj Dp-K1 Image 1	42	80.20	0.80	0.12
		Cam to Prj Dp-K1 Image 2	42	79.81	1.01	0.16
		Cam to Prj Dp-K2 Image 1	42	79.98	0.84	0.13
		Cam to Prj Dp-K2 Image 2	42	80.32	1.24	0.19
		Cam to Sys C-K1 Image 1	42	80.16	0.62	0.10
		Cam to Sys C-K1 Image 2	42	79.96	0.67	0.10
		Cam to Sys C-K2 Image 1	42	80.24	0.52	0.08
		Cam to Sys C-K2 Image 2	42	80.04	0.73	0.11

n = the total number of measurements taken on each grid.

(See page 113 for the definition of each variant).

The basic statistics for the settings test display a greater degree of variability than previous tests, particularly in terms of both the mean and standard deviation. One would expect such results due to the fact that changing the calibration settings is known to affect the capture process and hence the measured values (as described in section 4.2.6.). However it is the assessment of the actual effect on measured values caused by altering specific calibration variables that is of

interest. The Total Difference is the clearest measure of the effect that changing these calibration settings has, the results of which are detailed below. Note that for each setting, image 1 refers to an increase in the calibration settings, whereas image 2 refers to a decrease, each change being of the same magnitude in either direction.

Table 6.21. Total Difference: Settings Test

Variant	Image		
Calibration settings	Right Horizontal (mm) *n*=40	Right Vertical (mm) *n*=42	Sum (mm)
Base Grid	46.6	25.1	71.7
Fr Sp-Fld View Image 1	32.7	46.0	78.7
Fr Sp-Fld View Image 2	88.1	46.7	134.8
Cam to Prj Ht-Fr Sp Image 1	45.9	29.3	75.2
Cam to Prj Ht-Fr Sp Image 2	44.5	28.5	73.0
Cam to Prj Dp-Fr Sp Image 1	60.4	166.7	227.1
Cam to Prj Dp-Fr Sp Image 2	43.6	42.2	85.8
Cam to Prj Dp-K1 Image 1	49.9	27.8	77.7
Cam to Prj Dp-K1 Image 2	47.8	33.9	81.7
Cam to Prj Dp-K2 Image 1	56.9	27.2	84.1
Cam to Prj Dp-K2 Image 2	38.2	46.1	84.3
Cam to Sys C-K1 Image 1	30.8	21.5	52.3
Cam to Sys C-K1 Image 2	50.4	22.8	76.8
Cam to Sys C-K2 Image 1	23.9	17.2	41.1
Cam to Sys C-K2 Image 2	52.3	25.9	78.2

n = the total number of measurements taken on each grid.

By changing the calibration settings one would expect the Total Difference results to exceed that accounted for by the operator's influence in measurement, hence the comparisons for the TD results will focus comparing results once a change in the value of a calibration variable has taken place.

Fringe spacing – Field of View

By examining the effect of changing the Fringe Spacing and Field of View an increase in their values results in a small increase in the TD, whereas a decrease

in their values shows a notable increase in the TD. In both cases an increase in the vertical TD is apparent, however, the greatest impact is made in the horizontal direction, this is shown in the Total Difference table and in Figures 6.4. and 6.5. An increase in the settings for the Fringe Spacing and Field of View shows an improvement in the agreement with the true values in the horizontal direction by increasing the values slightly. However, in the vertical direction the values have increased to move the measured values further away from the true values. For a decrease in the value of the settings the converse is true, as the horizontal values have decreased from the original as have the vertical values, indicating why the TD for both the horizontal and vertical directions has increased.

Camera to Projector Height – Fringe Spacing

The Camera to Projector Height and Fringe Spacing show comparable TD results for both an increase and decrease in settings values, indicating that these variables in combination have a relatively minor effect on measured values, based upon the magnitude of change made to the settings in this instance. (See Figures 6.6 and 6.7)

Camera to Projector Depth – Fringe Spacing

The TD values for the Camera to Projector Depth and Fringe Spacing setting changes can be noted both from the table and also Figures 6.8 and 6.9. An increase in these values results in an increase in the horizontal TD, but more dramatically the vertical TD. Figure 6.8 illustrates how the vertical values have been increased away from the true values and also the deviation of the horizontal values indicates a non-uniform change. The greatest impact being made towards the bottom of the grid. By decreasing the values for the settings, however, the converse does not occur to the same magnitude. With the exception of the

increase in the movement of vertical values away from the true values the results are comparable with the original, any deviation being due to the movement of vertical values.

The Camera to Projector Depth setting is known to alter the z scaling in relation to x and y, as discussed in section 4.2.6, although its exact relationship to x and y is unknown, as the variable is not used in calibration by the manufacturers. The change in these settings illustrates a non-linear impact on measured values, as shown by the results. Hence the large difference in the TD results for this test, as an increase in this variable will not necessarily result in the same changes to measured values as a decrease.

Camera to Projector Depth – K1

When the Camera to Projector Depth is altered with the K1 setting the results remain comparable with the base grid with little change in the TD value. Figures 6.10 and 6.11, which illustrate the measured values against the true values also indicate little change when compared to the base grid. The conclusion that may be drawn therefore is that these variables in combination have a relatively minor effect on measurements values, based upon the magnitude of change made to the settings in this instance.

Camera to Projector Depth – K2

For the change in the Camera to Projector Depth and K2 settings the TD results are affected differently according to whether an increase or decrease was made in the value of the settings. For an increase in the settings the horizontal TD increases and the vertical TD increases fractionally. The shift in the measured horizontal values may be noted in Figure 6.12, as the measured values in the top right-hand corner in particular deviate away from the true values. For the

decrease in the value of the settings the TD for the horizontal direction has decreased, whilst the vertical difference has increased. Figure 6.13 illustrates the displacement of vertical measurements away from the true values.

The relationship that the Camera to Projector Depth setting has on measured values is non-linear, hence the results differ in magnitude when either increasing or decreasing this variable.

Camera to System Centre – K1

The TD results for the change in the Camera to System Centre and K1 settings indicate a decrease in the TD for the horizontal direction and a decrease in the vertical for an increase in the value of the settings. The shift in values is illustrated in Figure 6.14. Conversely when the settings are decreased the horizontal TD increases whilst the vertical TD remains similar to the original. The main difference illustrated in Figure 6.15 is the alteration in the degree of s-shaped distortion.

Camera to System Centre – K2

An increase in the value of the settings has reduced the overall TD to 41.1, with a greater improvement shown in the horizontal direction when compared to the findings for the Camera to System Centre and K1. Upon examination of Figure 6.16 a slight amount of s-shaped distortion is still noticeable however the majority has been removed and hence the overall matching of the measured and true values is much improved when compared to the base grid. Once the values for the settings are decreased the horizontal TD increases, whereas the values for the vertical TD stay approximately the same. The shift in values may be noted in Figure 6.17.

Figure 6.3. True vs. Measured Values: Settings Test - Base Grid

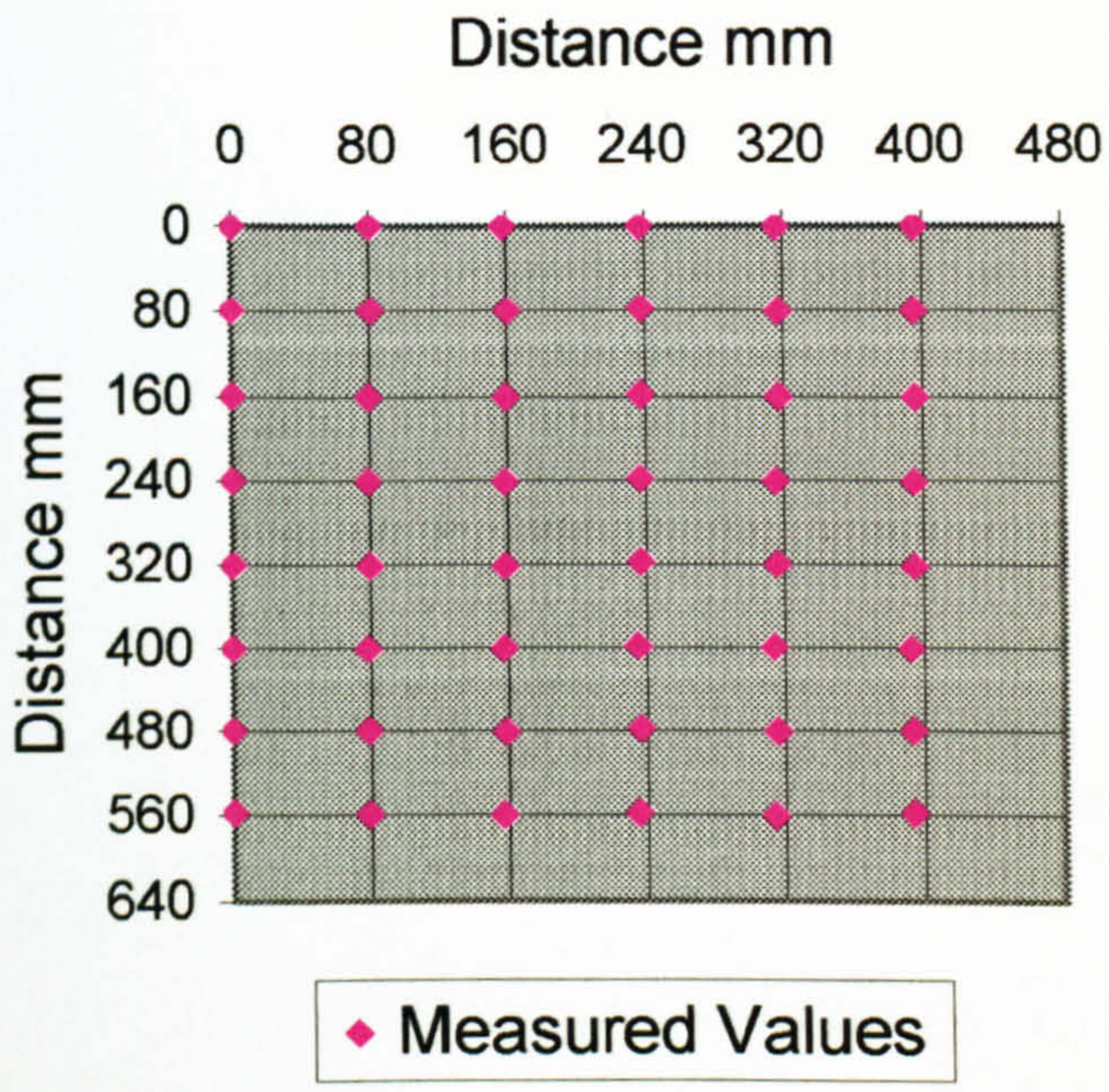

Figure 6.4. True vs. Measured Values: Settings Test - Fringe Spacing - Field of View Image 1

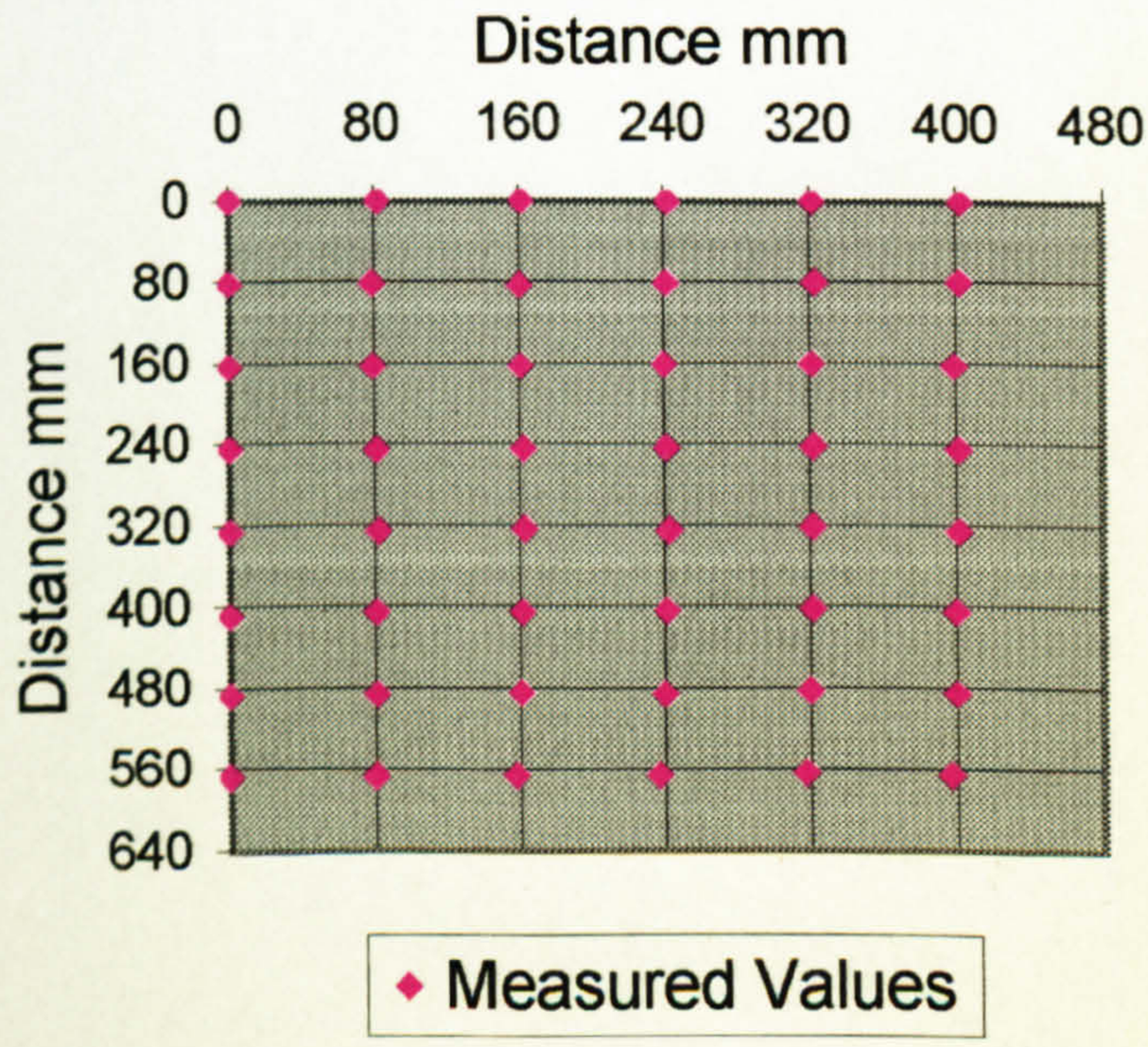

Figure 6.5. True vs. Measured Values: Settings Test - Fringe Spacing - Field of View Image 2

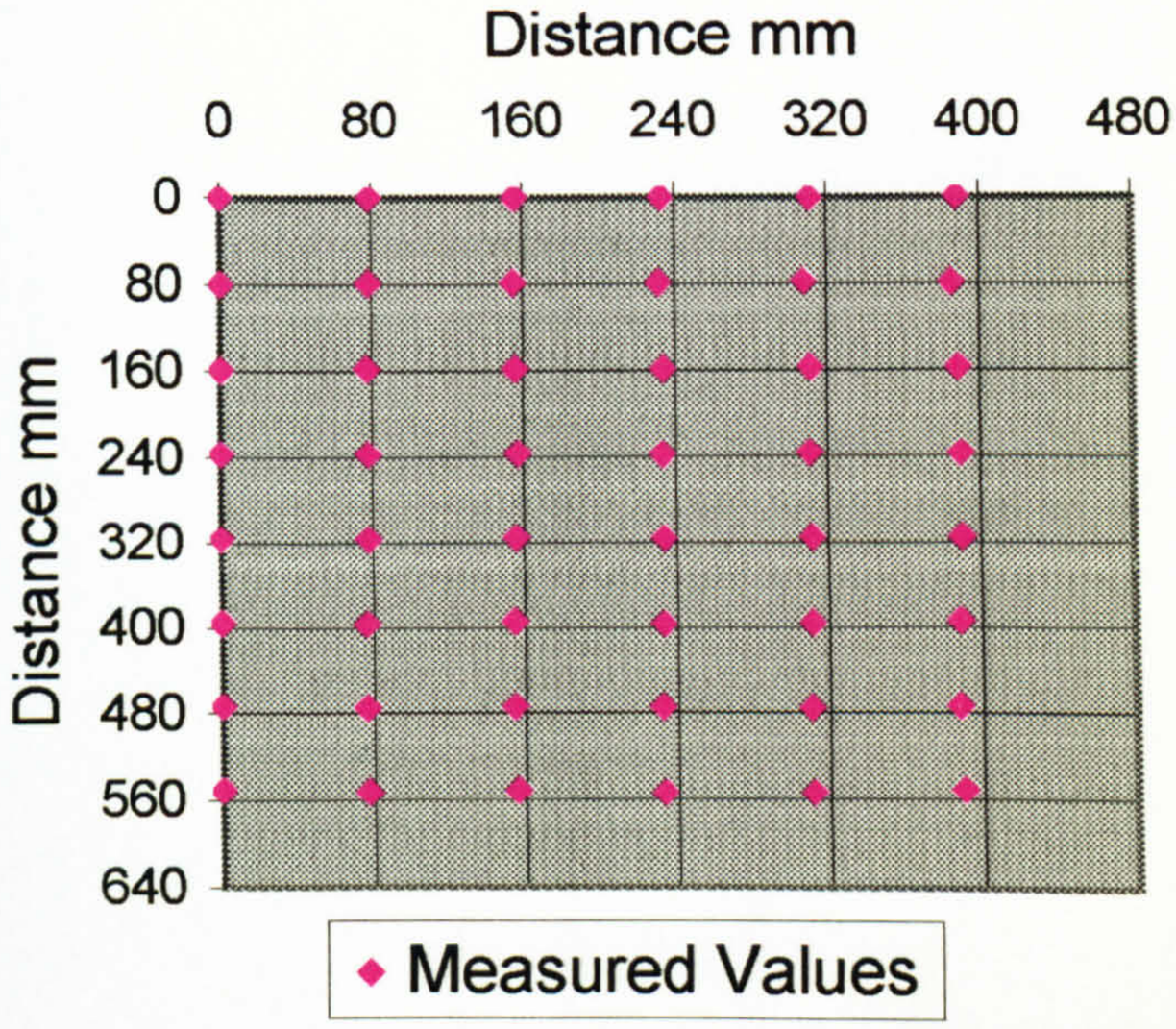

Figure 6.6. True vs. Measured Values: Settings Test - Camera to Projector Height - Fringe Spacing Image 1

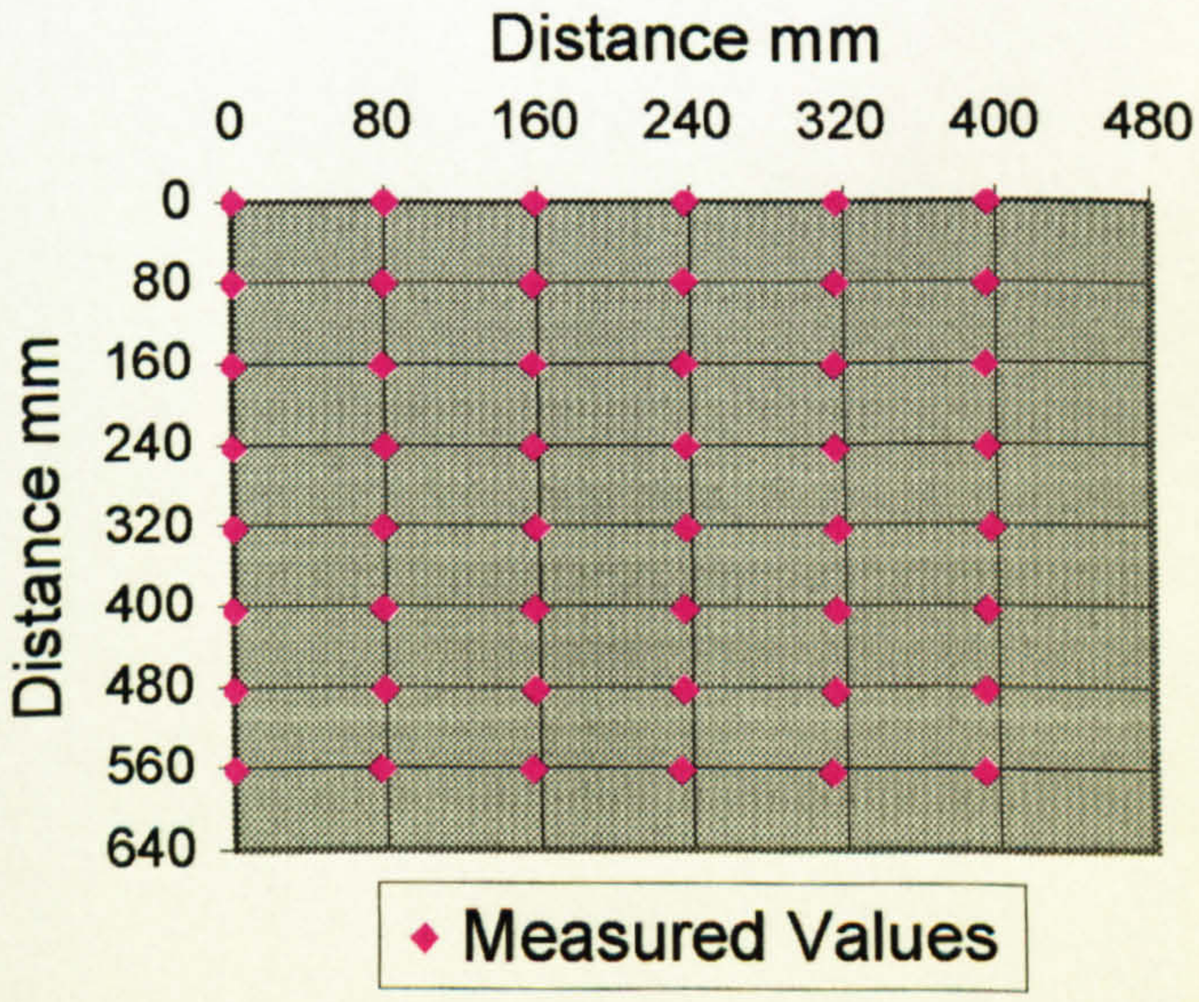

Figure 6.7. True vs. Measured Values: Settings Test - Camera to Projector Height - Fringe Spacing Image 2

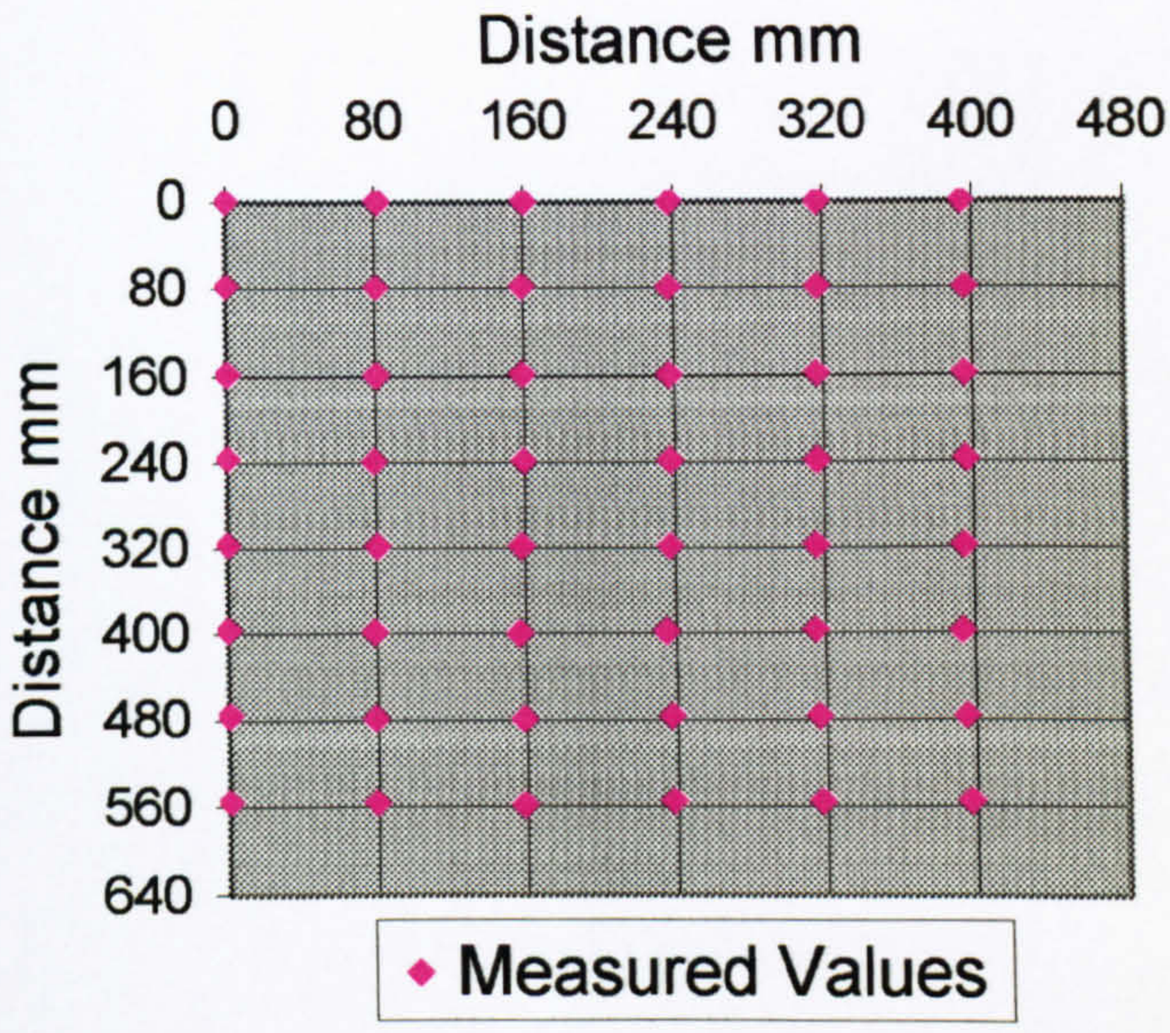

Figure 6.8. True vs. Measured Values: Settings Test - Camera to Projector Depth - Fringe Spacing Image 1

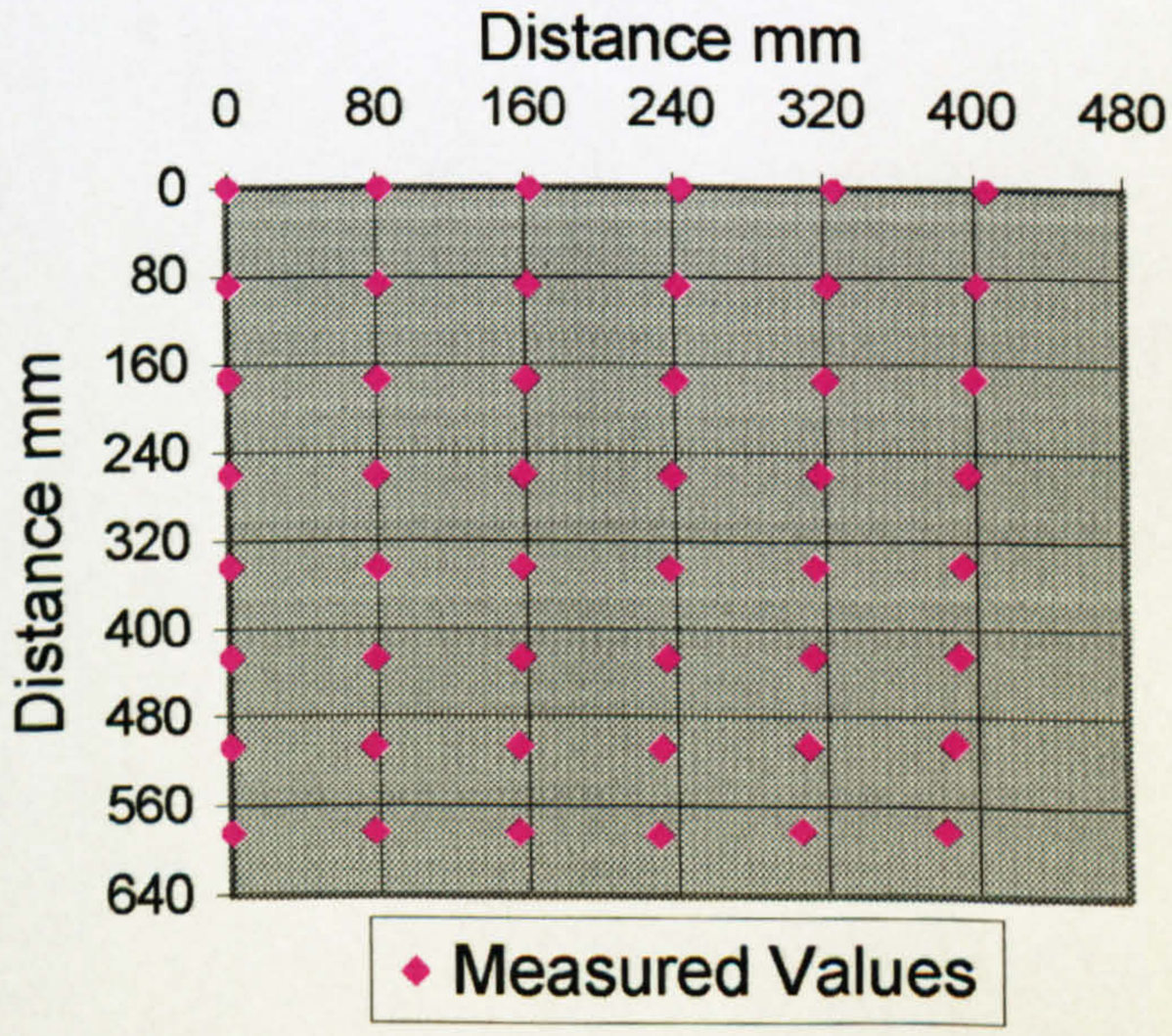

Figure 6.9. True vs. Actual Values: Settings Test - Camera to Projector Depth - Fringe Spacing Image 2

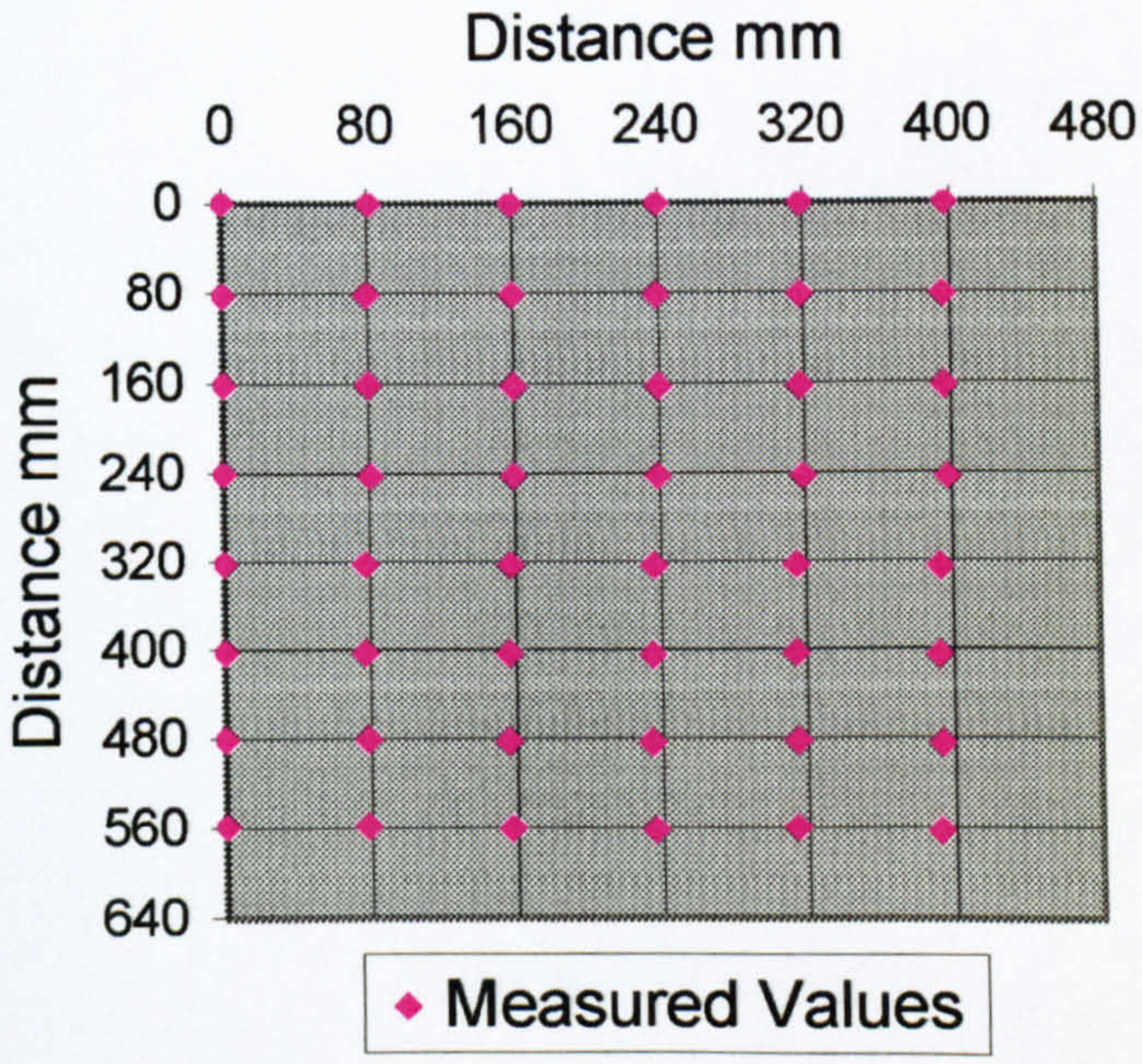

Figure 6.10. True vs. Actual Values: Settings Test - Camera to Projector Depth - K1 Image 1

Figure 6.11. True vs. Actual Values: Settings Test - Camera to Projector Depth - K1 Image 2

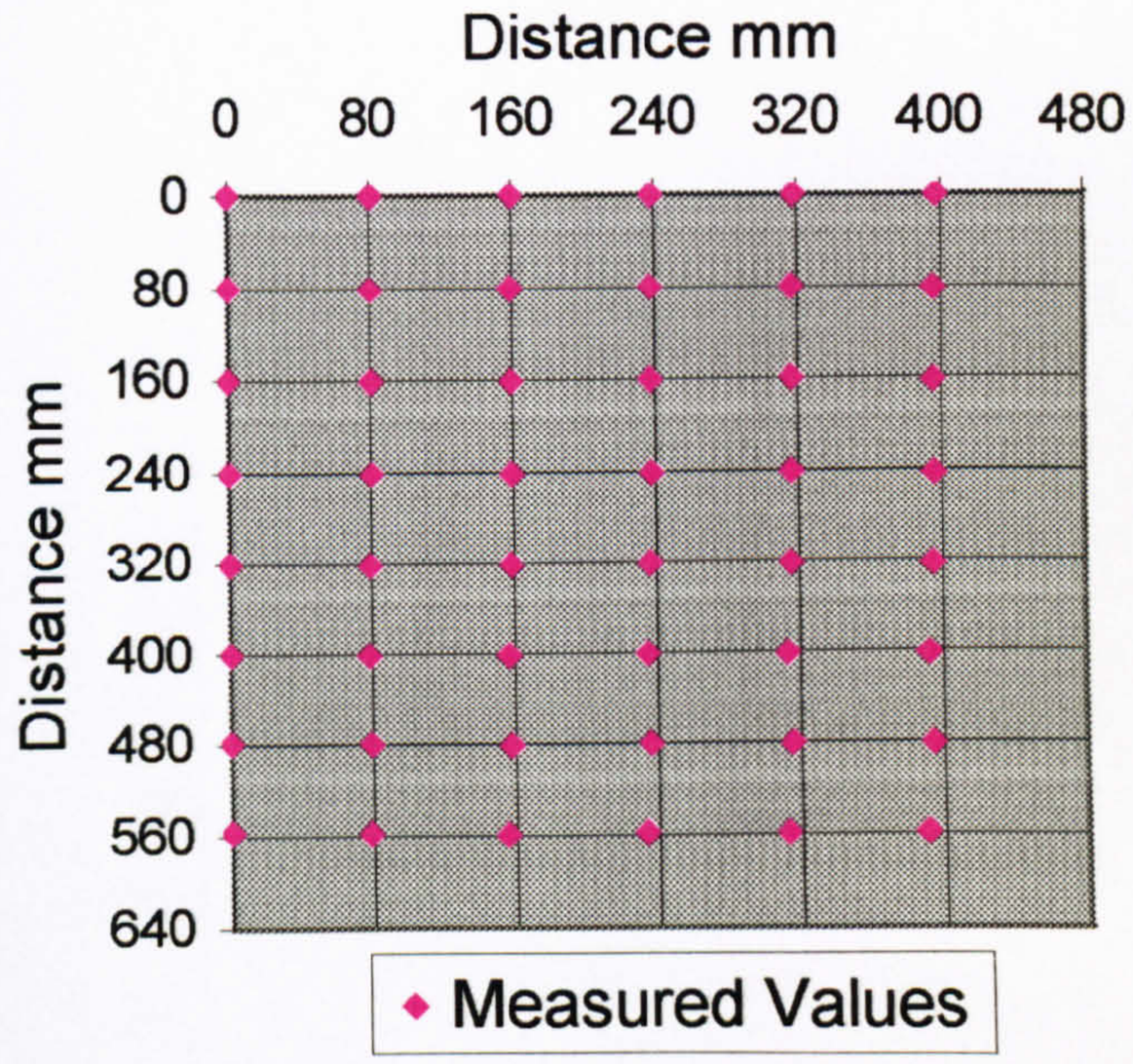

Figure 6.12. True vs. Actual Values: Settings Test - Camera to Projector Depth - K2 Image 1

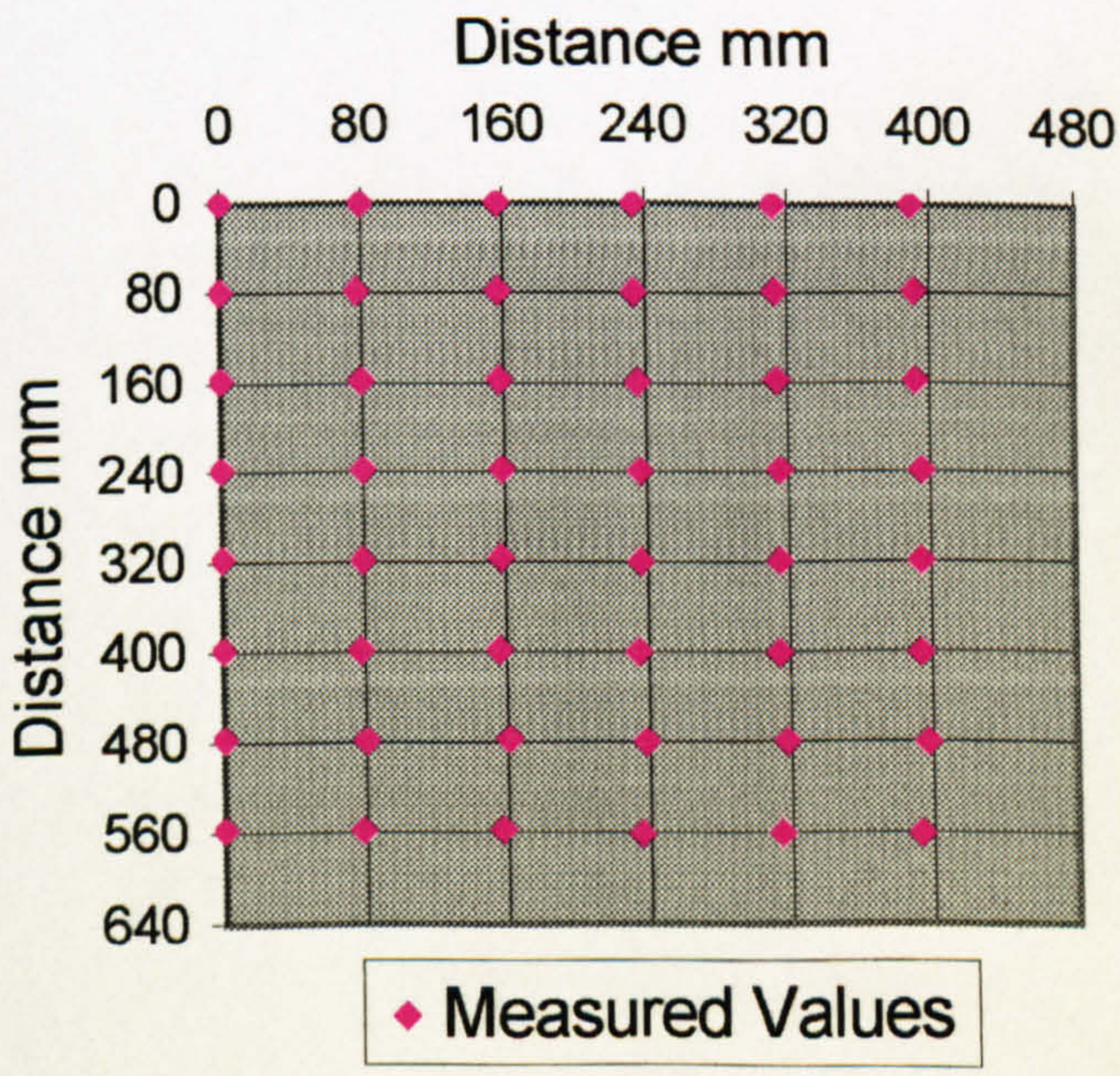

Figure 6.13. True vs. Actual Values: Settings Test - Camera to Projector Depth - K2 Image 2

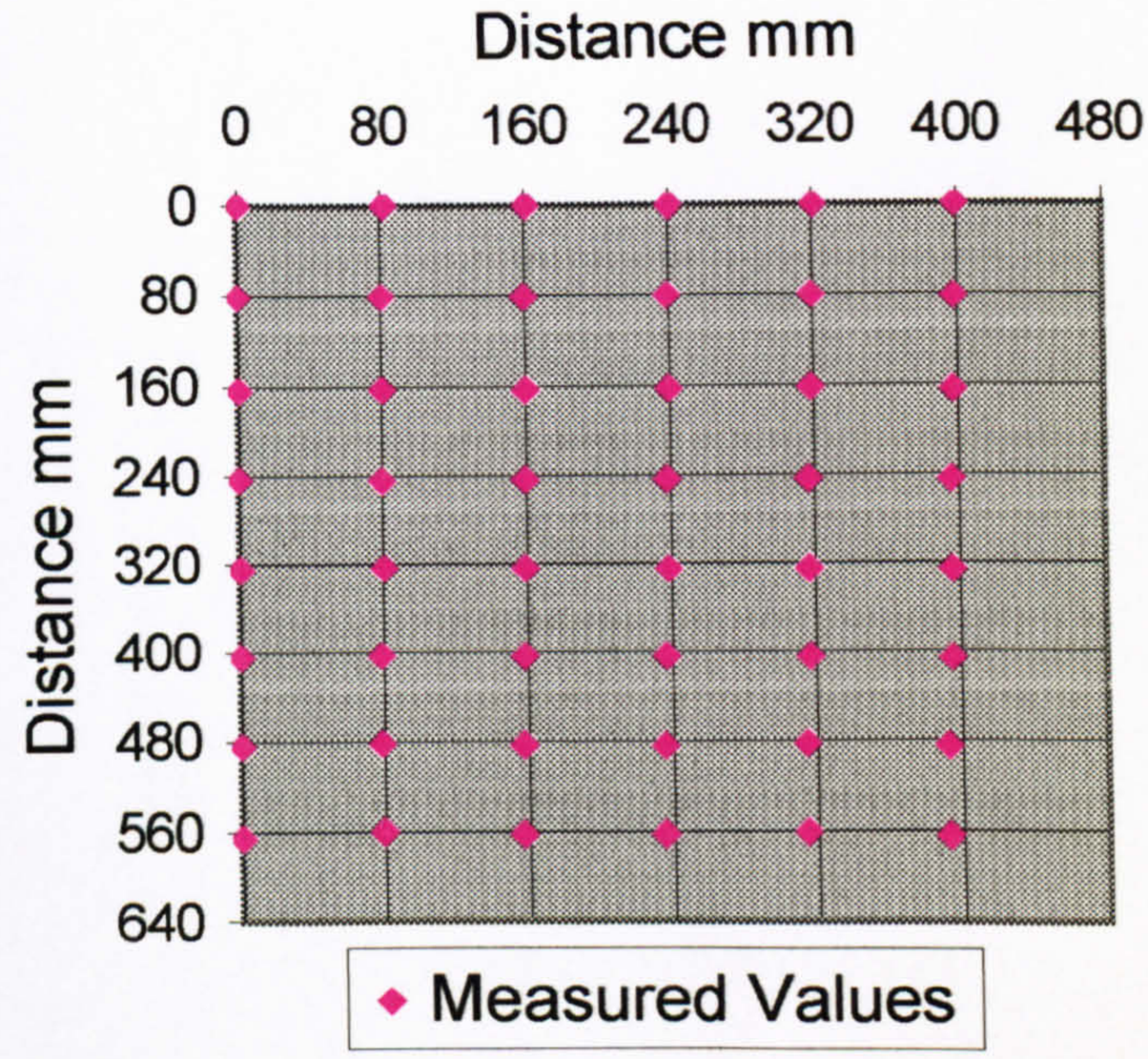

Figure 6.14. True vs. Actual Values: Settings Test - Camera to System Centre - K1 Image 1

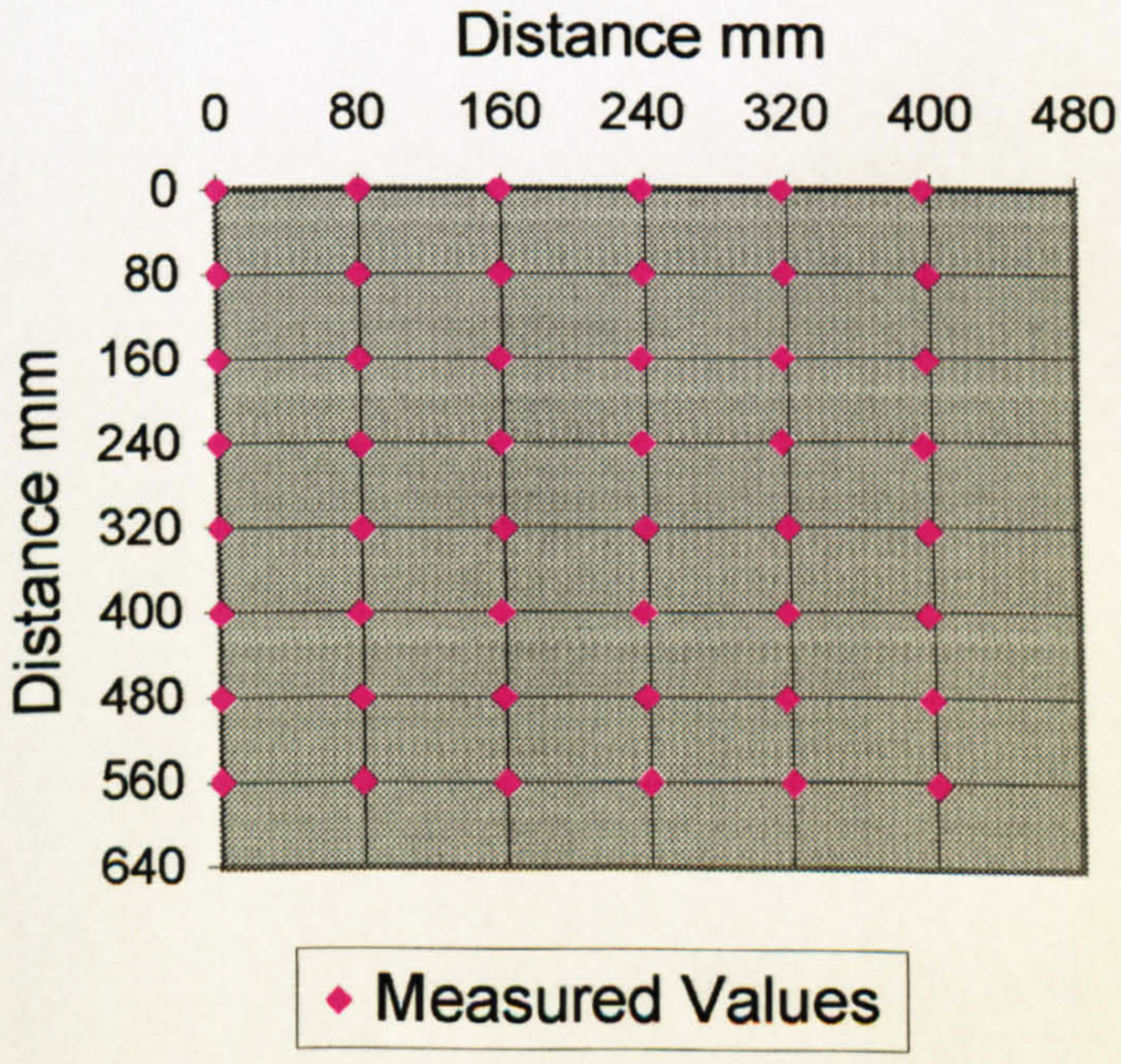

Figure 6.15. True vs. Actual Values: Settings Test - Camera to System Centre - K1 Image 2

Figure 6.16. True vs. Measured Values: Settings Test - Camera to System Centre - K2 Image 1

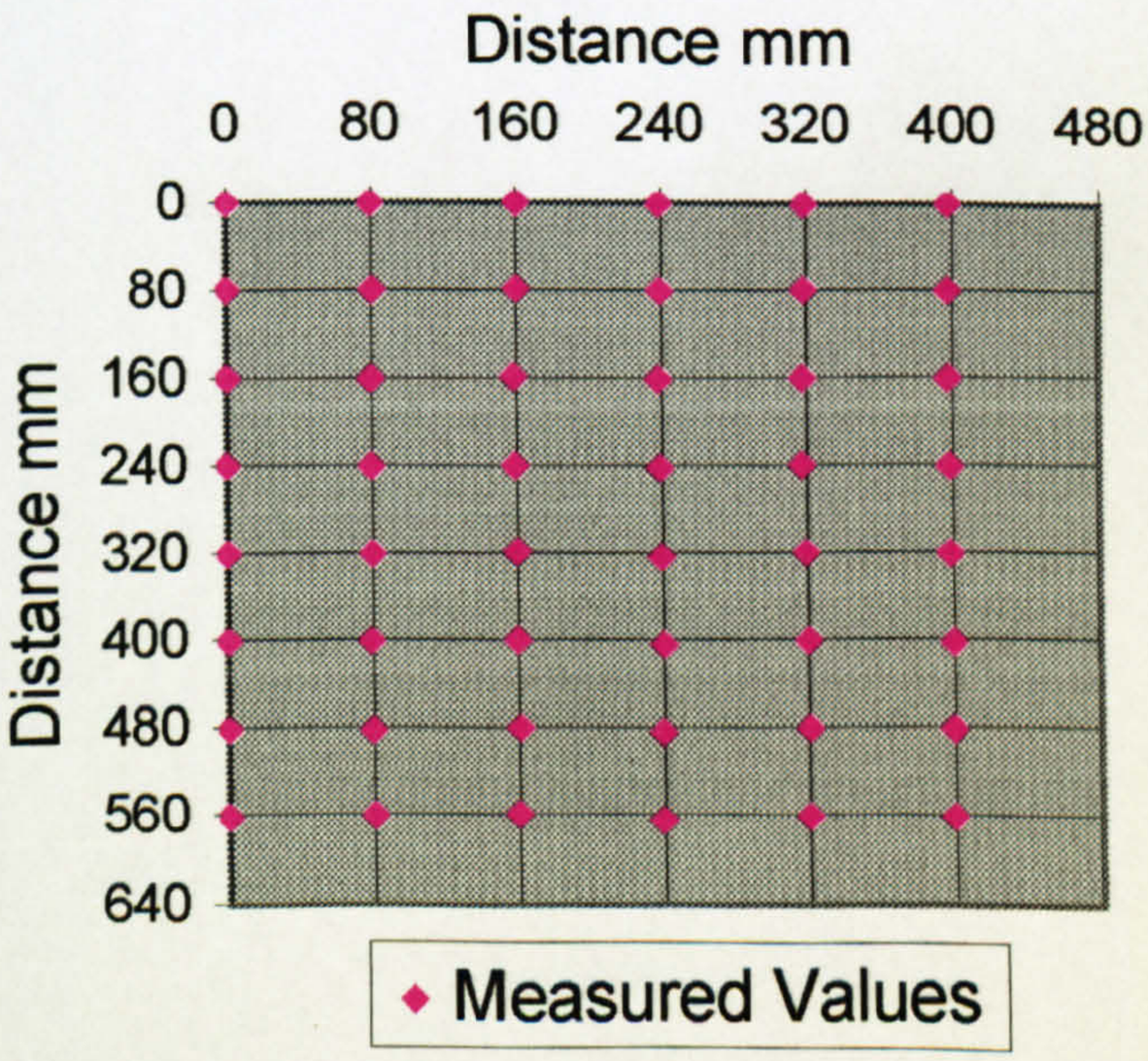

Figure 6.17. True vs. Actual Values: Settings Test - Camera to System Centre - K2 Image 2

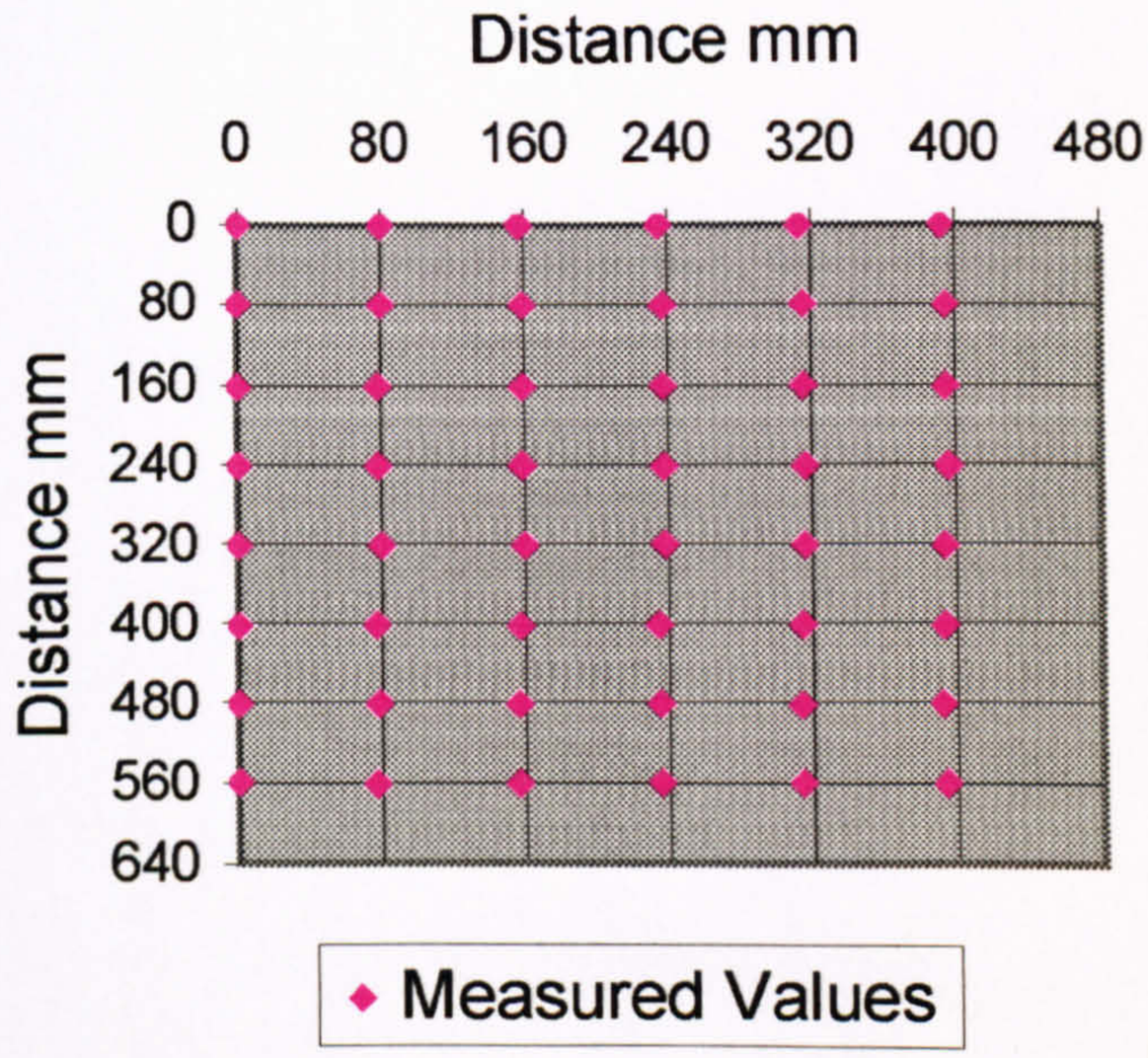

6.1.11. Vertical Grid Angle Position Test

Table 6.22. Basic Statistics: Vertical Grid Angle Position Test

View/ Direction	Measurement Type	Variant (Target object angle, degrees)	*n*	Mean (mm)	Standard Deviation (mm)	Standard Error of mean (mm)
Left/ Vertical	Shortest	0° (base grid)	42	79.80	0.82	0.13
		10° backwards	42	79.68	0.54	0.08
		20° backwards	42	79.80	0.56	0.09
		30° backwards	42	79.61	0.58	0.09
		10° forwards	42	79.42	0.65	0.10
		20° forwards	42	79.31	0.55	0.08
Right/ Vertical	Shortest	0° (base grid)	42	79.85	0.82	0.13
		10° backwards	42	79.43	0.58	0.09
		20° backwards	42	79.83	0.56	0.09
		30° backwards	42	79.48	0.80	0.12
		10° forwards	42	79.43	0.63	0.10
		20° forwards	42	79.27	0.67	0.10

n = the total number of measurements taken on each grid.

No notable difference, (within the confines of the test) may be noted between the basic statistics following each angle change, with the mean, standard deviation and standard error of the mean remaining consistent regardless of the vertical angle of the target object.

Table 6.23. Total Difference: Vertical Grid Angle Position Test

Variant	Image	
Target object angle (degrees)	Left Vertical (mm) *n*=42	Right Vertical (mm) *n*=42
0° (base grid)	27.7	
10° backwards	22.2	
20° backwards	20.4	
30° backwards	22.8	
10° forwards	30.0	
20° forwards	30.7	
0° (base grid)		28.0
10° backwards		28.6
20° backwards		19.2
30° backwards		33.4
10° forwards		28.6
20° forwards		35.6

n = the total number of measurements taken on each grid.

No notable differences in the Total Difference values are apparent between target positions. The TD in all cases is comparable with that which may be accounted for by the influence of the operator in measurement.

6.1.12. Horizontal Grid Angle Position Test

Table 6.24. Basic Statistics: Horizontal Grid Angle Position Test

View/ Direction	Measurement Type	Variant (Target object angle, degrees)	*n*	Mean (mm)	Standard Deviation (mm)	Standard Error of mean (mm)
Left/ Horizontal	Shortest	0° (base grid)	40	80.23	0.86	0.14
		10° anti-clockwise	40	80.30	0.71	0.11
		20° anti-clockwise	40	80.27	0.84	0.13
		30° anti-clockwise	40	79.88	0.72	0.11
		10° clockwise	40	80.35	0.92	0.15
		20° clockwise	40	80.47	0.64	0.10
		30° clockwise	40	80.39	0.61	0.10
Right/ Horizontal	Shortest	0° (base grid)	40	78.64	1.02	0.16
		10° anti-clockwise	40	79.40	0.66	0.10
		20° anti-clockwise	40	80.00	0.62	0.10
		30° anti-clockwise	40	80.57	0.51	0.08
		10° clockwise	40	77.77	0.66	0.10
		20° clockwise	40	77.04	0.88	0.14
		30° clockwise	40	76.47	0.89	0.14

n = the total number of measurements taken on each grid.

Whilst the basic statistics for the left image display a reasonable level of agreement, a greater degree of variability may be noted in the right image results. A distinct trend is apparent upon examination of the shortest distance results. From 0 to 30 degrees in the anti-clockwise direction the mean steadily increases with each angle increment and once the grid is turned in the opposite direction, (i.e. clockwise) the mean steadily decreases. It is also interesting to note that the standard deviation decreases as the grid is turned anti-clockwise and increases as the grid is turned clockwise.

Table 6.25. Total Difference: Horizontal Grid Angle Position Test

Variant	Image	
Target object angle, (degrees)	Left Horizontal (mm) n=40	Right Horizontal (mm) n=40
0° (base grid)	29.6	
10° anti-clockwise	24.4	
20° anti-clockwise	29.9	
30° anti-clockwise	23.7	
10° clockwise	30.5	
20° clockwise	25.4	
30° clockwise	23.7	
0° (base grid)		60.6
10° anti-clockwise		28.6
20° anti-clockwise.		18.3
30° anti-clockwise		25.6
10° clockwise		89.2
20° clockwise		118.5
30° clockwise		141.4

n = the total number of measurements taken on each grid.

The Total Difference results for the left image generally agree with one another however the results for the right image has a TD which generally decreases as the grid is turned anti-clockwise, but then increases dramatically as the grid is turned clockwise. This inequality in the magnitude of the TD is due to the distance by which the measured values deviate from the true value of 80mm. The horizontal direction of the right view has generally measured less than the true value in all single camera tests, in this test the TD at 0 degrees which reflects the original configuration of the system is 60.6. As the grid is turned anti-clockwise the measured values increase and hence the TD initially reduces, then begins to increase at 30 degrees anti-clockwise, as at this point the measured values begin to exceed the true value. Once the grid is turned in the opposite direction the TD increases at a more proportional rate relative to the angle of the target object.

As the target 2D grid is turned anti-clockwise the object becomes more perpendicular to the camera axis. Based upon the known geometry of the image capture system configuration the angle at which the 2D grid would be perpendicular to the camera axis is at 25 degrees (in the anti-clockwise

direction). This explains why the results are at their optimum in the +20 to +30 degree range of positions. Where the grid position deviates from the perpendicular, either by turning in excess of 30 degrees anti-clockwise or by turning in a clockwise direction, the measured results are affected, with values rising as the grid is turned further anti-clockwise and lowering as the grid is turned in the clockwise direction.

The results of the horizontal grid angle position test may not be fully explained by the influence of operator error. The TD values for the right view are in excess of the Total Difference for the operator error test, hence an instrumental source of error must also be present. The results in part may be due to the small amount of s-shaped distortion noted within the right view from the view comparison test. However the cosine effect is thought to be the primary reason for the distinct shift in measurement readings. The impact of the cosine effect would also explain the negative difference between the measured values and the true value, which is noticeable on all tests, resulting in a higher error for the horizontal direction for the right view, as the measured values consistently measure less than the true value.

The change in the level of agreement between the true and the measured values is shown in Figures 6.18-6.29. Figures 6.18-6.23 illustrate the performance for the left view, which appears to change little between grid positions. Whereas Figures 6.24-6.26 show a shift in the horizontal measurements for the right view from initially understating the measured values in respect to the true values, to providing measured values in excess of the true values. Figure 6.27-6.29, conversely, show a shift in the horizontal measurements which indicated the measured values decrease with respect to the true values, moving further away from the true values as the grid is rotated further in a clockwise direction. Note that the TriForm™ measurements used for Figures 6.18-6.29 are based upon measured horizontal distances and generated vertical distances that match

the true vertical values. This has been done for graphical purposes as no vertical measured readings exist for this test.

Figure 6.18. True vs. Measured Values: Horizontal Grid Angle Position Test - Left Image 10 Degrees Anti-clockwise

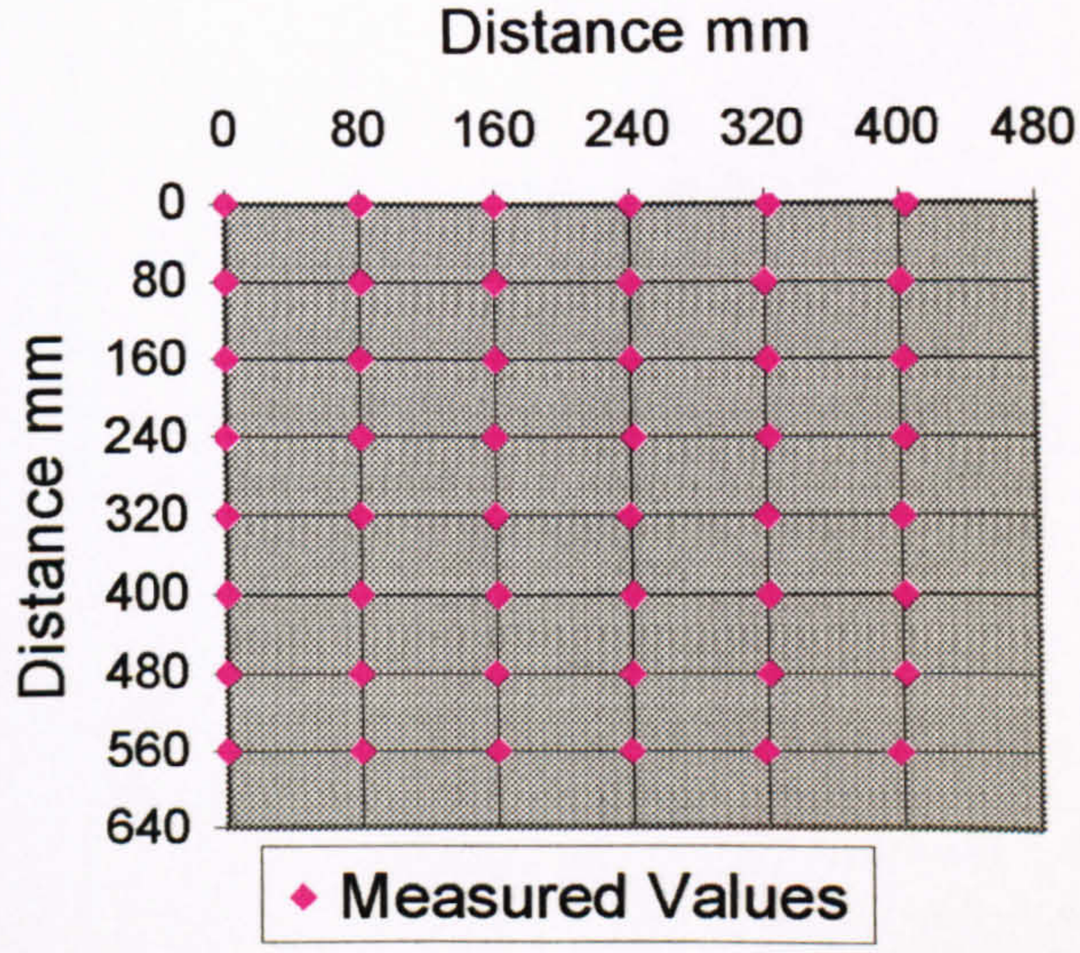

Figure 6.19. True vs. Measured Values: Horizontal Grid Angle Position Test - Left Image 20 Degrees Anti-clockwise

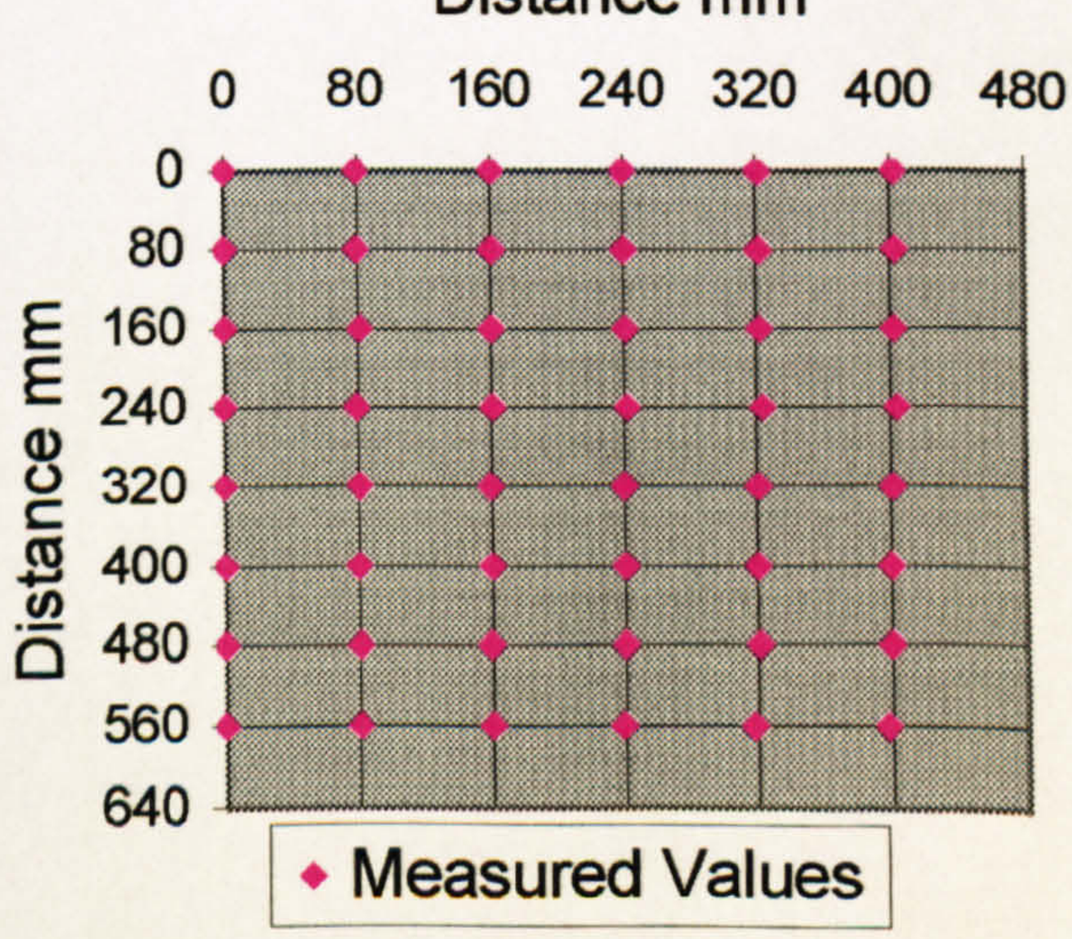

Figure 6.20. True vs. Measured Values: Horizontal Grid Angle Position Test - Left Image 30 Degrees Anti-clockwise

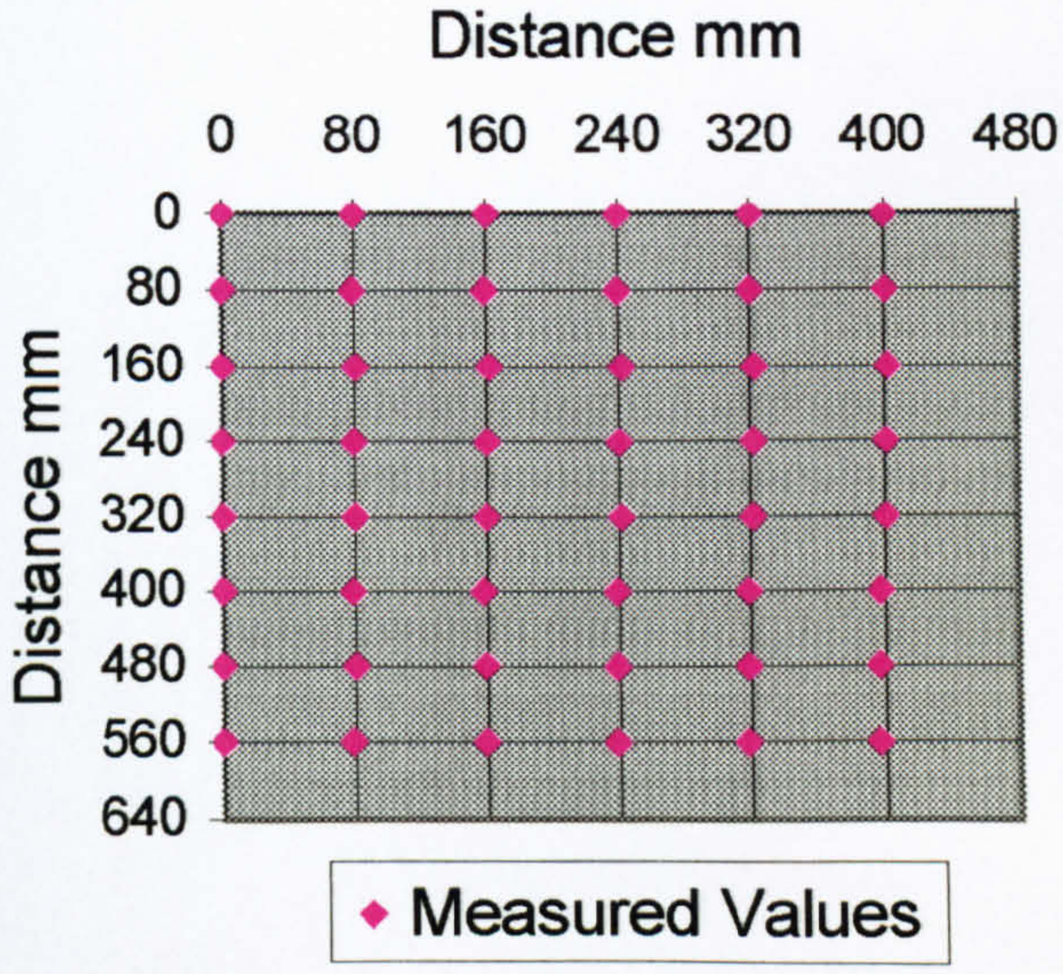

Figure 6.21. True vs. Measured Values: Horizontal Grid Angle Position Test - Left Image 10 Degrees Clockwise

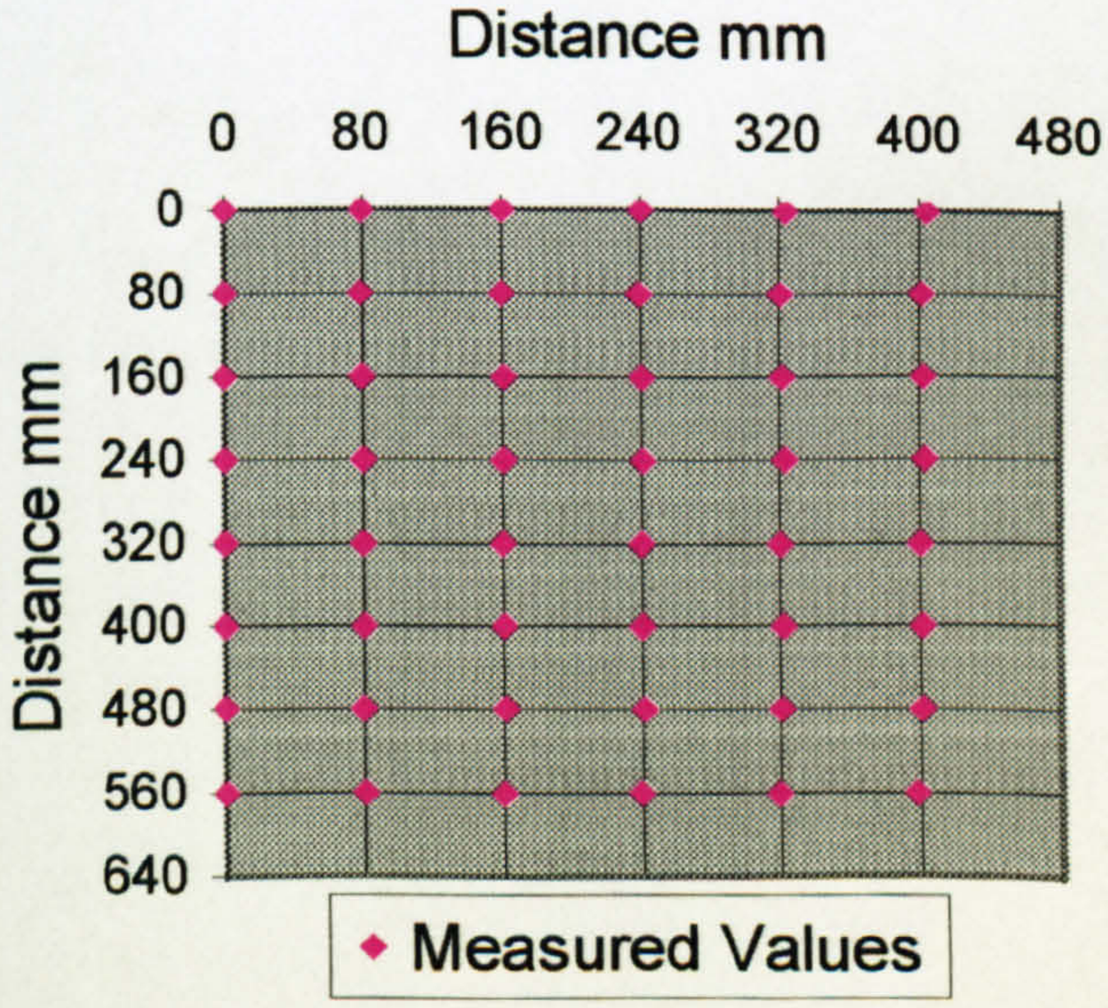

Figure 6.22. True vs. Measured Values: Horizontal Grid Angle Position Test - Left Image 20 Degrees Clockwise

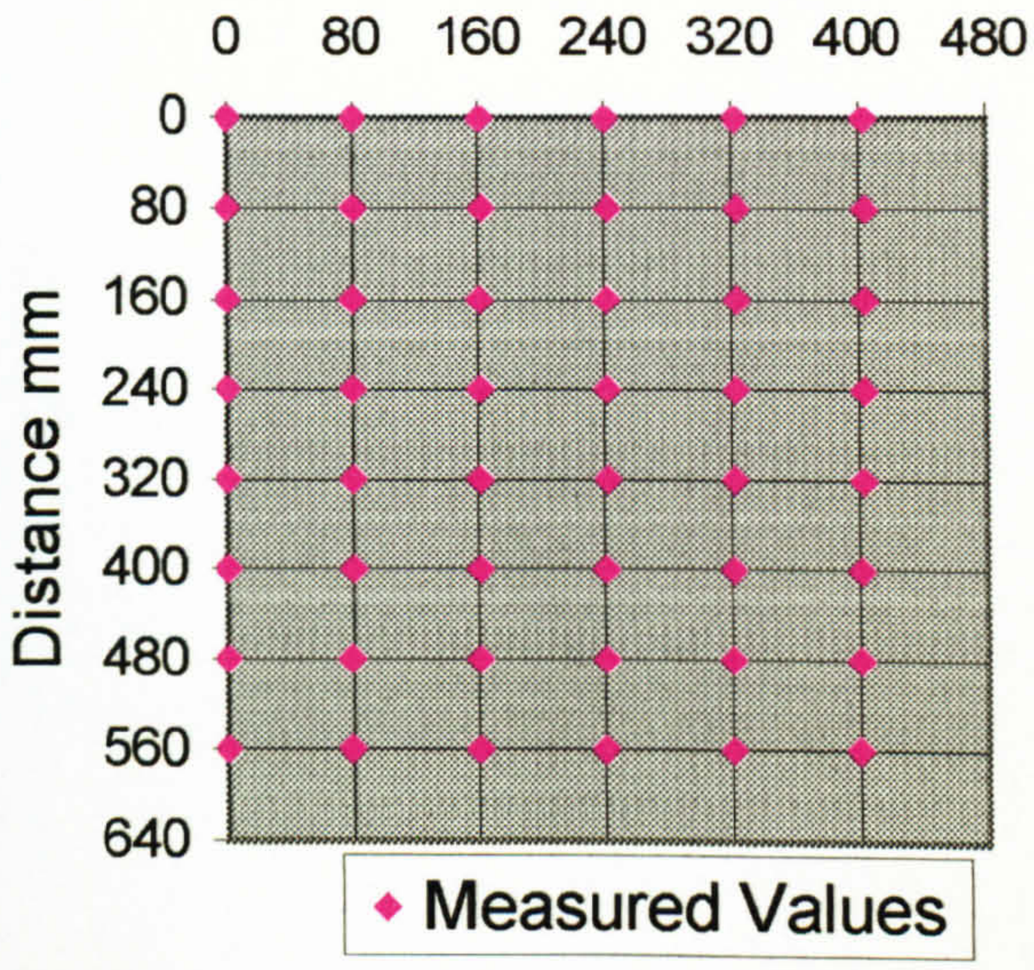

Figure 6.23. True vs. Measured Values: Horizontal Grid Angle Position Test - Left Image 30 Degrees Clockwise

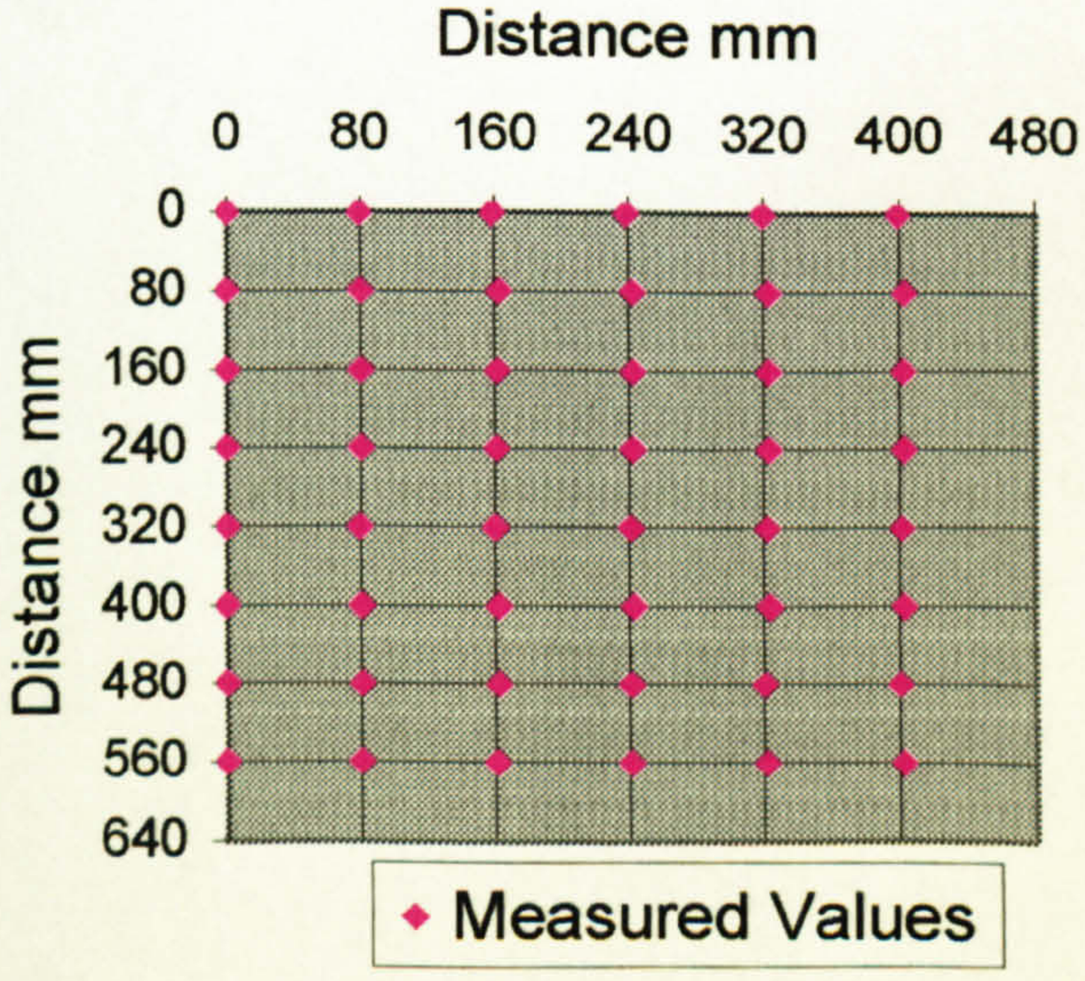

Figure 6.24. True vs. Measured Values: Horizontal Grid Angle Position Test - Right Image 10 Degrees Anti-clockwise

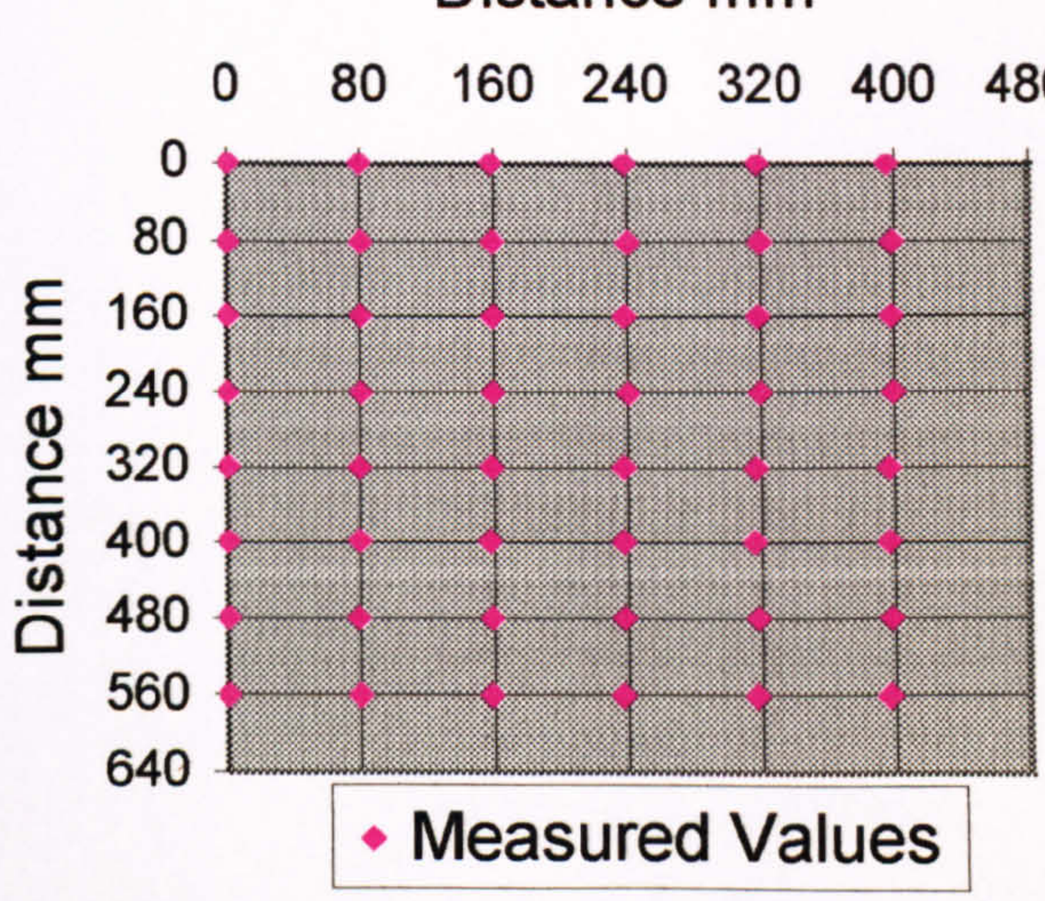

Figure 6.25. True vs. Measured Values: Horizontal Grid Angle Position Test - Right Image 20 Degrees Anti-clockwise

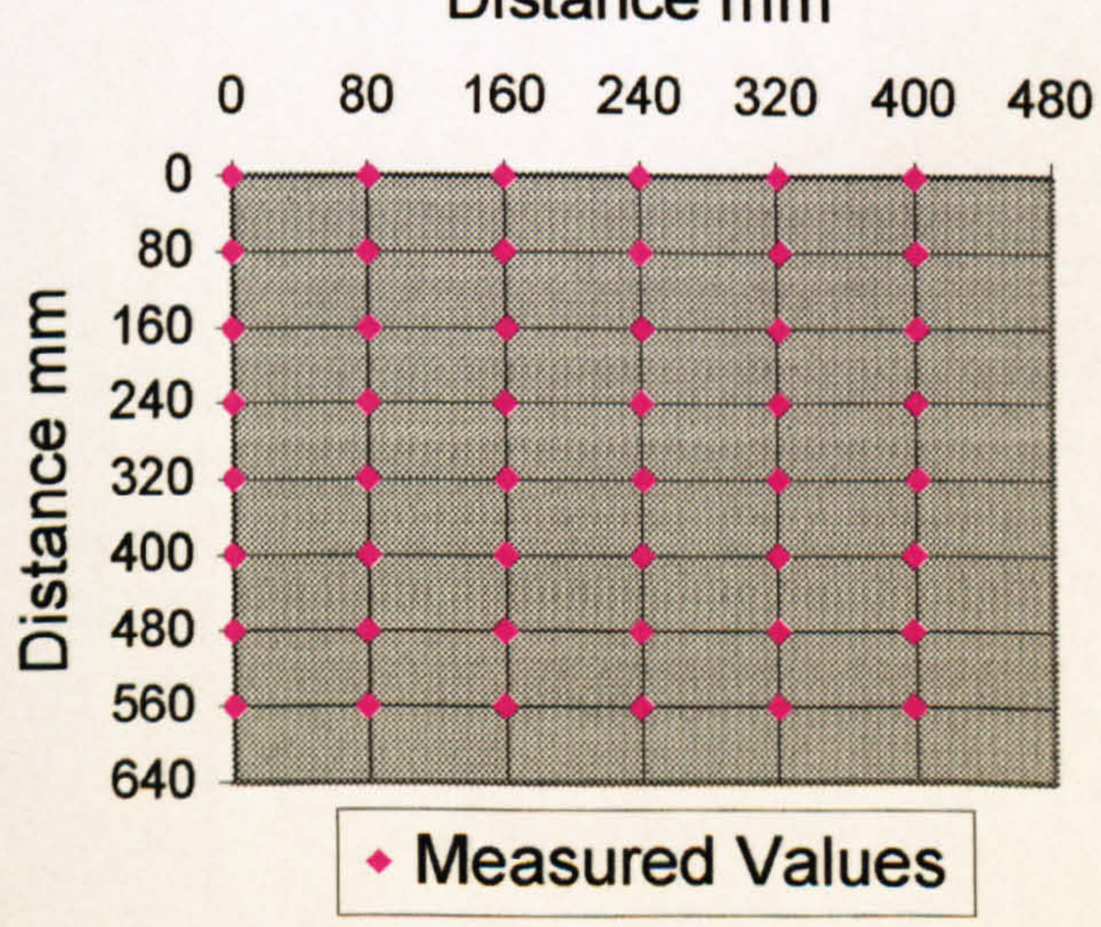

Figure 6.26. True vs. Measured Values: Horizontal Grid Angle Position Test - Right Image 30 Degrees Anti-clockwise

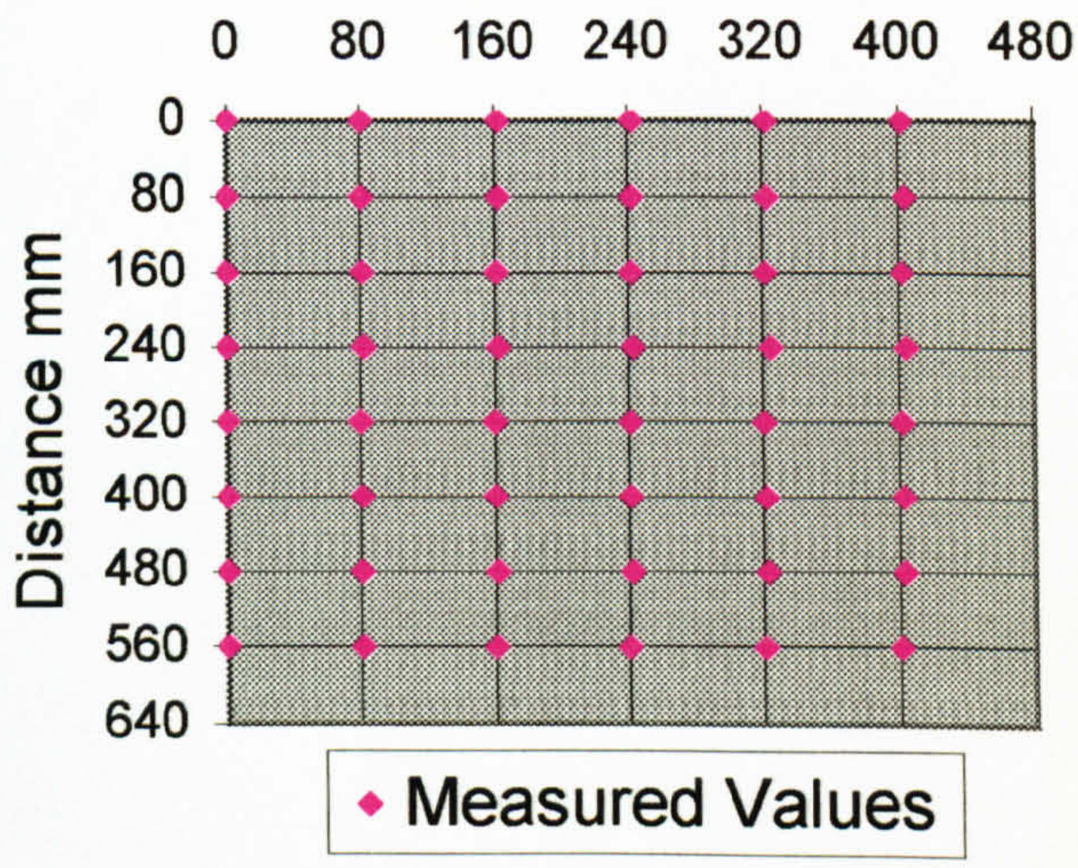

Figure 6.27. True vs. Measured Values: Horizontal Grid Angle Position Test - Right Image 10 Degrees Clockwise

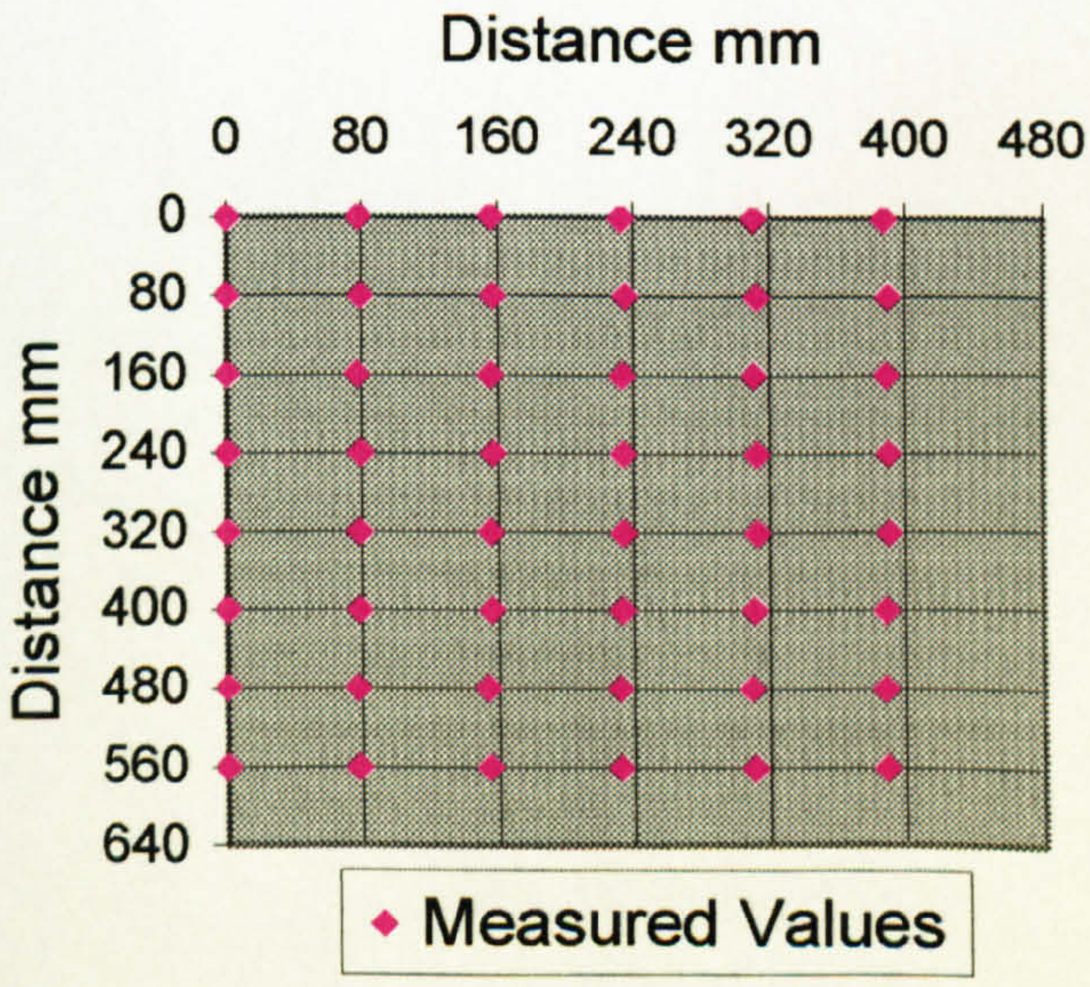

Figure 6.28. True vs. Measured Values: Horizontal Grid Angle Position Test - Right Image 20 Degrees Clockwise

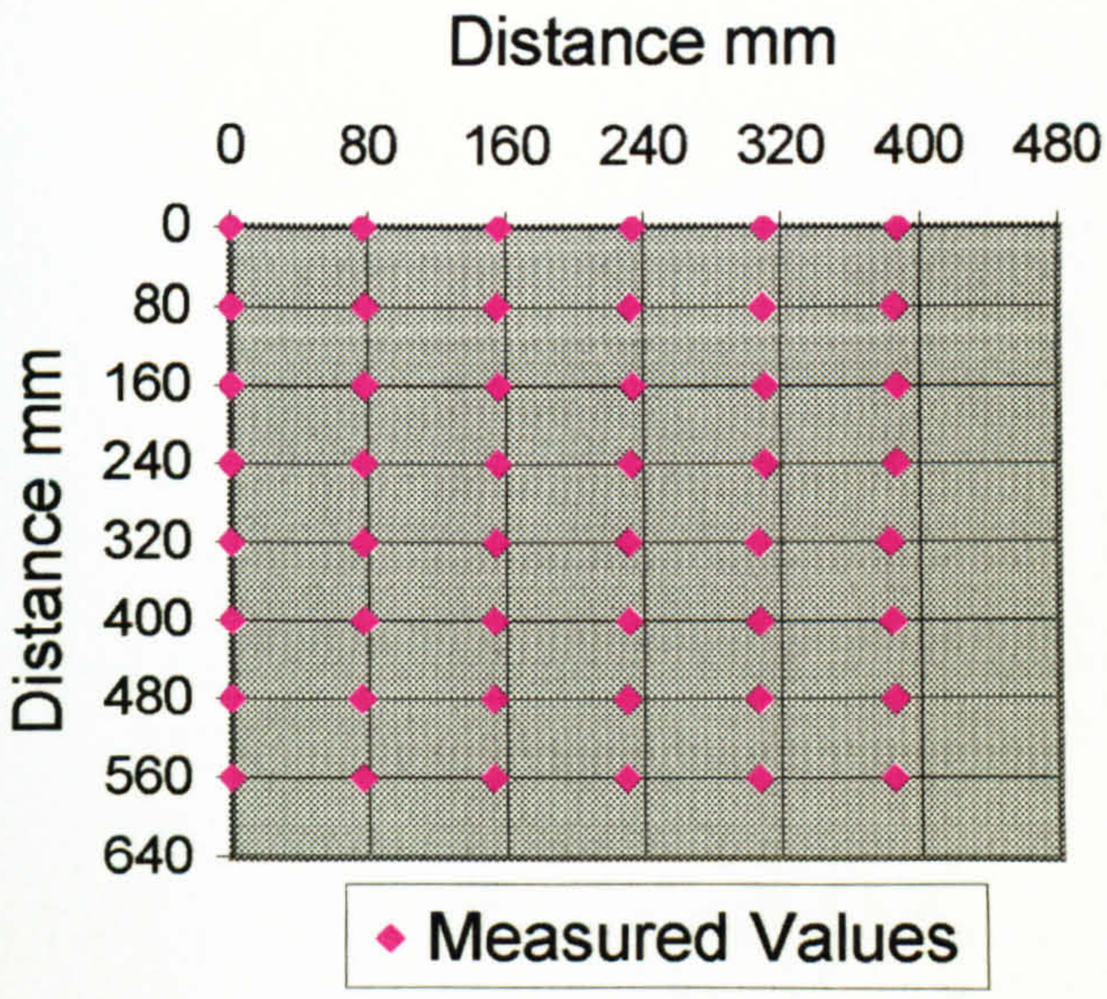

Figure 6.29. True vs. Measured Values: Horizontal Grid Angle Position Test - Right Image 30 Degrees Clockwise

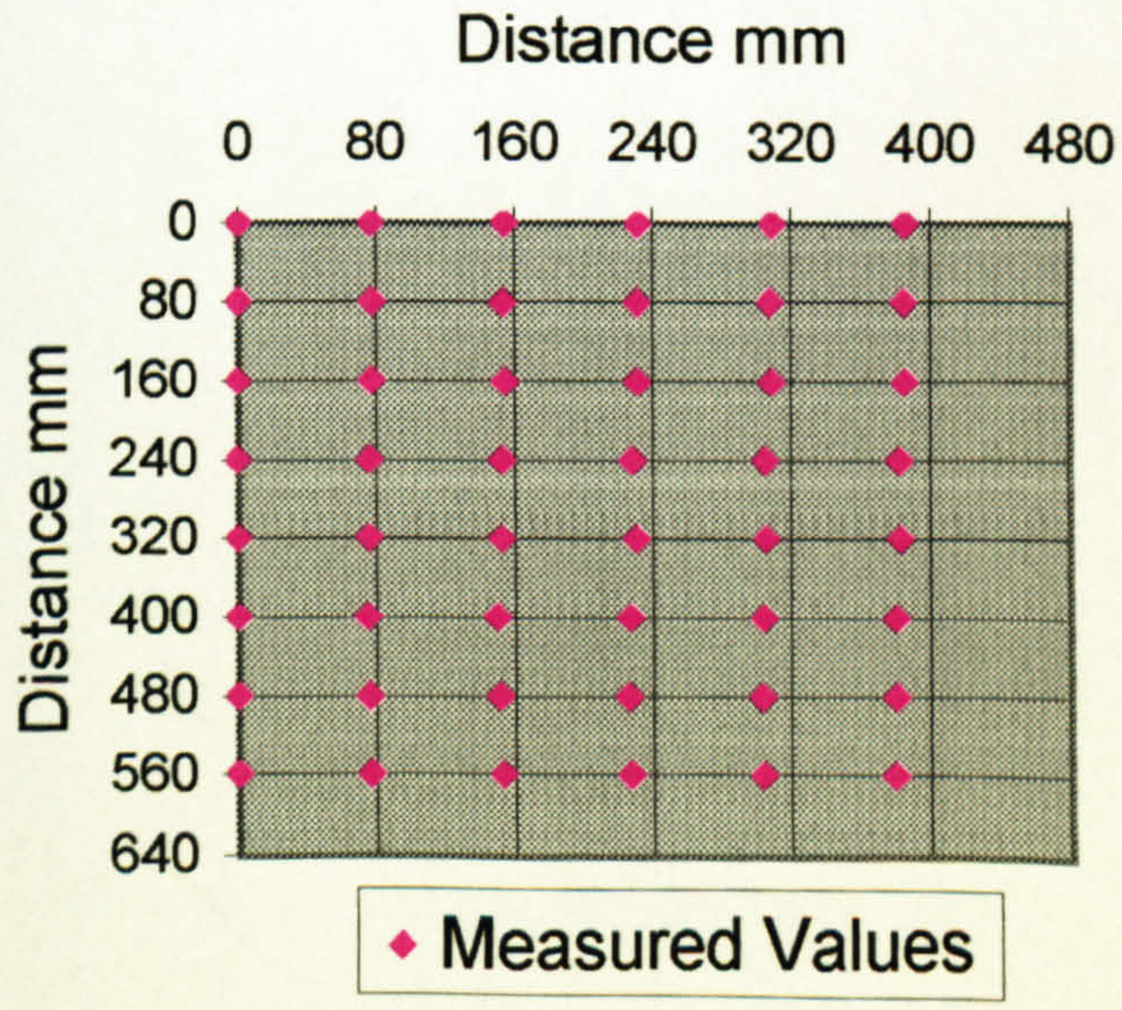

6.1.12.1. Further Findings

To investigate further the effect of the angle of the target object on measured values additional tests were undertaken using the same 2D grid. As the phenomenon was relevant to the right view only, the tests focussed on capturing images at 40 and 50 degrees in the anti-clockwise direction, measuring only the right view as the left view is not sufficiently captured. To provide more information on the impact of the angle nearer to the normal plane, i.e. 0 degrees, tests were also undertaken with the target object at 5 degrees in the anti-clockwise and 5 degrees in the clockwise direction.

Table 6.26. Basic Statistics: Horizontal Grid Angle Position Test (2)

View/ Direction	Measurement Type	Variant (Target object angle, degrees)	*n*	Mean (mm)	Standard Deviation (mm)	Standard Error of mean (mm)
Right/ Horizontal	Shortest	5° anti-clockwise	40	77.66	0.78	0.12
		5° clockwise	40	78.77	0.73	0.12
		40° anti-clockwise	40	80.73	0.57	0.09
		50° anti-clockwise	40	80.91	0.66	0.10

n = the total number of measurements taken on each grid.

The basic statistics follow the same trend in the extended angle range as those exhibited for the 10 – 30 degree ranges. To attempt to explain the relationship between the angle of the target object and the measured values, the relative error associated with each position was determined. This was calculated by expressing the absolute error as a percentage of the true value. The mean relative error of the 40 cells that were measured was then used to remove the dependency on the distance measured, mean values were used to minimise the influence of the operator. Figure 6.30 graphically illustrates the relationship between the angle of the target object and the relative error present within measurements.

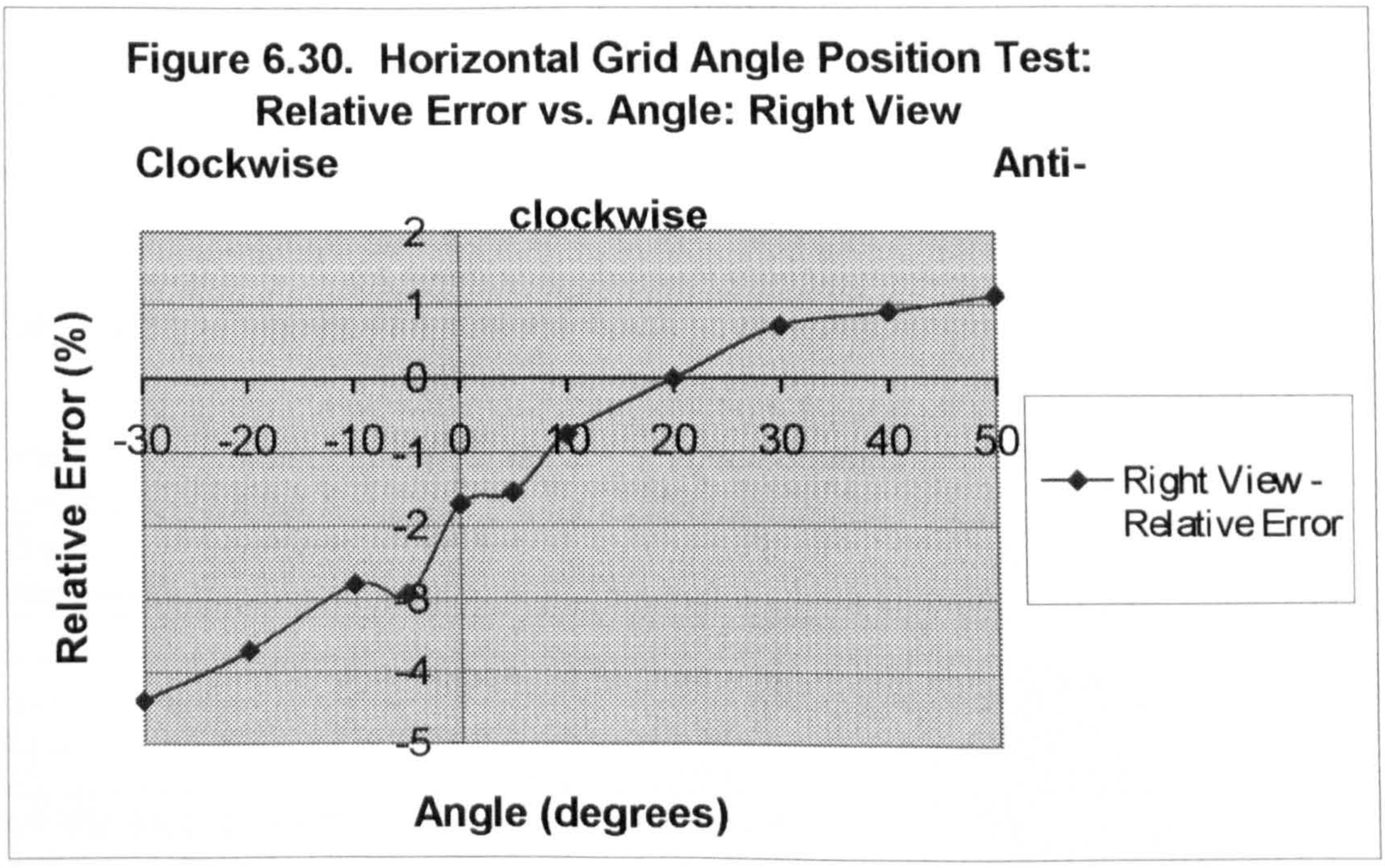

A linear relationship can be seen to exist between the angle of the target object and measured values, the linear region primarily covering the -30 to +30 degree range. Over the range of –10 - –30 degrees and +10 - +30 the relationship is particularly strong, however the relationship does appear to become weaker towards the +40/50 degree angle ranges. The relative error results over the –5/+5 degree range also deviate from the line of best fit, this is thought to be due to the difficulty by which accurate small differences in angle may be made using the target object.

6.1.13. Cylinder Test

From the results of the grid angle position test the accuracy of measured values appears to be angle dependent, however during the planar differences test this was not clear, as the 3D target object had only a limited range of surface curvature. Hence a cylinder of diameter 280mm was captured with the 2D grid carefully adhered to its surface, to check the impact of angle dependency, for the right view only. Due to the smaller available viewing area the cells were

Figure 6.30. Horizontal Grid Angle Position Test: Relative Error vs. Angle: Right View

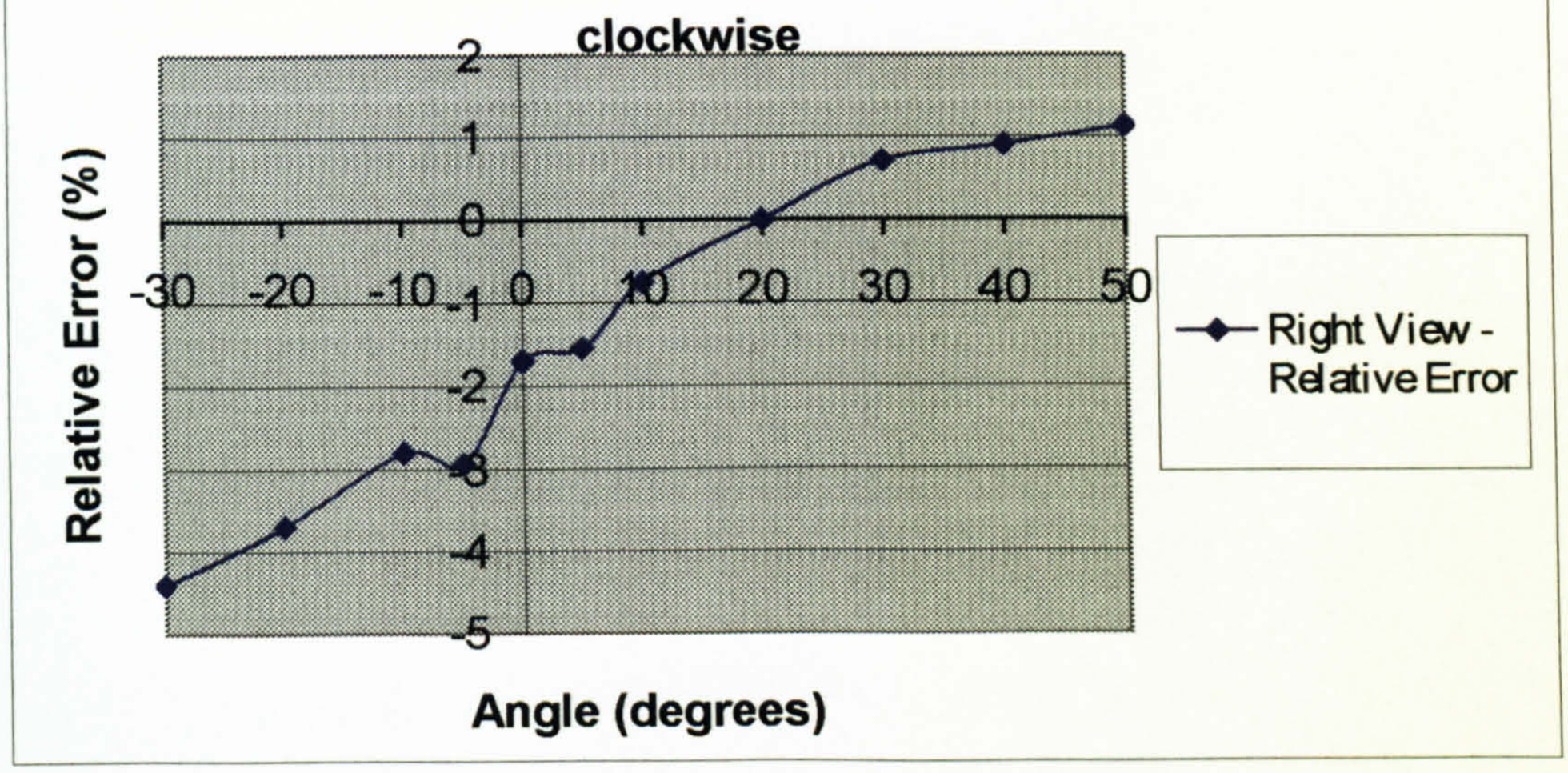

A linear relationship can be seen to exist between the angle of the target object and measured values, the linear region primarily covering the -30 to +30 degree range. Over the range of –10 - –30 degrees and +10 - +30 the relationship is particularly strong, however the relationship does appear to become weaker towards the +40/50 degree angle ranges. The relative error results over the –5/+5 degree range also deviate from the line of best fit, this is thought to be due to the difficulty by which accurate small differences in angle may be made using the target object.

6.1.13. Cylinder Test

From the results of the grid angle position test the accuracy of measured values appears to be angle dependent, however during the planar differences test this was not clear, as the 3D target object had only a limited range of surface curvature. Hence a cylinder of diameter 280mm was captured with the 2D grid carefully adhered to its surface, to check the impact of angle dependency, for the right view only. Due to the smaller available viewing area the cells were

measured in 40mm intervals and the mean measured results were recorded for each group of cells along the vertical length of the cylinder, the results of which are detailed in Table 6.27.

Table 6.27. Cylinder Test Mean Values: Horizontal Direction

View/ Direction	Measurement Type	Cell	Approximate Angle (°)	*n*	Mean (mm)
Right/ Horizontal	Surface	0-2	-16.37	8	39.35
		2-4	+16.37	8	39.91
		4-6	+32.74	8	40.40
		6-8	+49.11	8	41.38
		8-10	+65.48	8	41.95

n = the total number of measurements taken on each cell.

The relative errors of the measurements were again plotted to determine the relationship between the angle of the target object and the error incurred in measurement (Figure 6.31).

Figure 6.31. Cylinder Test Surface Distance: Relative Error vs. Angle - Right View

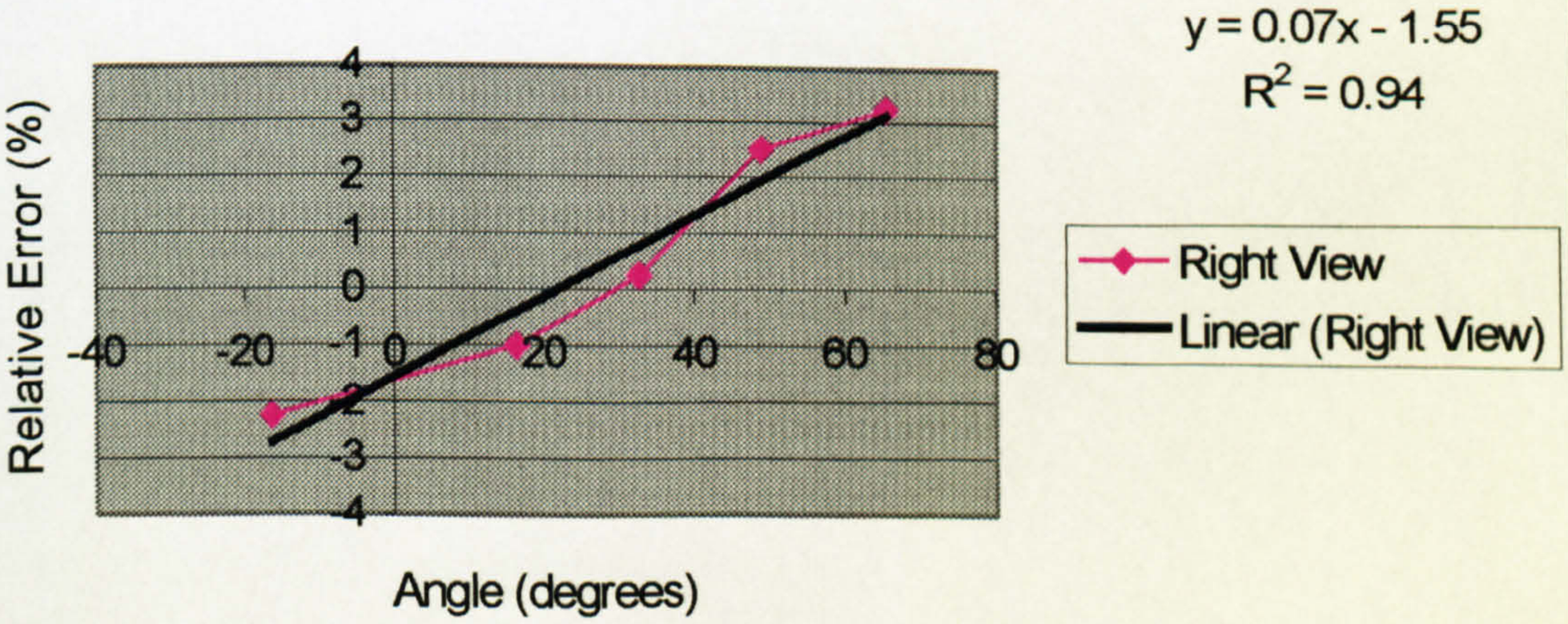

On examination of Figure 6.31 the linear relationship suggested by the grid angle position test is confirmed. The extent of the relationship is denoted by the R^2 value, which describes the proportion of the variance in y that is directly related to the variance in x. Hence R^2 denotes the quality of the linear relationship

between x and y. A value of 1 indicates true agreement, hence a value of 0.94 indicates a strong linear relationship between the angle and the relative error.

By examining the results of the horizontal grid angle position test and the cylinder test it is clear that the capture system gives an error dependent on the shape of the surface and the position of the points on the surface. To attempt to account for the errors noted in these tests a correction function was proposed to take account of the curvature of the surface and the length of the distance measured. The function calculates the magnitude of the absolute error by using the following equation.

$$\Delta = \int_L \delta(\varphi) dl, \tag{1}$$

where Δ is the absolute error

$\delta(\varphi)$ is a correction function;

φ is the angle between tangent to the surface and the front plane of the measuring device;

dl is an element of a distance along the surface;

L is the total length along the surface.

To evaluate the impact of the angle of the target object, two cases need to be considered.

1) Measuring the distance between two points on a plane in a horizontal direction, where no surface curvature exists.
2) Measuring the distance between two points on a cylinder in a horizontal direction where the surface forms a continuos curve.

Each will be considered in turn.

1) In the case of measuring the distance between two points on a plane, the surface has zero curvature hence the angle between the front plane of the device and the surface under consideration does not depend upon the position of points on the surface. The error in measuring depends only on the length of the distance.

$$\Delta = L_m - L_a \tag{2}$$

where Δ is the absolute error

L_a is the actual distance, between two points

L_m is the surface distance measured between two points.

2) In the case of measuring the distance between two points on a cylinder the error in measurement depends not only on the length of the distance, but also the position of points on the surface, thus there is a relationship between the distance measured on the surface and the angle φ. Figure 6.32 illustrates the situation.

Figure 6.32. Two Points on a Cylinder.

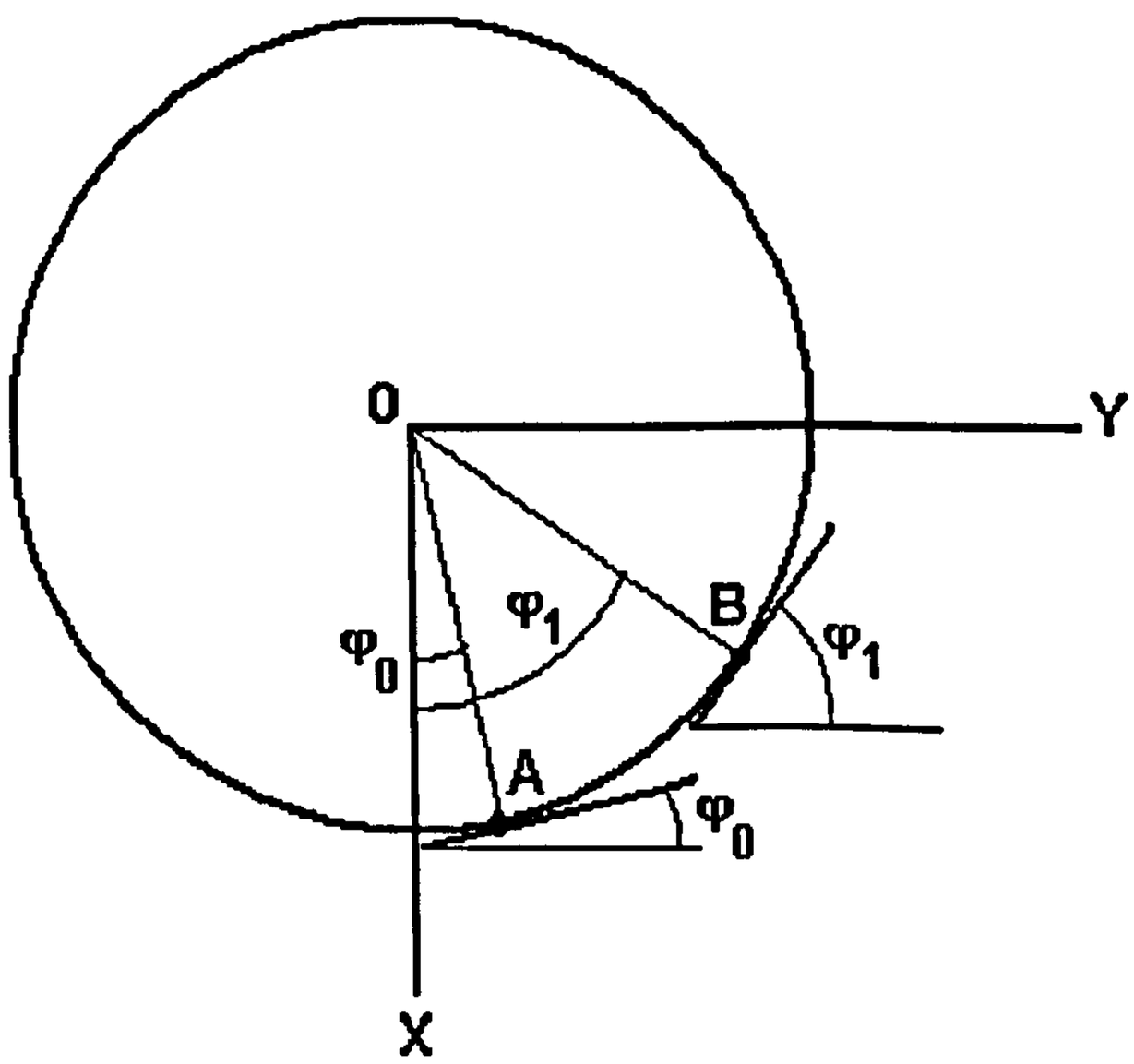

Two points, A and B, are on the surface of the cylinder at the same distance from the plane $X0Y$. Their position on the surface is characterised by two angles, φ_0 and φ_1, respectively, as shown in Figure 6.32, hence in the case of the cylinder the angle φ is no longer a constant. Therefore the errors in measuring each small part of the surface will be different depending on their position on the surface of the cylinder. The relationship between the distance measured and the angle φ may be expressed as follows:

$$dl = r\, d\varphi, \tag{3}$$

where dl is an element of a distance along the surface;

r is the radius of a cylinder;

φ is the angle between tangent to the surface and the front plane of the measuring device.

Following the results of the horizontal grid angle position test the relationship between the relative error and the angle φ may be approximated by using the least square method by the polynomial of the 4th degree, see Figure 6.33. As a cylinder of known radius is being measured, the angle has been expressed in radians to provide information on the distance measured between specified points based on the known angle.

The following equation expresses the polynomial relationship.

$$\delta_1(\varphi) = a_4\varphi^4 + a_3\varphi^3 + a_2\varphi^2 + a_1\varphi + a_0. \tag{4}$$

where a is a constant, relative to the polynomial function.

By testing the fit of polynomials at various levels the 4th degree polynomial was found to provide the optimum fit to the data. Increasing the polynomial to the 5th and 6th degrees were tested but found to show little improvement.

Figure 6.33. Horizontal Grid Angle Position Test Surface Distance: Relative Error vs Angle - Right View

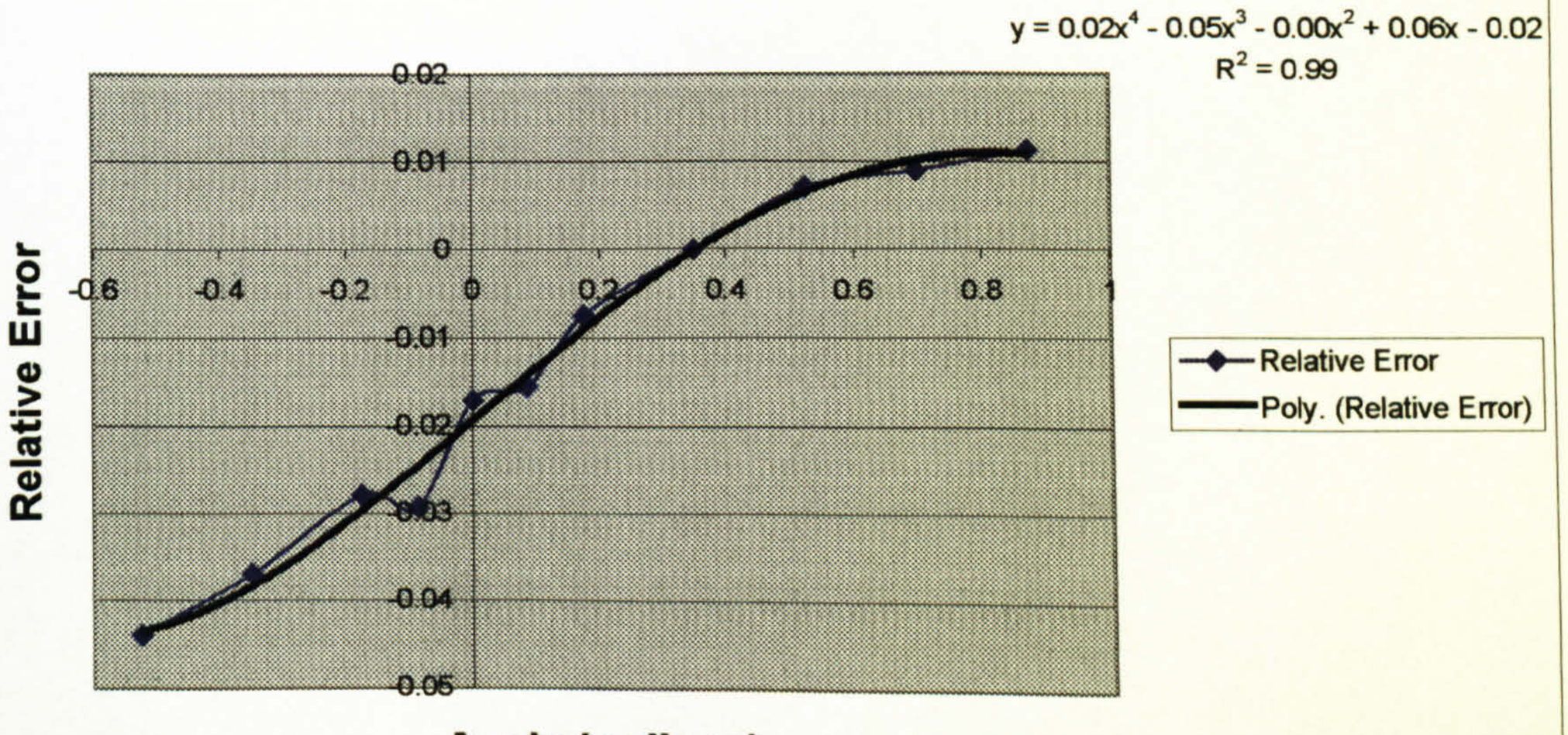

By substituting formulae (3) and (4) into the equation (1):

$$\Delta = \int_L \delta(\varphi) dl = r \int_{\varphi_0}^{\varphi_1} (a_4\varphi^4 + a_3\varphi^3 + a_2\varphi^2 + a_1\varphi + a_0) d\varphi, \quad (6)$$

where φ_0 and φ_1 are angles related to the start and end point on the surface, for points A and B respectively.

Therefore integrating the equation (6) results in the formula for calculating the absolute error for curved surfaces:

$$\Delta = r[\frac{a_4}{5}(\varphi_1^5 - \varphi_0^5) + \frac{a_3}{4}(\varphi_1^4 - \varphi_0^4) + \frac{a_2}{3}(\varphi_1^3 - \varphi_0^3) + \frac{a_1}{2}(\varphi_1^2 - \varphi_0^2) + a_0(\varphi_1 - \varphi_0)] \quad (7)$$

To test the accuracy of the formula a revised cylinder test was undertaken, to enable the comparison of the predicted error with the absolute error obtained during measurement. A specially designed grid was drawn using a computer so the measured divisions were placed at specified angles from the central 0 degrees point. The following distances were then measured:

Table 6.28. Cylinder Test (2) Measured Divisions

Area Measured	Corresponding Surface Distance
0 degrees to -20 degrees	49mm
0 degrees to -10 degrees	25mm
0 degrees to +10 degrees	25mm
0 degrees to +20 degrees	49mm
0 degrees to +30 degrees	74mm
0 degrees to +40 degrees	98mm
0 degrees to +50 degrees	123mm

Note that the grid was only able to be drawn in divisions of 1mm, hence the distances required to produce the desired angle were rounded to the nearest millimetre

The grid was adhered to the same cylinder that had previously been used. The specified distances as detailed in Table 6.28 were measured 40 times to ensure the value *n* remained equal for both the horizontal grid angle position test results and the second cylinder test. By maintaining the same value for *n* and using average values theoretically any random errors would be minimised.

The absolute error for the revised cylinder test was calculated according to measured values and plotted along with the calculated absolute error which was predicted by the application of equation (7), as shown in Figure 6.34.

Figure 6.34. Cylinder Test (2) Surface Distance: Absolute Error Predicted vs. Measured - Right View

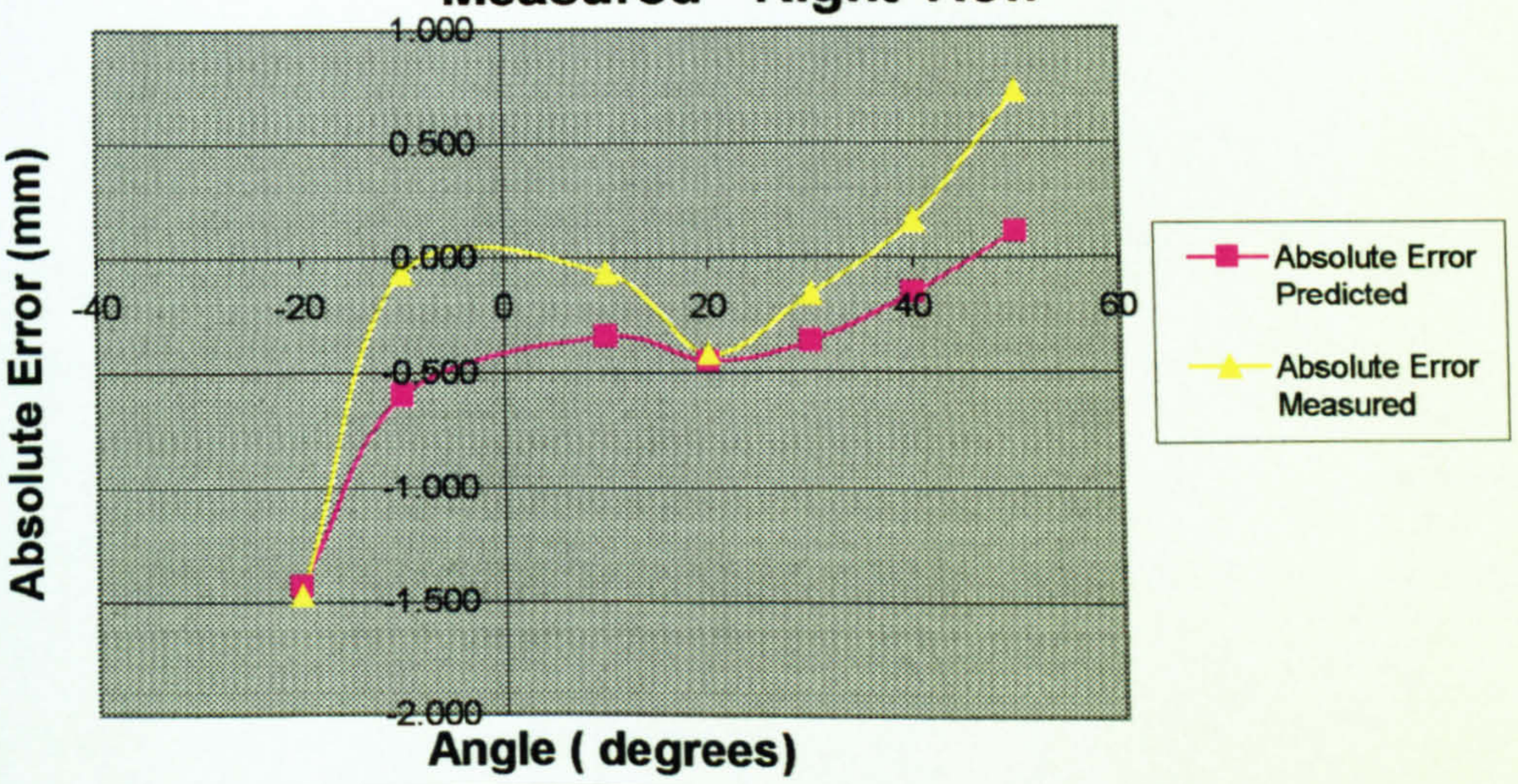

From Figure 6.34 it can be seen that the results from the prediction model and measured results are in agreement at the –20 and +20 degree points. However nearer the central area around 0 degrees and towards the +40/50 degree area the level of agreement is diminished. As noted however with Figure 6.30, the linearity of the relationship between angle and error is diminished in these positions, hence this may in part responsible for the lower levels of accuracy of error prediction. Particularly as the 5 degree angle position was difficult to produce with the 2D grid. The influence of random errors will also make the accuracy of any error prediction model variable, even where averaging was undertaken to assist in the removal of the influence of such errors.

It can be noted that the calculated absolute error consistently underestimates the impact of the error, this is likely to be due to the surface distance being greater

than the shortest distance results when measuring a 2D surface, (although in theory the two measurement types should return the same result). The shortest distance results were used as a basis for the predictive equation as the shortest distance has proved throughout the investigation to be the most reliable measure. As even with the improvements in the accuracy of surface measurement the surface distance results still show greater variability and tend to slightly over estimate the distance.

6.2. Summary

The main findings of the single camera system evaluation may be summarised as follows:

Operator Error Test

By taking repeated measurements of identical captured images the influence of the operator on measured values was determined. The results of which are summarised as follows:

- Repeat measurements over the same images were found to be consistent with one another, especially for the left view.

- The maximum errors related to the measurement of a single cell of 80mm were found to be in the range of –2.30mm to +2.80mm for the horizontal direction and –2.20mm to +1.90mm for the vertical direction. However as the error is random in nature it is unlikely the maximum error would be encountered.

- The likely mean absolute error for the measurement of a single cell of 80mm was found to be 0.69±0.04mm in the horizontal direction and

0.80±0.04mm in the vertical direction. The mean Total Difference for the operator error test was calculated to be 27.5mm for the horizontal direction and 33.6mm for the vertical direction.

The influence of the operators prior knowledge of the dimensions of the grid was also tested by creating a grid of unknown dimensions, however the measured results indicate that this prior knowledge has no effect on measured values.

Directional Bias Test

The direction of measurement was tested to determine whether it had any bearing on measured values. However, no notable difference was found between measuring in either direction. Hence for the current operator it is not a factor in the accuracy of measured results, however this test is valid for checking individual operators who may be more susceptible to its influence.

View Comparison Test:

By comparing the measured values gained from the left and right view based on the same image capture process the following differences were apparent:

- In the vertical direction both views produced similar measured results, however in the horizontal direction the left view measures fractionally in excess of the true value (80.23mm, mean shortest distance), whereas the right view measures less than the true value (78.64mm, mean shortest distance).

- By examining the Total Difference results the horizontal direction for the right view has a TD value in excess of that accounted for by the operator error hence an instrumental error was noted of 33.1mm.

Distance Test:

With the target object captured at various distances the measured values taken from the images produced were compared. Within the range of the test, distance was not found to be a significant factor in the accuracy of measured values. However the test was conducted with distance as an independent factor following the results of the grid angle position test it is the author's opinion that distance in combination with angle could potentially affect measured values.

Angle in Computer Test

By examining the effects of changing the angle in the configuration settings no notable difference in the vertical direction could be found in measured values which could directly be attributed to the change in the setting. For the horizontal direction however, an improvement in the TD value was noted reducing the TD from 60.6 at 50 degrees to 47.2 at 0 degrees and 56.4 at 100 degrees. Conversely for the left view the TD increases from 29.6 at 50 degrees to 40.8 at 0 degrees and 35.0 at 100 degrees, indicating an instrumental error which is related to the angle setting.

Image Enlargement Test

The potential for measured values to be affected by the enlargement of the captured image on screen prior to measurement was evaluated and was found to show a slight improvement in the closeness of measured values to the true value.

Rotation Test

The effects of measuring the captured image at a range of rotated positions of ± 15 degrees was examined however this was not found to have any detrimental effect on measured values regardless of the direction in which the image was rotated.

Planar Differences Test

The potential differences associated with measuring a three-dimensional surface as opposed to the two-dimensional surface used for the majority of the tests were tested and found to have the following results on measured values:

- Essentially an improvement in measured values was noted when comparing the results from the two-dimensional surface with the same in three-dimensions in concave and convex vertical and horizontal combinations.

Stitching Test

To test the effects of stitching two independent views together a range of stitching options were undertaken. Within the boundaries of the test the stitching process was not found to make any notable difference to measured values. Discounting the auto-align function and the placement of points for stitching as potential sources of error.

Calibration Settings Test

The settings test was based upon altering the calibration settings for the right view to test their impact on measured values. The summarised results of these tests are detailed below by setting combination.

Fringe Spacing – Field of View

An increase in both variables resulted in an increase in horizontal values and hence an improved level of agreement with the true value and an increase in vertical values, thus making the measured vertical values in excess of the true value. A decrease in the value of the settings had the opposite effect.

Camera to Projector Height – Fringe Spacing

In the case of both an increase and decrease in the value of these settings, only a minor effect on measured values was noted, based upon the magnitude of change made to the settings in this instance.

Camera to Projector Depth – Fringe Spacing

The alteration of these variables in combination produced a non-linear impact on measured values. An increase in the variables results in an increase in the overall deviation from the true value for the horizontal direction and a dramatic deviation for the vertical direction, conversely for a decrease in settings only a relatively small difference in the horizontal and vertical directions may be noted.

Camera to Projector Depth – K1

In the case of both an increase and decrease in the value of these settings, only a minor effect on measured values was noted, based upon the magnitude of change made to the settings in this instance.

Camera to Projector Depth – K2

The alteration of these variables in combination produced a non-linear impact on measured values. An increase in the variables results in an increase in the overall deviation from the true value for the horizontal direction, whereas the vertical direction remains relatively constant, conversely for a decrease in settings, the deviation in the horizontal direction decreases, whereas in the vertical direction it increases.

Camera to System Centre – K1

A decrease in the settings results in an overall improved level of agreement with the true value in the vertical direction, however for the horizontal direction the agreement with the true value is diminished. Conversely for an increase in settings both directions show improved results which are illustrated by the removal of s-shaped distortion in the image.

Camera to System Centre – K2

The results for the alteration of settings are much the same as those described for the Camera to System Centre and K1. However a more marked improvement in the results of the horizontal direction are noted following an increase in the value of the settings.

Vertical Grid Angle Position Test

By examining the effects of changing the vertical angle of the target object in relation to the Capture Unit no notable difference could be found in measured values which could directly be attributed to the change in the target object position.

Horizontal Grid Angle Position Test

Contrary to the results of the vertical grid angle position test, the impact of rotating the target object in the horizontal plane did affect measured values. The primary results of the test are summarised below:

- For the left view the alteration in angle appears to have little effect.

- For the right view a distinct linear relationship may be noted between the angle of the target object and the measured results. As the target is turned anti-clockwise the measured values increase from a mean value of 78.64mm at 0 degrees to 80.57mm at 30 degrees. As the target is turned in a clockwise direction the measured values decrease from a mean value of 78.64mm at 0 degrees to 76.47mm at 30 degrees clockwise. Whilst this may in part be explained by s-shaped distortion in the authors opinion it is likely that it is primarily due to the impact of the cosine effect.

Cylinder Test

A cylinder was measured to check the results of the horizontal grid angle position test. The same linear relationship was displayed when examining the results across the curved surface.

6.3. Relevance to Actual Body Form Measurements

Whilst the findings from the evaluation of the single camera Triform™ system were based upon the measurement of a grid adhered to a 2D or 3D surface they may be applied to the body form to suggest how they may affect body dimension measurements. The dimensional differences between the two views will impact on the values obtained by measurement. Any measurements taken directly from the left view should provide relatively accurate measurement results as the deviation from the true value for that view is minimal, on average the deviation is +0.23mm, +0.73mm or +0.54mm dependent on which measurement type is used. Conversely as the right view underestimates the true value this will result in any an under-representation of the actual size of the dimension being measured. The right view can deviate by as much as –1.36mm over a distance of 80mm, however this only represents a relative error of 1.7%.

As the results for the planar differences test showed an improvement in the proximity of measured values to true values these discrepancies in the dimensions for each view should be minimised, particularly where the surface is convex. By stitching two individual views together, which is most likely for body form measurements, the dimensional differences between views are likely to even out as noted during the stitching test. Although it is expected in this case that the right side of the joined image would measure slightly less than it should whereas the left side should provide results very close to the true value, due to the dimensional differences between views.

The distance of the target object to the Unit as an independent variable was found to not affect measured values. This enables greater flexibility in positioning the subject, as providing the subject is within the capture area the measured values should be consistent with one another.

Enlarging and rotating the image on-screen were found to not have any notable affect on measured values hence the operator is able to position the form on-screen to provide the clearest view for measurement, thus avoiding the potential mis-location of landmarks on the body.

The influence of the operator in measurement will remain an issue for body form measurement. The likely mean absolute error for the measurement of a single cell of 80mm was found to be approximately 0.69mm in the horizontal direction and 0.80mm in the vertical direction, this relates to relative errors of 0.86% and 1% in the horizontal and vertical directions respectively. This relative error will therefore apply to any body form measurement taken. Maximum errors were recorded as high as –2.30mm to +2.80mm in the horizontal direction and –2.20mm to +1.90mm in the vertical direction, hence relative errors as high as 2.88% and 3.5% for the horizontal and 2.75% and 2.38% vertical directions respect are also possible, although unlikely.

The angle dependency factor noted in the horizontal direction in both the horizontal grid angle position test and the cylinder test is likely to affect measurements taken over the horizontal plane on a body form. Where a girth may be taken e.g. waist girth it is likely that any error related to angle dependency will be cancelled out. As that which falls at an anti-clockwise direction to the Unit will measured in excess of the true value whilst that clockwise to the Unit will measure less than the true value. However where measurements are taken over only a portion of the image, i.e. the right or left side they may be subject to this error leading to either a higher or lower measurement result dependent on the angle of the portion of the body to the Unit.

CHAPTER 7

CONCLUSION

7.1. Introduction

The overall aim of the investigation was to establish test procedures for the determination of errors in a 3D optical measurement system. An evaluation of the optical measurement system was undertaken and its suitability for providing dimensional information for bespoke clothing manufacture was assessed. The process of evaluation enabled the creation of a systematic test procedure and whilst the methodology was established using a single optical measurement system the test procedure may be applied to other optical measurement systems working on the same principle.

7.2. The Overall Performance of the Image Capture System and Test Procedure

The investigation has been based upon the fulfilment of a number of objectives specified in Chapter 2. To illustrate their contribution to the creation of a systematic test procedure each will be considered in turn.

1. To isolate the potential sources of error associated with one optical measurement system.

   A total of eighteen potential sources of error were identified for the image capture system under evaluation. Those sources found to be most significant include

The angle of the target object to the Capture Unit

The dimensional differences between views

The operator error present during measurement (includes the error related to the size of the marker)

The different types of measuring tools

The impact of amending the values of the calibration variables on measured values (specific to the device under investigation)

The value of the angle setting in the configuration parameters.

The remaining variables that were investigated were discounted as sources of error following the investigation and thus were found to not have any notable effect on measured values, within the boundaries of the specified test procedures.

The repeatability of the capture process over timed intervals

The consistency of results throughout the capture area

The impact of rotating the image on-screen.

The impact of enlarging the image on-screen.

The error related to the stitching algorithm

The positioning of the stitching points

Any operator bias in measuring in a specified direction

The planar differences between 2D and 3D target objects

The vertical angle of the target object in relation to the Capture Unit.

The distance of the target object to the Capture Unit.

The repeatability of measurements following software reboot

2. To quantify the magnitude of error associated with each tested variable and establish the effect on measured values.

The effect of each source of error was evaluated and quantified as part of the test procedure, the results of which appear in Chapters 4 and 6. To identify the error basic statistics were employed such as the mean, standard deviation and standard error of the mean. A measure designed specifically for the investigation, Total Difference (TD), was also used which enabled the absolute error for the entire grid to be calculated thus providing a measure between results within each test. Where possible errors were also categorised to attempt to identify the contributions of operator and instrumental error. This was facilitated by the use of the Total Difference measure.

The likely operator error present during measurement was calculated by using the mean absolute error and was found to be 0.69±0.04mm in the horizontal direction and 0.80±0.04mm in the vertical direction, based on the measurement of a single cell of 80mm. This equates to a mean Total Difference of 27.5mm for the horizontal direction and 33.6mm for the vertical direction, based on the measurement of 40, 80mm cells in the horizontal direction and 42 in the vertical direction.

Dimensional differences between views have identified mean absolute errors of +0.23mm and –1.36mm for the shortest horizontal distance in the left and right views respectively. The error noted in the right view could not be accounted for purely by operator error, hence it may be considered as primarily an instrumental error, as the discrepancy is a product of the image capture system.

The angle of the target object to the Capture Unit was also noted as a variable that affects measured values. The mean absolute error within the –30 degrees to +30 degrees ranged from +0.57mm to –3.53mm respectively. Indicating an error

that is a product of the image capture system and relative to the angle of the target object.

3. To identify the corrective action required, and retest following the correction of errors within the system.

During the investigation the findings of any tests have been supplied to the system manufacturers. Following the results of the manikin test and the initial grid test a systematic error was noted in the shortest distance measurement results, s-shape distortion was noted in captured images and the surface distance measurement tool was proved to be highly variable and inaccurate. Following these findings the system was re-calibrated by the system manufacturers which minimised both the s-shaped distortion and the systematic error. Further work as part of the preliminary investigation identified the mis-alignment of the LCD in the projector (identified during the grid angle position test). Both the LCD housing and the surface distance measurement process were subsequently changed by the manufacturers. For the single camera evaluation a more robust LCD housing was used, although the angle dependency issue which first implied an LCD error still remained, suggesting a further source of error other than just the LCD. The surface distance measure was altered and was found to provide much improved results that were consistent with both the shortest distance and tape measure distance results.

The findings from the single camera system formed the latter part of the investigation and hence the correction of these factors did not occur within the time frame of the practical research. However suggestions are made for the correction of these errors.

The findings of measurement point displacement and the relationship between the angle of the target object and the accuracy of measured values require

changes to the algorithms set within the software. The measurement point displacement is random in nature and hence may be estimated if the surface is a continuous flat surface to enable the operator to attach an uncertainty to any measurements based on its presence. Where the surface is not continuous the error may not be quantified as its effect will be related to the area being measured. The angle dependency factor, however, forms a clear relationship with measured value and hence its systematic nature enables the production of a corrective algorithm to apply to measured values based on the known angle of the target object. Whilst the current error prediction model is only accurate under certain conditions, by the removal of additional sources of error, such as point displacement and the operators influence the same methodology could be employed to provide more accurate results.

Whilst s-shaped distortion is still present to a minor extent, its presence can be minimised further, by the adjustment of the distortion correction factors K1 and K2 and related calibration variables. The inequality between measurement directions and views also may be minimised further, however, in the present system the capability does not exist by which to alter the x and y dimensions individually. Therefore limitations in achieving the correct values exist due to inequalities in the measurements between directions. Both the inequalities and the s-shaped distortion exist due to slight differences in the mirrors and the mounting of those mirrors that introduce variability. The impact of the cosine effect will also alter the measured results even where the target is set at 0 degrees to the front of the Unit, as it is still essentially at an angle in respect to the light path of the right view. Measured values decrease as the target is turned towards the clockwise direction, hence this is the likely primary reason for the underestimation of measured values in the horizontal direction of the right view. Once corrected the measured values could be considerably improved without affecting the values in the y dimension.

Random and systematic errors are present within the image capture and measurement process. The systematic errors such as the cosine effect and measurement inequalities have been discussed. In theory any systematic errors may be either calibrated out or removed by altering the algorithms in the software. The random errors however, are not easily removed or accounted for, these include such factors as the operator's influence in measurement, the operator's influence in selecting the alignment points for the stitch process and the measurement point displacement. All these random errors may be removed from the process by further software development. The measurement process could be altered from what is essentially a manual process to an automated measurement extraction procedure whereby measurements on a form could be extracted based upon predetermined areas to measure. The alignment process could be automated by having points of known orientation on the target object, which could be automatically detected by each view and recognisable within the software, which could be used for an automated alignment, and stitching process. The measurement point displacement could be removed by altering the area and hence the threshold limit within which the nearest point may be selected. At present there are eight additional locations that could be selected instead of the central point, which the operator originally selected, hence the available search area is too large and should be reduced to avoid measurement point displacement.

Following the investigation the manufacturers have now introduced a number of improvements that resolve a number of issues raised during this investigation making the system suitable for the provision of data for bespoke clothing production. An automatic calibration procedure has been introduced, to avoid the potential discrepancies involved in a manual calibration procedure. A number of additional improvements have also been made such as a software correction for the point selection displacement noted in section 5.5 and the facility to alter the x, y and z dimensions independently, thus reducing the

inequality between measurement directions. The system is now commercially used for body dimension surveys and is still in a process of constant development, with the prime aim of providing the highest possible quality 3D data.

4. To evaluate the suitability of the system for providing detailed dimensional information on the human body for bespoke clothing production.

The system in its current form has a limited application to the capture of the human body for bespoke clothing production. The configuration of the single camera system is designed for capturing the torso area of the body and can adequately capture this area on a person within a limited height range. Due to the fixed nature of the system particularly shorter or taller persons cannot be accommodated in the same way and hence a slightly different portion of their body would be captured. The system will capture the front portion of the body and hence ½ circumference measurements are possible, however this again is based on persons of an expected size range and hence on larger persons this area will be reduced somewhat. The time which is taken for the image capture process to complete could result in some minor problems in ensuring the subject stays still during the procedure, body sway, posture and breathing being significant problems in the repeatability of the image capture process on human subjects. Occlusion is another factor in taking adequate three-dimensional images of the body, as areas such as under the arms can often be masked.

As the image capture system under investigation is based upon a light projection method only ambient light can be present during image capture, otherwise the light projections are affected. In a laboratory environment this is not an issue, however in a retail store environment a roofed booth would have to be built to mask any bright lighting. The lighting method in this case also has limitations in

terms of the colours that may be adequately captured. Therefore very dark skinned subjects, dark underwear and shiny fabrics could potentially cause difficulties in obtaining an adequate captured image.

The actual accuracy of the results gained from the system, in terms of the point cloud generation and measurement process are fundamental to the performance of the image capture system for capturing the shape and dimensions of the body. The calibration procedure that has been employed during this investigation has been essentially a manual process, whereby calibration variables are set according to predetermined levels or by measurement and then subsequently adjusted to attempt to improve the accuracy of the image and the measured results. One could compare the process to tuning a television, the quality of the picture being based on the skill of the tuner, hence the procedure is not 100% robust. The inability to alter the x, y and z dimensions independently is another major factor which limits the potential to ensure continuity between views and measurement directions.

The issue of the cosine effect on measured values in the horizontal direction of the right view image is another limitation to the current system, as is the measurement point displacement. However these may be removed with further software development or in the case of the cosine effect by the application of a corrective model.

The reliance upon manual intervention for the measurement and stitching processes are additional limitations to the system. The potential for introducing error is apparent as mean relative errors of 0.86% in the horizontal direction and 1% in the vertical direction have been determined during measurement. With accuracy requirements for bespoke manufacture being so small any sources of error must be kept to an absolute minimum. The operator's influence is random and whilst systematic errors may be removed by calibration or correction

algorithms, random errors add uncertainty to measurements which may not be adequately taken into account.

In terms of evaluating the system against the accuracy requirements for bespoke manufacture the ISO standard 8559 (1989) may be used as a guide. The standard suggests an accuracy of ± 1% or ±5mm whichever is the smaller. The current performance of the system under investigation exceeds the accuracy requirement and hence cannot be deemed to be suitable for the measurement of the body production of bespoke clothing based on the ISO requirement. However the requirement stipulated by ISO is higher than what is generally obtainable through anthropometric measurement. This coupled with the lack of repeatability between repeat anthropometric measurements means the ISO accuracy stipulation is somewhat unrealistic.

When comparing the repeatability of the image capture system taking measurements with manual anthropometric measurements the image capture system provides more consistent results, as shown in the manikin test. Therefore the image capture system is superior in performance to manual measurement. In comparison with the manufacturers accuracy specification of ±2mm the majority of results within this investigation fall well within this tolerance. However it must be noted that this is in comparison to means and based on Total Difference calculations over a fixed area, however upon examination of the single measurement results, (which provide the raw data), the incidence of exceeding this specification is extremely rare and occurs within specific tests, such as the horizontal grid angle position test. The system therefore proves to be fit for purpose in terms of the manufacturer's accuracy specification. Once the instrumental sources of error noted during the investigation are corrected, namely the cosine effect error, the inequality between views and directions and the displacement of measurement points, the system would in the authors opinion be suitable for the extraction of dimensional information for bespoke clothing

production. The system is capable of providing more consistent and accurate measurements than those achievable through traditional manual anthropometric measurement.

It must be noted that the system under investigation has been designed to fall within a specific price bracket, which is relatively low for image capture systems. Potential therefore exists for additional improvements in the production of the 3D data by the introduction of alternative hardware, thus improving the performance of the image capture system. For example, an improvement in the resolution of the data may be gained by upgrading the camera array, higher quality lens will assist in reducing any potential for lens distortion and so on.

5. To document the individual tests undertaken to evaluate the potential for error when altering defined variables.

As a by-product of the investigation all test procedures have been documented regardless of whether the source was found to contribute to the error in measured values. Enabling tests to be undertaken by other researchers on alternative image capture systems.

6. To provide recommendations for the automation of the manual test procedure presented in this thesis.

Recommendations for an automated test procedure have been developed and are included in Chapter 8.

CHAPTER 8

RECOMMENDATIONS

8.1. Recommendations for an Automated Test Procedure

The test procedure implemented has enabled the identification of errors that would otherwise have been indeterminable. The variables associated with the operation of the system have been isolated and individually evaluated for their impact on measured values, to enable their importance in the overall test procedure. The use of the simple 2D surface has proved to be more than adequate for determining the errors within an optical measurement system, enabling curved surfaces, such as those found on the human body, to be simulated.

The tests undertaken during the investigation could be incorporated into an automated error determination and evaluation procedure, which could be used for both new systems and re-calibration following the movement of equipment. This would improve the accuracy by which the methodology may be applied, as the operator error would be removed plus the procedure would have a distinct speed advantage.

A number of issues exist in testing the performance of any image capture system: Calibration is necessary once the system is manufactured and also at predetermined intervals based on the environment in which the system is used. In terms of the initial manufacturing calibration it is imperative that an error determination and evaluation procedure is also undertaken to ensure the system is working to its optimum. Issues also exist related to inter-camera variation and intra-camera performance for multiple view systems.

For the purpose of calibration an automated procedure could be designed based upon a fine grid of markers that are recognisable within the software so that any deviations from the known true locations could be automatically assessed. This simple calibration procedure could be used for calibration of both individual Capture Units and also multiple Capture Units where the convergence of views could be checked. Any deviations from these locations could be corrected automatically or designed to alert the operator to run more critical error determination and evaluation tests where the deviation exceeds a threshold set as acceptable in everyday use. An example of this would be the use of transportable image capture systems, such as those mounted inside vehicles, where movement vibrations may affect the lens mounting.

For the purpose of a more rigorous error determination and evaluation procedure a series of factors would need to be assessed to ensure that all potential errors were checked. This principally applies to single Capture Units/views where the performance of a single image generator is assessed independently. Any errors, which are purely software dependent, may be evaluated and where possible eliminated or taken into account at the manufacturing stage. Such factors that may need to be considered are:

- The effect of rotating the image on-screen
- The effect of enlarging the image on-screen
- The potential for displacement of measuring points

Whilst the rotation and magnification factors did not result in any detrimental effect on measured values in the investigation it is still valid to ensure that this is still the case following software revisions.

The rotation and magnification of on-screen views may be tested using pre-captured images, using predetermined amounts of rotation or magnification

based upon testing the system to its limits relative to the surface being measured. Known areas of each image could be measured before and after rotation to ensure that no detrimental effect occurred. Ideally this would be based upon an automated measurement procedure for reasons of speed and also for the reduction in the error related to taking repeat measurements manually.

The potential for the displacement of measurement points may be checked by identifying the exact points used during measurement once the image is enlarged sufficiently to be viewed as a point cloud. Once corrected the factor will only need rechecking following alterations to the surface construction or following changes to other software variables that may affect threshold limits.

Other additional factors exist which whilst based on software are to some extent also hardware dependent or related to the surface being capture, these include:

- The accuracy of the measurement tools
- The consistency of the results throughout the capture area

The accuracy of the measurement tools may be assessed by measuring a surface which enables each type of measurement tool to be tested, i.e. the shortest, surface and tape measure distances. Such a surface would therefore need to combine curved and flat surfaces, to enable each tool to be tested. By measuring areas of known dimensions the accuracy of each measurement tool may be assessed. Again there is no reason why these areas could not be measured automatically through further software development.

The consistency of the results throughout the capture area may be determined by the measurement of an object that would essentially fill the available capture area. By checking the dimensions of a known object in each part of the capture area any deviations due to for example, s-shaped distortion could be evaluated.

The remaining factor is dependent on the physical configuration of the target object to the image capture system and relates to the distance between the target object and the Capture Unit

The acceptable range of distance between the target and the capture source will need to be determined to ensure the limits for adequate image capture are identified and then can be adhered to by the operator. Once set this factor need only be rechecked following alterations to the calibration settings.

For a multiple Capture Unit system it is imperative that each Unit is assessed independently according to the aforementioned procedure to ensure that each Unit is performing to an adequate standard. Following this the quality of the combination of these multiple views can be addressed. Theoretically by using a system of markers of known geometry for calibration the stitching of multiple views may also be undertaken automatically. If the scaling of each single view can be guaranteed through calibration, then the orientation of each view to one another then just needs to be determined to provide an automated stitching procedure. The quality of the stitch then may be determined through measurement of areas where the two point clouds overlap, this will identify where any discrepancies in the stitching process may lie.

For the purpose of image capture system evaluation the target object would need to comprise of a range of surfaces to enable all sources of error to be tested. Hence, the author suggests that potentially two target objects are used. A 2D grid would be ideal for such factors as checking the consistency throughout the capture area. However for the tests which require a range of surfaces and multiple view testing, concave and convex curved surfaces could be combined with flat surfaces to provide 2D, concave and convex surfaces in both the horizontal and vertical planes. By creating the object to a defined specification

and marking the object with a grid of known dimensions the accuracy of the dimensions of the grid may be assessed for all surfaces.

8.2. Recommendations for Further Work

The research presented has revealed a number of areas worthy of further investigation to progress this area of research.

1. The application of the test methodology presented to alternative image capture systems.

2. The construction of the suggested calibration object and the creation of an automated calibration and diagnostic procedure as suggested in the conclusion.

3. An evaluation of the effects of the combination of angled surfaces in both the horizontal and vertical planes; to assess whether these factors in combination have a direct effect on measured values.

4. The full evaluation of the interdependency between calibration parameters and the determination of the relationship between the parameters in combination and their effect on measured values.

5. The evaluation of difficulties concerned with human body capture, which would include the following elements:

   5.1 The effects of body sway, breathing, and posture.

   5.2. The ability of systems to capture subjects of differing skins tones

   5.3. The ability of systems to capture a range of fabrics, (used for undergarments).

GLOSSARY

Absolute Error — The difference between the measured value and the true value (Eckschlager 1969).

Accuracy — The accuracy of a result refers to its consistency with the true value.

Angle in Computer — Refers to a setting in the configuration parameters of the measurement system software that specifies the physical angle formed at the target object when viewed by the two views. The principle is illustrated in the diagram below.

Figure 4.6. Angle Determination

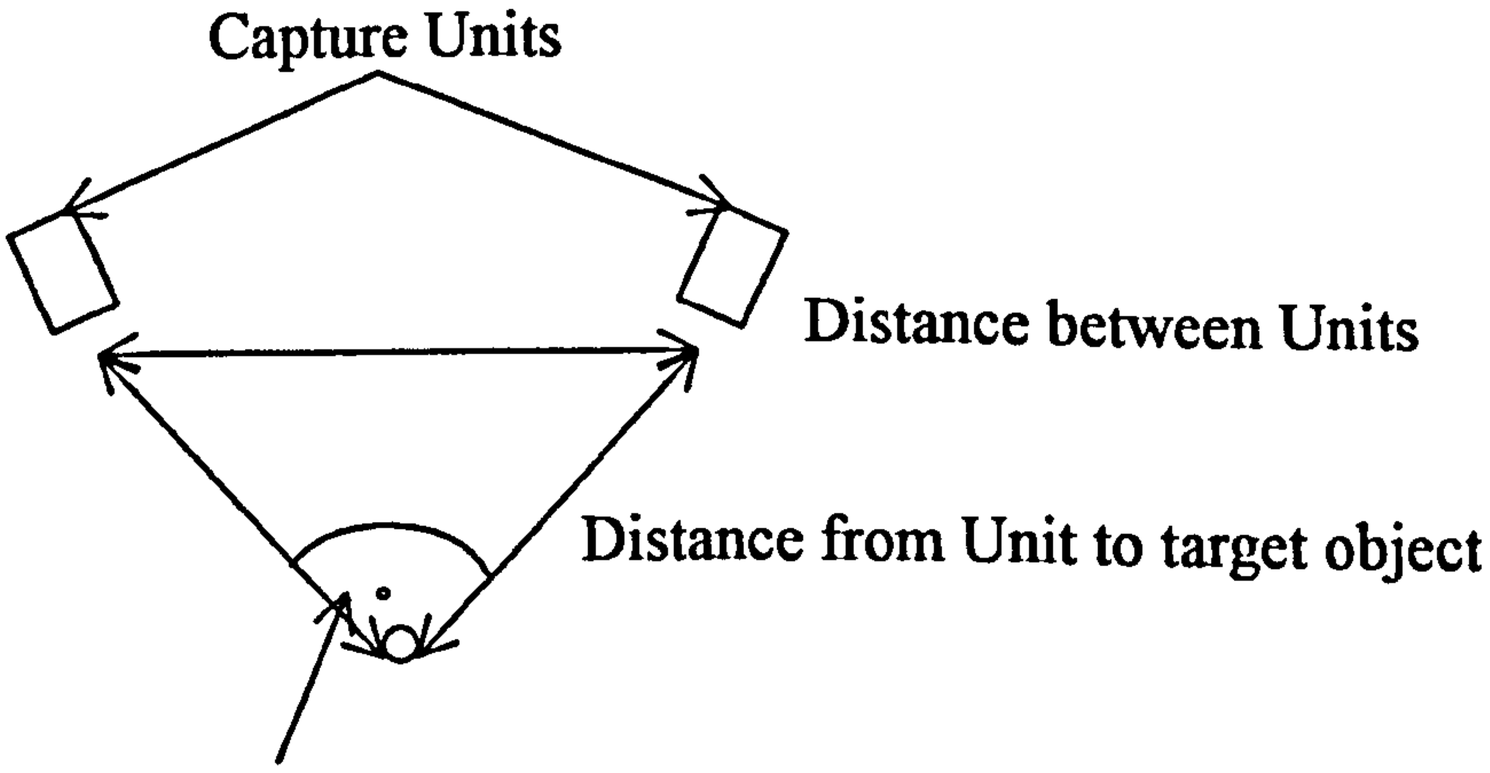

Angle in Computer Test — A test designed to evaluate whether amending the value of the angle setting in the configuration parameters would effect measured values.

Anthropometric Measurement — The physical manual measurement of the human body.

Base Grid	The control grid that provides the basis for all comparisons within each test. The image is captured using the calibration settings specified by the manufacturers and is taken in the configuration shown in Figure 4.5 at a fixed distance and angle from the Capture Units. Direct comparisons may then be made between the base grid and the other variants for each test.
CCD	Charge-Coupled Device.
Camera to Projector Depth	The physical depth distance between the front of the camera and the front of the projector.
Camera to Projector Height	The physical distance between the camera and the projector as they are situated within the Capture Unit.
Camera to System Centre	The physical distance in millimetres from the camera lens to the centre of the target object.
Capture Frame Delay	Capture frame delay is a hardware variable that is used to regulate the speed of the projected pattern change against the running speed of the computer.
Capture Unit	The combined camera and projector unit that facilitates the capture of 3D data.
Capture Unit Comparison Test	A test designed to evaluate any differences between the Capture Units by comparing the measurement results from one Unit with another.
Capture Unit Timed Test	A test designed to evaluate whether the Units were subject to any thermal effect.

Cosine Effect	The effect of the viewing the target at an alternative angle to the normal. As the projector and the camera view the scene from an angle, corrections need to be employed to cover the variation arising from the cosine effect. As the Capture Unit views the target object from an angle, the distance from the Capture Unit to the target is variable across its length and thus this needs to be incorporated into the software to ensure the cosine effect does not impact on measured values.
Cylinder Test	A test designed to evaluate the effects of angle and distance on measured values, by using a cylindrical target object.
Depth Dimension	Relates to the distance from the system centre to the target object.
Distance Test	A test designed to evaluate the effect of capturing images with the target object at different distances from the Capture Units.
Distortion Correction K1	A correction factor used in calibration to remove any convexity or concavity in the captured image.
Distortion Correction K2	A correction factor used in calibration to remove any 'S' shaped distortion in the image that remains after K1 is optimised.
Fringe Spacing	A calibration setting based on the distance between fringes on a flat surface. The variable may also be used to adjust the vertical orientation of the captured object.
Field of View	A calibration setting based on the physical view width at the target object. The setting may also be used to adjust the x and y values.
Gross Error	Errors due to mistakes in procedure, incorrect methodology or numerical errors in calculation (Eckschlager 1969).
Horizontal Dimension	The dimension in the horizontal plane (x plane).

Horizontal Grid Angle Position Test	A test designed to evaluate the effect of capturing images with the target object at different angles in the horizontal plane.
Image Enlargement Test	A test designed to evaluate the effect of enlarging the captured image within the software.
Instrumental Error	An error that may be directly attributed to the use of equipment.
Inter-Observer Error	The error in measurement between observers.
Intra-Observer Error	The error within repeat measurements by the same observer.
Inter-Observer Variability	The variability in measurement between observers.
Intra-Observer Variability	The variability within repeat measurements by the same observer.
Mass Customisation	The process by which mass-market goods are individualised at an affordable cost based upon a defined customer requirement (Gerber [No date]a).
Mean Difference	The difference between mean values.
Mean Range	The upper and lower values for the mean.
Measured Values	The results from measuring a specified area.
Observer Error	An error that may be directly attributed to the influence of the operator.
Operator Error	The resultant error due to the operator's influence.
Physical View Height	The height of the available capture area. Determined by physical measurement of the lit area with the 2D grid perpendicular to the camera axis.

Physical View Width	The width of the available capture area. Determined by physical measurement of the lit area with the 2D grid perpendicular to the camera axis.
Point Cloud	A collection of 3D points in space.
Point Pitch	The spacing of individual points within the point cloud.
Precision	The precision of a result refers to how exactly it is expressed.
Process Time	The time taken to process the raw 3D data into a cleaned image.
Random Error	A chance occurrences that occur in measurement (Eckschlager 1969).
Range of Difference	The upper and lower values for the difference between mean values.
Relative Error	An expression of the accuracy of the result, derived from the absolute error divided by the true value (Eckschlager 1969).
Reliability	The degree of consistency in repeat measurements on the same test (Carmines & Zeller 1979).
Resolution	As a calibration variable the resolution refers to the quality at which the data is stored.
Scan Time	The time taken to capture the raw 3D data.
Shortest Distance	The shortest distance between two points in space.
Software Reboot Test	A test designed to evaluate whether rebooting the software would have any effect on measured values.
Standard Deviation Range	The upper and lower values for the difference between standard deviation values.
Standard Error of the Mean	An estimate of the error of the sample's mean. Standard error of the mean = $\frac{\text{standard deviation}}{\sqrt{n}}$

Standard Error of the Mean Range	The upper and lower values for the difference between standard error of the mean values.
Stitching	The joining of multiple points clouds into one seamless image.
Structured Light	Structured light is a method using projected light patterns to provide three-dimensional information. This is achieved by analysing the distortion of the light patterns as they meet the object to be captured.
Surface Distance	The distance between two points taken along the surface of the image, i.e. following both the contours and convex surfaces.
Systematic Error	A non-random error which forms a constant pattern of results.
Tape Measure Distance	The distance between two points taken along the surface of the image, following the contours but spanning the convex surfaces. Designed to replicate the action of a physical tape measure.
Total Difference	$TD = \sum \lvert \text{Absolute error for each cell} \rvert$
True Value	The accepted value for a measurement.
Units	The Capture Units of the image capture system.
Validity	The degree that a measurement actually measures what it is supposed to (Carmines & Zeller 1979).
Variant	Refers to the description given to the altered variable in each test.
Vertical Dimension	The dimension in the vertical plane (y plane).
Vertical Grid Angle Position Test	A test designed to evaluate the effect of capturing images with the target object at different angles in the vertical plane.
X Plane	The horizontal plane.
Y Plane	The vertical plane.
Z Plane	The depth plane.

REFERENCES

ADDLEMAN, S. (1997) Whole-Body 3D scanner and scan data report. In: THREE-DIMENSIONAL IMAGE CAPTURE, *Proceedings SPIE-the international society for optical engineering, SPIE-The International Society for Optical Engineering. San Jose, California, 11 February 1997.* Washington, USA, SPIE-The International Society for Optical Engineering. Vol. 3023. 2-5.

ANDERSON, L.J. BRANNON, E.L. ULRICH, P.V. MARSHALL, T. STAPLES, N. OLIVER, B. BUTENHOFF, P. BENINATI, M. [No date] Discovering the process of mass customization: A paradigm shift for competitive manufacturing [WWW] Available from: http://ntc.tx.ncsu.edu/html/REPORTS/ANN-RB-FOLDER/ar1.html [Accessed 22 July 1998].

ATC (2000) *Project Identification* [WWW] Available from: http://www.atc.gr/e-tailor/project_Frame. [Accessed 3 March 2000].

BATOUCHE, M. BENLAMRI, R. KHOLLADI, M.K. (1996) A computer vision system for diagnosing scoliosis using moiré images. *Computers in Biology and Medicine*, 26 (4), 339-353.

BELL, J. (1987) Automation beckons the garment industry. *New Scientist*, 13 August, 42-43.

BROOKE-WAVELL, K. JONES, P.R.M. WEST, G.M. (1994) Reliability and repeatability of 3-D body scanner (LASS) measurements compared to anthropometry. *Annals of Human Biology*, 21 (6), 571-577.

BRUNER, D. (1999) Private Communication.

BRUNER, D. (1999a) Application of body scanning technology. *Bobbin Americas Seminar Programme, Bobbin Americas, Atlanta, Georgia, 1 October 1999.* (Unpublished)

BURNSIDES, D.B. (1997) Software for visualization, analysis, and manipulation of laser scan images. In: THREE-DIMENSIONAL IMAGE CAPTURE, *Proceedings SPIE-the international society for optical engineering, SPIE-The International Society for Optical Engineering. San Jose, California, 11 February 1997.* Washington, USA, SPIE-The International Society for Optical Engineering. Vol. 3023. 159-168.

BYRNE, C. [1995] The industrial and social impact of new technology in the clothing industry into the 2000's [WWW] Manchester, UK: David Rigby Associates. Available from: http://www.dratex.co.uk/publications/clotech1.html [Accessed 30 March 1998].

CALDWELL, L.F. WORKMAN, J.E. (1991) Retailers' perceptions of the effects of garment complexity on interest in customized patterns. *Clothing and Textiles Research Journal*, 9 (3), 1-6.

CARMINES, E.G. ZELLER, R.A. (1979) Reliability and validity assessment. In: SULLIVAN, J.L. NIEMI, R.G. (eds) Series: *Quantative applications in the social sciences*. California, Sage University Papers, Sage Publications Inc.

CLARITY FIT TECHNOLOGIES. [No date] Solving the Internet e-commerce apparel shopping problem through the use of true 3-D technology for a virtual try-on and size prediction application [WWW]. Available from: http://www.clarityfit.com/marketing.htm [Accessed 6 October 1999].

CONNER, M. (1995) Body modelling: Pattern blocks from computerised measurements. *Apparel International*, January, 19-20.

COOKSON, C. (1998) Shops get ready for the invasion of the body scanners. *Financial Times*, Friday, 4 December, 1.

COX, D.R. (1992) *Planning of experiments*, 2nd ed., NewYork, John Wiley & Sons Inc.

CRONEY, J. (1980) *Anthropometry for designers*. 2nd ed. London, Batsford Academic and Educational Ltd., 51.

CYBERWARE (1998) Cyberware whole body scanning [WWW]. Cyberware. Available from: http://ghiberti.cyberware.com/products/WholeBody.html [Accessed 4 March 1998].

DAANEN, H. TAYLOR, S.E. BRUNSMAN, M.A. NURRE, J.H. (1997) Absolute accuracy of the Cyberware WB4 whole body scanner. In: THREE-DIMENSIONAL IMAGE CAPTURE, *Proceedings SPIE-the international society for optical engineering, SPIE-The International Society for Optical Engineering. San Jose, California, 11 February 1997.* Washington, USA, SPIE-The International Society for Optical Engineering. Vol. 3023. 6-12.

DEKKER, L. BUXTON, B. (1998) Automated landmarking for virtual human modelling. In: IEE COLLOQUIUM ON COMPUTER VISION FOR VIRTUAL HUMAN MODELLING, *The Institution of Electrical Engineers, London, 9 July 1998*. London, The Institution of Electrical Engineers. Ref:1998/433. 8/1-8/3.

DELONG, M. ASHDOWN, S. BUTTERFIELD, L. TURNBLADH, K.F. (1993) Data specification needed for apparel production using computers. *Clothing and Textiles Research Journal*, 11 (3), 1-7.

DEMERS, M.H. HURLEY, J.D. WULPERN, R.C. GRINDON, J.R (1997) Three dimensional surface capture for body measurement using projected sinusoidal patterns. In: THREE-DIMENSIONAL IMAGE CAPTURE, *Proceedings SPIE-the international society for optical engineering, SPIE-The International Society for Optical Engineering. San Jose, California, 11 February 1997*. Washington, USA, SPIE-The International Society for Optical Engineering. Vol. 3023. 13-25.

DIETRICH, C.F. (1973) *Uncertainty, calibration and probability: The statistics of scientific and industrial measurement*, London, Adam Hilger, 2-3.

DOCTER, G.J. ENSINK, (1985) Automatic measurement of body shape by means of raster stereography. In: WHITTLE, M. HARRIS, D. (eds) *Biomechanical measurement in orthopaedic practice*. Oxford, Clarendon Press.

DOUTY, H.I. (1968) "Visual somatometry" in health related research. *Journal of the Alabama Academy of Science*, 39 (1), 21-34.

EARLY, J. [No date] Body measurement system [WWW]. Textile/Clothing Technology Corporation. Available from: http://hubcap.clemson.edu/~apparel/projects/3D.html [Accessed 1998].

ECKSCHLAGER, K. (1969) *Errors, measurement and results in chemical analysis*, London, Van Nostrand Reinhold Company.

FARRELL-BECK, J.A. POULIOT, C.J. (1983) Pants alteration by graphic somatometry techniques. *Home Economics Research Journal*, 12 (1), 95-105.

FINCH, J. (1994) How we have changed shape. *Daily Express*, May 12, 42.

GERBER [No date] Made to measure or mass customization: Is it for you? *Cuttings*, 18 (1) [WWW] Available from: http://www.ggt.com/library/cuttings/181.mtm.htm. [Accessed 6 August 1998].

GERBER [No date]a What is mass customization? [WWW] Available from: http://www.mass-customization.com. [Accessed 7 September 2000].

GERBER, H.J. (1983) Visions: Tomorrows apparel production. *Bobbin*, February, 89-102.

GODHWANI. A. BHATIA, G. VANNIER, M.W. (1994) Calibration of a multisensor structured light range scanner. *Optical Engineering*, 33 (4), 1359-1367.

GOLDSBERRY, E. SHIM, S. REICH, N. (1996) Women 55 years and older: Part I. Current body measurements as contrasted to the PS 42-70 data. *Clothing and Textiles Research Journal*, 14 (2) 108-120.

GORDON, C.C. BRADTMILLER, B. (1992) Interobserver error in a large scale anthropometric survey. *American Journal of Human Biology*, 4, 253-263.

GORDON, C.C. BRADTMILLER, B. CHURCHILL, T. CLAUSER, C.E. McCONVILLE, J.T. TEBBETTS, I. WALKER, R.A. (1989) *1998 Anthropometric survey of U.S. army personnel: Methods and summary statistics.* Technical Report No. Natick/TR-89/044.

GRAY, S. (1996) Personalisation: IT systems for the next century's clothing customer. In: NICHES IN THE WORLD OF TEXTILES. *Proceedings of the Textile Institute's 77th world conference, Tampere, Finland, May 1996.* Manchester, UK, Textile Institute. Vol. 1 (2), 303-314.

HAMAMATSU (1997) *BL Scanner.* Hamamatsu Photonics K.K.

HEALY, M.R.J. (1989) Measuring measuring errors. *Statistics in Medicine*, 8, 893-906.

HEISEY, F.L. BROWN , P. JOHNSON, R.F. (1986) A mathematical analysis of the graphic somatometry method of pattern alteration. *Home Economics Research Journal*, 15 (2), 115-123.

HEISEY, F. BROWN, P. JOHNSON, R.F. (1990) Three-dimensional pattern drafting. Part I: Projection. *Textile Research Journal*, November, 690-696.

HEISEY, F. BROWN, P. JOHNSON, R.F. (1990) Three-dimensional pattern drafting. Part II: Garment modelling. *Textile Research Journal*, December, 731-737.

HIMES, J.H. (1989) Reliability of anthropometric methods and replicate measurements. *American Journal of Physical Anthropology*, 79, 77-80.

HINDS, B.K. McCARTNEY, J. HADDEN, C. DIAMOND, J. (1992) 3D CAD for garment design. *International Journal of Clothing Science and Technology*, 4 (4), 6-14.

HOLUSHA, J. (1996) Producing custom-made clothes for the masses. *The New York Times*, Monday, February 19.

HORN, M.J. GUREL, L.M. (1981) *The second skin: An interdisciplinary study of clothing*. 3rd ed. Boston, Houghton Mifflin Company, 368.

HUTCHINSON, R. *The geometrical requirements of patterns for women's garments to achieve satisfactory fit.* MPhil, Leeds University, 1977.
ISO 8559: (1989) *Garment construction and anthropometric surveys – Body dimensions*. Switzerland, ISO.

JAMISON, P.L. ZEGURA, S.L. A univariate and multivariate examination of measurement error in anthropometry. *American Journal of Physical Anthropometry*, 40, 197-204.

JOINT CLOTHING COUNCIL LTD. (1957) *Women's measurements and sizes*. London, HMSO.

JONES, P.R.M. LI, P. BROOKE-WAVELL, K. WEST, G.M. (1995) Format for human body modelling from 3-D body scanning. *International Journal of Clothing Science and Technology*, 7 (1), 7-16.

JONES, P.R.M. WEST, G.M. BROOKE-WAVELL, K. (1993) Interrogation of 3D body data for applications in manufacturing industries, In: APPLICATION OF COMPUTERS TO MANUFACTURING ENGINEERING, *Proceedings of the SERC research conference, Directorate of the Science and Engineering Research Council. Sheffield, UK, 1993*. SERC. 20-25.

KAUFMANN, K. (1997) Invasion of the body scanners. *Circuits and Devices*, May, 12-17.

KEE, L. (1993) Sizing for clothing. *Textile Asia*, October, 89 -93.

KNIGHT, A. CASSILL, N. (1994) 3-D Body scanning gets high marks. *Apparel Industry Magazine*, August, 98-103.

KREIBICH, J. (1994) Introduction to the cyber scanner [WWW] Beckman InstituteVisualization Lab. Available from: http://vizlab.beckman.uiuc.edu/people/greg/old/cyberscanner/cyberUG.html [Accessed 28 September 1999].

LEONARD, T. (1997) Women's fashion takes a fresh look at the bottom line. *Daily Telegraph*, 3 February, 8.

LEWIS, J.R.T. SOPWITH, T. (1986) Measuring the human chest with structured lighting. *Pattern Recognition Letters*, 4, 359-366.

LI, P. JONES, P.R.M. (1994) Anthropometry-based surface modelling of the human torso. In: COMPUTERS IN ENGINEERING, *Proceedings of the 1994 ASME international computers in engineering conference and exhibition, The American Society of Mechanical Engineers. Minneapolis, Minnesota, September 11/14 1994.* New York, The American Society of Mechanical Engineers. Vol. 1, 469-474.

MAGGS, R. *'Sizing'-A study of female body measurements in relation to age.* BSc. De Montfort University. 1998.

MARKS, G.C. HABICHT, J. MUELLER, W.H. (1989) Reliability, dependability, and precision of anthropometric measurements. *American Journal of Epidemiology,* 130 (3), 578-587.

MARTORELL, R. MENDOZA, F. MUELLER, W.H. PAWSON, I.G. (1988) Which side to measure: Right or left? In: LOHMAN, T.G. ROCHE, A.F. MARTORELL, R. (eds.) *Anthropometric Standardization Reference Manual.* Champaign, IL, Human Kinetics, 87.

MANUFACTURING CLOTHIER (1983) Does clothing need 3D grading? *Manufacturing Clothier*, April, 41/47.

MUELLER, W.H. MARTORELL, R. (1988) Reliability and accuracy of measurement. In: LOHMAN, T.G. ROCHE, A.F. MARTORELL, R. (eds). *Anthropometric Standardization Reference Manual.* Champaign, IL. Human Kinetics, 83.

NEDSCAN. (1999) NedScan [WWW] Available from: http://www.nedscan.nl/meetuk.htm [Accessed 8 September 1999].

NG, R. CHAN, C.K. AU, R. PONG, T.Y. (1993) Computational technique for 3-D pattern design. *Textile Asia*, September, 62-64.

NUKI, P. (1999) Talking clothes get our measure. *The Sunday Times*, 21 March, 9.

O'BRIEN, R. SHELTON, W.C. (1941) *Women's measurements for garment and pattern construction.* Publication No. 454. U.S. Department of Agriculture.

ODY, P. (1998) The cutting edge. *The Daily Telegraph*, 3 September, 6.

OLIVER, S. HENDRIE, C. (1996) Does size really matter. *The Mail on Sunday* , 4 February, 40-41.

PENTZ, M. SHOTT, M. (1988) *Handling experimental data.* Milton Keynes, Open University Press, 17-22.

PFISTER, H.L. PFISTER, H.D. (1991) Noncontact body measurement for automated apparel manufacturing. *Factory Automation and Information Management*, 529-536.

PHEASANT, S. (1986) *Bodyspace: Anthropometry, ergonomics and design.* London, Taylor and Francis, 28.

RENNESSON, J. (1998) 2D and 3D Automated Body Measurement, Mass Customisation and Made-to-Measure. In: IS MASS CUSTOMISATION POSSIBLE? Textile Institute, *Nottingham, UK, April 1998*, (Unpublished).

ROSS, T. (1996) CAD/CAM experts look to the year 2000. *Canadian Apparel Manufacturer*, 20 (3), 20-22.

RUSSELL, E. (1999) Taking the measure of whole body scanning. *World Clothing Manufacturer*, April, 15.

SAE [No date] Civilian American and European Surface Anthropometry Resource Project - CAESAR™ [WWW] Available from: http://www.sae.org/TECHCMTE/caesumm.htm [Accessed 10 January 1997].

SANDERSON, P.M. [No date] Human factors in human-machine systems [WWW]. Available from: http://aviation.uiuc.edu/institute/acadprog/epjp/Anthropom.html [Accessed 30 September 1997].

SHELDON, W.H. STEVENS, S.S. TUCKER, W.B. (1940) *The varieties of human physique.* New York, Harper & Bros.

SHEN, L. HUCK, J. (1993) Bodice pattern development using somatographic and physical data. *International Journal of Clothing Science and Technology*, 5 (1), 6-16.

STOKES, G. (1997) CAESAR™ measures the U.S. and Europe. *ASTM Standardization News*, August, 22-25.

TAMBURRINO, N. (1992) Apparel sizing issues, Part 1. *Bobbin*, April, 44-46.

TAMBURRINO, N. (1992a) Sized to sell. *Bobbin*, June, 68 & 72-74.

TAMBURRINO, N. (1992b) Apparel sizing issues: Part 2. *Bobbin*, May, 52-60.

TAYLOR, J.R. (1982) *An introduction to error analysis: The study of uncertainties in physical measurements*, California, University Science Books, 3&7.

TECMATH [No date] High tech perfection [WWW] TecMath. Available from: http://www.tecmath.com/Menschmodellierung/measurement/flyer_cont1.html [Accessed 30 November 1999].

TECMATH [No date]a Contour/ArmyFit: Touchless body measuring and automatic clothing size determination [WWW] TecMath Human Modelling. Available from: http://arn.iitri.org/docs/scan/articles/tmarmy [Accessed 8 March 1999].

TECMATH [No date]b Clothing made to measure [WWW] Framework "Production 2000" of the Federal Ministry of Edukation, Science, Research and Technology, Germany (BMBF). Available from: http://www.tecmath.com/Menschmode...projekte/produktion_2000_eng.html. [Accessed 8 October 1999].

TECMATH (1998) *European Center of Individual production* [WWW] Available from: http://www.tecmath.com [Accessed 27 January 2000].

TELMAT (1999) *Symcad turbo flash/3D*, July.

TELMAT (1999a) *Symcad: Automated 3D body measurement*, March.

TRELEAVEN, P. DEKKER, L. (1998) The Challenge of 3D Data Capture. In: IS MASS CUSTOMISATION POSSIBLE? Textile Institute, *Nottingham, UK, April 1998*, (Unpublished).

TRELEAVEN, P. BUXTON, B. SLATER, M. (1999) *Centre for 3D electronic commerce*. Foresight LINK Award Application. University College London. (Unpublished).

TURNER-SMITH, A.R. HARRIS, D. (1985) Shape measurement in the Scoliosis clinic. In: WHITTLE, M. HARRIS, D. (eds) *Biomechanical measurement in orthopaedic practice*. Oxford, Clarendon Press.

ULIJASZEK, S.J. LOURIE, J.A (1994) Intra- and inter-observer error in anthropometric measurement. In: ULIJASZEK, S.J. MASCIE-TAYLOR, C.G.N. (eds.). *Anthropometry: the individual and the population*. UK, Cambridge University Press, 30-55.

VALKENBURG, R.J. McIVOR, A.M. (1998) Accurate 3D measurement using a structured light system. *Image and Vision Computing*, 16, 99-110.
VINCOUREK, V. (1990) Statistics for clothiers. *Textile Asia*, July, 85-88.

VITRONIC [No date] Vitus whole body scanner [WWW] Vitronic. Available from: http://www.vitronic.de/vitus_e1.htm [Accessed 8 September 1999].

VOUYOUKA, A. VOUYOUKA, I. (1997) Solutions to female size variations for accurate style interpretation in order to generate consumer demand. In: TEXTILES AND THE INFORMATION SOCIETY, *Proceedings of the 78th world conference of the Textile Institute, Textile Institute. Thessaloniki, Greece, 1997*. Manchester, Textile Institute. Vol. 1, 353-368.

WARD, J. ROGERS, N. BROWN, R. JEFFRIES, G. WRIGHT, D. (1996) Techniques for the measurement of the human body and its actions: application to design for physically disabled people. *Journal of Rehabilitation Sciences*, 9 (2), 34-45.

WENG, J. COHEN, P. HERNIOU, M. (1992) Camera calibration with distortion models and accuracy evaluation. *IEEE Transactions on Pattern Analysis and Machine Intelligence*, 14 (10), 965-980.

WEST, G.M. *Loughborough Anthropometric Shadow Scanner (LASS)*. MPhil, Loughborough University of Technology, 1987, 34-35.

WICKS & WILSON LTD. (1999) Private Communication.

WICKS & WILSON LTD. (2000) Private Communication.

WILMORE, J.H. STANFORTH, P.R. DOMENICK, M.A. GAGNON, J. DAW, E.W. LEON, A.S. RAO, D.C. SKINNER, J.S. (1997) Reproducibility of anthropometric and body composition measurements: the HERITAGE family study. *International Journal of Obesity*, 21, 297-303.

WORLD CLOTHING MANUFACTURER (1999) Mass Customisation. *World Clothing Manufacturer*, 16 November, 16.

WWW.IC3D.COM. (1999) Interactive custom clothes company & ic3d jeans ~ In the news [WWW] Available from: http://www.ic3d.com/aboutus/press_release_0399.htm [Accessed 27 May 1999].

WYATT, J. (1999) The challenge of clothing for disabled and elderly people. Paper in preparation.

YANG, Z. WANG, Y.F. (1996) Error analysis of 3D shape construction from structured lighting. *Pattern Recognition*, 29 (2), 189-206.

APPENDICES

APPENDIX A

PRELIMINARY IMAGE CAPTURE SYSTEM EVALUATION: MANIKIN TEST

A1. Introduction

At this time the objective of the evaluation of the image capture system was to ascertain its performance in terms of its capability to accurately capture the shape and dimensions of the human body. The investigation was focussed towards using the system to characterise the torso area for ladies with Scoliosis, as discussed in section 1.2. To evaluate the performance of the system a test was devised based on measuring areas of the torso of a female manikin to ascertain how closely the measurements generated by the image capture system compared to those taken by anthropometric measurement.

A2. Manikin Test

The test was undertaken using a standard size 18 female tailor's manikin, without arms, chosen for a number of reasons.

1) It was of an appropriate size for the capture volume set within the system.
2) It provided a symmetrical form, which may be measured from either side without the encumbrance of adopted body poses found on most display manikins.
3) The form is rigid and therefore will provide more consistent anthropometric measurement results than that of a human body which is malleable and subject to change through slight differences in pose adoption.

A2.1. Measurement Methodology

The selected measurements covered several planes, utilising the different types of measurement offered by the TriForm™ system. Both the capture system and anthropometric measurement readings were recorded for each dimension for comparative purposes. The tests were undertaken by two observers each taking 27 measurements. This measurement process was then repeated by each observer, both with the TriForm™ system and by anthropometric means to provide information on intra- and inter-observer variability.

A number of measurements were selected to enable characterisation of the female torso.

Figures A1 – A4 illustrate the measurement locations on the manikin.

Figure A1. Manikin: Front View

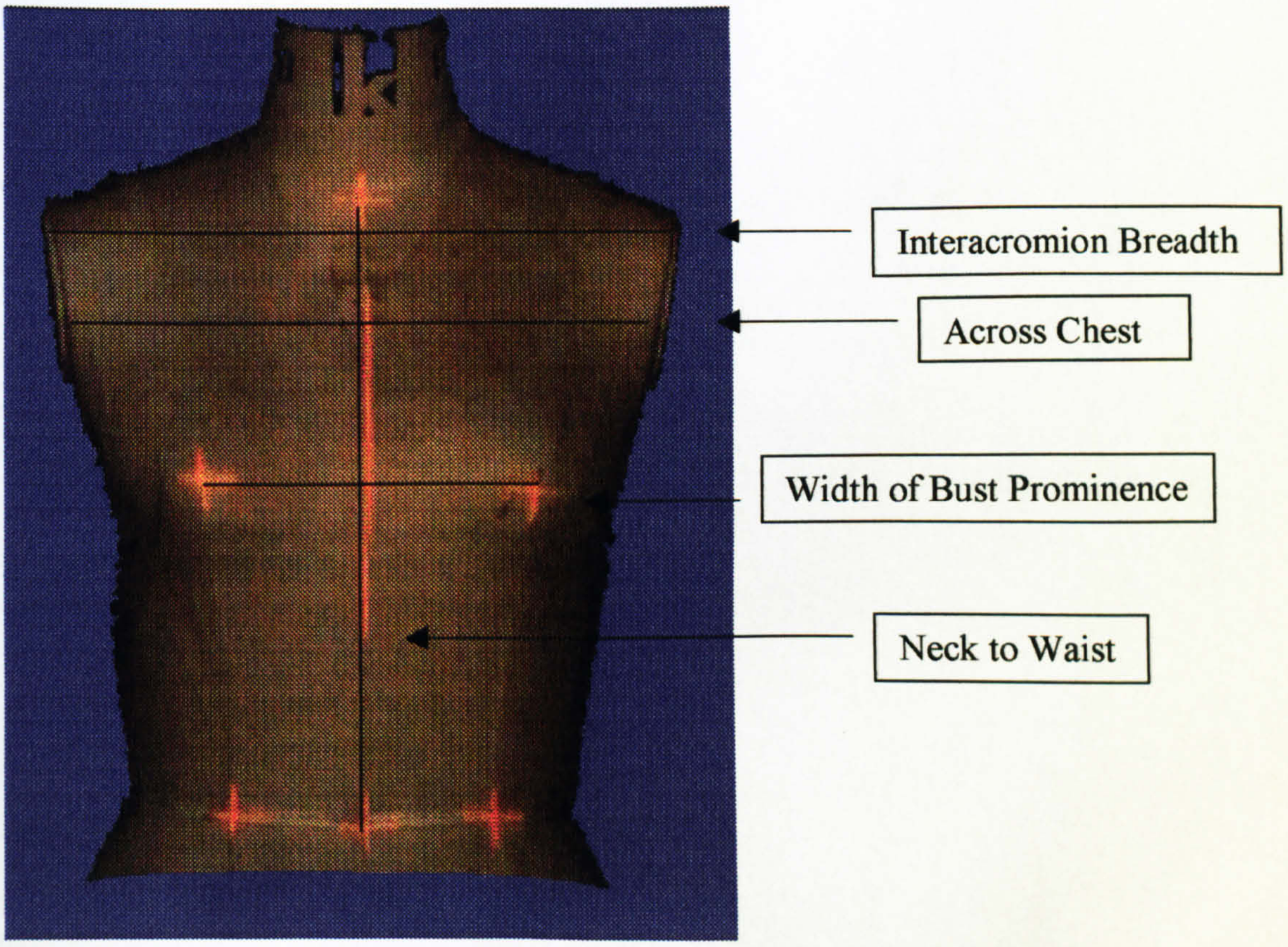

Figure A2. Manikin: Right Side View

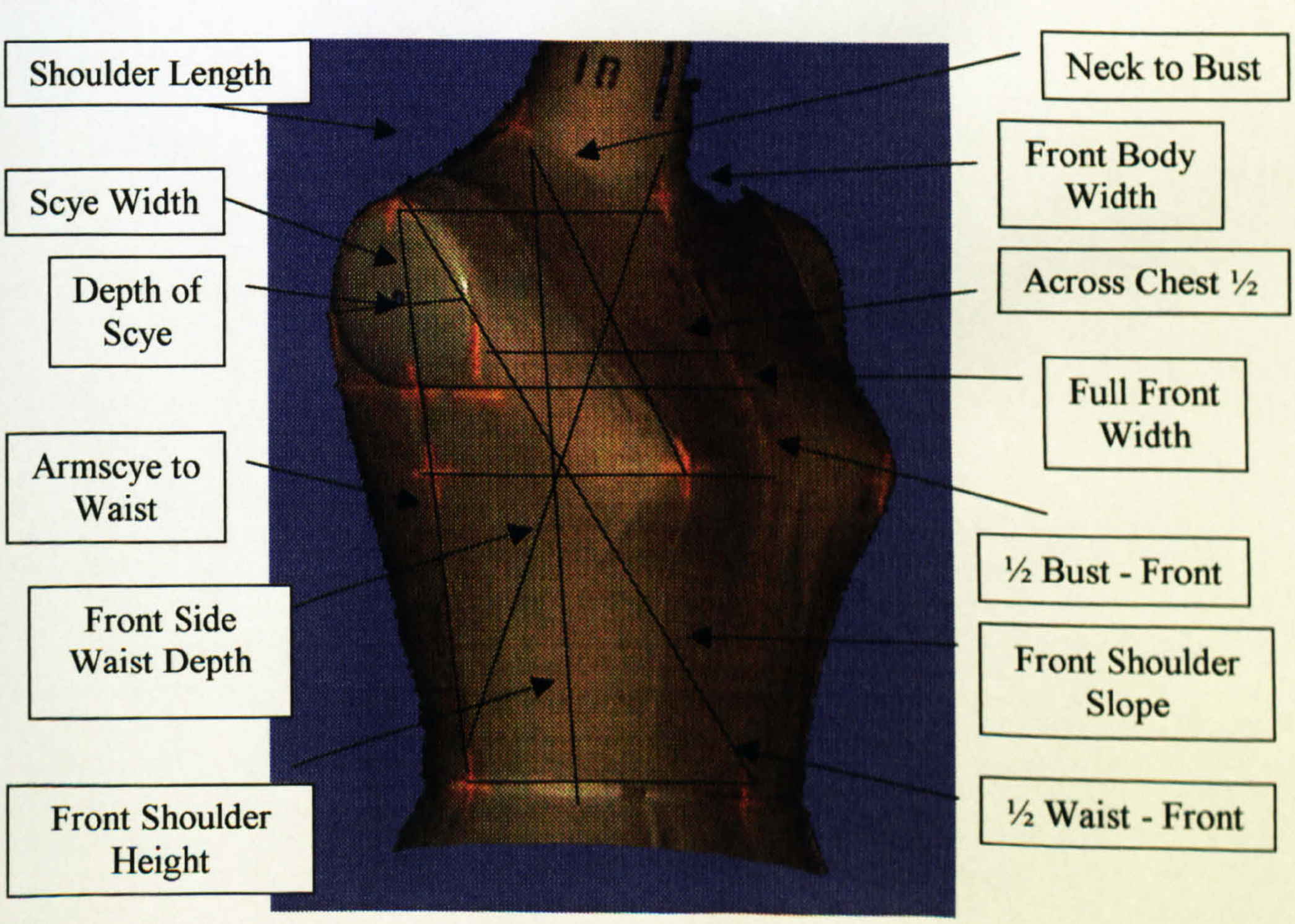

Figure A3. Manikin: Back View

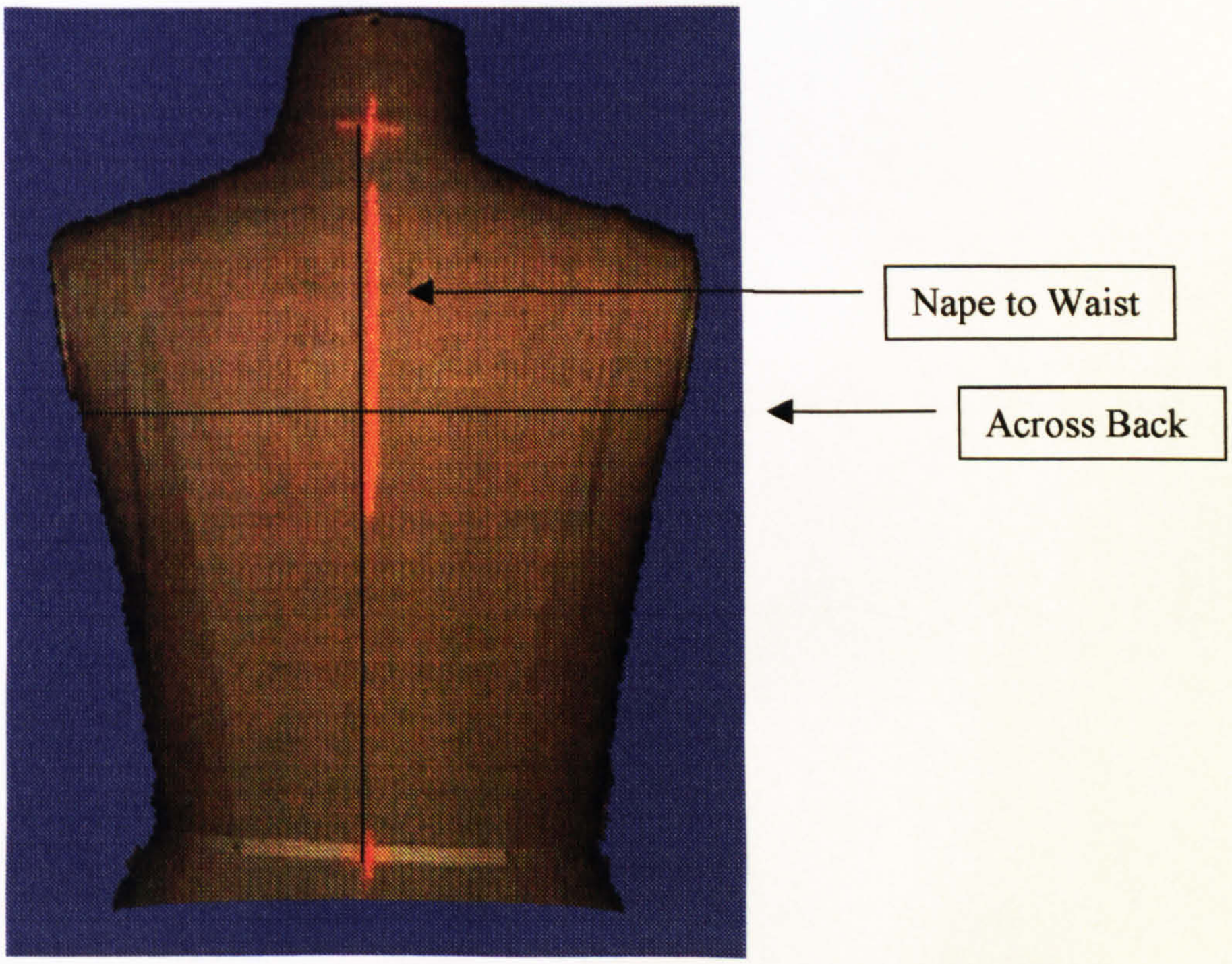

Figure A4. Manikin: Left Side View

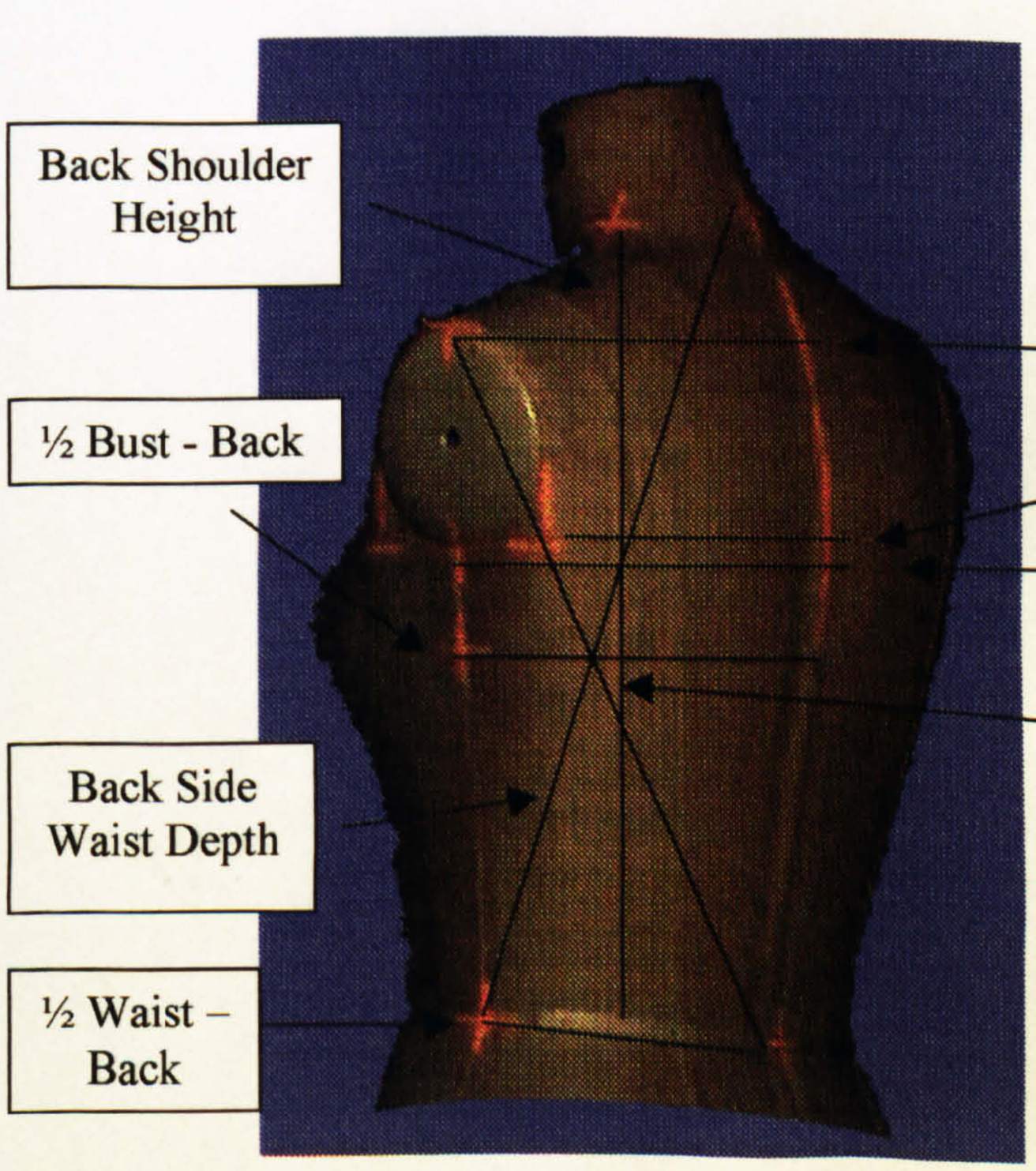

The relevant body sites were marked prior to measurement by strips of orange fluorescent adhesive paper measuring approximately 3mm wide. Both the colour and size of the markers were chosen for visibility on-screen. All measurements were taken directly on the fabric of the surface using the landmarks on the manikin as reference points.

A2.2. Anthropometric Measurements

The shortest distance measurements were taken using a Harpenden Anthropometer (Holtain Ltd, Dyfed), whilst the surface and 'tape measure' measurements were taken using a Rabone Chesterman Miniflex steel anatomical tape (Cranlea & Company, Birmingham). Anthropometric measurements were taken by each technique (shortest, surface & tape measure distance) with the exception of the following:

Tape measure distance -	Interacromion breadth
Surface distance –	Interacromion breadth
	Width of bust prominence
	Across Chest (Full)
	Front shoulder slope
	Front side waist depth

These anthropometric measurements were omitted, as taking the measurement was found to be impractical. The tape measure distance on the interacromion breadth is unworkable as the neck area interferes with the line of the tape measure. For the remaining surface distance measurements it was found to be very difficult to ensure the tape measure remains in full contact with the body, as each of the five measurements noted contain both convex and concave areas. The measurements therefore could not be relied upon as being accurate and thus were omitted.

A2.3. TriForm™ Measurements

The images were initially taken using a single Capture Unit system. A total of four were taken. Front, right side, back and left side. These allowed all of the landmarks to be viewed to enable measurement of the form. The positions for each of the images captured are shown in Figures A1-A4. Each of the side views needed to be rotated on-screen to enable clearer viewing of the remaining landmark points.

Following this, images of the front and back view positions of the manikin were captured on a two-camera system. The images were then rotated, on-screen, to enable viewing of all the landmark points.

A2.4. Evaluation of the Measurement Results

The measurement results were examined by comparison between anthropometric and TriForm™ results for each camera configuration and for each measurement technique. The mean, standard error of the mean, mean difference and inter and intra-observer variability were calculated using Microsoft Excel 97. These were used to assess the degree of agreement between the two systems of measurement, between successive measurements and between observers. The mean error range and mean difference were both calculated to two decimal places. The reported precision of the TriForm™ measurement is 0.1mm and as the results concern mean values the precision by which the measurement may be stated should increase. Therefore the decision was made to calculate to two decimal places to illustrate the differences between systems of measurements even though the known accuracy of the system is only ± 2.0mm for any distance measurement.

A2.5. Mean and Standard Error Variability

The full tabulated results for the mean, standard error of the mean and the mean difference may be found in section A4, with Tables A3, A4, and A5 referring to the shortest, surface and tape measure distances for a single camera, and Tables A6, A7 and A8, for a two-camera system respectively.

Table A1. Range of the Mean Error

(Based upon the standard error of the mean)

	Total Number of Measurements (*n*)		Anthropometry (mm)	TriForm™ (mm) Single Camera System	TriForm™ (mm) Two-Camera System
	Anthropometry	TriForm™			
Shortest Distance	*n*=108	*n*=108	0.25 – 2.75	0.18 – 1.56	0.09 – 1.62
Surface Distance	*n*= 88	*n*=108	0.00 – 1.31	0.77 – 12.60	0.06 – 5.74
Tape Measure Distance	*n*=104	*n*=108	0.00 – 1.32	0.22 – 3.40	0.10 – 4.36

n = individual measurements measured four times.

The anthropometric surface and tape measure distance results indicate a lower variability than the shortest distance results. The maximum mean error being 1.31mm, 1.32mm and 2.75mm respectively. Conversely the TriForm™ measurements displayed a maximum mean error of 1.56mm (shortest distance), 3.40mm (tape measure distance) and 12.60mm (surface distance). For the two-camera system (TriForm™ measurement only) the shortest distance and the surface distance display a maximum mean error of 1.62mm and 5.74mm respectively, with a maximum mean error of 4.36mm for the tape measure measurement. However, to put this into perspective, the majority of TriForm™ measurements show mean errors of less than 10mm.

The standard error of the mean is virtually the same for the surface and tape measure anthropometric measurements, whereas it is almost twice as large for the shortest distance measurement. This indicates the variability in taking this type of measurement over areas that are difficult to measure. For the TriForm™ measurements the standard error remains very similar for the shortest distance when changing from a single to a two-camera system. However, for the surface distance the error is considerably smaller and for the tape measure distance the standard error is greater when using the two-camera system. The variability in the range of the standard error for the surface distance illustrates the inconsistency within the TriForm™ system as it is unlikely that the difference is related to the change in the number of cameras.

The results of the standard error of the mean display a significantly higher degree of variability in the TriForm™ measurements for the surface and tape measure distances, when compared to those recorded during anthropometric measurement. However, the variability for the shortest distance is smaller for the TriForm™ measurements than for anthropometry. Indicating that the TriForm™ system provides greater consistency in undertaking repeat shortest distance measurements than anthropometry.

A2.6. Mean Differences Between Anthropometry & TriForm™

Table A2. Range of Difference Between TriForm™ and Anthropometry

		Total Number of Measurements (*n*)	Range of Difference (mm) (Triform™ - Anthropometry)	% Range of Difference
Single Camera System	Shortest Distance	*n*=108	-17.70 – 49.70	-9.39 – 31.86
	Surface Distance	*n*= 88	-27.43 – 36.65	-6.22 – 27.00
	Tape Measure Distance	*n*=104	-46.58 – 3.07	-11.63 – 1.44
Two-Camera System	Shortest Distance	*n*=108	-27.50 – 47.28	-10.54 – 30.30
	Surface Distance	*n*= 88	-33.03 – 4.95	-11.58 – 3.65
	Tape Measure Distance	*n*=104	-49.45 – -2.90	-1.64 – -11.74

n = individual measurements measured four times.

The variation between the anthropometric measurements and those taken using TriForm™ vary from -17.70 to 49.70mm for the shortest distance, (however, just under half of the total measurements exhibit a difference of less than 5mm), from –27.43 to 36.65mm for the surface distance and -46.58 to 3.07mm for the tape measure distance. For the two-camera system the variation between the anthropometric measurements and those taken using TriForm™ vary from –27.50 to 47.28mm, for the shortest distance, from -33.03 to 4.95mm, for the surface distance and from -49.45 to –2.90mm for the tape measure distance.

The majority of measurements (both locations and types) display an increase in difference between the anthropometric and TriForm™ results when changing

from a single to a two-camera system. However, the overall range of difference remains similar regardless of the system. One potential reason is the introduction of additional errors following the stitching process, which may have affected individual measurements. The difference between the TriForm™ and anthropometric measurements are generally below 10mm for a single camera system, however, when changing to a two-camera system only the shortest distance follows this trend, with the majority of the surface and tape measure differences falling outside this limit.

A2.7. Inter and Intra-Observer Variability

Figures A5, A6, and A7 refer to the inter-observer variability and Figures A8, A9 and A10 refer to intra-observer variability for a single camera system. Figures A11, A12 and A13 and Figures A14, A15 and A16 refer to a two-camera system, for inter and intra-observer variability respectively.

Measurement Key:

1. Interacromion Breadth
2. Depth of Scye
3. Scye Width
4. Width of Bust Prominence
5. Shoulder Length
6. Neck to Waist
7. Front Shoulder Height
8. Front Body Width
9. Across Chest Full
10. Across Chest Half
11. Front Shoulder Slope
12. Full Front Width
13. Front Side Waist Depth
14. Across Back Full
15. Across Back Half
16. Back Body Width
17. Full Back Width
18. Back Shoulder Slope
19. Back Side Waist Depth
20. Nape to Waist
21. Back Shoulder Height
22. Neck to Bust
23. Armscye to Waist
24. ¼ Bust Girth – Front
25. ¼ Bust Girth – Back
26. ¼ Waist Girth – Front
27. ¼ Waist Girth – Back

For use with Figures A5 – A16.

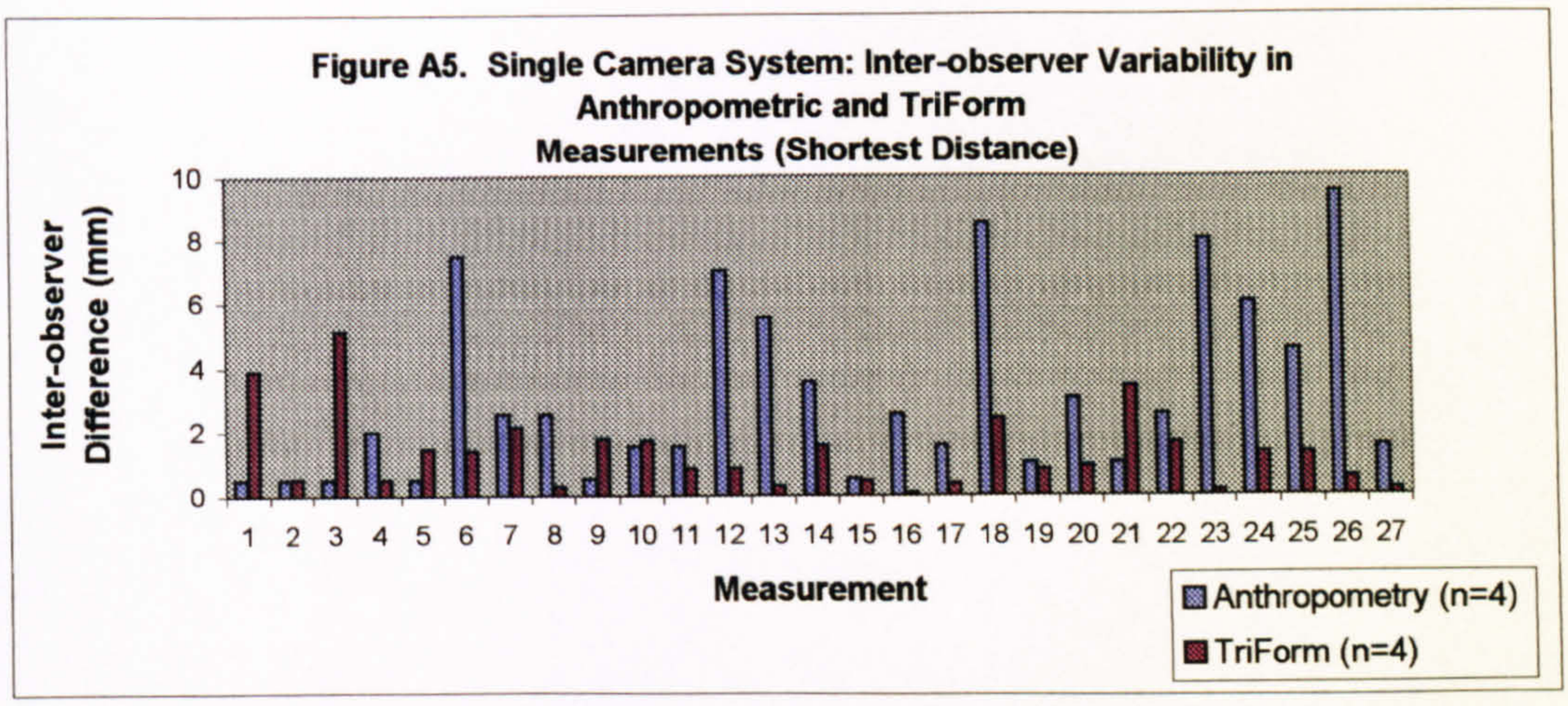

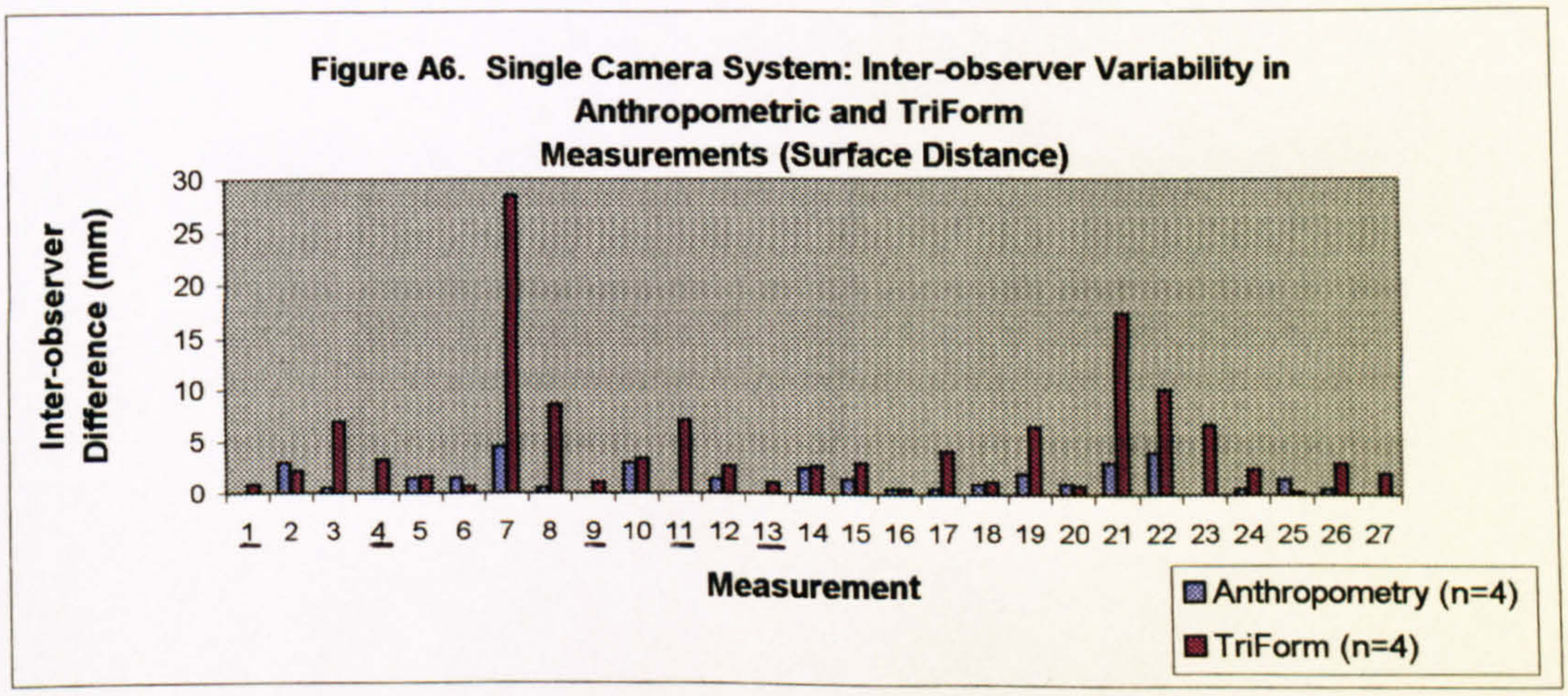

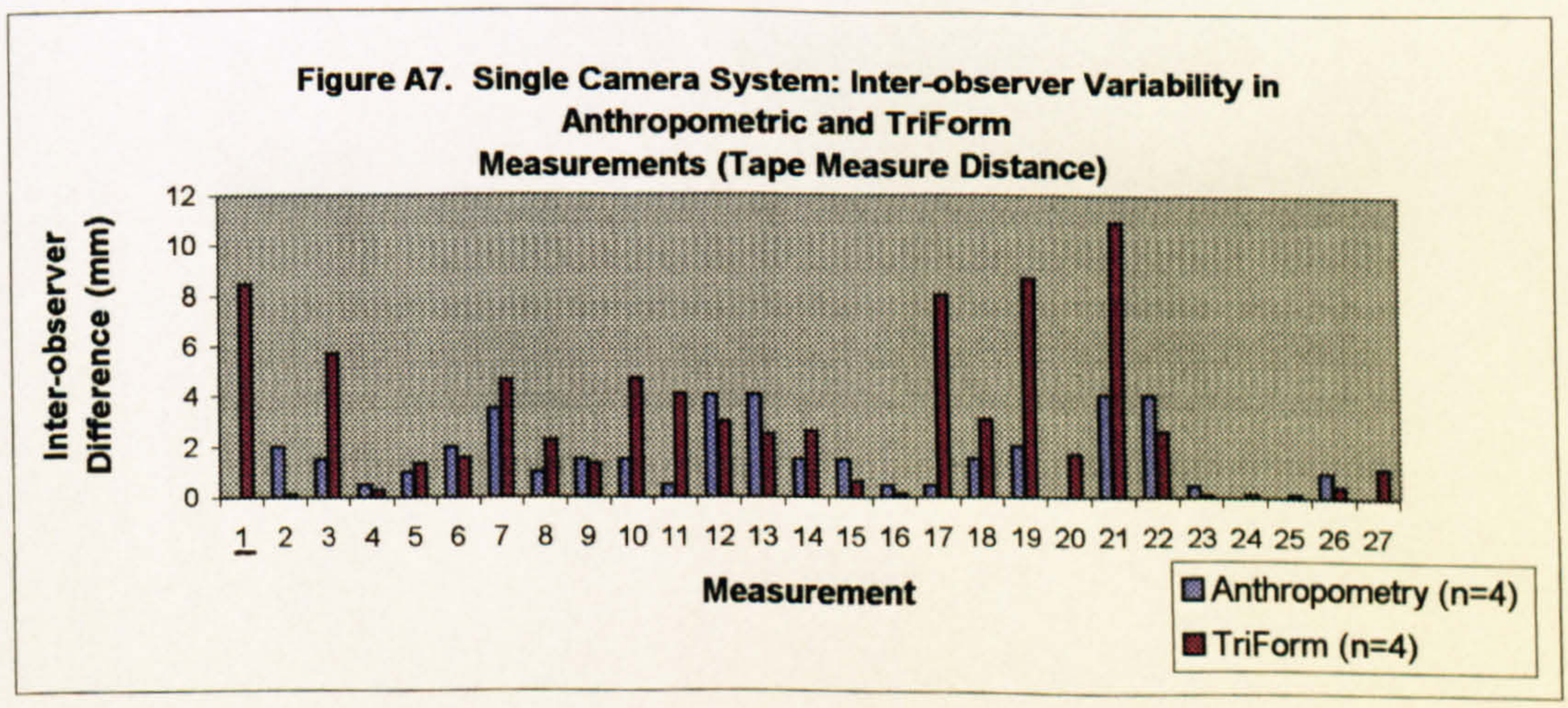

Key: _____ Manual measurements omitted
n = Number of repeat measurements

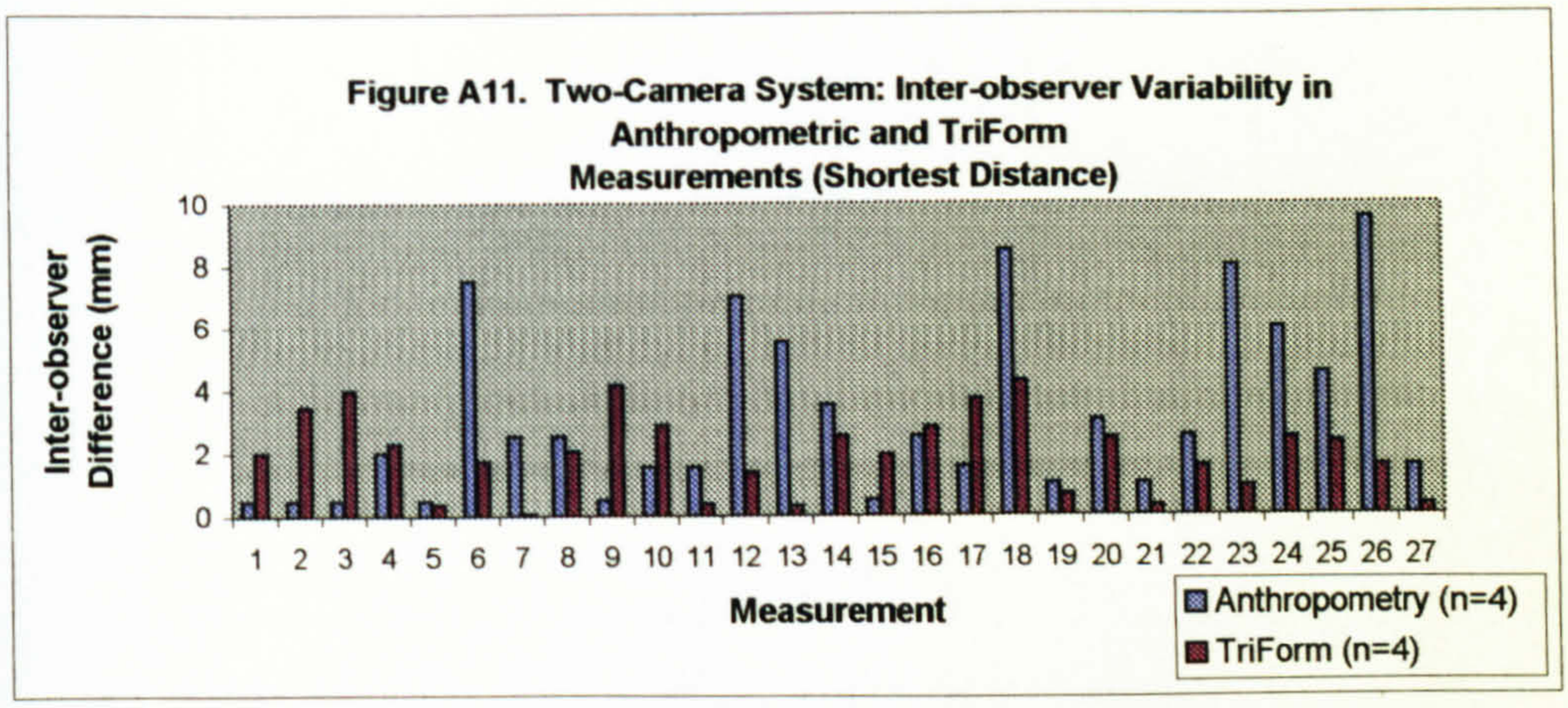

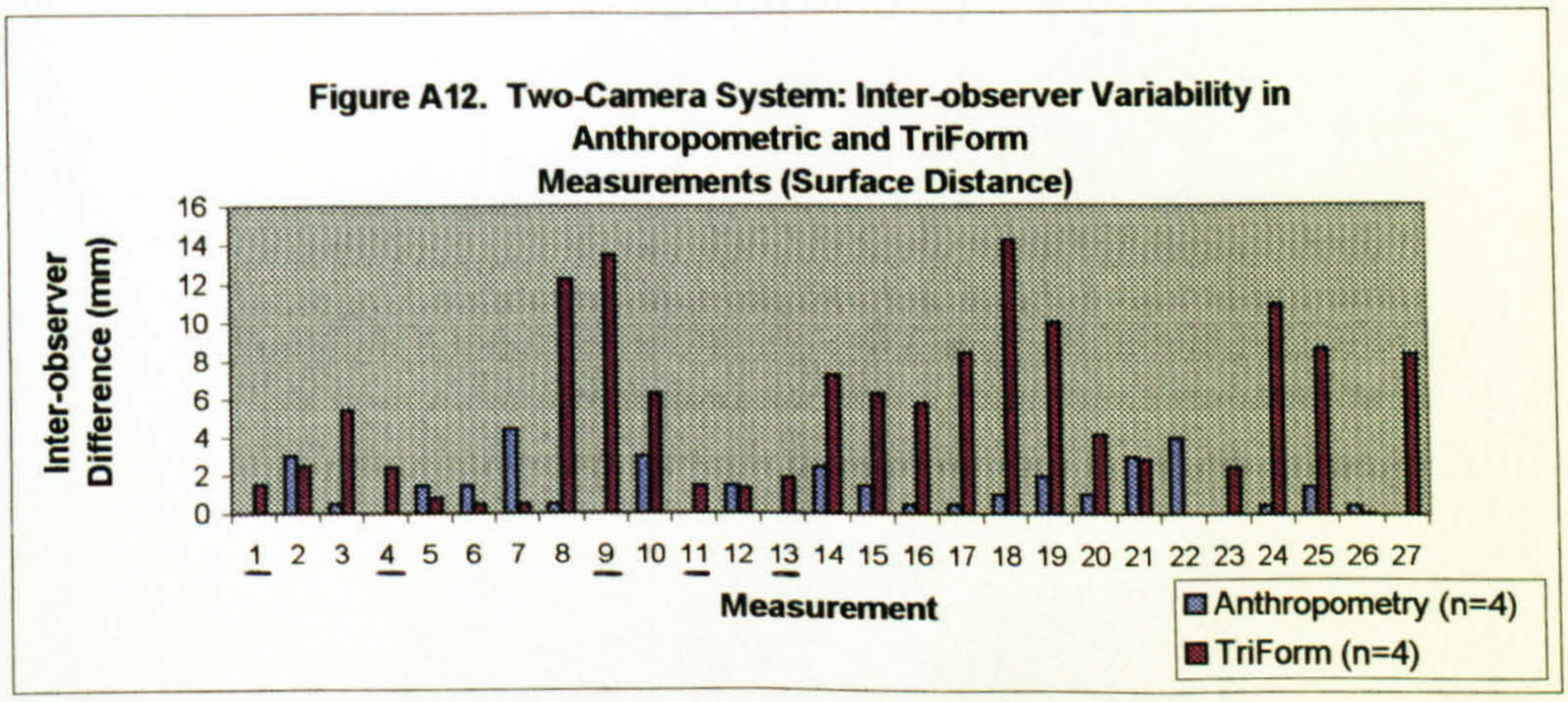

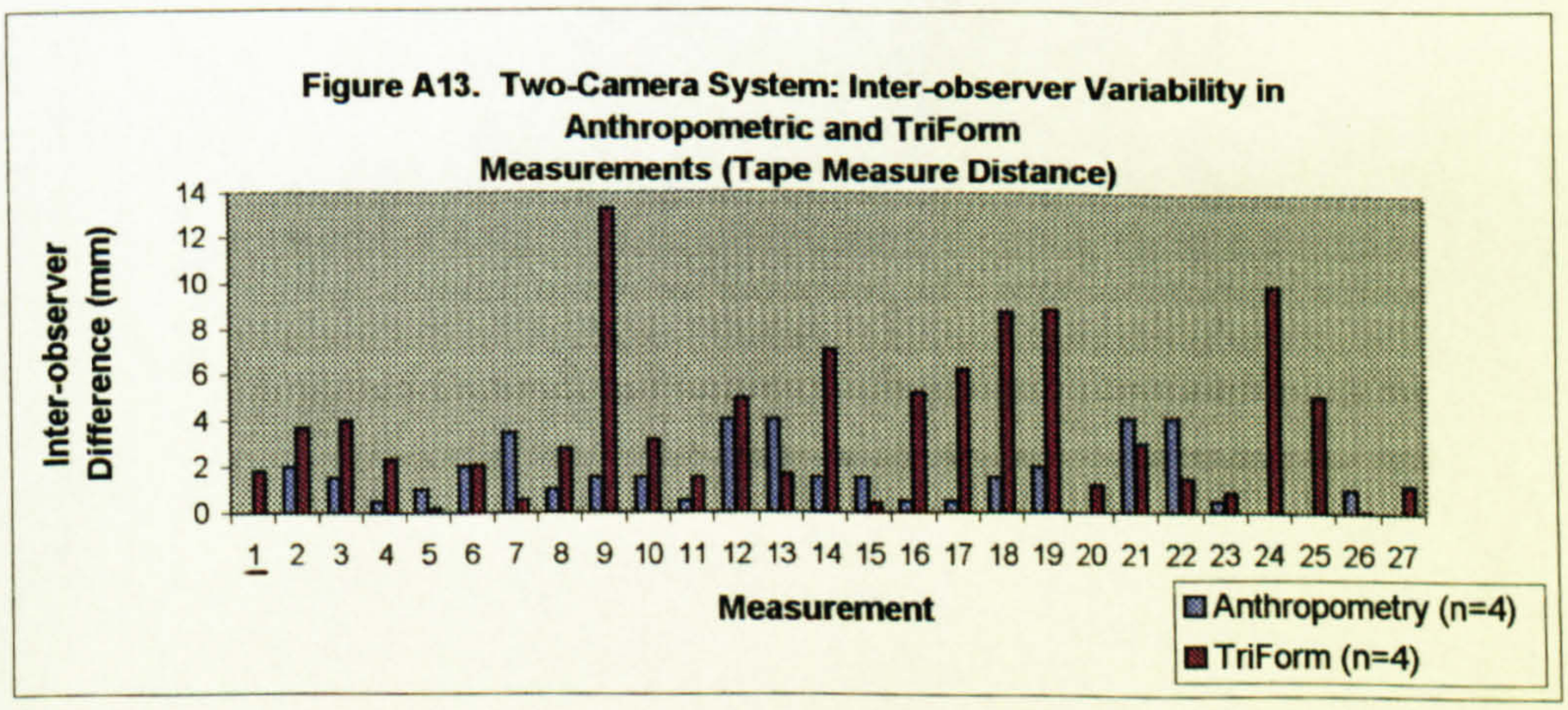

Key: ——— Manual measurements omitted
n = Number of repeat measurements

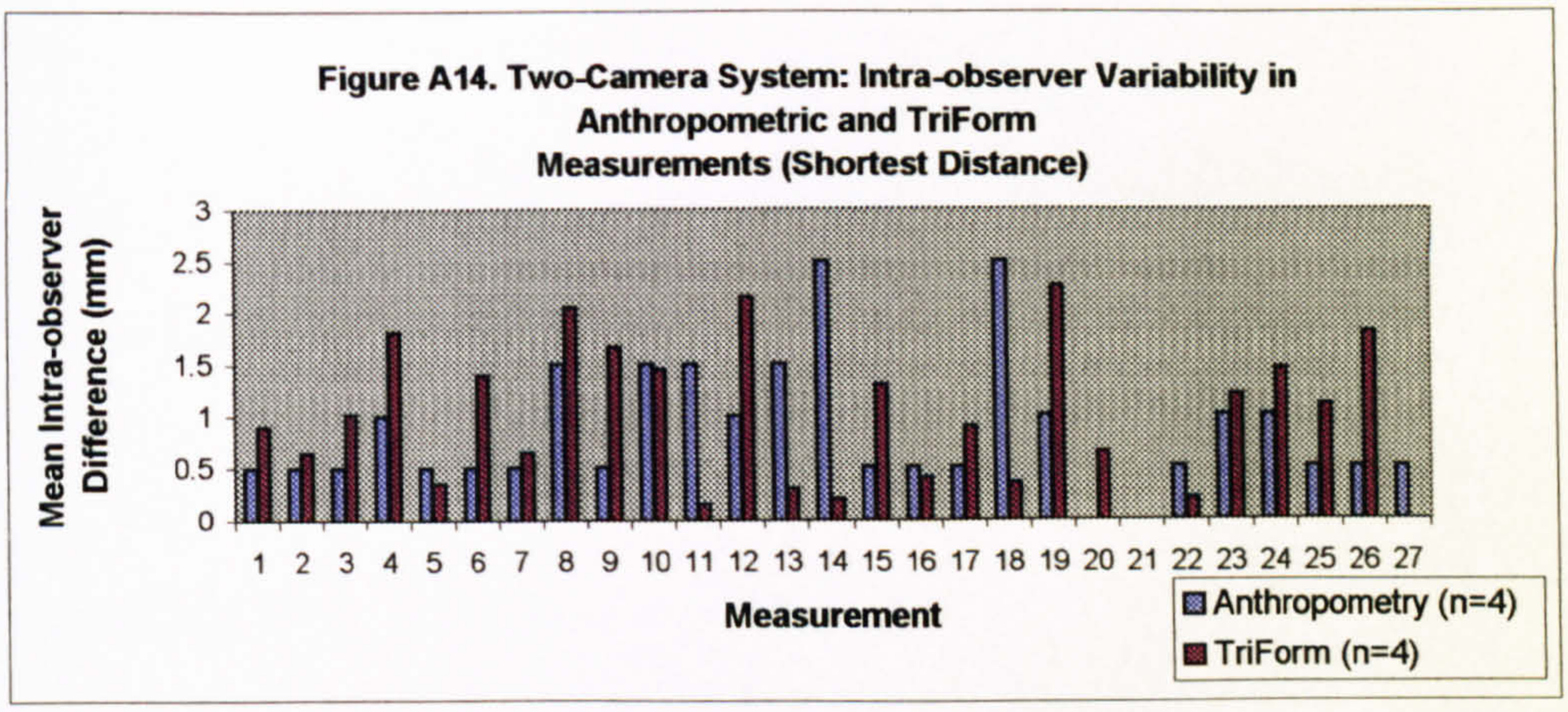

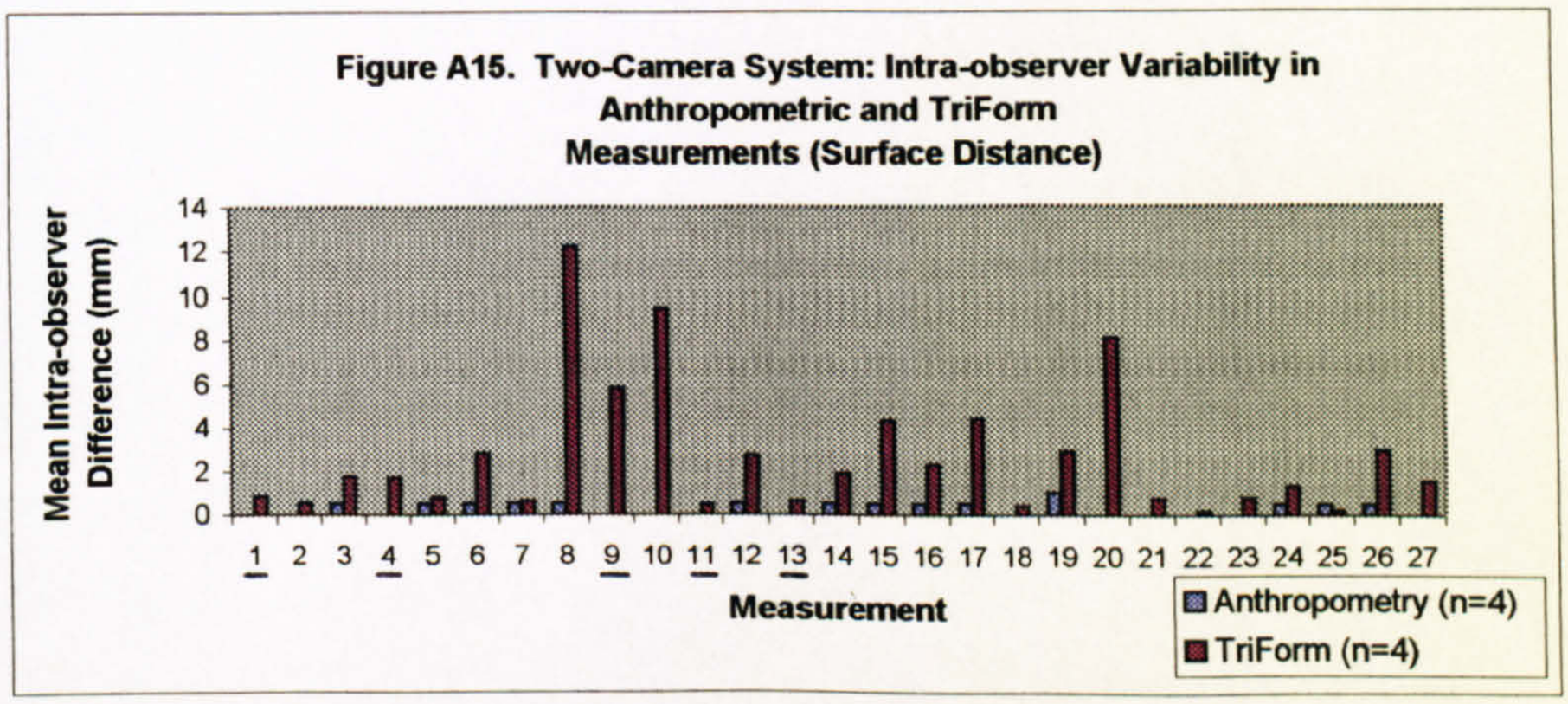

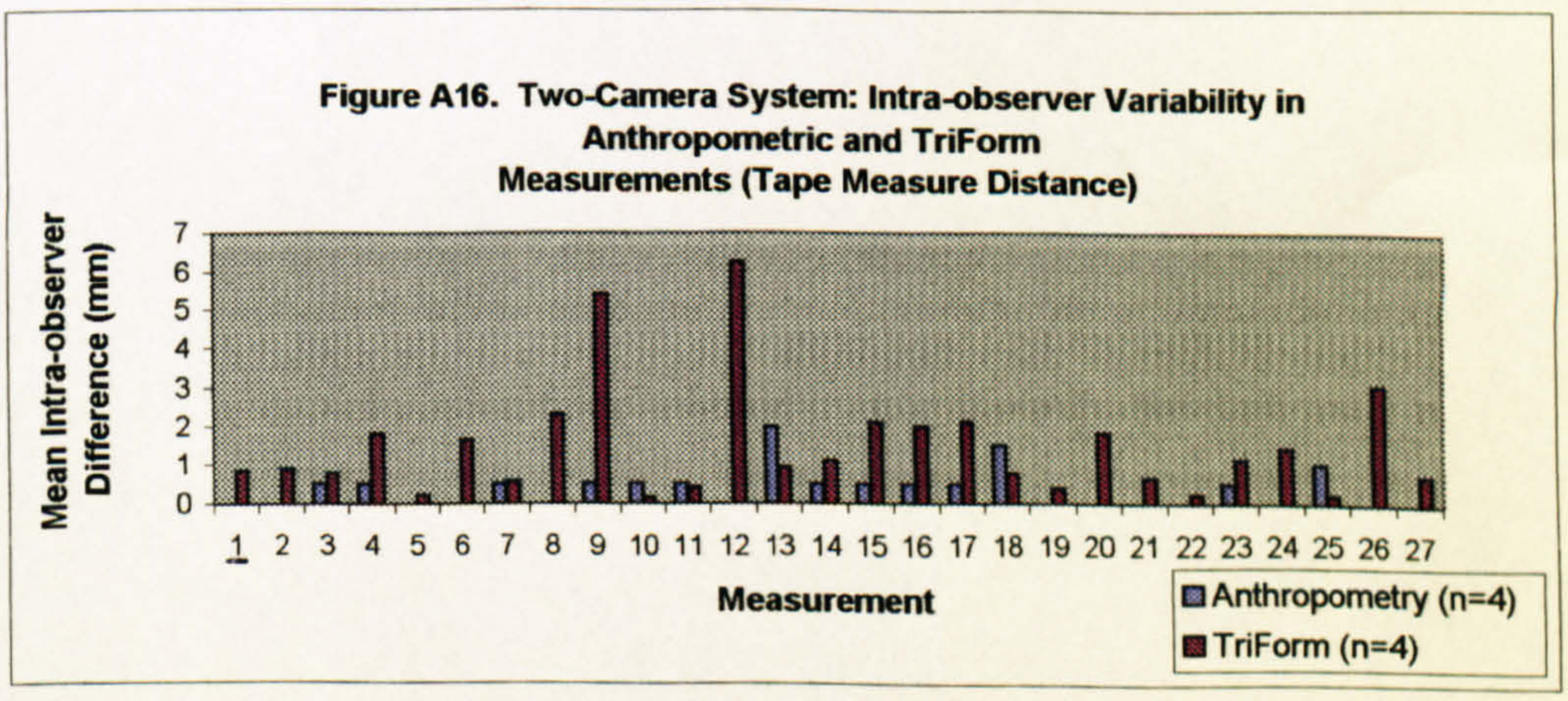

Key: ____ Manual measurements omitted
n = Number of repeat measurements

Generally less variability was noted between observers shortest distance measurements when using the TriForm™ system than those recorded through anthropometric measurements. The results from the inter and intra observer variability support the findings of the mean error and mean difference results discussed in section A2.5. Those measurements which display greater variability using the TriForm™ system were generally more difficult to measure due to difficulties encountered in locating the appropriate landmark points on-screen. Significantly large surface distance differences can be noted in both the single and two-camera results recorded between observers when using the TriForm™ system. These may be explained by irregular surface measurement readings, which occurred intermittently during the whole test procedure. The majority of the measurements show an increase in variability in all measurement types between the observers changing from a one to a two-camera system. One potential reason may be greater variability in the possible positioning of the captured object on-screen, which could compromise the accuracy of any surface or tape measure measurements by restricting the plane of measurement to one which does not match that used when manually taking the anthropometric measurement. Another is the introduction of the stitching process as previously mentioned.

A high level of agreement between successive measurements is exhibited in all measurement types. The spread of the variability between measurements being greater for the TriForm™, as opposed to those taken by anthropometric means. The greater variability in specific TriForm™ measurements can be explained by difficulties in viewing the landmarks on-screen by the limited Field of View currently offered with the TriForm™ system. This case stands for all measurement types and for both single and dual camera systems.

A3. Conclusion

The variability between observers and successive measurements is generally below 10mm for TriForm™ and anthropometric measurements, the exceptions being the irregular surface measure results which were prevalent using the TriForm™ system and certain specific measurements, which are more difficult to take on-screen. Both issues will need to be addressed if the variability is to be reduced. The TriForm™ shortest distance measurements however, have proved to be more repeatable than the anthropometric shortest distance measurements.

The range of difference between TriForm™ and anthropometric measurements remains high for across all measurement types and techniques, with differences as high as 49.70mm and 47.28mm for the single and two-camera systems respectively. Whilst this may be the case for specific measurements, the majority of differences for each measurement are under 10mm for the single camera system, however, for the two-camera system less than half the measurements were under 10mm difference.

It may be noted that any measurement taken by the TriForm™ system is subject to a degree of error, based upon the accuracy of the image generated by the system and the operators skill in determining the correct point selection for measurement. At this stage the available information is limited, as any assessment must be made on the basis of the accuracy specification given by the manufacturer, the operator error influence has not been evaluated at this time as it is beyond the scope of the current analysis. The estimated error, which is likely for an individual measurement, is therefore covered more fully in the latter parts of the investigation, where it is most relevant.

The accuracy of the TriForm™ measurements was not satisfactory at this stage. Illustrated by differences of up to 49.70mm between anthropometric and

TriForm™ measurements which are practically the same as the intervals used for pattern grading. In light of this the investigation into the characterisation of the torso of women with Scoliosis was suspended, as critical surface measurements to obtain information over the curved back could not be relied upon and thus would not enable accurate pattern development rules to be created.

Whilst the manikin test highlighted some of the issues applicable to automated measurement, it could not form a satisfactory base for further development until more fundamental tests had been completed. Using the complex 3D form of the manikin did not allow the nature and sources of error to be identified and other approaches, which would allow this, needed to be established. These may then highlight the major sources of error to enable further development work to be undertaken.

A4. Full Measurement Results

Table A3. Single Camera System: Shortest Distance Test Statistics (n=4)

Measurement	Anthropometry (mm)	TriForm™ (mm)	Difference (mm)	%
			(TriForm – Anthropometry)	
Interacromion Breadth	378.75 ± 0.25	361.05 ± 1.30	-17.70	-4.67
Depth of Scye	111.25 ± 0.25	109.68 ± 0.66	-1.57	-1.42
Scye Width	102.75 ± 0.25	93.10 ± 1.56	-9.65	-9.39
Width of Bust Prominence	196.50 ± 0.65	193.45 ± 0.25	-3.05	-1.55
Shoulder Length	133.75 ± 0.25	131.38 ± 0.83	-2.38	-1.78
Neck to Waist	368.25 ± 2.21	363.00 ± 0.45	-5.25	-1.43
Front Shoulder Height	411.25 ± 0.85	409.80 ± 0.83	-1.45	-0.35
Front Body Width	194.75 ± 0.85	194.75 ± 0.64	0	0
Across Chest	334.25 ±.0.25	333.88 ± 0.61	-0.38	-0.11
Across Chest ½	171.75 ± 0.63	182.80 ± 0.52	11.05	6.43
Front Shoulder Slope	420.75 ± 0.75	412.68 ± 0.25	-8.07	-1.92
Full Front Width	167.00 ± 2.04	207.83 ± 0.42	40.83	24.45
Front Side Waist Depth	383.75 ± 1.80	379.50 ± 0.52	-4.25	-1.11
Across Back	344.75 ± 1.31	344.10 ± 0.45	-0.65	-0.19
Across Back ½	179.75 ± 0.25	176.03 ± 0.18	-3.72	-2.07
Back Body Width	204.75 ± 0.85	204.65 ± 0.37	-0.10	-0.05
Full Back Width	193.25 ± 0.48	202.18 ± 0.21	8.93	4.62
Back Shoulder Slope	408.75 ± 2.56	400.95 ± 1.25	-7.80	-1.91
Back Side Waist Depth	441.50 ± 0.50	434.45 ± 0.35	-7.05	-1.60
Nape to Waist	423.50 ± 0.87	409.05 ± 0.26	-14.45	-3.41
Back Shoulder Height	413.50 ± 0.29	401.13 ± 1.07	-12.38	-2.99
Neck to Bust	254.25 ± 0.85	254.45 ± 0.62	0.20	0.08
Armscye to Waist	237.00 ± 2.35	235.33 ± 0.51	-1.68	-0.71
½ Bust - Front	156.00 ± 1.78	205.70 ± 0.67	49.70	31.86
½ Bust – Back	178.75 ± 1.38	193.30 ± 0.57	14.55	8.14
½ Waist – Front	135.25 ± 2.75	172.38 ± 0.24	37.13	27.45
½ Waist - Back	137.75 ± 0.63	162.25 ± 0.56	24.50	17.79

Table A4. Single Camera System: Surface Distance Test Statistics (*n*=4)

Measurement	Anthropometry (mm)	TriForm™ (mm)	Difference (mm)	%
			(TriForm – Anthropometry)	
Interacromion Breadth	x	378.13 ± 5.24	x	x
Depth of Scye	115.50 ± 0.87	125.45 ± 2.11	9.95	8.61
Scye Width	107.75 ± 0.25	109.40 ± 7.31	1.65	1.53
Width of Bust Prominence	x	198.18 ± 0.98	x	x
Shoulder Length	135.75 ± 0.48	172.40 ± 1.48	36.65	27.00
Neck to Waist	390.25 ± 0.48	381.48 ± 2.05	-8.77	-2.25
Front Shoulder Height	469.25 ± 1.31	461.53 ± 12.60	-7.73	-1.65
Front Body Width	202.25 ± 0.25	203.60 ± 2.85	1.35	0.67
Across Chest	x	373.35 ± 1.15	x	x
Across Chest ½	203.00 ± 0.91	206.85 ± 3.58	3.85	1.90
Front Shoulder Slope	x	432.58 ± 2.07	x	x
Full Front Width	247.25 ± 0.48	244.85 ± 0.83	-2.40	-0.97
Front Side Waist Depth	x	429.78 ± 1.59	x	x
Across Back	371.25 ± 0.75	362.50 ± 1.20	-8.75	-2.36
Across Back ½	187.25 ± 0.48	186.53 ± 1.07	-0.72	-0.39
Back Body Width	212.25 ± 0.25	223.10 ± 0.77	10.85	5.11
Full Back Width	241.75 ± 0.25	239.20 ± 3.42	-2.55	-1.05
Back Shoulder Slope	441.00 ± 0.41	413.58 ± 1.50	-27.43	-6.22
Back Side Waist Depth	478.00 ± 0.71	468.50 ± 2.02	-9.50	-1.99
Nape to Waist	434.50 ± 0.29	421.70 ± 1.37	-12.80	-2.95
Back Shoulder Height	451.50 ± 0.87	438.45 ± 5.31	-13.05	-2.89
Neck to Bust	270.00 ± 1.15	263.30 ± 2.93	-6.70	-2.48
Armscye to Waist	245.00 ± 0.00	241.30 ± 3.78	-3.70	-1.51
½ Bust - Front	270.75 ± 0.25	256.08 ± 1.05	-14.68	-5.42
½ Bust – Back	228.75 ± 0.48	224.23 ± 2.27	-4.53	-1.98
½ Waist – Front	195.25 ± 0.25	191.80 ± 2.02	-3.45	-1.77
½ Waist - Back	184.00 ± 0.00	178.33 ± 2.14	-5.67	-3.08

Table A5. Single Camera System: Tape Measure Distance Test Statistics (n=4)

Measurement	Anthropometry (mm)	TriForm™ (mm)	Difference (mm)	%
			(TriForm – Anthropometry)	
Interacromion Breadth	x	368.88 ± 2.88	x	x
Depth of Scye	114.00 ± 0.58	114.50 ± 0.80	0.50	0.44
Scye Width	105.75 ± 0.48	93.45 ± 1.78	-12.30	-11.63
Width of Bust Prominence	197.75 ± 0.25	193.55 ± 0.22	-4.20	-2.12
Shoulder Length	134.50 ± 0.29	133.83 ± 0.96	-0.68	-0.50
Neck to Waist	390.00 ± 0.58	376.98 ± 0.58	-13.03	-3.34
Front Shoulder Height	469.25 ± 1.03	447.08 ± 1.44	-22.18	-4.73
Front Body Width	204.00 ± 0.41	197.93 ± 1.30	-6.07	-2.98
Across Chest	399.25 ± 0.48	371.78 ± 1.13	-27.48	-6.88
Across Chest ½	202.75 ± 0.48	200.30 ± 1.37	-2.45	-1.21
Front Shoulder Slope	476.75 ± 0.48	430.18 ± 1.22	-46.58	-9.77
Full Front Width	248.00 ± 1.15	242.00 ± 0.87	-6.00	-2.42
Front Side Waist Depth	455.50 ± 1.32	424.80 ± 1.46	-30.70	-6.74
Across Back	371.75 ± 0.48	361.65 ± 1.14	-10.10	-2.72
Across Back ½	187.25 ± 0.48	181.98 ± 0.47	-5.28	-2.82
Back Body Width	213.25 ± 0.25	216.33 ± 0.56	3.07	1.44
Full Back Width	242.25 ± 0.25	228.15 ± 3.38	-14.10	-5.82
Back Shoulder Slope	442.25 ± 0.95	411.43 ± 0.98	-30.83	-6.97
Back Side Waist Depth	480.00 ± 0.82	464.88 ± 2.53	-15.13	-3.15
Nape to Waist	434.00 ± 0.00	416.45 ± 0.52	-17.55	-4.04
Back Shoulder Height	452.00 ± 1.15	434.65 ± 3.40	-17.35	-3.84
Neck to Bust	269.00 ± 1.15	257.18 ± 0.83	-11.83	-4.40
Armscye to Waist	243.75 ± 0.25	235.43 ± 0.47	-8.32	-3.42
½ Bust - Front	271.00 ± 0.00	253.50 ± 0.66	-17.50	-6.46
½ Bust – Back	229.00 ± 0.41	220.23 ± 1.70	-8.77	-3.83
½ Waist – Front	196.00 ± 0.41	188.93 ± 0.83	-7.07	-3.61
½ Waist - Back	184.00 ± 0.00	176.30 ± 1.38	-7.70	-4.18

Table A6. Two-Camera System: Shortest Distance Test Statistics (n=4)

Measurement	Anthropometry (mm)	TriForm™ (mm)	Difference (mm)	%
			(Triform – Anthropometry)	-
Interacromion Breadth	378.75 ± 0.25	356.70 ± 0.66	-22.05	-5.82
Depth of Scye	111.25 ± 0.25	109.83 ± 1.02	-1.43	-1.28
Scye Width	102.75 ± 0.25	93.41 ± 1.62	-9.34	-9.09
Width of Bust Prominence	196.50 ± 0.65	178.65 ± 0.99	-17.85	-9.08
Shoulder Length	133.75 ± 0.25	128.38 ± 0.17	-5.38	-4.02
Neck to Waist	368.25 ± 2.21	361.20 ± 0.80	-7.05	-1.91
Front Shoulder Height	411.25 ± 0.85	408.53 ± 0.33	-2.72	-0.66
Front Body Width	194.75 ± 0.85	190.93 ± 0.90	-3.82	-1.96
Across Chest	334.25 ±.0.25	324.38 ± 1.33	-9.88	-2.95
Across Chest ½	171.75 ± 0.63	176.83 ± 0.93	5.07	2.95
Front Shoulder Slope	420.75 ± 0.75	410.23 ± 0.60	-10.53	-2.50
Full Front Width	167.00 ± 2.04	204.93 ± 0.78	37.93	22.71
Front Side Waist Depth	383.75 ± 1.80	374.55 ± 0.39	-9.20	-2.40
Across Back	344.75 ± 1.31	317.25 ± 0.72	-27.50	-7.98
Across Back ½	179.75 ± 0.25	160.80 ± 0.70	-18.95	-10.54
Back Body Width	204.75 ± 0.85	195.05 ± 1.21	-9.70	-4.74
Full Back Width	193.25 ± 0.48	188.85 ± 1.14	-4.40	-2.28
Back Shoulder Slope	408.75 ± 2.56	392.03 ± 1.26	-16.73	-4.09
Back Side Waist Depth	441.50 ± 0.50	428.98 ± 0.69	-12.53	-2.84
Nape to Waist	423.50 ± 0.87	410.43 ± 0.84	-13.08	-3.09
Back Shoulder Height	413.50 ± 0.29	399.95 ± 0.10	-13.55	-3.28
Neck to Bust	254.25 ± 0.85	252.95 ± 0.49	-1.30	-0.51
Armscye to Waist	237.00 ± 2.35	234.75 ± 0.55	-2.25	-0.95
½ Bust - Front	156.00 ± 1.78	203.28 ± 0.92	47.28	30.30
½ Bust – Back	178.75 ± 1.38	177.05 ± 0.75	-1.70	-0.95
½ Waist – Front	135.25 ± 2.75	167.15 ± 0.85	31.90	23.59
½ Waist - Back	137.75 ± 0.63	148.60 ± 0.09	10.85	7.88

Table A7. Two-Camera System: Surface Distance Test Statistics (n=4)

Measurement	Anthropometry (mm)	TriForm™ (mm)	Difference (mm)	%
			(Triform – Anthropometry)	
Interacromion Breadth	x	372.38 ± 0.57	x	x
Depth of Scye	115.50 ± 0.87	112.13 ± 0.72	-3.38	-2.92
Scye Width	107.75 ± 0.25	95.28 ± 1.81	-12.48	-11.58
Width of Bust Prominence	x	181.70 ± 0.98	x	x
Shoulder Length	135.75 ± 0.48	140.70 ± 0.40	4.95	3.65
Neck to Waist	390.25 ± 0.48	376.60 ± 0.86	-13.65	-3.50
Front Shoulder Height	469.25 ± 1.31	446.70 ± 0.23	-22.55	-4.81
Front Body Width	202.25 ± 0.25	199.35 ± 5.74	-2.90	-1.43
Across Chest	x	394.28 ± 4.51	x	x
Across Chest ½	203.00 ± 0.91	200.75 ± 3.82	-2.25	-1.11
Front Shoulder Slope	x	430.68 ± 1.19	x	x
Full Front Width	247.25 ± 0.48	237.23 ± 0.88	-10.03	-4.05
Front Side Waist Depth	x	425.90 ± 0.66	x	x
Across Back	371.25 ± 0.75	338.23 ± 2.30	-33.03	-8.90
Across Back ½	187.25 ± 0.48	172.65 ± 2.45	-14.60	-7.80
Back Body Width	212.25 ± 0.25	210.33 ± 2.97	-1.93	-0.91
Full Back Width	241.75 ± 0.25	219.48 ± 2.78	-22.28	-9.21
Back Shoulder Slope	441.00 ± 0.41	413.10 ± 4.14	-27.90	-6.33
Back Side Waist Depth	478.00 ± 0.71	468.03 ± 3.50	-9.98	-2.09
Nape to Waist	434.50 ± 0.29	425.15 ± 3.22	-9.35	-2.15
Back Shoulder Height	451.50 ± 0.87	432.13 ± 0.95	-19.38	-4.29
Neck to Bust	270.00 ± 1.15	253.50 ± 0.06	-16.50	-6.11
Armscye to Waist	245.00 ± 0.00	237.65 ± 0.79	-7.35	-3.00
½ Bust - Front	270.75 ± 0.25	247.55 ± 3.20	-23.20	-8.57
½ Bust – Back	228.75 ± 0.48	206.33 ± 2.53	-22.43	-9.80
½ Waist – Front	195.25 ± 0.25	182.45 ± 1.23	-12.80	-6.56
½ Waist - Back	184.00 ± 0.00	173.50 ± 2.53	-10.50	-5.71

Table A8. Two-Camera System: Tape Measure Distance Test Statistics (n=4)

Measurement	Anthropometry (mm)	TriForm™ (mm)	Difference (mm)	%
			(TriForm – Anthropometry)	
Interacromion Breadth	x	370.53 ± 0.64	x	x
Depth of Scye	114.00 ± 0.58	111.10 ± 1.11	-2.90	-2.54
Scye Width	105.75 ± 0.48	93.70 ± 1.57	-12.05	-11.39
Width of Bust Prominence	197.75 ± 0.25	178.65 ± 0.99	-19.10	-9.66
Shoulder Length	134.50 ± 0.29	129.50 ± 0.10	-5.00	-3.72
Neck to Waist	390.00 ± 0.58	374.93 ± 0.87	-15.08	-3.87
Front Shoulder Height	469.25 ± 1.03	443.03 ± 0.23	-26.23	-5.59
Front Body Width	204.00 ± 0.41	192.95 ± 1.05	-11.05	-5.42
Across Chest	399.25 ± 0.48	392.70 ± 4.36	-6.55	-1.64
Across Chest ½	202.75 ± 0.48	194.23 ± 0.94	-8.52	-4.20
Front Shoulder Slope	476.75 ± 0.48	427.30 ± 1.16	-49.45	-10.37
Full Front Width	248.00 ± 1.15	234.23 ± 2.56	-13.78	-5.55
Front Side Waist Depth	455.50 ± 1.32	422.43 ± 0.67	-33.07	-7.26
Across Back	371.75 ± 0.48	334.88 ± 2.11	-36.88	-9.92
Across Back ½	187.25 ± 0.48	166.40 ± 0.62	-20.85	-11.13
Back Body Width	213.25 ± 0.25	207.75 ± 2.56	-5.50	-2.58
Full Back Width	242.25 ± 0.25	216.10 ± 1.93	-26.15	-10.79
Back Shoulder Slope	442.25 ± 0.95	405.00 ± 2.53	-37.25	-8.42
Back Side Waist Depth	480.00 ± 0.82	463.60 ± 2.62	-16.40	-3.42
Nape to Waist	434.00 ± 0.00	419.50 ± 0.64	-14.50	-3.34
Back Shoulder Height	452.00 ± 1.15	430.83 ± 0.94	-21.18	-4.68
Neck to Bust	269.00 ± 1.15	252.93 ± 0.49	-16.08	-5.98
Armscye to Waist	243.75 ± 0.25	234.78 ± 0.53	-8.98	-3.68
½ Bust - Front	271.00 ± 0.00	245.60 ± 2.89	-25.40	-9.37
½ Bust – Back	229.00 ± 0.41	202.13 ± 1.55	-26.88	-11.74
½ Waist – Front	196.00 ± 0.41	181.48 ± 1.25	-14.53	-7.41
½ Waist - Back	184.00 ± 0.00	167.83 ± 0.44	-16.18	-8.79

APPENDIX B

PRELIMINARY IMAGE CAPTURE SYSTEM EVALUATION: PART 1

B1. Introduction

In light of the findings of the manikin test the investigation into the characterisation of the torso of women with Scoliosis was suspended. To attempt to identify any possible reasons for the problems noted during the manikin test, a more simplistic surface was used. Namely a two-dimensional board marked with a grid of predetermined dimensions. The theory being the lack of curvature may assist in clearer identification and quantification of errors.

B2. Methodology Justification

The human body comprises of a series of complex concave and convex surfaces, which makes the identification of any source of error and the magnification associated with it unfeasible. The individual areas of the body that are constant in curvature are so small it is difficult to identify whether errors are the result of surface curvature, or a product of the operator or the image capture system. Some areas may be subject to errors more than others, for example, concave areas where the lighting of the object may be below optimum. The lack of surface continuity also makes the assessment of any image distortion near impossible, as the surface does not provide a critical enough base upon which to examine such issues. Therefore for the purpose of evaluation a more simplistic surface was utilised once the presence of errors became apparent to the investigator. A two-dimensional board was used as the surface to capture as it was deemed as the most critical, enabling the isolation of individual sources of error and thus the evaluation of their contribution to the overall error.

B3. Measurement Procedure

A large white flat board was marked with a grid of square cells. The grid was produced by computer with each cell measuring 20mm x 20mm. The lines were drawn in red on a white background so as to be clearly visible on-screen after image capture, a line thickness of 1.5mm was chosen for ease of viewing on-screen. The grid situated so as to form a triangle with the two Capture Units, as shown in Figure B1. Its position was assured by measuring the exact distances between the Units and the target object.

Figure B1. Angle Determination

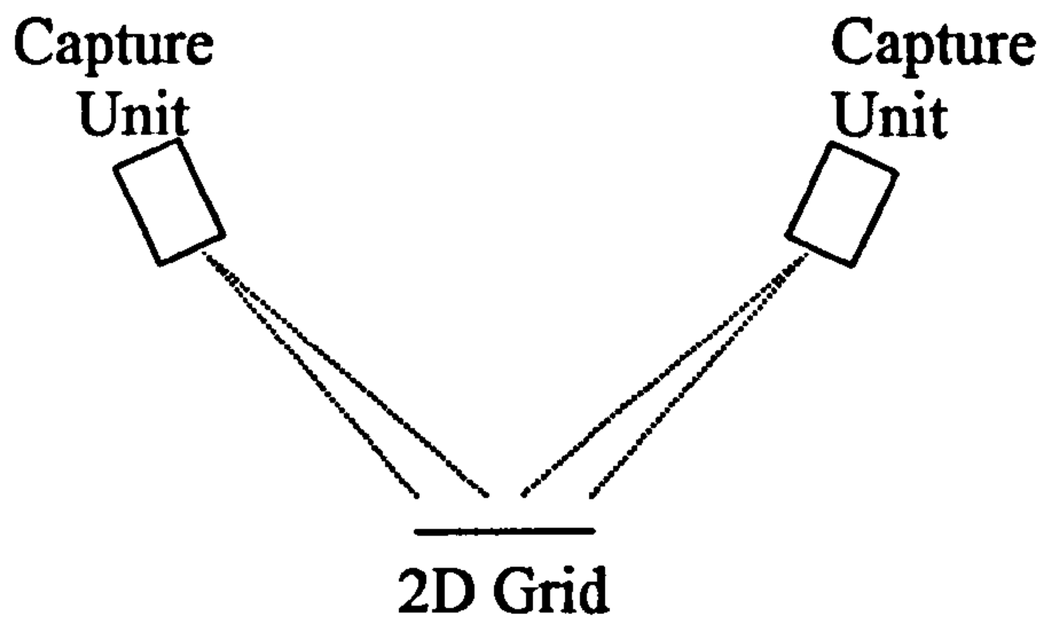

The both units in the two-camera system were used to capture the target object from which 3 variations were measured:

1. The image from Unit A
2. The image from Unit B.
3. The stitched image

Note that only the shortest distance results were considered in this test, as the surface and tape measure distances had already been deemed as the least accurate measurement types. Plus in theory, the surface under investigation is flat hence all three measurement types should, (if the system were measuring correctly), be approximately the same as that recorded for the shortest distance.

A single set of measurements were taken, initially over 2 cells (40 mm), then subsequently over 4 cells, 6 cells, 8 cells and so on, the process being repeated in both the horizontal and vertical direction. The TriForm™ measurements were then compared to the known measurements of the computer generated grid.

The layout of the system and the calibration & configuration settings remained constant from those used in the manikin test.

B4. Evaluation Procedure

In order to analyse the results the measurement readings were graphically plotted for each measured line, as was the actual measurement distance for the same area. Bitmaps of the images produced from Units A, B plus the stitched image produced by combining the two views were also examined for their likeness to the original target object.

B5. Results

The graphical results for the plotted measurement readings may be seen in Figures B2, and B3, B4 and B5, and B6 and B7 for Units A, B, and the stitched image respectively.

Figure B2. Grid Test: Camera A Image TriForm
Horizontal Distance vs. Actual Distance

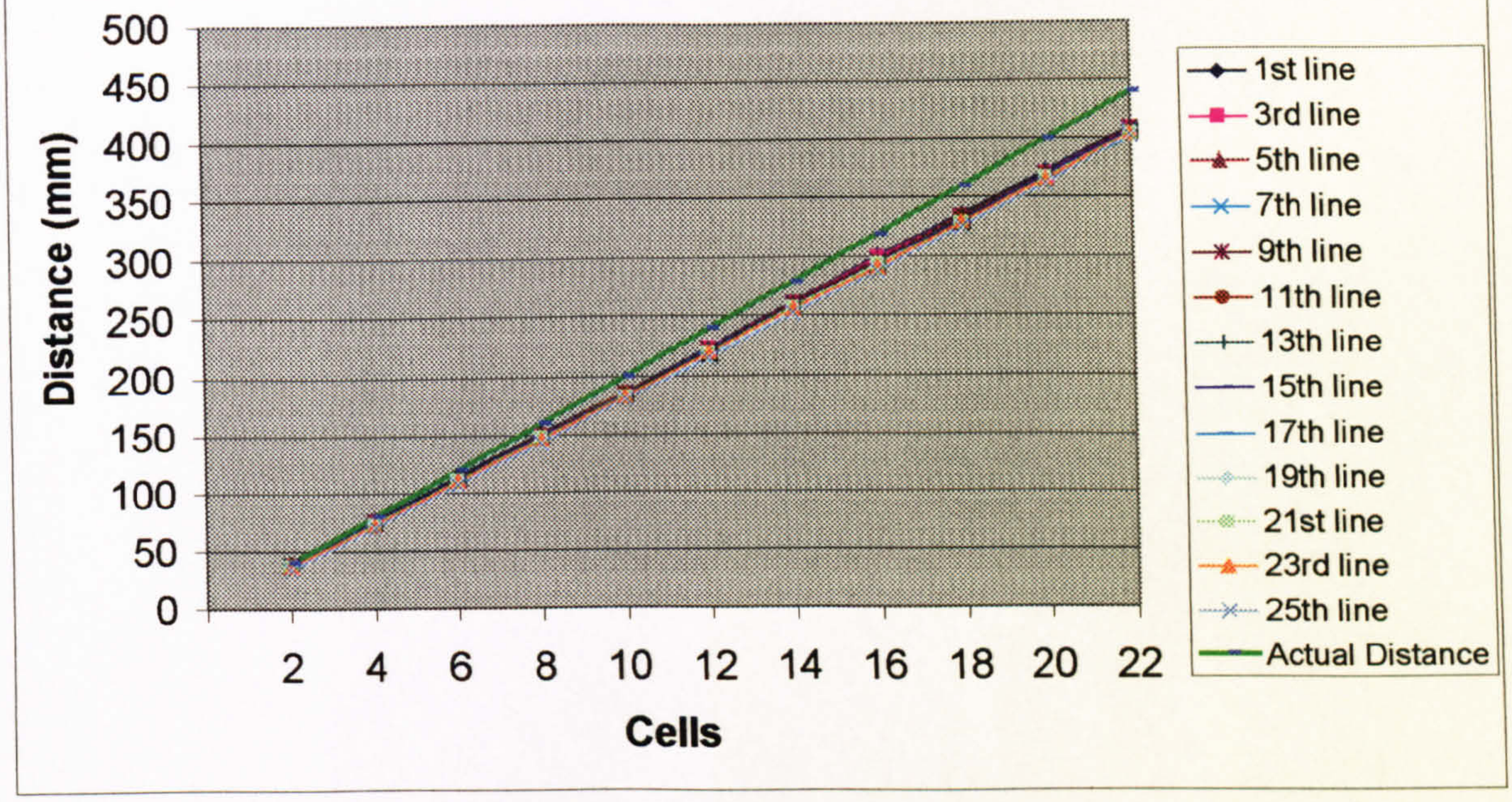

Figure B3. Grid Test: Camera A Image TriForm
Vertical Distance vs. Actual Distance

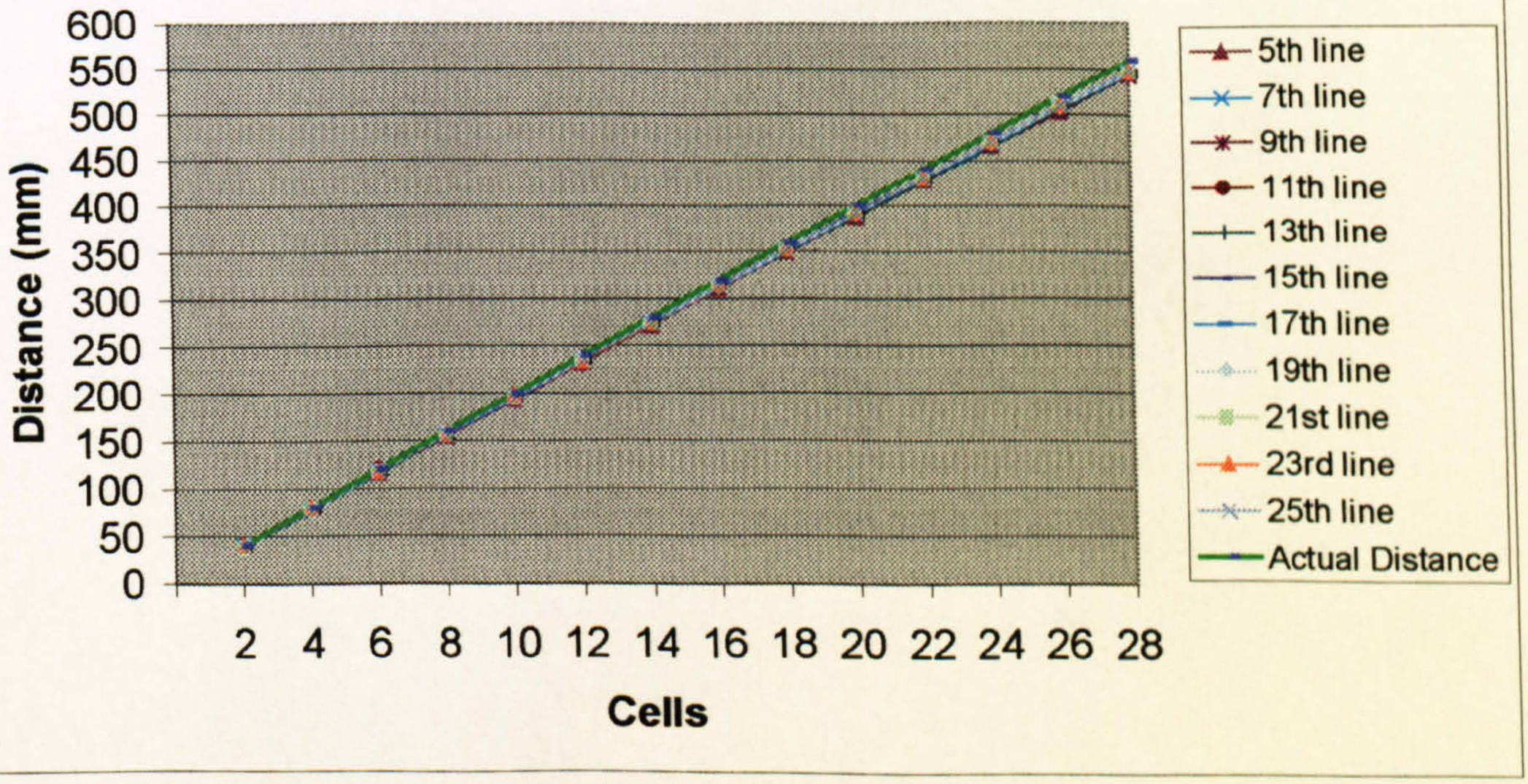

Figure B4. Grid Test: Camera B Image TriForm Horizontal Distance vs. Actual Distance

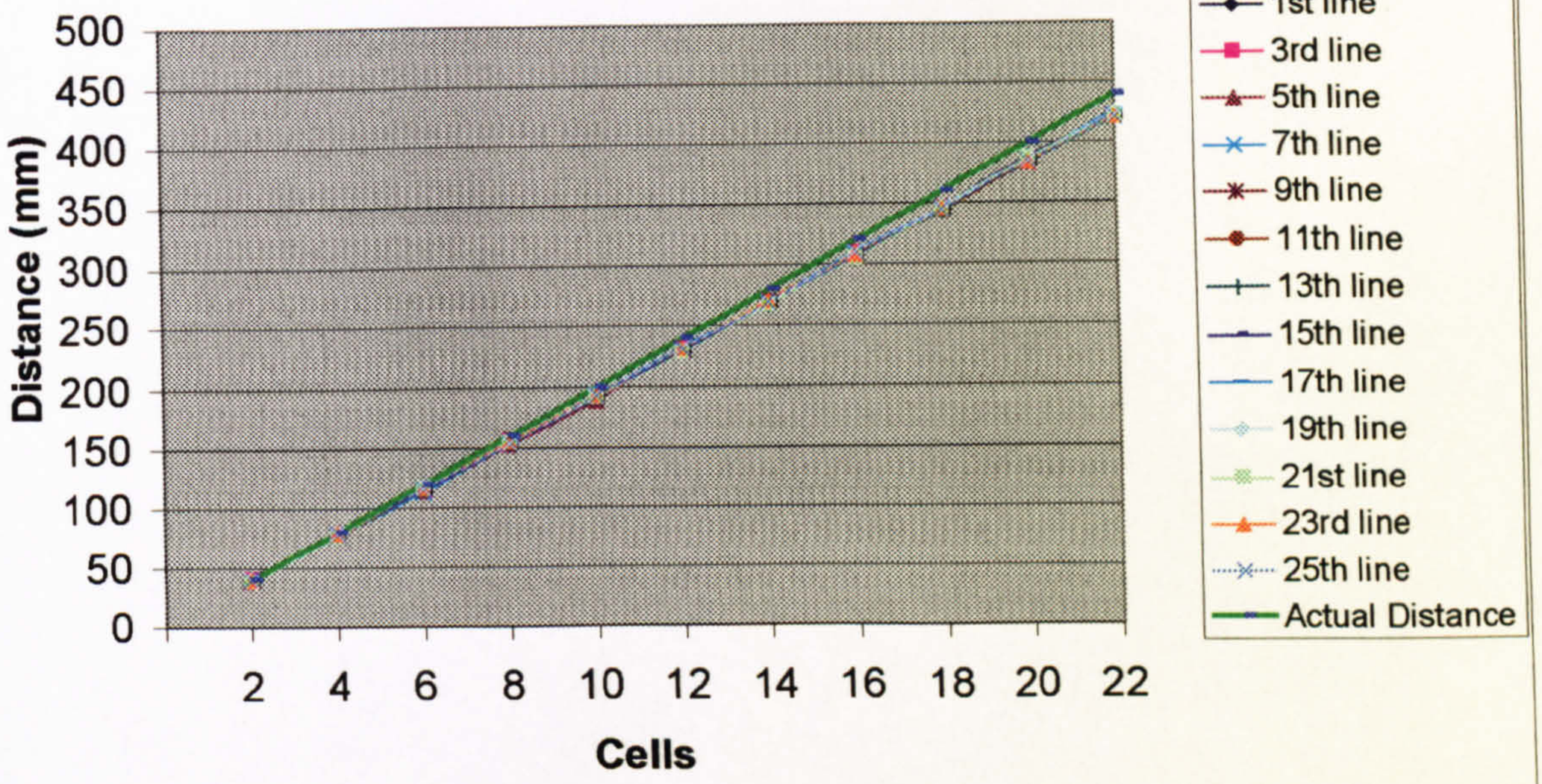

Figure B5. Grid Test: Camera B Image TriForm Vertical Distance vs. Actual Distance

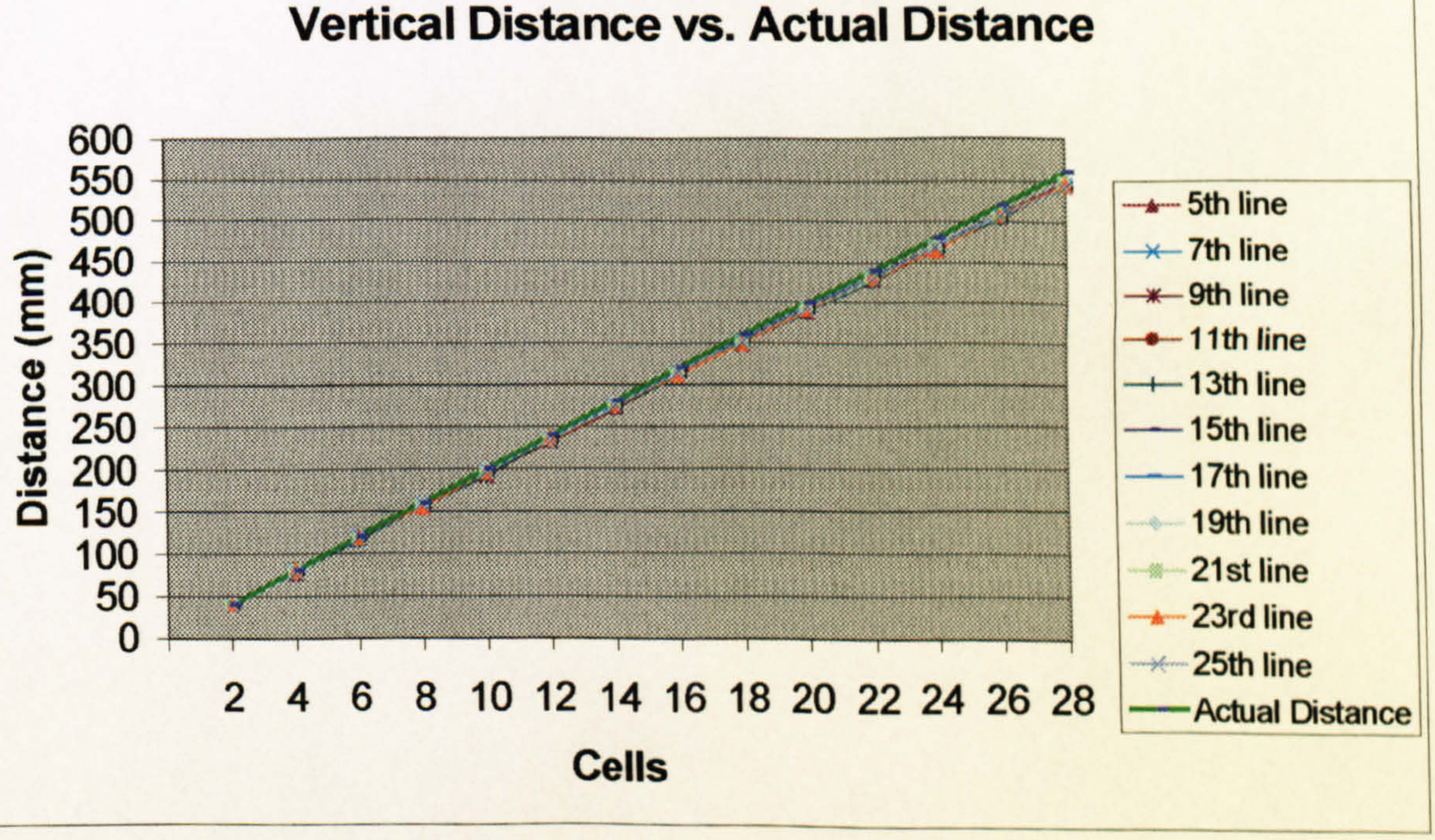

Figure B6. Grid Test: Stitched Image TriForm Horizontal Distance vs. Actual Distance

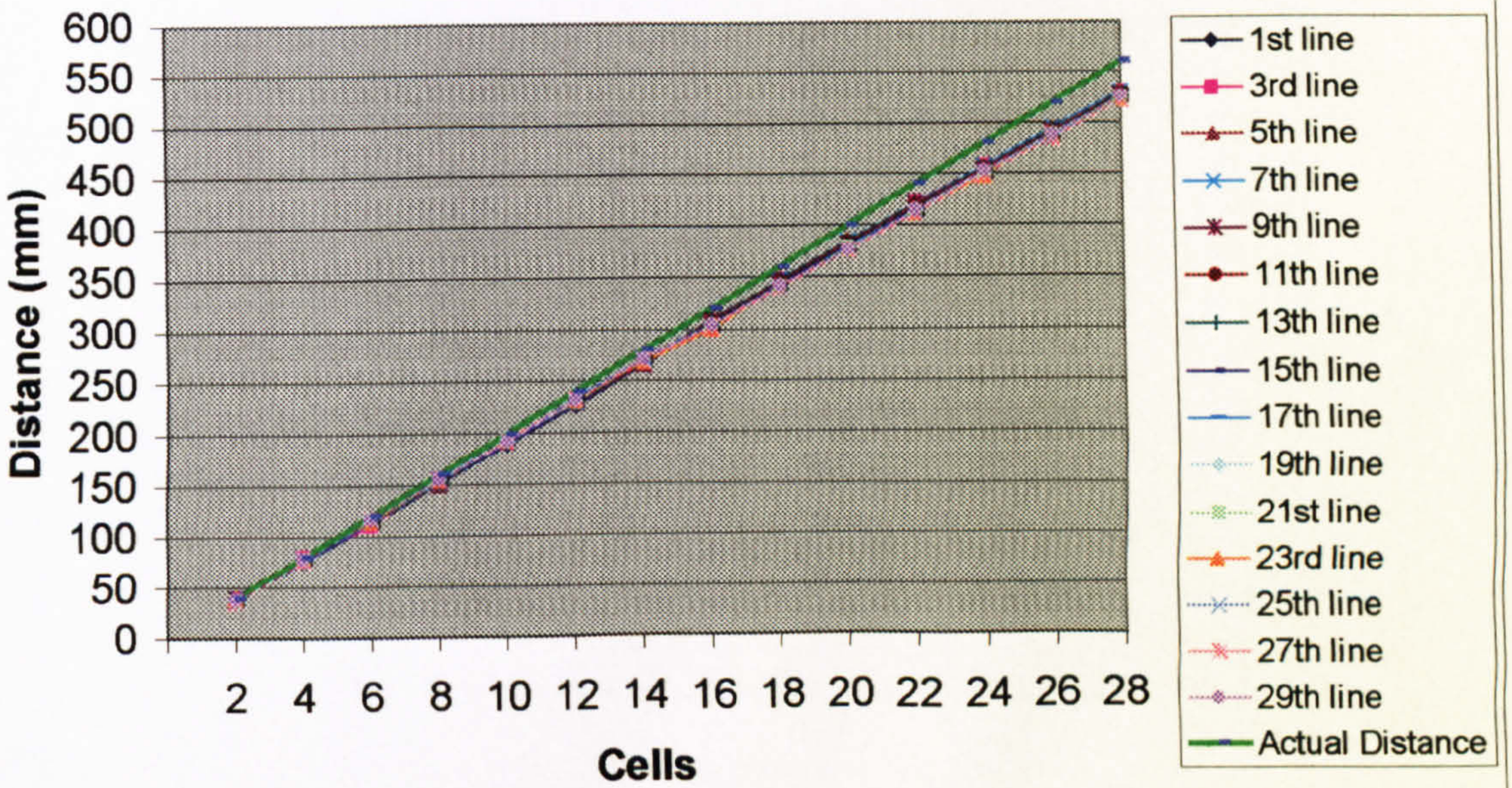

Figure B7. Grid Test: Stitched Image TriForm Vertical Distance vs. Actual Distance

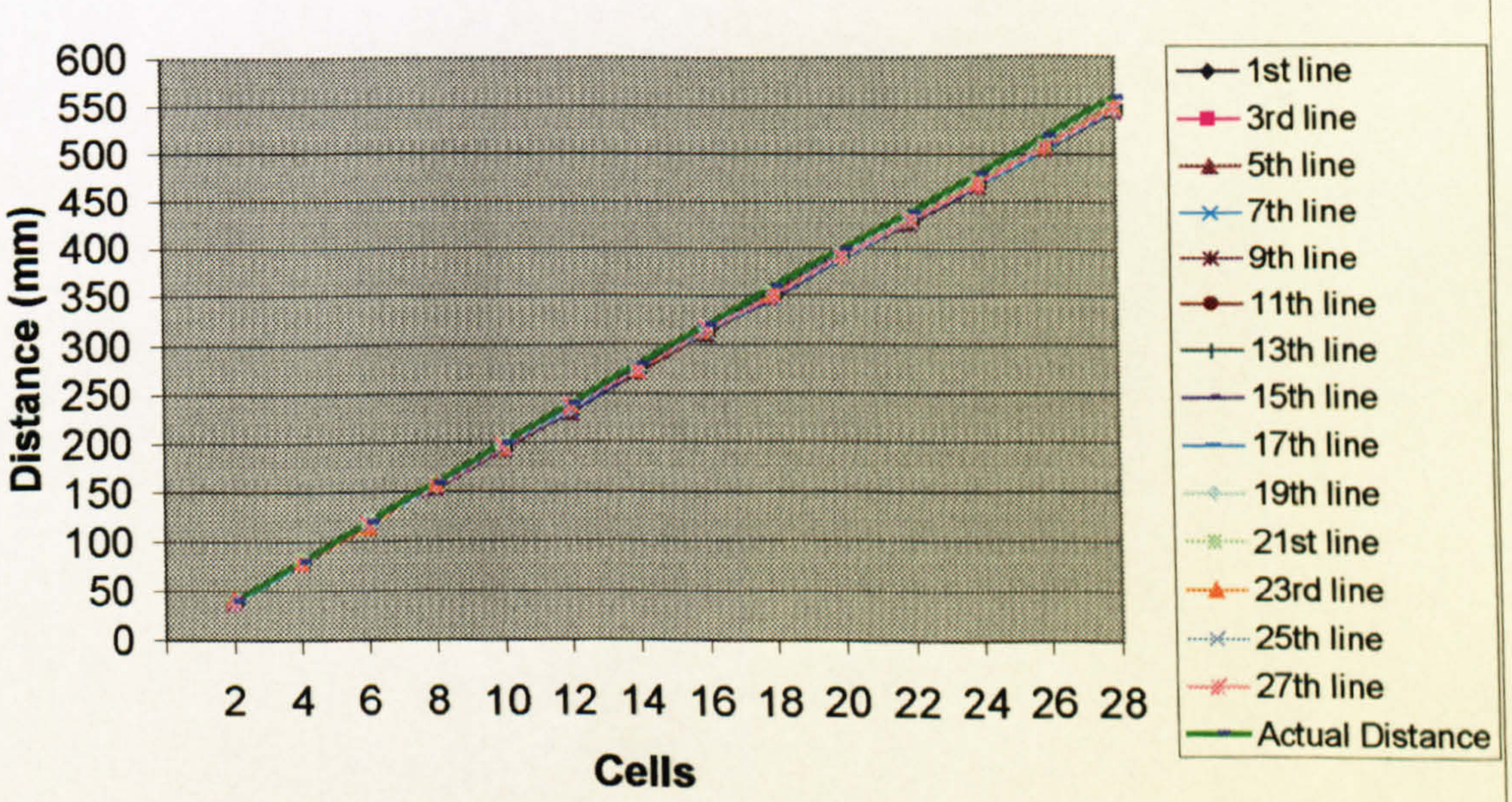

The results display systematic errors for both Units, which were present in each of the image tests, apparent in both the horizontal and vertical directions, which may be clearly seen from Figures B2-B7. The error can be identified as systematic as the graphs display a constant pattern showing a distinct shift in the measurements away from the true value The TriForm™ readings being consistently less than the actual grid measurements. The error in the horizontal direction displays the greatest magnitude on average reaching approx. 6%, whereas the error in the vertical direction is approx. 2.5%. Both of these errors are position dependent, the maximum error being approximately 10%. Whilst there is an error of ±2mm associated with any measurement taken using the TriForm™ system (according to the specification, detailed in section 4.2.2), this error alone does not account for the magnitude displayed by the results. Whilst the nature of the measurement procedure must be subject to some variability, due to the operator influence, it is likely that this would cause a random error as opposed to the distinct and consistent shift in the measurement readings which is apparent in Figures B2-B7.

Screen captures of the images of the grid are shown as bitmaps in Figures B8, B9 for the single camera images and Figure B10 for the stitched image to evaluate the accuracy of the representation of the target object.

Figure B8. Screen Capture of the Camera A Image

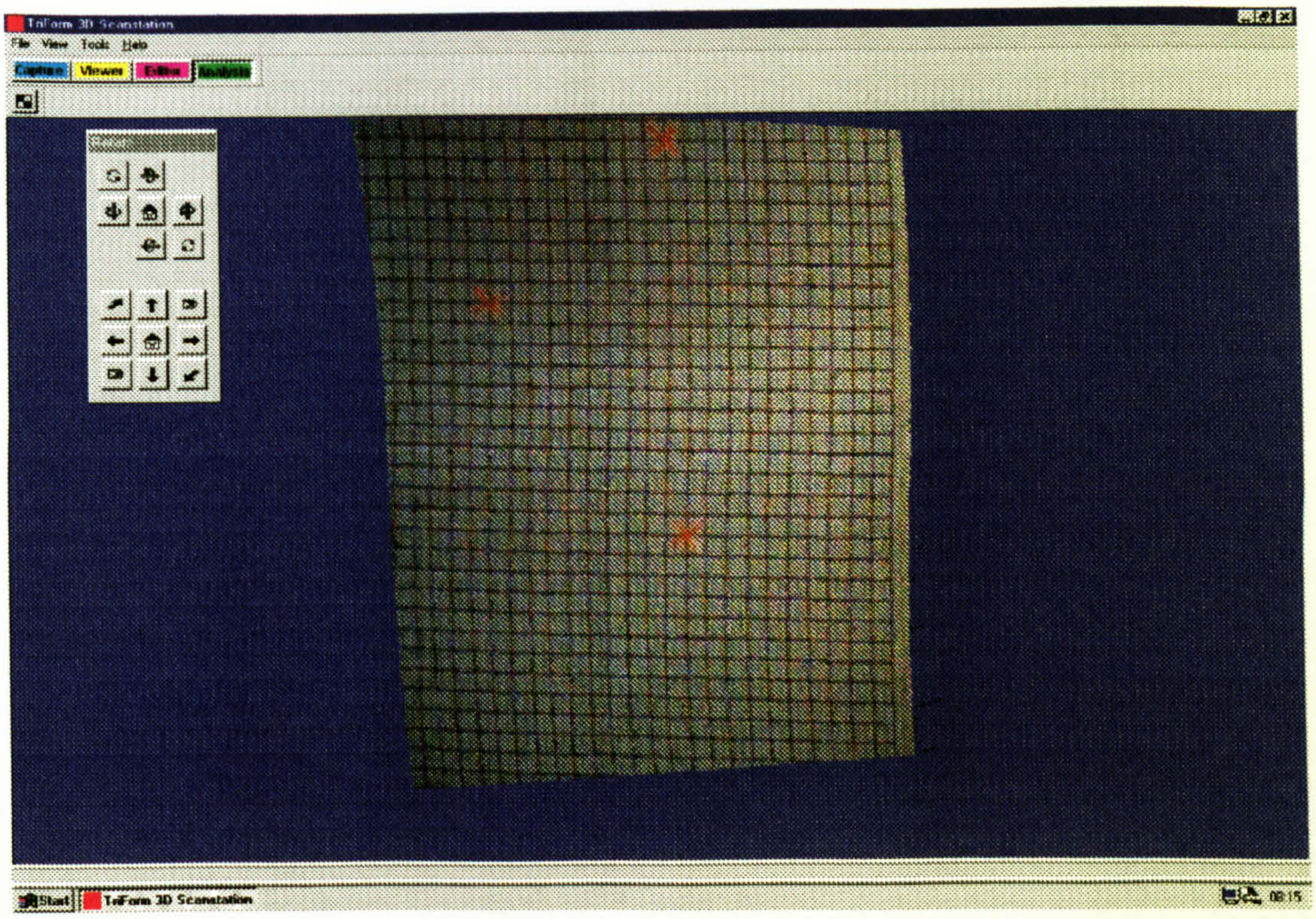

Figure B9. Screen Capture of the Camera B Image

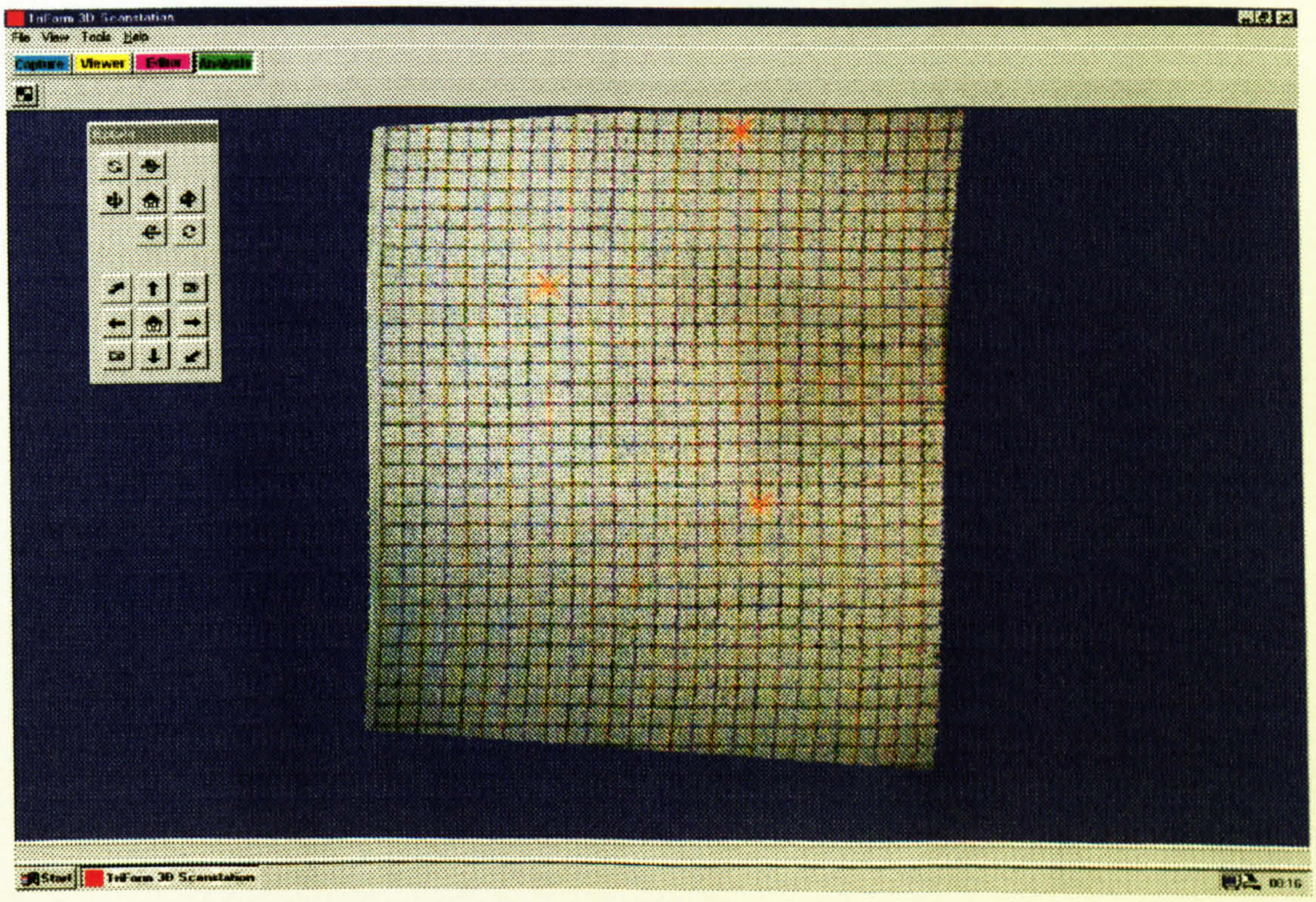

Figure B10. Screen Capture of the Two-Camera Stitched Image

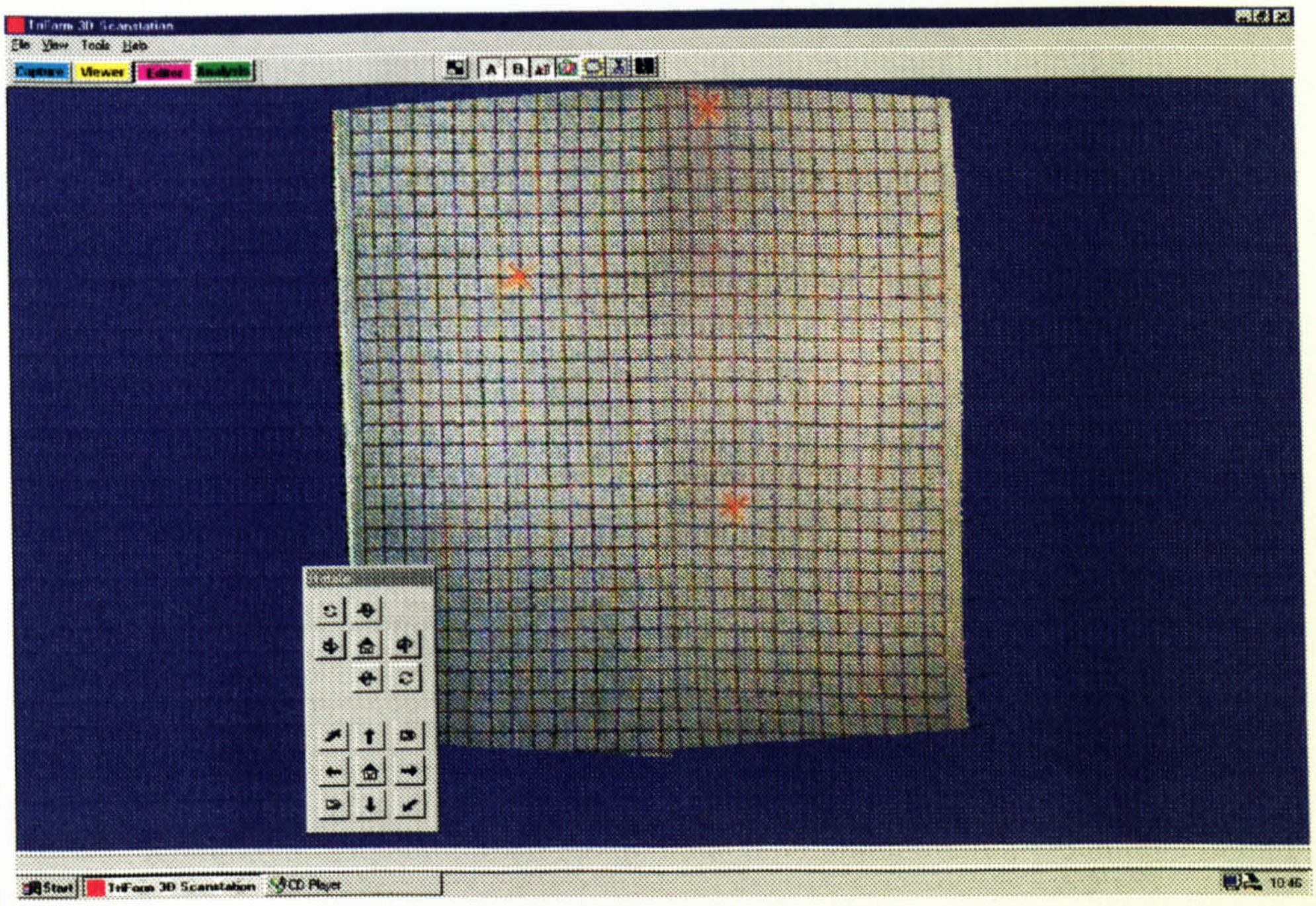

The on-screen images of the grid were seen to be clearly distorted (see Figures B7, B8 for the single unit images). The two-camera stitched imaged (Figure B9) displays a more pronounced degree of distortion, especially around the stitching line. This 'S' type distortion deforms the squares of the grid, which in turn could be responsible for the distortion of the dimensions of the cell at that point. It is likely that the distortion is greater in the stitched image due to the combination of two distorted images, however there is also a potential error introduced by the operator in selecting the points for alignment.

B6. Conclusion

A systematic error is clearly apparent for the single camera and stitched images, which is position dependent. The error is evident in both the horizontal and vertical direction, however, it is clearly more pronounced in the horizontal direction in all cases. The accuracy specification for the TriForm™ system is ±2mm for both the horizontal and vertical directions, however the error shown in

the results exceeds this specification. Whilst it is feasible that the vertical error could be accounted for by the systems error combined with the operators error, the error noted in the horizontal direction cannot be accounted on the same basis.

The images produced by the image capture system clearly have a degree of 'S' type distortion present. This results in images that are not accurate representations of the physical object, which must, in turn, impact upon the measurements taken on-screen. This distortion is also apparent when the two views are stitched together as the cells in the upper portion of the joined grid appear wider whilst the cells in the lower portion of the joined grid appear narrower than the actual 20mm x 20mm cells.

B7. Summary

The two-dimensional grid has proved to be a useful tool for identifying errors in a three-dimensional image capture system. The absence of surface curvature has enabled the deviation in the TriForm™ system measurements to be clearly quantified against the actual distances marked on the grid. The simplicity of the object has also illustrated the distortion present during image capture. Neither of these problems could be clearly identified using the manikin as a test object.

The findings have indicated the depth of the problems associated with providing accurate and precise three-dimensional data for the purpose of bespoke products. It is clear from the results that the performance of the image capture system may only be clearly evaluated and improved by further calibration and the undertaking of additional tests. The investigation therefore now concentrated on the evaluation of the performance of the optical measurement system under investigation. The system at this stage is not suited to fulfilling the functions of accurately capturing the human body. Therefore the aim of the investigation shifted towards the determination and evaluation of the errors inherent within the

system. This was achieved by the creation of a test procedure that could isolate these sources and enable the quantification of their impact upon measurement readings.

APPENDIX C

PRELIMINARY IMAGE CAPTURE SYSTEM EVALUATION: PART 2

C1. Introduction

Following the results of the initial grid test modifications were made to the image capture system configuration and the calibration settings. The objective was to improve the current performance of the prototype system, to enable the full evaluation to be undertaken with the system performing at its optimum level.

C2. System Configuration

The configuration of the Capture Units was changed, primarily to improve the layout of the system within the confinements of the room in which it was housed. The distance between each Unit was altered, as was the distance from each Unit to the object, this is illustrated in Figure C1.

Figure C1. The Two-Camera TriForm™ 3D Image Capture System

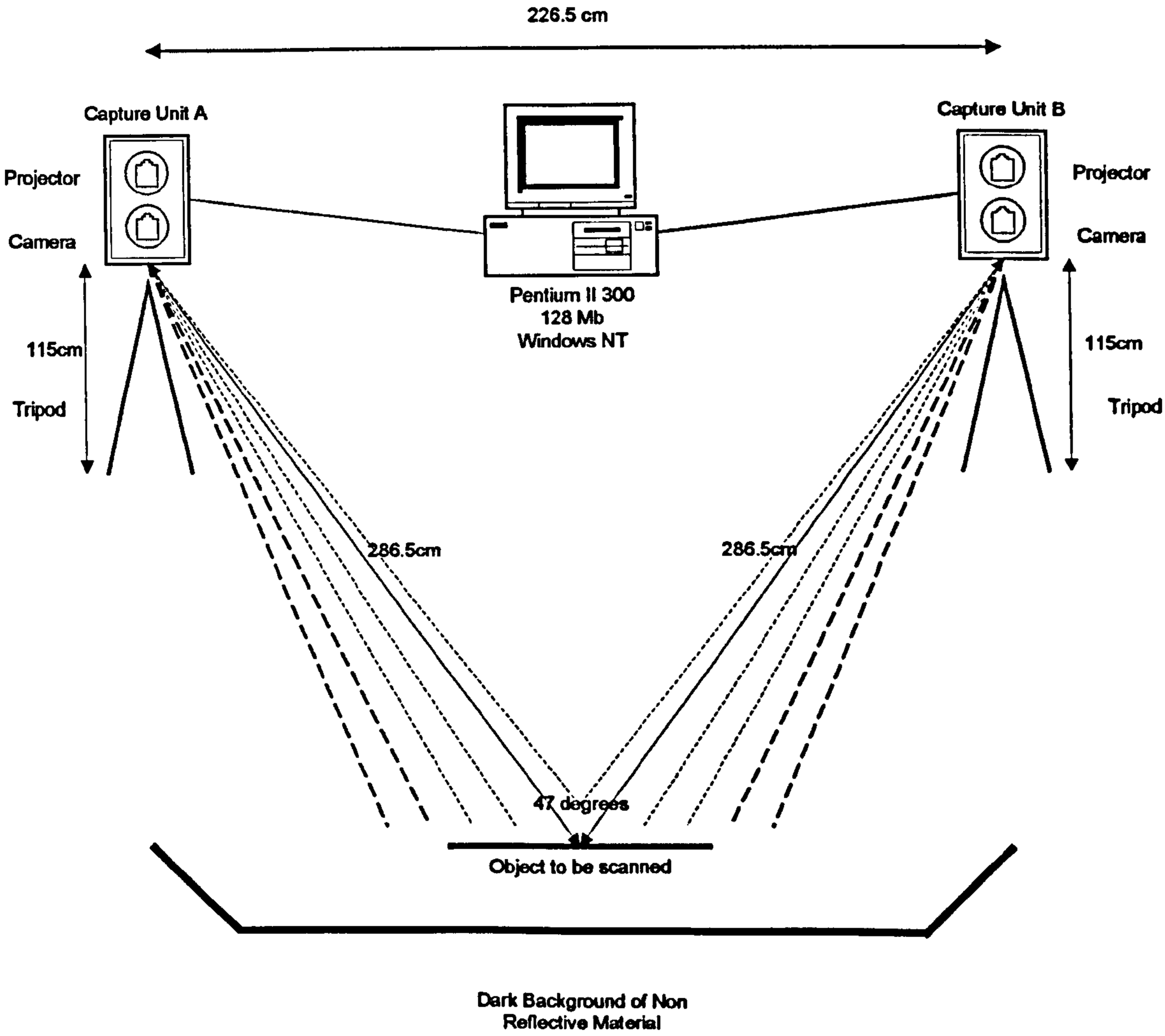

C3. Calibration

The system was re-calibrated using the method described in Chapter 4 for the new system configuration. Each Unit being calibrated in turn, with the target object (in this case a computer generated grid mounted on a white board) being placed parallel to the front of the Unit.

The settings were changed as follows:

	Old Settings	New Settings
Unit A		
Fringe Spacing	9.93059	9.9
Field of View	559	587
Camera to Projector Height	443	443
Camera to Projector Depth	0	0
Camera to System Centre	3500	3500
Capture Frame Delay	350	350
Resolution	10	10
Distortion Correction K1	0	0
Distortion Correction K2	0	0.04
Unit B		
Fringe Spacing	9.98192	9.98
Field of View	553	593
Camera to Projector Height	450	450
Camera to Projector Depth	0	0
Camera to System Centre	3500	3500
Capture Frame Delay	350	350
Resolution	10	10
Distortion Correction K1	0	0.04
Distortion Correction K2	0	0.05

The modification made to the calibration settings, included a change to the Fringe Spacing, Field of View and K2 factor for each camera, plus an alteration to the setting of K1 for Capture Unit B. The Field of View was increased for

both Capture Units to try to improve upon the discrepancy noted between the measured distance and the actual distance readings (which were primarily apparent in the x direction). The K factors were altered to try to correct the S distortion that was present in each image, particularly Capture Unit B. A process of trial and error determined the amended values for K1 and K2. The values were altered in intervals whilst the effect on the on-screen image was noted. This process was repeated until the visual distortion was minimised.

It may be noted that the Camera to System Centre parameter was not changed, even though the physical distance between the Capture Units and the target object had been reduced. As explained in section 4.2.6, it is not necessary that the value used for this parameter is correct to the actual physical measurement between the camera and the target objects centre, but rather the importance lies in the calibration procedure once this value is chosen. For ease, therefore this value was kept constant, as changing this parameter would have meant total re-calibration as opposed to amending the remaining calibration values.

C4. Measurement Objects

For the purpose of the main investigation, a 2D (20mm x 20mm) grid was used similar to that used in the preliminary investigation. The only exception being that the overall size was altered to fit onto A2 paper to improve ease by which the grid could be printed. The squares, in this instance were measured in 80mm blocks, as opposed to 40mm blocks, as used in the preliminary investigation to reduce the likelihood of operator fatigue affecting the measurement results. The areas of the grid were also now measured in series of 80mm blocks as opposed to the cumulative measuring carried out in the preliminary investigation. This was undertaken to reduce the dependence on the 1st line of the grid (either horizontal or vertical) as any problems in that particular area could potentially be carried forward in each measurement. The reason for the continued inclusion of such a

fine grid was to help to the visual perception of any deformity in the grid which could have easily been overlooked on a larger grid. The grids in each case were measured both in the horizontal and vertical directions, unless specified otherwise.

C5. Methodology Justification

For the purpose of calibration investigators have used various target objects such as spheres (Bruner 1999), cylinders and boxes (Daanen et al. 1997) which provide various surface representations which are mirrored to some degree in the human form. Whilst these test procedures are acknowledged, their application to the methodology being created by the author remains limited. For calibration, the manufacturers of the image capture equipment often have known tolerances within which their particular system needs to operate, therefore the object is merely a medium by which the required performance may be checked.

The use of objects such as spheres and cylinders are particularly relevant to 360° multiple Capture Unit systems, as a single object can provide a calibration reference for multiple Units. However, the objective of this particular investigation is to create a test methodology to evaluate the performance of an image capture system, which then may be universally applied to other capture systems working on the same principle. Thus the investigation is primarily based upon the performance of a single Capture Unit, as the methodology may then be applied to alternative systems with differing numbers of Capture Units. By evaluating the errors in a single Unit the individual errors present within a system may be identified without the interference of joining together multiple views, which in its own right can introduce further errors. Further test procedures may then be developed to test the performance of combining multiple views for each system.

The methodology used within this investigation is based upon the configuration as laid out in Figure C1. This enables the evaluation of each Capture Unit independently, however it may be noted that the view from each Unit is offset from the normal. A number of the image capture systems concerned with human body capture utilise Capture Units which are configured in a similar manner (for example [TC]2). The reason for using this configuration as opposed to testing each Unit separately using the 2D grid running parallel to the front of the Unit is due to incorporating the impact of the cosine effect (which is discussed further in section 4.2). Hence the same configuration has been employed for all tests, unless otherwise stated. The two Units have been used to view the image simultaneously enabling comparison between the Units to check the consistency between views. This configuration also enables the optimum Field of View to be generated when the two views are combined. Hence it is necessary to test each view with the target object offset from the normal, as this is the format which is taken when multiple views in such a system are combined.

A two-dimensional board provides a more critical surface for the determination of individual errors than a curved surface. By using a 2D surface, a curved surface may still be simulated by varying the physical geometry of the object. Viewing a 2D surface, as shown against the cylinder in Figure C2, illustrates that by the movement of the 2D surface in terms of angle and distance a curved surface may also be simulated.

Figure C2. Curved Surface Simulation

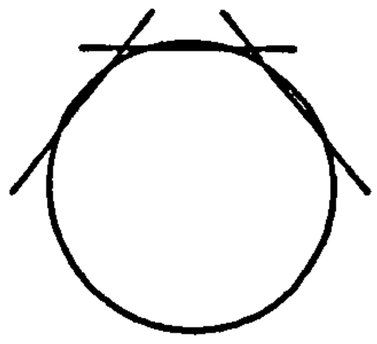

The use of a two-dimensional board is preferable when the aim of each test within the methodology is to keep all variables constant with the exception of the

one under investigation. With a 2D surface the System Centre and hence the distance may be kept constant for any point across the board, whereas for a curved surface the distance and angle of various points does not remain constant across the surface. Thus increasing the number of known variables that could be responsible for the source of error.

As the capture volume of each Unit is limited to a vertical cylinder of 700mm in diameter, with a maximum view of 120°, the size of sphere or cylinder that could be used is limited. A curved surface differs across the horizontal plane in terms of the angle and distance. Therefore when evaluating distances over the horizontal direction within the system it is not feasible to compare areas within the capture volume for continuity of results, such as checking for any lens distortion towards the outer areas of the capture volume. A two-dimensional surface however provides a far clearer representation of any distortion that may be present, as the surface itself is not subject to any curvature and the grid area may be constructed to cover the majority of the capture volume. This is an important issue as the number of variables present within the image capture procedure and the combination of these additional factors make the identification and evaluation of errors more difficult. Any additional variability which may be introduced by the target object selection could result in the misidentification of the source of error or the incorrect proportioning of each individual variables contribution to total error. The added variability associated with a curved surface also makes the evaluation of operator error as an individual entity subject to outside influences and thus open to error. However, to ensure the application of the findings to curved surfaces, (as the human body is subject to a high degree of curvature), a curved surface was used for a limited range of testing. This is discussed further in section 5.8.8.

C6. Design of the Investigation

Following the preliminary investigation a list of the sources of potential error for the image capture system were determined. These broadly fell into three categories, optical, measurement and geometric. The design of the study was based around identification of possible sources of error and the creation of test procedures to isolate each variable and determine the magnitude of its impact upon the error of the system as a whole. The test procedures were divided into categories according to whether either the physical set up or the configuration/calibration settings needed adjustment. A summary table of potential sources of error and test procedures is shown in Table C1. The primary reason for this restriction is to maintain continuity through like test procedures so that no additional variation is introduced which could impede the isolation of each single factor under investigation.

Table C1. Potential Sources of Error

Error Type	Potential sources of error	Required Action
System	The repeatability of measurements following software reboot	No movement in set up, no changes in software settings
System	The repeatability of the capture process over timed intervals	
System	The consistency of results throughout the capture area	
System	Effects of rotation	
System	Effects of enlarging the image	
System	The error related to the stitching algorithm	
System	Positioning of the stitching points	
System	The comparative performance of each Unit	
System (Measurement)	The accuracy of the measurement tool itself	
System (Measurement)	The different types of measurements and the way they work	
Operator	The operator error present during measurement	
Operator	Any operator bias in measuring in a specified direction	
System	The relationship between measured values and the calibration variables	No movement in set up required, changes in software settings
System	The effect of changing the angle setting in the software	
Object	The error related to the size of the marker	Movement in set up required, no changes in software settings
Object	Planar differences (2D vs. 3D objects)	
Object	The angle of the target object to the Unit	
Object	The distance between the target object & the Unit	Movement in set up required, and changes in software settings

C7. Evaluation Procedure

For each test, both camera images were measured, over intervals of 80mm, in both the horizontal and vertical directions, (unless otherwise stated). The images of each camera were compared separately, to provide a check for each camera, as were the two directions. Initially the mean, standard deviation and standard error of the mean were calculated for each measurement type, the results of which may be found in section C9. The results have again been calculated to two decimal places to illustrate the differences generated between tests, (the number of measurements contained within the mean justifies this increase in reported precision).

z or *t* tests for matched samples were also undertaken for hypothesis testing to ascertain whether any significant difference did exist between the test results. *z* tests were employed for all the hypothesis testing with the exception of the distance test, where *t* tests were employed. The reason for this change is based upon the size of the sample, *z* tests requiring a minimum sample size of 25, as opposed to *t* tests, which are restricted, by a maximum sample size of 30. The reduced dataset for the distance test therefore requires this change in evaluation.

z and *t* tests for matched samples test for differences between population means. The null hypothesis of 'no difference' was tested to determine whether the source of potential error under investigation is a factor that impacts on measured values. This was achieved by comparing an original captured image with that captured following a change in a specified variable, relative to each particular test. The *z* or *t* values have been calculated to two and three decimal places respectively to allow like comparison with the critical values for each. The confidence intervals have been calculated to two decimal places as they refer to the mean value and therefore have been expressed to the same degree of precision. Note that only the shortest distance was considered in the hypothesis tests, as this was found to be the most reliable indicator.

C7.1. Software Reboot Test

To test whether the software is subject to any changes after rebooting, repeat measurements were taken, comparing the results from the image captured after 60 minutes in the camera timed test, with the measurement readings taken on the same grid after rebooting the software.

C7.2. Camera Timed Test

To test whether the Units were subject to any thermal effect associated from start up, tests were undertaken involving repeat captures of an identical set up at 0 minutes, 15 minutes, 30 minutes and 60 minutes. To ascertain any difference between the results the two extreme images were measured at 0 minutes and 60 minutes.

C7.3. Distance Test

To ascertain the effect of distance on measured values, images were captured with the target 2D grid at various distances from the Capture Units. A total of nine images were taken at the following distances and angle settings:

Image	Distance (cm)	Angle Set in Software (°)
1	**286.5**	**46.56**
2	266.5	46.56
3	**266.5**	**50.3**
4	246.5	46.56
5	**246.5**	**54.7**
6	306.5	46.56
7	**306.5**	**43.37**
8	326.5	46.56
9	**326.5**	**40.6**

For each distance the angle was altered to the correct geometric angle, (based upon the calculation of the angle between the two Units projection at the target object), as described in section 4.2.6, and also left at 46.56, as on the original image (image 1). The objective being to test the influence of the angle setting in the configuration settings. The range of distances enabled comparisons of like areas of the grid, however, at the more extreme distances the visible area of the grid is greatly diminished, hence using *t* tests as the sample size was smaller. The boundaries of the test were therefore set at +/- 40cm to ensure an adequate captured area was obtained.

C7.4. Horizontal Grid Angle Position Test

To test the effect of altering the angle of the target object to the camera axis the 2D grid was used, being rotated on the central axis by 10° intervals.

Image 1	0 degrees
Image 2	10 degrees clockwise
Image 3	20 degrees clockwise
Image 4	10 degrees anti-clockwise
Image 5	20 degrees anti-clockwise

As the test focuses on changes in the horizontal plane only the horizontal distances were recorded for this test.

C7.5. Capture Unit Comparison Test

To test for any difference between the two Unit images, the measurement results from the camera timed test were examined, comparing both the horizontal and vertical planes. The results the two extreme images (0 minutes and 60 minutes) were used, comparing the Unit A measurements with the Unit B measurements for each plane to identify if any distinct differences existed.

C8. Results

C8.1 Basic Statistics

The Capture Unit comparison test results were omitted from the basic statistics as the results used were duplicates of those generated from the Capture Unit timed test.

Table C2 summarises the basic statistics, for the shortest distance, showing the range for the mean, standard deviation and standard error of the mean. The complete tables of results for each test, covering each measurement type, may be found in section C9.

Table C2. Shortest Distance Basic Statistics Summary

Tue value = 80mm

Unit /Direction	Test	*n*	Mean Range (mm)	Standard Deviation Range (mm)	Standard Error of the Mean Range (mm)
Unit A/ Horizontal	Reboot Test	80	78.07-78.09	1.15-1.27	0.18-0.20
	Capture Unit Timed Test	80	77.77-78.07	1.04-1.27	0.16-0.20
	Distance Test	263	78.11-78.82	0.97-1.47	0.19-0.31
	Horizontal Grid Angle Position Test	200	75.07-79.43	1.09-1.44	0.17-0.23
Unit A/ Vertical	Reboot Test	84	80.88-81.34	1.32-1.46	0.20-0.23
	Capture Unit Timed Test	84	80.88-80.96	1.32-1.54	0.20-0.24
	Distance Test	286	80.64-81.93	0.84-1.43	0.17-0.27
Unit B/ Horizontal	Reboot Test	80	81.45-81.49	1.18-1.19	0.19-0.19
	Capture Unit Timed Test	80	81.40-81.45	1.04-1.18	0.16-0.19
	Distance Test	250	80.85-81.93	0.88-1.68	0.16-0.30
	Horizontal Grid Angle Position Test	200	80.44-81.48	1.20-1.49	0.19-0.24
Unit B/ Vertical	Reboot Test	84	82.47-82.82	1.45-1.52	0.22-0.23
	Capture Unit Timed Test	84	82.24-82.47	1.22-1.52	0.19-0.23
	Distance Test	276	82.08-83.46	0.86-1.47	0.17-0.35

n = the number of measurements taken per grid multiplied by the number of variations measured for each test.

By examining the results comparisons may be drawn by measurement direction, by Unit, by measurement type and by test. These will each be examined in turn.

C8.1.1. Measurement Direction

Looking at the range for the mean across all common tests (namely the reboot, Capture Unit timed and distance tests) it is clear that regardless of Unit, the vertical measurement results are higher than those recorded for the horizontal direction. The range being 78.07-78.82mm and 80.85-81.93mm for the horizontal direction, for Unit's A and B respectively, and 80.64-81.93mm and 82.08-83.46mm for the vertical direction. The standard deviation and standard error of the mean, however, for each of these samples remains fairly consistent ranging from 0.84-1.68mm and 0.16-0.35mm for the standard deviation and standard error of the mean respectively across the samples.

The difference found between results in each direction is not of paramount importance in comparative testing. The importance lies in comparing one set of results with another once a change in circumstances has been implemented. Hence as long as like-for-like comparisons are being made (i.e. comparing like directions) this inequality is inconsequential. However, the discrepancy between horizontal and vertical results suggests that the inequality may not be removed by calibration. Under the current set of parameters it is not possible to alter the x and y dimensions independently. For example, by altering the calibration variables for Unit A it may be possible to increase the measured values in the x dimension to more accurately reflect the true value. However as the x and y dimensions would both be affected the y values would also be increased. This would result in the vertical direction providing measured values far in excess of the true value.

C8.1.2. Unit

There is a clear discrepancy between the measured values for the two images. The mean range, for all the tests, being 75.07-79.43mm and 80.44-81.93mm for the horizontal direction for Unit's A and B respectively and 80.64-81.93mm and 82.08-83.46mm for the vertical direction (shortest distance only). It is not imperative that the results are correct at this time as all the tests are comparative between the Units and not to the true value. One of the Units could have been re-calibrated to alter the x, y and z dimensions, so as to produce more consistent measured readings between the two Units, however, this was not undertaken as it was viewed as unnecessary in light of the tests being undertaken. One of the main concerns of the test procedures was to keep all variables constant so as to maintain comparable results. Re-calibration part way through the tests would have made comparison between test results invalid.

The variability of the results across the tests remained fairly consistent ranging from 0.84-1.54mm and 0.86-1.68mm for the standard deviation for Units A and B and 0.16-0.31 and 0.16-0.35 for the standard error of the mean for Units A and B respectively. This suggests that whilst the mean values differed markedly, the variability for the measurement results remained consistent between the two.

C8.1.3. Measurement Type

Table C3. Mean Range by Measurement Type

Unit/ Direction	*n*	Shortest Distance (mm)	Surface Distance (mm)	Tape Measure Distance (mm)	Difference Surface – shortest (mm)	Difference tape measure – shortest (mm)
Unit A/ Horizontal	623	75.07-79.43	80.12-87.06	75.16-79.67	5.05- 7.63	0.09-0.24
Unit B/ Horizontal	610	80.44-81.93	86.18-91.78	80.67-82.10	5.74- 9.85	0.03-0.17
Unit A/ Vertical	454	80.64-81.93	83.41-91.84	80.67-82.07	2.77- 9.91	0.03-0.14
Unit B/ Vertical	444	82.08-83.46	85.89-94.02	82.13-83.62	3.81-10.56	0.05-0.16

n = the total number of measurements taken per grid multiplied by the number of variations for all tests.

By examination of Table C3 a large discrepancy can be clearly seen between the surface and shortest measurement results. A discrepancy may also be noted between the tape measure and shortest distance results, although this is to a far lesser degree. The object being measured is a flat surface, hence each measurement type should give the same or at least very similar results as opposed to the notable difference recorded in Table C3. An obvious fault must therefore be noted, which illustrates the decision to primarily use the shortest measurement results, as these appeared to be the most applicable and consistent measurement type to use as a basis for the tests.

Table C4. Standard Deviation Range by Measurement Type

Unit/ Direction	*n*	Shortest Distance (mm)	Surface Distance (mm)	Tape Measure Distance (mm)
Unit A/ Horizontal	623	0.97-1.47	3.31- 8.41	1.03-1.76
Unit B/ Horizontal	610	0.88-1.68	4.30- 7.46	0.86-1.87
Unit A/ Vertical	454	0.84-1.54	2.58-10.09	0.85-1.68
Unit B/ Vertical	444	0.86-1.52	3.83-12.16	0.89-1.52

n = the total number of measurements taken per grid multiplied by the number of variations for all tests.

Table C5 Standard Error of the Mean Range by Measurement Type.

Unit/ Direction	*n*	Shortest Distance (mm)	Surface Distance (mm)	Tape Measure Distance (mm)
Unit A/ Horizontal	623	0.16-0.31	0.69-1.42	0.17-0.31
Unit B/ Horizontal	610	0.16-0.30	0.68-2.15	0.16-0.30
Unit A/ Vertical	454	0.17-0.27	0.67-1.71	0.18-0.28
Unit B/ Vertical	444	0.17-0.35	0.92-1.88	0.19-0.33

n = the total number of measurements taken per grid multiplied by the number of variations for all tests.

Tables C4 and C5 illustrate the degree of variability in the results for each measurement type. On comparison of the standard deviation, the results for the shortest distance and tape measure distance are fairly comparable, showing a similar level of variability for each measurement type. Similar results may also be noted for the range of the standard error of the mean, where the results are almost identical. However the surface distance results show a substantial degree of variability in both the standard deviation and standard error of the mean results. Therefore whilst the shortest and tape measure results remain fairly

consistent throughout the test results, the surface distance is subject to a high degree of variability.

C8.1.4. Test

Table C6. Shortest Distance Test Statistics

Unit/ Direction	Test	Variant	*n*	Mean (mm)	Standard Deviation (mm)	Standard Error of the Mean (mm)
Unit A/ Horizontal	Reboot Test	Before	40	78.07	1.27	0.20
		After	40	78.09	1.15	0.18
	Capture Unit Timed Test	0 mins.	40	77.77	1.04	0.16
		60 mins.	40	78.07	1.27	0.20
	Distance Test	Image 1	40	78.18	1.23	0.19
		Image 2	26	78.6	1.20	0.24
		Image 3	29	78.59	1.18	0.22
		Image 4	12	78.11	1.09	0.31
		Image 5	12	78.68	0.97	0.28
		Image 6	40	78.75	1.41	0.22
		Image 7	40	78.82	1.27	0.20
		Image 8	32	78.54	1.44	0.25
		Image 9	32	78.26	1.47	0.26
	Horizontal Grid Angle Position Test	Image 1	40	77.11	1.44	0.23
		Image 2	40	76.12	1.38	0.22
		Image 3	40	75.07	1.43	0.23
		Image 4	40	78.34	1.18	0.19
		Image 5	40	79.43	1.09	0.17
Unit B/ Horizontal	Reboot Test	Before	40	81.45	1.18	0.19
		After	40	81.49	1.19	0.19
	Capture Unit Timed Test	0 mins.	40	81.40	1.04	0.16
		60 mins.	40	81.45	1.18	0.19
	Distance Test	Image 1	40	81.05	1.01	0.16
		Image 2	21	81.03	1.38	0.30
		Image 3	21	81.29	1.03	0.22
		Image 4	12	80.85	0.88	0.25
		Image 5	12	81.01	0.99	0.29
		Image 6	40	81.33	1.31	0.21
		Image 7	40	81.27	1.49	0.24
		Image 8	32	81.90	1.41	0.25
		Image 9	32	81.93	1.68	0.30
	Horizontal Grid Angle Position Test	Image 1	40	81.24	1.23	0.19

n = the total number of measurements taken for each variant.

Table C6. Shortest Distance Test Statistics (continued)

Unit/ Direction	Test	Variant	*n*	Mean (mm)	Standard Deviation (mm)	Standard Error of the Mean (mm)
Unit B/ Horizontal	Horizontal Grid Angle Position Test	Image 2	40	81.10	1.28	0.20
		Image 3	40	81.32	1.21	0.19
		Image 4	40	81.48	1.20	0.19
		Image 5	40	80.44	1.49	0.24
Unit A/ Vertical	Reboot Test	Before	40	80.88	1.32	0.20
		After	40	81.34	1.46	0.23
	Capture Unit Timed Test	0 mins.	40	80.96	1.54	0.24
		60 mins.	40	80.88	1.32	0.20
	Distance Test	Image 1	42	81.15	1.43	0.22
		Image 2	29	80.64	1.22	0.23
		Image 3	31	81.36	1.30	0.23
		Image 4	15	81.19	1.06	0.27
		Image 5	15	80.74	0.84	0.22
		Image 6	42	81.52	1.12	0.17
		Image 7	42	81.81	1.35	0.21
		Image 8	35	81.91	1.41	0.24
		Image 9	35	81.93	1.38	0.23
Unit B/ Vertical	Reboot Test	Before	40	82.47	1.52	0.23
		After	40	82.82	1.45	0.22
	Capture Unit Timed Test	0 mins.	40	82.24	1.22	0.19
		60 mins.	40	82.47	1.52	0.23
	Distance Test	Image 1	42	82.24	1.22	0.19
		Image 2	25	82.08	1.13	0.23
		Image 3	25	82.54	1.33	0.27
		Image 4	15	82.15	0.86	0.22
		Image 5	15	82.09	1.37	0.35
		Image 6	42	82.96	1.20	0.19
		Image 7	42	82.59	1.13	0.17
		Image 8	35	83.13	1.18	0.20
		Image 9	35	83.46	1.47	0.25

n = the total number of measurements taken for each variant.

On examination of the basic statistics presented in Table C6, for the shortest distance it is clear that the results for the reboot test, Capture Unit timed test and

distance test, the mean, standard deviation and standard error of the mean are generally consistent with one another for both units.

For the grid angle position test, (which was only concerned with the horizontal direction) a clear pattern may be noted in the results for Unit A. The mean decreases as the target object was turned in the clockwise direction (images 2 and 3) and increases as the object was turned towards the anti-clockwise direction (images 4 and 5). The results, however, for Unit B, do not follow this trend, indicating a difference between the images produced by each Unit.

C8.2. Hypothesis Testing

C8.2.1. Software Reboot Test

Table C7. Hypothesis Test Results: Software Reboot Test

z Test for Matched Samples				Confidence Interval	
Test	*N*	*z*	Hypothesis Not Rejected/ Rejected	Lower Limit (mm)	Upper Limit (mm)
Unit A Horizontal Before – After	40	-0.09	Not Rejected	-0.40	0.36
Unit A Vertical Before – After	42	1.73	Not Rejected	-0.98	0.60
Unit B Horizontal Before – After	40	0.24	Not Rejected	-0.39	0.31
Unit B Vertical Before – After	42	1.30	Not Rejected	-0.88	0.18

n = the total number of measurements taken on each grid.

Significance Level 5%
z_{CRIT} ±1.96

For each Unit image and each direction the null hypothesis is not rejected at the 95% confidence interval. Therefore there is no evidence of a difference between

the images produced after rebooting the software. Dismissing the influence of rebooting the software as a potential source of error.

C8.2.2. Capture Unit Timed Test

Table C8. Hypothesis Test Results: Capture Unit Timed Test

z Test for Matched Samples				Confidence Interval	
Test	*n*	*z*	Hypothesis Not Rejected/ Rejected	Lower Limit (mm)	Upper Limit (mm)
Unit A Horizontal 60 – 0 mins.	40	1.20	Not Rejected	-0.25	1.23
Unit A Vertical 60 – 0 mins.	42	-0.31	Not Rejected	-0.60	0.44
Unit B Horizontal 60 – 0 mins.	40	0.22	Not Rejected	-0.40	0.50
Unit B Vertical 60 – 0 mins.	42	0.82	Not Rejected	-0.33	0.79

n = the total number of measurements taken on each grid.

Significance Level	5%
z_{CRIT}	±1.96

For each Unit image and each direction the null hypothesis is not rejected at the 95% confidence interval. As no evidence exists of a difference between the images produced at 0 minutes when compared to those captured at 60 minutes. Dismissing the influence of a thermal effect on the Units as a potential source of error.

C8.2.3. Distance Test

Table C9. Hypothesis Test Results: Distance Test – Unit A Horizontal

t Test for Matched Samples					Confidence Interval	
Test	*n*	*T*	Critical value for *t*	Hypothesis Not Rejected/ Rejected	Lower Limit (mm)	Upper Limit (mm)
Unit A Horizontal Image 1-Image 2	12	0.415	2.201	Not Rejected	-0.64	0.94
Unit A Horizontal Image 1 – Image 3	12	0.098	2.201	Not Rejected	-0.97	0.89
Unit A Horizontal Image 1 – Image 4	12	1.769	2.201	Not Rejected	-0.16	1.50
Unit A Horizontal Image 1 – Image 5	12	0.209	2.201	Not Rejected	-0.95	1.15
Unit A Horizontal Image 1 – Image 6	12	-0.800	2.201	Not Rejected	-1.66	0.77
Unit A Horizontal Image 1 – Image 7	12	-0.429	2.201	Not Rejected	-1.17	0.79
Unit A Horizontal Image 1 – Image 8	12	2.026	2.201	Not Rejected	-1.34	0.86
Unit A Horizontal Image 1 – Image 9	12	-0.158	2.201	Not Rejected	-0.71	2.07
Unit A Horizontal Image 4 – Image 8	6	-1.387	2.571	Not Rejected	-2.55	0.73
Unit A Horizontal Image 5 – Image 9	6	0.573	2.571	Not Rejected	-1.96	3.12

n = the total number of measurements taken on each grid.

Table C10. Hypothesis Test Results: Distance Test – Unit A Vertical

t Test for Matched Samples					Confidence Interval	
Test	*n*	*T*	Critical value for *t*	Hypothesis Not Rejected/ Rejected	Lower Limit (mm)	Upper Limit (mm)
Unit A Vertical Image 1- Image 2	15	-0.025	2.262	Not Rejected	-1.82	1.83
Unit A Vertical Image 1 – Image 3	15	-1.367	2.262	Not Rejected	-1.41	0.40
Unit A Vertical Image 1 – Image 4	15	0.785	2.262	Not Rejected	-0.85	1.67
Unit A Vertical Image 1 – Image 5	15	1.592	2.262	Not Rejected	-0.31	1.94
Unit A Vertical Image 1 – Image 6	15	-0.506	2.262	Not Rejected	-2.32	1.51
Unit A Vertical Image 1 – Image 7	15	-0.394	2.262	Not Rejected	-2.43	1.70
Unit A Vertical Image 1 – Image 8	15	-1.852	2.262	Not Rejected	-2.21	0.20
Unit A Vertical Image 1 – Image 9	15	-0.714	2.262	Not Rejected	-2.22	0.53
Unit A Vertical Image 4 – Image 8	15	0.793	2.262	Not Rejected	-5.40	2.64
Unit A Vertical Image 5 – Image 9	15	-2.081	2.262	Not Rejected	-3.21	0.01

n = the total number of measurements taken on each grid.

Table C11. Hypothesis Test Results: Distance Test – Unit B Horizontal

t Test for Matched Samples					Confidence Interval	
Test	*n*	*T*	Critical value for *t*	Hypothesis Not Rejected/ Rejected	Lower Limit (mm)	Upper Limit (mm)
Unit B Horizontal Image 1 – Image 2	12	-0.929	2.201	Not Rejected	-1.38	0.56
Unit B Horizontal Image 1 – Image 3	12	-0.871	2.201	Not Rejected	-0.18	0.40
Unit B Horizontal Image 1 – Image 4	12	-0.384	2.201	Not Rejected	-1.01	0.71
Unit B Horizontal Image 1 – Image 5	12	-0.639	2.201	Not Rejected	-1.08	0.46
Unit B Horizontal Image 1 – Image 6	12	-1.032	2.201	Not Rejected	-1.44	0.40
Unit B Horizontal Image 1 – Image 7	12	-2.032	2.201	Not Rejected	-2.30	0.01
Unit B Horizontal Image 1 – Image 8	12	-2.199	2.201	Not Rejected	-2.81	-0.45
Unit B Horizontal Image 1 – Image 9	12	-1.831	2.201	Not Rejected	-2.69	-0.25
Unit B Horizontal Image 4 – Image 8	6	-1.602	2.571	Not Rejected	-3.94	0.98
Unit B Horizontal Image 5 – Image 9	6	-2.517	2.571	Not Rejected	-2.64	0.32

n = the total number of measurements taken on each grid.

Table C12. Hypothesis Test Results: Distance Test – Unit B Vertical

t Test for Matched Samples					Confidence Interval	
Test	*n*	*T*	Critical value for *t*	Hypothesis Not Rejected/ Rejected	Lower Limit (mm)	Upper Limit (mm)
Unit B Vertical Image 1 – Image 2	10	-0.037	2.262	Not Rejected	-1.85	1.79
Unit B Vertical Image 1 – Image 3	10	-0.710	2.262	Not Rejected	-2.55	1.33
Unit B Vertical Image 1 – Image 4	10	0.330	2.262	Not Rejected	-1.81	2.41
Unit B Vertical Image 1 – Image 5	10	0.246	2.262	Not Rejected	-1.23	1.53
Unit B Vertical Image 1 – Image 6	10	-0.227	2.262	Not Rejected	-2.19	1.79
Unit B Vertical Image 1 – Image 7	10	-0.248	2.262	Not Rejected	-2.03	1.63
Unit B Vertical Image 1 – Image 8	10	0.331	2.262	Not Rejected	-1.34	1.72
Unit B Vertical Image 1 – Image 9	10	-0.972	2.262	Not Rejected	-2.93	1.16
Unit B Vertical Image 4 – Image 8	10	-0.192	2.262	Not Rejected	-1.97	-0.41
Unit B Vertical Image 5 – Image 9	10	-1.338	2.262	Not Rejected	-2.77	0.71

n = the total number of measurements taken on each grid.

On comparison of the measurements taken from the captured object at various distances, the null hypothesis is not rejected at the 95% confidence interval for each Unit image and each direction. Therefore no evidence of a difference is reported between the images when the target object is placed at various distances from the Capture Units. The effect of changing the angle setting also appears to have no significant effect. Thus both factors may be dismissed as a source of measurement error.

For the reboot, Capture Unit timed test and distance tests the null hypothesis of no difference was not rejected at the 95% confidence interval. This indicates that within confidence limits of 95% no difference existed between the population

means. Therefore when like Units and directions are compared neither of these factors substantially affects the measurement readings from the TriForm™ system. Whilst these are only applicable to the boundaries set for each test, the author believes the tests constitute the maximum level of variation which would generally arise when undertaking the image capture process and hence the tests provide a complete evaluation for each variable.

C8.2.4. Horizontal Grid Angle Position Test

Table C13. Hypothesis Test Results: Horizontal Grid Angle Position Test

z Test for Matched Samples				Confidence Interval	
Test	*n*	*z*	Hypothesis Not Rejected/ Rejected	Lower Limit (mm)	Upper Limit (mm)
Unit A Image 1 – Image 2	40	2.93	Rejected	-0.12	2.10
Unit A Image 1 – Image 3	40	6.46	Rejected	n/a	n/a
Unit A Image 1 – Image 4	40	-4.18	Rejected	n/a	n/a
Unit A Image 1 – Image 5	40	7.80	Rejected	n/a	n/a
Unit A Image 3 – Image 5	40	14.25	Rejected	n/a	n/a
Unit B Image 1 – Image 2	40	0.52	Not Rejected	-0.41	0.69
Unit B Image 1 – Image 3	40	-0.36	Not Rejected	-0.56	0.40
Unit B Image 1 – Image 4	40	-0.79	Not Rejected	-0.84	0.36
Unit B Image 1 – Image 5	40	2.67	Rejected	-0.19	1.79
Unit B Image 3 – Image 5	40	2.89	Rejected	-0.13	1.89

n = the total number of measurements taken on each grid.

Significance Level 5%
z_{CRIT} ±1.96

Image 1 0 degrees
Image 2 10 degrees clockwise
Image 3 20 degrees clockwise
Image 4 10 degrees anti-clockwise
Image 5 20 degrees anti-clockwise

For the Unit A image the null hypothesis is rejected. Conversely, for the Unit B image, the null hypothesis failed to be rejected at 95% for images 1-2, 1-3 and 1-4, whilst the null hypothesis is rejected for images 1-5 and 3-5. Therefore a significant difference is reported between the images produced after rotating the target object, especially for Unit A. Image 5 positioned the target object 20 degrees towards Unit A, and hence away from Unit B. Therefore the available view from Unit B was still complete, however, by the results it indicates that positioning the object at an angle of 20 degrees away from the capture source does impede the quality of the image and therefore the measurement results gained from it.

From the results the limitations of the positioning of the target object to the Capture Unit must be at no greater angle than 10 degrees towards any particular Capture Unit. Whilst the hypothesis was not rejected for image 3 which was placed at 20 degrees towards Unit B, the same principle should apply if Unit A were functioning correctly. The comparison of images 3 and 5 illustrate the extremes of the angle position and hence the null hypothesis rejection is most likely because of the placement of the object in image 5. One would expect that if the two Units were working perfectly, that the limitations in terms of the angle of the target object to the Units should be within 10 degrees in each Unit direction.

C8.2.5. Capture Unit Comparison Test

Table C14. Hypothesis Test Results: Capture Unit Comparison Test

z Test for Matched Samples				Confidence Interval	
Test	*n*	*z*	Hypothesis Not Rejected/ Rejected	Lower Limit (mm)	Upper Limit (mm)
Unit A-B Horizontal 0 mins.	40	-14.2	Rejected	n/a	n/a
Unit A-B Vertical 0 mins.	42	4.4	Rejected	n/a	n/a
Unit A-B Horizontal 60mins.	40	4.2	Rejected	n/a	n/a
Unit A-B Vertical 60mins.	42	5.6	Rejected	n/a	n/a

n = the total number of measurements taken on each grid.

Significance Level 5%
z_{CRIT} ±1.96

The two Capture Units were compared in both directions to see whether the discrepancies in the horizontal direction and vertical direction, shown in the basic statistics and horizontal grid angle position test were significant enough to reject the null hypothesis of no difference at the 95% confidence interval. When comparing the results from each Unit in the horizontal and vertical directions the null hypothesis is rejected at the 95% confidence interval. Therefore a significant difference can be reported between the Unit A image and the Unit B image, indicating the importance of evaluating the impact of changes in variables independently on each Unit.

The measured values from each Unit image were plotted against the true value of 80mm per cell for the whole grid to enable a visual comparison of the results. These can be seen in Figures C3and C4 for Units A and B respectively.

Figure C3. Measured Values Vs. True Values - Unit A

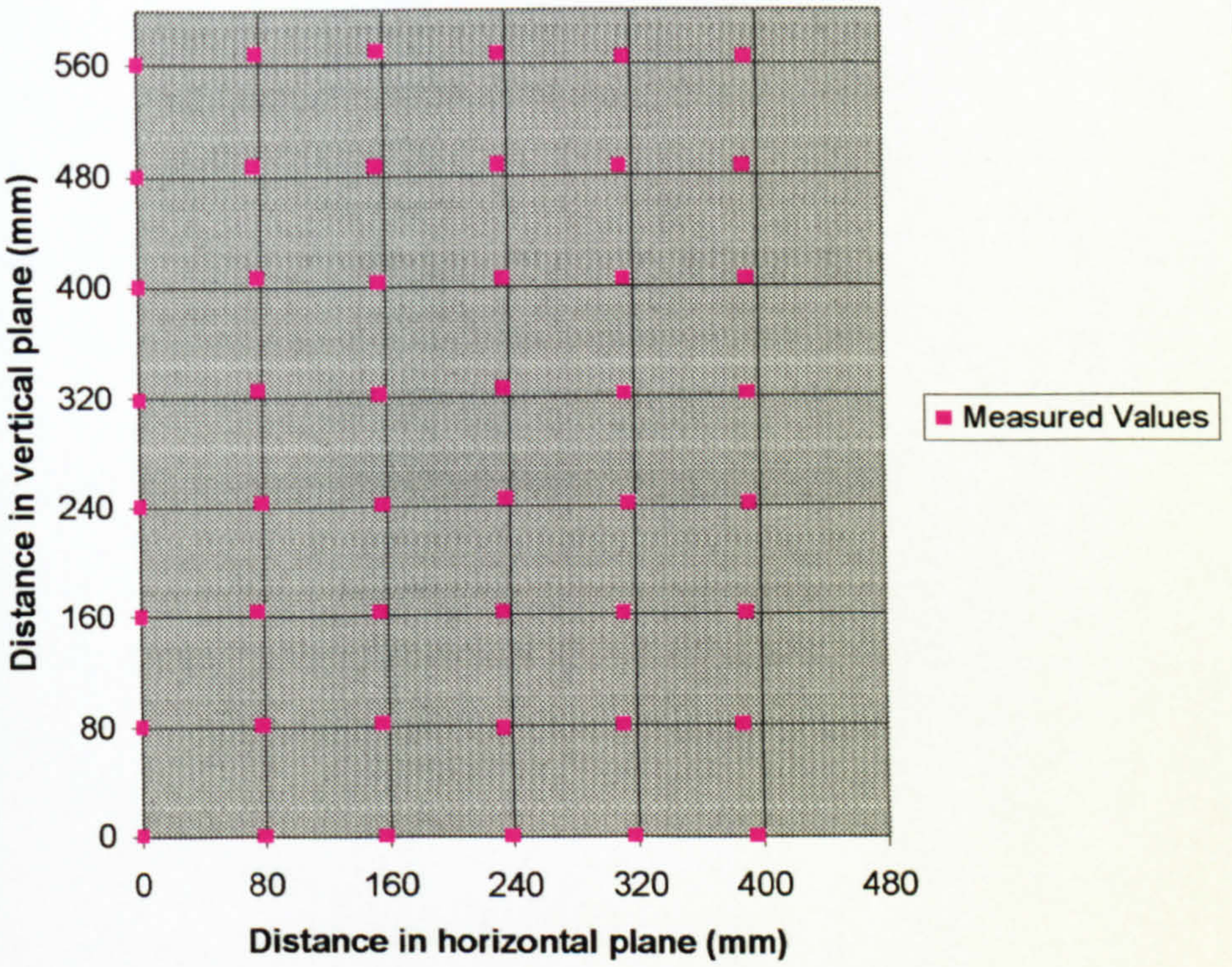

Figure C4. Measured Values vs. True Values - Unit B

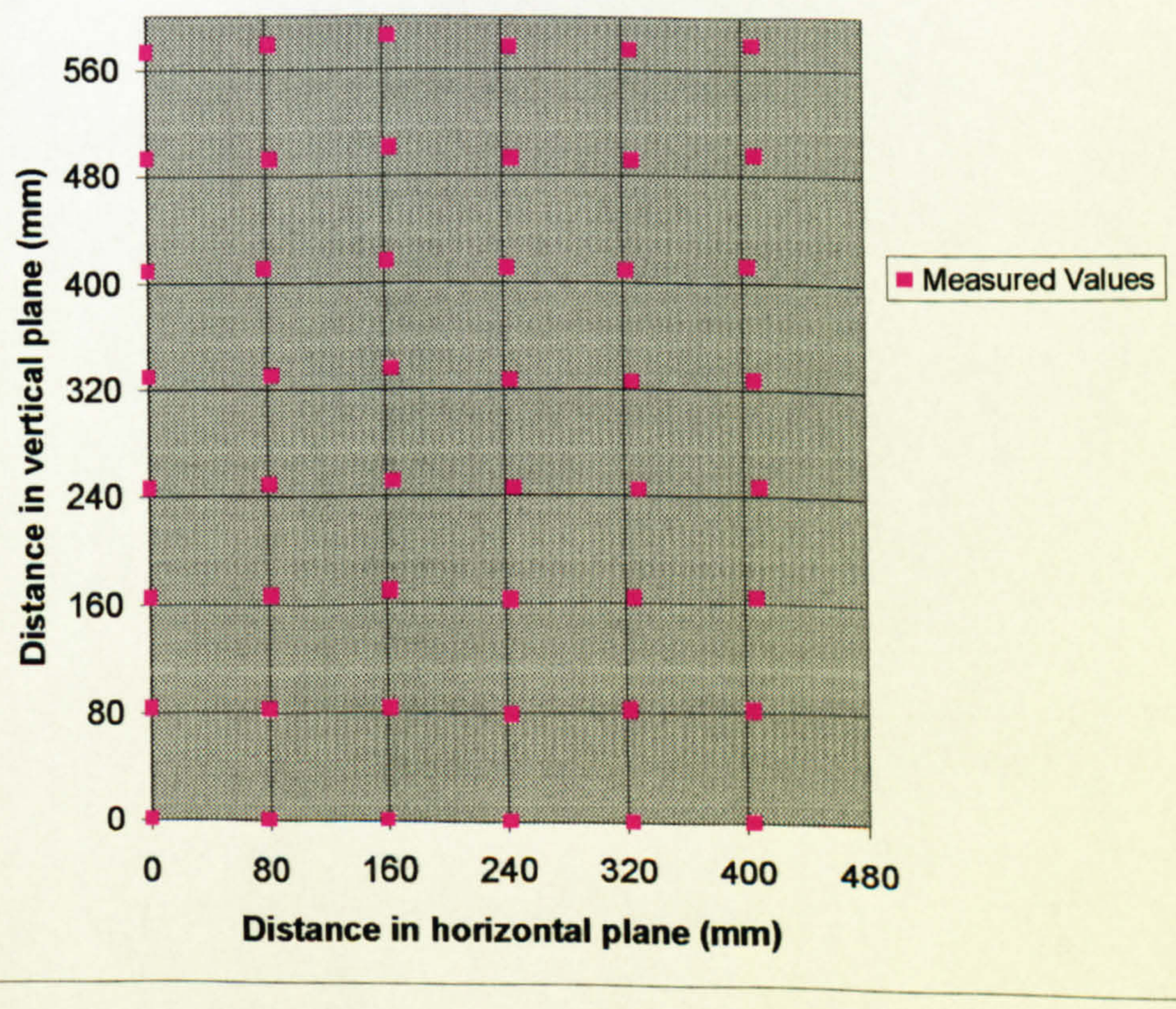

The null hypothesis was rejected for each image comparison for Unit A, in contrast with Unit B where only in comparing opposite angles was the hypothesis rejected. This illustrates the importance of testing images from both Units. By means of this comparison results may be verified and the source of error more easily identified.

The results from Unit A indicate a problem with the Unit where the accuracy of the measured results appears to be angle dependent. Whilst inherent errors exist in the image generation and the measuring procedure the pattern of results noted during the horizontal grid angle position test relates directly to the angle of the target object, suggesting a linear relationship between the target object angle and the error in measured values.

The Capture Unit comparison test which was undertaken following the results of the horizontal grid angle position test, proved the distinct difference between Units A and B which was suggested in the basic statistics and brought to light primarily by the horizontal grid angle position test. The null hypothesis of no difference was rejected on all occasions, both in the horizontal and vertical direction.

The apparent problem with the Unit A image was thought to originate from one of two potential causes of error, one being an error in the z plane, and the other being a problem with the mounting of the LCD in the projector. To check for any error in the z plane a target object, (illustrated in Figure C5), was captured and rotated on-screen so that the top of the right angle was visible. This proved to be a clear right angle reflecting the object captured. Any problem with z would have shown a distorted right angle and would have required a change in the calibration settings.

Figure C5. Z Error Test Target Object

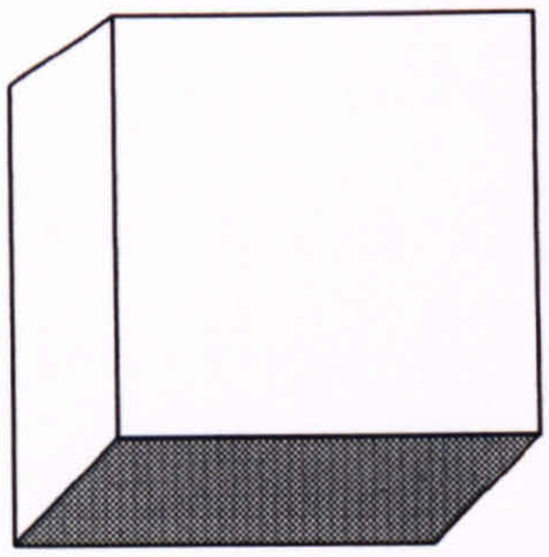

Following this the Unit A image from a previous test was re-examined and rotated to check for twist in the on-screen image which would indicate a problem with the mounting of the LCD. When rotating the Unit A image forward the image distorts before tilting forward through 90°, as shown in Figure C6:

Figure C6. Rotation of Unit A Image

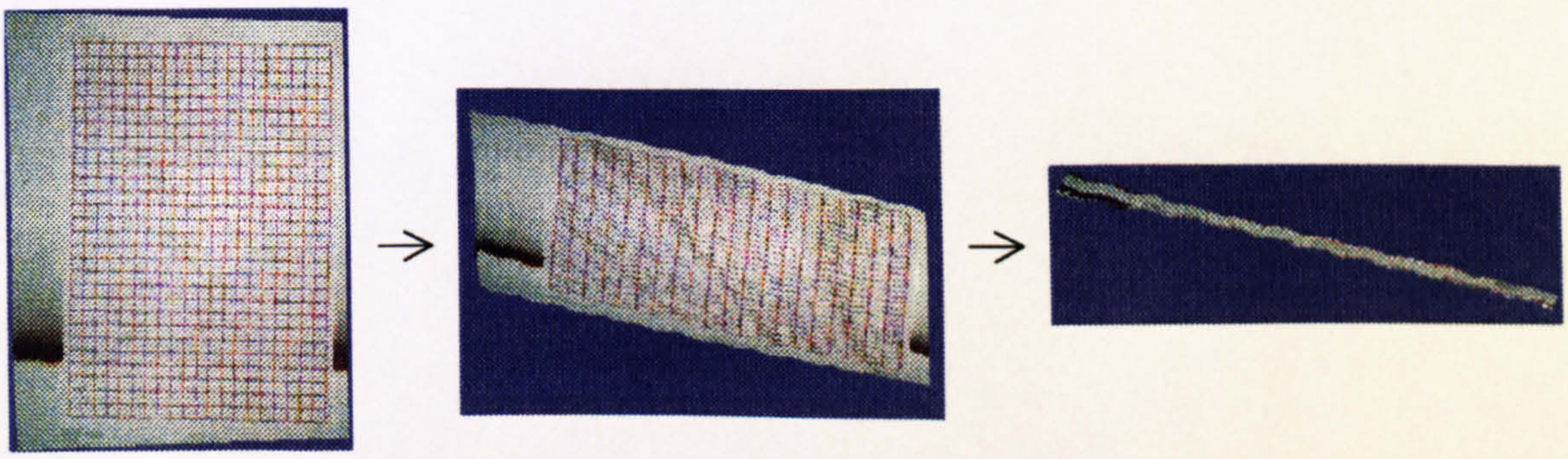

When viewing the Unit A image from above the image does not appear flat as one would expect. Whilst the overall appearance is flat the opposite corners show slight concavity indicating a twist in the image. S-shaped distortion was also noted in both images, which only further magnifies any apparent twist. As previous tests had compared like with like images, the horizontal grid angle position test, by rotating the object, indicated the difference. It was only by distorting the view of the object that the twist in the image became apparent. It is possible therefore that the results noted in the horizontal grid angle position test were a result of the twist present within the image, generated by the misalignment of the LCD.

C8.3. Measured Values versus True Values

Whilst it is known that the results gained from either Unit are not consistently in keeping with the true value of 80mm, it must be noted that discrepancies are bound to exist between the true value and the measured value, however good the calibration. The lines on the grid are 1.5mm thick and therefore the markers used for measurement on-screen could be incorrectly placed. The accuracy of the point cloud and associated colour data must be taken into account, as discussed in section 4.3, with the accuracy in the x dimension being specified by the manufacturer as ±1.5mm and ±2.0mm in the y and z dimensions. Also the measurements are all undertaken by the operator and hence are subject to some operator error, although one would assume that the error related to the marker size and point pitch would be included within any measure of operator variability. It is unlikely therefore that one would ever get absolute agreement with the true value.

One would expect that these error factors would impact on the various distances to the same extent. Whilst a slight error in the z dimension would affect the surface (and tape measure) distances to a greater extent, it is highly unlikely that it would explain the deviation noted in the results. The deviation in the shortest distance measurement however could be accounted for by taking into account the previously stated sources of error, which would impact on every measurement taken. However the deviation exhibited in the horizontal grid angle position test cannot be explained in this manner and therefore must be subject to an additional source of error, identified as an error in the mounting of the LCD.

C8.4. Conclusion

Only limited conclusions may be drawn at this stage in the investigation, as the sources of error that have been evaluated are limited. However, a number of

general conclusions can be formed on the performance of the system. The measurement readings from the horizontal and vertical directions for each Unit are inconsistent with one another and the opportunity to equalise the two is not available under the calibration settings. This is not a problem whilst comparative testing is taking place, it does not assist in the objective of obtaining more accurate measurement results. At present the discrepancies result in a systematic error for each direction.

The differences between the two Capture Units when used independently are manageable, however when stitching multiple views together, the problem would lead to scaling errors between the two images, which would result in an inaccurate stitching process. The problem highlighted with Unit A means that corrective work will need to be undertaken on the Unit to improve the LCD mounting and thus the results obtainable. It is clear from the measurement results that the shortest and tape measure distances are the only reliable measurement indicators, the surface distance proving to be both inaccurate and inconsistent. Whilst the shortest distance only is being used for comparisons, this issue is of no great importance, however, for three-dimensional objects, the surface distance is a measure of paramount importance in replicating anthropometric measurement. Therefore it is imperative that the large discrepancy between the three types of measurement is reduced and brought to a more acceptable level.

Following the feedback given to the system manufacturers from the research carried out on the two-camera system the software was revised. The new software update included a modified method of generating the surface distance measurement, by using more reference points along the length of the measurement and restricting the spread of points so that only those directly in the path of the measurement would be included. The remaining modifications related to the user interface and primarily consisted of changes in the Analysis

mode. The update provided the same capabilities as the previous version, but with the additional capabilities of being able to measure from one point on, for example, the side of the body over to the opposite side. This is achieved by being able to select a start point for a measurement, then being able to rotate the object before selecting the end measurement point.

A test was designed to provide a comparison between the performance of the new measurement software against that used previously with the two-camera system. This used an image that had been previously measured in the old software and comprised of re-measuring it in the latest software and comparing the results to identify whether any improvements in the measurement accurcay were apparent.

Table C15. Basic Statistics: Software Comparison Test

Unit/ Direction	*n*	Mean Shortest Distance (mm)		Mean Surface Distance (mm)		Mean Tape Measure Distance (mm)	
		Old Software	New Software	Old Software	New Software	Old Software	New Software
Unit A/ Horizontal	40	78.07	78.26	84.31	79.02	78.18	78.71
Unit A/ Vertical	42	80.88	80.67	90.27	81.69	81.01	81.37
Unit B/ Horizontal	40	81.45	81.47	88.77	82.30	81.70	82.03
Unit B/ Vertical	42	82.47	81.92	94.02	83.21	82.60	82.98

n = the total number of measurements taken per grid.

The most significant difference may be noted in the surface distance, which highlights the improvements made in the calculation of surface distance.

By measuring the same image in two different software editions the following points may be noted:

- A greater range of variability in measured values was present when measuring in the old software when compared to the newer version.

- A notable improvement in the accuracy of the surface distance measurement results were apparent when measuring in the newer software.

- The shortest distance results were found to have closer agreement to the true value in the latest software as opposed to the previous edition.

C9. Full Measurement Results

Table C16. Two-Camera System: Surface Distance Test Statistics - Camera A Horizontal Direction

Test	Variant	*n*	Mean (mm)	Standard Deviation (mm)	Standard Error of the Mean (mm)
Reboot Test	Before	40	84.31	5.65	0.89
	After	40	83.33	5.09	0.80
Camera Timed Test	0 mins.	40	83.92	5.78	0.91
	60 mins.	40	84.31	5.65	0.89
Distance Test	Image 1	40	83.95	4.69	0.74
	Image 2	26	82.22	3.70	0.73
	Image 3	29	82.36	3.73	0.69
	Image 4	12	80.12	3.31	0.96
	Image 5	12	82.39	4.04	1.17
	Image 6	40	86.89	8.41	1.33
	Image 7	40	86.22	7.18	1.14
	Image 8	32	85.33	6.48	1.15
	Image 9	32	85.97	8.01	1.42
Horizontal Grid Angle Position Test	Image 1	40	83.29	5.99	0.95
	Image 2	40	81.26	4.91	0.78
	Image 3	40	82.06	5.87	0.93
	Image 4	40	85.17	6.24	0.99
	Image 5	40	87.06	6.30	1.00

n = the total number of measurements taken per grid.

Table C17. Two-Camera System: Tape Measure Distance Test Statistics - Camera A Horizontal Direction

Test	Variant	*n*	Mean (mm)	Standard Deviation (mm)	Standard Error of the Mean (mm)
Reboot Test	Before	40	78.18	1.25	0.20
	After	40	78.14	1.16	0.18
Camera Timed Test	0 mins.	40	77.90	1.07	0.17
	60 mins.	40	78.18	1.28	0.20
Distance Test	Image 1	40	78.45	1.30	0.21
	Image 2	26	78.69	1.20	0.24
	Image 3	29	78.76	1.20	0.22
	Image 4	12	78.20	1.07	0.31
	Image 5	12	78.86	1.03	0.30
	Image 6	40	79.01	1.39	0.22
	Image 7	40	79.21	1.40	0.22
	Image 8	32	78.85	1.42	0.25
	Image 9	32	78.63	1.76	0.31
Horizontal Grid Angle Position Test	Image 1	40	77.22	1.45	0.23
	Image 2	40	76.30	1.36	0.22
	Image 3	40	75.16	1.48	0.23
	Image 4	40	78.47	1.31	0.21
	Image 5	40	79.67	1.07	0.17

n = the total number of measurements taken per grid.

Table C18. Two-Camera System: Surface Distance Test Statistics - Camera B Horizontal Direction

Test	Variant	*n*	Mean (mm)	Standard Deviation (mm)	Standard Error of the Mean (mm)
Reboot Test	Before	40	88.77	5.62	0.89
	After	40	88.83	6.24	0.99
Camera Timed Test	0 mins.	40	88.00	7.39	1.17
	60 mins.	40	88.77	5.62	0.89
Distance Test	Image 1	40	89.23	7.15	1.13
	Image 2	21	86.18	4.31	0.94
	Image 3	21	87.46	5.89	1.29
	Image 4	12	86.46	4.67	1.35
	Image 5	12	88.46	7.46	2.15
	Image 6	40	87.35	4.89	0.77
	Image 7	40	88.34	5.11	0.81
	Image 8	32	86.48	4.80	0.85
	Image 9	32	88.01	5.34	0.94
Horizontal Grid Angle Position Test	Image 1	40	86.34	5.26	0.83
	Image 2	40	89.10	6.50	1.03
	Image 3	40	91.78	6.83	1.08
	Image 4	40	86.30	4.30	0.68
	Image 5	40	89.52	5.73	0.91

n = the total number of measurements taken per grid.

Table C19. Two-Camera System: Tape Measure Distance Test Statistics - Camera B Horizontal Direction

Test	Variant	*n*	Mean (mm)	Standard Deviation (mm)	Standard Error of the Mean (mm)
Reboot Test	Before	40	81.70	1.26	0.20
	After	40	81.61	1.20	0.19
Camera Timed Test	0 mins.	40	81.84	1.87	0.30
	60 mins.	40	81.70	1.26	0.20
Distance Test	Image 1	40	81.19	1.02	0.16
	Image 2	21	81.23	1.39	0.30
	Image 3	21	81.48	1.00	0.22
	Image 4	12	81.06	0.86	0.25
	Image 5	12	81.08	0.96	0.28
	Image 6	40	81.48	1.35	0.21
	Image 7	40	81.33	1.51	0.24
	Image 8	32	82.03	1.44	0.25
	Image 9	32	82.10	1.70	0.30
Horizontal Grid Angle Position Test	Image 1	40	81.29	1.26	0.20
	Image 2	40	81.22	1.39	0.22
	Image 3	40	81.51	1.28	0.20
	Image 4	40	81.69	1.24	0.20
	Image 5	40	80.67	1.49	0.24

n = the total number of measurements taken per grid.

Table C20. Two-Camera System: Surface Distance Test Statistics - Camera A Vertical Direction

Test	Variant	*n*	Mean (mm)	Standard Deviation (mm)	Standard Error of the Mean (mm)
Reboot Test	Before	40	90.27	8.85	1.37
	After	40	89.27	8.80	1.36
Camera Timed Test	0 mins.	40	87.24	7.38	1.14
	60 mins.	40	90.27	8.85	1.37
Distance Test	Image 1	42	86.94	6.68	1.03
	Image 2	29	84.34	4.35	0.81
	Image 3	31	87.55	4.90	0.88
	Image 4	15	84.66	3.59	0.93
	Image 5	15	83.41	2.58	0.67
	Image 6	42	91.14	9.41	1.45
	Image 7	42	90.02	9.07	1.40
	Image 8	35	91.76	9.26	1.57
	Image 9	35	91.84	10.09	1.71

n = the total number of measurements taken per grid.

Table C21. Two-Camera System: Tape Measure Distance Test Statistics - Camera A Vertical Direction

Test	Variant	*n*	Mean (mm)	Standard Deviation (mm)	Standard Error of the Mean (mm)
Reboot Test	Before	40	81.01	1.38	0.21
	After	40	81.59	1.68	0.26
Camera Timed Test	0 mins.	40	81.05	1.57	0.24
	60 mins.	40	81.01	1.38	0.21
Distance Test	Image 1	42	81.24	1.42	0.22
	Image 2	29	80.67	1.21	0.22
	Image 3	31	81.48	1.29	0.23
	Image 4	15	81.33	1.08	0.28
	Image 5	15	80.76	0.85	0.22
	Image 6	42	81.64	1.16	0.18
	Image 7	42	81.90	1.37	0.21
	Image 8	35	82.06	1.47	0.25
	Image 9	35	82.07	1.40	0.24

n = the total number of measurements taken per grid.

Table C22. Two-Camera System: Surface Distance Test Statistics - Camera B Vertical Direction

Test	Variant	*n*	Mean (mm)	Standard Deviation (mm)	Standard Error of the Mean (mm)
Reboot Test	Before	42	94.02	12.16	1.88
	After	42	93.22	11.65	1.80
Camera Timed Test	0 mins.	42	91.84	9.59	1.48
	60 mins.	42	94.02	12.16	1.88
Distance Test	Image 1	42	89.57	9.55	1.47
	Image 2	25	86.07	4.59	0.92
	Image 3	25	86.34	4.72	0.94
	Image 4	15	85.89	4.49	1.16
	Image 5	15	86.43	3.83	0.99
	Image 6	42	91.72	7.80	1.20
	Image 7	42	89.52	6.41	0.99
	Image 8	35	91.65	8.27	1.40
	Image 9	35	91.39	7.93	1.34

n = the total number of measurements taken per grid.

Table C23.Two-Camera System: Tape Measure Distance Test Statistics - Camera B Vertical Direction

Test	Variant	*n*	Mean (mm)	Standard Deviation (mm)	Standard Error of the Mean (mm)
Reboot Test	Before	42	82.60	1.52	0.23
	After	42	82.93	1.43	0.22
Camera Timed Test	0 mins.	42	82.32	1.27	0.20
	60 mins.	42	82.60	1.52	0.23
Distance Test	Image 1	42	82.39	1.40	0.22
	Image 2	25	82.13	1.16	0.23
	Image 3	25	82.65	1.31	0.26
	Image 4	15	82.19	0.89	0.23
	Image 5	15	82.17	1.29	0.33
	Image 6	42	83.08	1.22	0.19
	Image 7	42	82.71	1.21	0.19
	Image 8	35	83.23	1.23	0.21
	Image 9	35	83.62	1.47	0.25

n = the total number of measurements taken per grid.

Table C24. Software Comparison Test: Basic Statistics

View/ Direction	Measurement Type	Variant	*n*	Mean (mm)	Standard Deviation (mm)	Standard Error of mean (mm)
Left/ Horizontal	Shortest	Old Software	40	81.45	1.18	0.19
		New Software	40	81.47	0.88	0.14
	Surface	Old Software	40	88.77	5.62	0.89
		New Software	40	82.30	0.97	0.15
	Tape Measure	Old Software	40	81.70	1.26	0.20
		New Software	40	82.03	0.92	0.15
Left/ Vertical	Shortest	Old Software	42	82.47	1.52	0.23
		New Software	42	81.92	0.55	0.08
	Surface	Old Software	42	94.02	12.16	1.88
		New Software	42	83.21	0.95	0.15
	Tape Measure	Old Software	42	82.60	1.52	0.23
		New Software	42	82.98	0.94	0.15
Right/ Horizontal	Shortest	Old Software	40	78.07	1.27	0.20
		New Software	40	78.26	1.09	0.17
	Surface	Old Software	40	84.31	5.65	0.89
		New Software	40	79.02	1.07	0.17
	Tape Measure	Old Software	40	78.18	1.25	0.20
		New Software	40	78.71	1.11	0.18
Right/ Vertical	Shortest	Old Software	42	80.88	1.32	0.20
		New Software	42	80.67	0.97	0.15
	Surface	Old Software	42	90.27	8.85	1.37
		New Software	42	81.69	0.98	0.15
	Tape Measure	Old Software	42	81.01	1.38	0.21
		New Software	42	81.37	0.96	0.15

n = the total number of measurements taken per grid.

APPENDIX D

THE PERFORMANCE OF THE SINGLE CAMERA TRIFORM™ SYSTEM

Table D1. Operator Error Test: Basic Statistics

View/ Direction	Measurement Type	Variant (Measurement of the image)	*n*	Mean (mm)	Standard Deviation (mm)	Standard Error of mean (mm)
Left/ Horizontal	Shortest	Base Grid	40	80.19	0.85	0.13
		Remeasure 1A	40	80.33	0.80	0.13
		Remeasure 2A	40	80.35	0.93	0.15
		Remeasure 3A	40	80.17	1.02	0.16
		Base Grid	40	80.23	0.86	0.14
		Remeasure 1C	40	80.38	0.78	0.12
		Base Grid	40	80.62	0.86	0.14
		Remeasure 1E	40	80.51	0.88	0.14
	Surface	Base Grid	40	80.71	0.81	0.13
		Remeasure 1A	40	80.80	0.81	0.13
		Remeasure 2A	40	80.82	0.96	0.15
		Remeasure 3A	40	80.63	0.96	0.15
		Base Grid	40	80.73	0.90	0.14
		Remeasure 1C	40	80.76	0.72	0.11
		Base Grid	40	81.16	0.86	0.14
		Remeasure 1E	40	81.01	0.90	0.14
	Tape Measure	Base Grid	40	80.52	0.84	0.13
		Remeasure 1A	40	80.63	0.78	0.12
		Remeasure 2A	40	80.62	0.96	0.15
		Remeasure 3A	40	80.47	0.96	0.15
		Base Grid	40	80.54	0.87	0.14
		Remeasure 1C	40	80.60	0.75	0.12
		Base Grid	40	80.92	0.85	0.13
		Remeasure 1E	40	80.80	0.92	0.15
Left/Vertical	Shortest	Base Grid	42	79.90	0.91	0.14
		Remeasure 1A	42	79.91	0.82	0.13
		Remeasure 2A	42	79.92	0.89	0.14
		Remeasure 3A	42	79.82	0.74	0.11
		Base Grid	42	79.80	0.82	0.13
		Remeasure 1C	42	79.85	0.77	0.12
		Base Grid	42	80.06	0.69	0.11
		Remeasure 1E	42	80.00	0.51	0.08
	Surface	Base Grid	42	80.85	1.09	0.17
		Remeasure 1A	42	80.76	1.02	0.16
		Remeasure 2A	42	80.82	0.99	0.15
		Remeasure 3A	42	80.81	0.86	0.13
		Base Grid	42	80.75	0.95	0.15
		Remeasure 1C	42	80.65	0.90	0.14
		Base Grid	42	80.95	0.96	0.15
		Remeasure 1E	42	80.85	0.64	0.10

Table D1. Operator Error Test: Basic Statistics (cont.)

View/ Direction	Measurement Type	Variant (Measurement of the image)	*n*	Mean (mm)	Standard Deviation (mm)	Standard Error of mean (mm)
Left/Vertical	Tape Measure	Base Grid	42	80.56	1.06	0.16
		Remeasure 1A	42	80.53	0.95	0.15
		Remeasure 2A	42	80.54	0.93	0.14
		Remeasure 3A	42	80.54	0.80	0.12
		Base Grid	42	80.47	0.96	0.15
		Remeasure 1C	42	80.51	0.85	0.13
		Base Grid	42	80.69	0.88	0.14
		Remeasure 1E	42	80.60	0.62	0.10
Right/ Horizontal	Shortest	Base Grid	40	78.26	1.08	0.17
		Remeasure 1B	40	78.32	0.76	0.12
		Base Grid	40	78.64	1.02	0.16
		Remeasure 1D	40	78.94	0.80	0.13
	Surface	Base Grid	40	78.62	1.06	0.17
		Remeasure 1B	40	78.68	0.74	0.12
		Base Grid	40	79.01	0.99	0.16
		Remeasure 1D	40	79.36	0.81	0.13
	Tape Measure	Base Grid	40	78.44	1.04	0.16
		Remeasure 1B	40	78.56	0.79	0.12
		Base Grid	40	78.83	1.01	0.16
		Remeasure 1D	40	79.20	0.82	0.13
Right/ Vertical	Shortest	Base Grid	42	79.14	0.92	0.14
		Remeasure 1B	42	79.45	0.82	0.13
		Base Grid	42	79.85	0.82	0.13
		Remeasure 1D	42	79.75	0.65	0.10
	Surface	Base Grid	42	79.76	0.92	0.14
		Remeasure 1B	42	80.04	0.92	0.14
		Base Grid	42	80.56	0.88	0.14
		Remeasure 1D	42	80.64	0.72	0.11
	Tape Measure	Base Grid	42	79.62	0.93	0.14
		Remeasure 1B	42	79.90	0.88	0.14
		Base Grid	42	80.36	0.88	0.14
		Remeasure 1D	42	80.31	0.69	0.11

n = the total number of measurements taken per grid.

Table D2. Directional Bias Test: Basic Statistics

View/ Direction	Measurement Type	Variant (Measurement of the image)	*n*	Mean (mm)	Standard Deviation (mm)	Standard Error of mean (mm)
Left/ Horizontal	Shortest	Base grid	40	80.23	0.86	0.14
	Surface		40	80.73	0.90	0.14
	Tape Measure		40	80.54	0.87	0.14
Left/ Horizontal	Shortest	Remeasure in opposite direction	40	80.11	0.80	0.13
	Surface		40	80.65	0.78	0.12
	Tape Measure		40	80.42	0.83	0.13
Left/ Vertical	Shortest	Base grid	42	79.80	0.82	0.13
	Surface		42	80.75	0.95	0.15
	Tape Measure		42	80.47	0.96	0.15
Left/ Vertical	Shortest	Remeasure in opposite direction	42	79.69	0.58	0.09
	Surface		42	80.81	0.80	0.12
	Tape Measure		42	80.53	0.82	0.13

n = the total number of measurements taken per grid.

Table D3. View Comparison Test: Basic Statistics

View/Direction	Measurement Type	*n*	Mean (mm)	Standard Deviation (mm)	Standard Error of mean (mm)
Left/Horizontal	Shortest	40	80.23	0.86	0.14
Right/Horizontal		40	78.64	1.02	0.16
Left/Vertical		42	79.80	0.82	0.13
Right/Vertical		42	79.85	0.82	0.13
Left/Horizontal	Surface	40	80.73	0.90	0.14
Right/Horizontal		40	79.01	0.99	0.16
Left/Vertical		42	80.75	0.95	0.15
Right/Vertical		42	80.56	0.88	0.14
Left/Horizontal	Tape Measure	40	80.54	0.87	0.14
Right/Horizontal		40	78.83	1.01	0.16
Left/Vertical		42	80.47	0.96	0.15
Right/Vertical		42	80.36	0.88	0.14

n = the total number of measurements taken per grid.

Table D4. Distance Test: Basic Statistics

View/ Direction	Measurement Type	Variant (Distance from Capture Unit, cm)	*n*	Mean (mm)	Standard Deviation (mm)	Standard Error of mean (mm)
Left/ Horizontal	Shortest	171cm	32	80.12	0.96	0.17
		145cm (base grid)	40	80.19	0.85	0.13
		100cm	14	80.96	0.92	0.25
	Surface	171cm	32	80.62	0.93	0.16
		145cm (base grid)	40	80.71	0.81	0.13
		100cm	14	81.47	0.99	0.26
	Tape Measure	171cm	32	80.45	0.94	0.17
		145cm (base grid)	40	80.52	0.84	0.13
		100cm	14	81.34	1.02	0.27
Left/ Vertical	Shortest	171cm	35	79.86	1.02	0.17
		145cm (base grid)	42	79.90	0.91	0.14
		100cm	18	80.18	0.57	0.13
	Surface	171cm	35	80.97	1.20	0.20
		145cm (base grid)	42	80.85	1.09	0.17
		100cm	18	81.02	0.81	0.19
	Tape Measure	171cm	35	80.69	1.22	0.21
		145cm (base grid)	42	80.56	1.06	0.16
		100cm	18	80.84	0.74	0.17
Right/ Horizontal	Shortest	171cm	40	79.10	0.74	0.12
		145cm (base grid)	40	78.26	1.08	0.17
		100cm	14	78.32	0.57	0.15
	Surface	171cm	40	79.40	0.78	0.12
		145cm (base grid)	40	78.62	1.06	0.17
		100cm	14	78.82	0.69	0.18
	Tape Measure	171cm	40	79.26	0.75	0.12
		145cm (base grid)	40	78.44	1.04	0.16
		100cm	14	78.66	0.65	0.17
Right/ Vertical	Shortest	171cm	42	80.04	1.13	0.17
		145cm (base grid)	42	79.14	0.92	0.14
		100cm	18	79.04	0.85	0.20
	Surface	171cm	42	80.65	1.04	0.16
		145cm (base grid)	42	79.76	0.92	0.14
		100cm	18	79.68	0.92	0.22
	Tape Measure	171cm	42	80.50	1.03	0.16
		145cm (base grid)	42	79.62	0.93	0.14
		100cm	18	79.54	0.93	0.22

n = the total number of measurements taken per grid.

Table D5. Angle in Computer Test: Basic Statistics

View/ Direction	Measurement Type	Variant (Angle setting, degrees)	*n*	Mean (mm)	Standard Deviation (mm)	Standard Error of mean (mm)
Left/ Horizontal	Shortest	0°	40	80.51	1.09	0.17
		50° (base grid)	40	80.23	0.86	0.14
		100°	40	80.70	0.83	0.13
	Surface	0°	40	80.91	1.07	0.17
		50° (base grid)	40	80.73	0.90	0.14
		100°	40	81.20	0.83	0.13
	Tape Measure	0°	40	80.73	1.09	0.17
		50° (base grid)	40	80.54	0.87	0.14
		100°	40	80.97	0.82	0.13
Left/ Vertical	Shortest	0°	42	80.32	0.95	0.15
		50° (base grid)	42	79.80	0.82	0.13
		100°	42	79.83	0.93	0.14
	Surface	0°	42	81.16	1.08	0.17
		50° (base grid)	42	80.75	0.95	0.15
		100°	42	80.56	0.98	0.15
	Tape Measure	0°	42	80.97	1.02	0.16
		50° (base grid)	42	80.47	0.96	0.15
		100°	42	80.39	0.95	0.15
Right/ Horizontal	Shortest	0°	40	78.90	0.90	0.14
		50° (base grid)	40	78.64	1.02	0.16
		100°	40	78.71	1.14	0.18
	Surface	0°	40	79.22	0.86	0.14
		50° (base grid)	40	79.01	0.99	0.16
		100°	40	79.20	1.14	0.18
	Tape Measure	0°	40	79.08	0.88	0.14
		50° (base grid)	40	78.83	1.01	0.16
		100°	40	78.98	1.13	0.18
Right/ Vertical	Shortest	0°	42	78.18	1.34	0.21
		50° (base grid)	42	79.85	0.82	0.13
		100°	42	79.82	0.89	0.14
	Surface	0°	42	80.51	1.01	0.16
		50° (base grid)	42	80.56	0.88	0.14
		100°	42	80.66	0.99	0.15
	Tape Measure	0°	42	80.37	0.96	0.15
		50° (base grid)	42	80.36	0.88	0.14
		100°	42	80.42	0.98	0.15

n = the total number of measurements taken per grid.

Table D6. Image Enlargement Test: Basic Statistics

View/ Direction	Measurement Type	Variant (%magnification)	*n*	Mean (mm)	Standard Deviation (mm)	Standard Error of mean (mm)
Left/ Horizontal	Shortest	0% (base grid)	40	80.19	0.85	0.13
	Surface		40	80.71	0.81	0.13
	Tape Measure		40	80.52	0.84	0.13
Left/ Vertical	Shortest	0% (base grid)	42	79.90	0.91	0.14
	Surface		42	80.85	1.09	0.17
	Tape Measure		42	80.56	1.06	0.16
Left/ Horizontal	Shortest	25%	40	80.28	0.59	0.09
	Surface		40	80.84	0.55	0.09
	Tape Measure		40	80.63	0.55	0.09
Left/ Vertical	Shortest	25%	42	79.97	0.55	0.08
	Surface		42	81.02	0.87	0.13
	Tape Measure		42	80.82	0.80	0.12

n = the total number of measurements taken per grid.

Table D7. Rotation Test: Basic Statistics

View/ Direction	Measurement Type	Variant (Rotation, degrees)	*n*	Mean (mm)	Standard Deviation (mm)	Standard Error of mean (mm)
Left/ Horizontal	Shortest	0° (base grid)	40	80.19	0.85	0.13
		15°clockwise	40	80.31	0.66	0.10
		15° anti-clockwise	40	80.37	0.71	0.11
	Surface	0° (base grid)	40	80.71	0.81	0.13
		15°clockwise	40	80.85	0.64	0.10
		15° anti-clockwise	40	80.89	0.73	0.12
	Tape Measure	0° (base grid)	40	80.52	0.84	0.13
		15°clockwise	40	80.64	0.64	0.10
		15° anti-clockwise	40	80.68	0.73	0.12
Left/ Vertical	Shortest	0° (base grid)	42	79.90	0.91	0.14
		15°clockwise	42	79.96	0.60	0.09
		15° anti-clockwise	42	80.07	0.60	0.09
	Surface	0° (base grid)	42	80.85	1.09	0.17
		15°clockwise	42	80.92	0.77	0.12
		15° anti-clockwise	42	80.93	0.73	0.11
	Tape Measure	0° (base grid)	42	80.56	1.06	0.16
		15°clockwise	42	80.69	0.75	0.12
		15° anti-clockwise	42	80.68	0.69	0.11

n = the total number of measurements taken per grid.

Table D8. Planar Differences Test: Basic Statistics

View/ Direction	Measurement Type	Variant (Surface)	*n*	Mean (mm)	Standard Deviation (mm)	Standard Error of mean (mm)
Left/ Horizontal	Shortest	2D (base grid)	40	80.62	0.86	0.14
		Concave Horizontal	30	80.25	0.82	0.14
		Concave Vertical	30	80.23	0.82	0.13
		Convex Horizontal.	24	80.43	0.66	0.11
		Convex Vertical.	30	79.92	0.41	0.06
	Surface	2D (base grid)	40	81.16	0.86	0.14
		Concave Horizontal	30	80.70	0.80	0.13
		Concave Vertical	30	80.64	0.85	0.13
		Convex Horizontal.	24	80.88	0.70	0.12
		Convex Vertical.	30	80.31	0.37	0.06
	Tape Measure	2D (base grid)	40	80.92	0.85	0.13
		Concave Horizontal	30	80.50	0.82	0.14
		Concave Vertical	30	80.51	0.86	0.14
		Convex Horizontal.	24	80.75	0.66	0.11
		Convex Vertical.	30	80.20	0.39	0.06
Left/ Vertical	Shortest	2D (base grid)	42	80.06	0.69	0.11
		Concave Horizontal	30	80.04	0.52	0.09
		Concave Vertical	30	79.64	0.74	0.11
		Convex Horizontal.	24	80.12	0.53	0.10
		Convex Vertical.	30	79.56	0.65	0.10
	Surface	2D (base grid)	42	80.95	0.96	0.15
		Concave Horizontal	30	81.14	0.84	0.14
		Concave Vertical	30	80.60	0.84	0.13
		Convex Horizontal.	24	80.81	0.70	0.13
		Convex Vertical.	30	80.41	0.65	0.10
	Tape Measure	2D (base grid)	42	80.69	0.88	0.14
		Concave Horizontal	30	80.95	0.80	0.14
		Concave Vertical	30	80.25	0.81	0.12
		Convex Horizontal.	24	80.66	0.60	0.11
		Convex Vertical.	30	80.07	0.69	0.11

n = the total number of measurements taken per grid.

Table D8. Planar Differences Test: Basic Statistics (cont.)

View/ Direction	Measurement Type	Variant (Surface)	*n*	Mean (mm)	Standard Deviation (mm)	Standard Error of mean (mm)
Right/ Horizontal	Shortest	2D (base grid)	40	78.85	0.85	0.13
		Concave Horizontal	30	78.85	1.07	0.18
		Concave Vertical	30	78.75	0.71	0.11
		Convex Horizontal.	24	78.76	0.71	0.12
		Convex Vertical.	30	79.21	0.43	0.07
	Surface	2D (base grid)	40	79.36	0.88	0.14
		Concave Horizontal	30	79.35	1.04	0.17
		Concave Vertical	30	79.12	0.71	0.11
		Convex Horizontal.	24	79.12	0.73	0.12
		Convex Vertical.	30	79.68	0.45	0.07
	Tape Measure	2D (base grid)	40	79.14	0.87	0.14
		Concave Horizontal	30	79.14	1.04	0.17
		Concave Vertical	30	78.97	0.70	0.11
		Convex Horizontal.	24	78.98	0.74	0.12
		Convex Vertical.	30	79.49	0.46	0.07
Right/ Vertical	Shortest	2D (base grid)	42	79.93	0.63	0.10
		Concave Horizontal	30	79.98	0.60	0.10
		Concave Vertical	30	79.32	0.66	0.10
		Convex Horizontal.	24	79.76	0.60	0.10
		Convex Vertical.	30	79.57	0.60	0.09
	Surface	2D (base grid)	42	80.72	0.63	0.10
		Concave Horizontal	30	80.83	0.94	0.16
		Concave Vertical	30	80.15	0.73	0.11
		Convex Horizontal.	24	80.12	0.52	0.09
		Convex Vertical.	30	80.52	0.65	0.10
	Tape Measure	2D (base grid)	42	80.52	0.65	0.10
		Concave Horizontal	30	80.66	0.89	0.15
		Concave Vertical	30	79.80	0.70	0.11
		Convex Horizontal.	24	80.03	0.53	0.09
		Convex Vertical.	30	80.21	0.68	0.10

n = the total number of measurements taken per grid.

Table D9. Stitching Test: Basic Statistics

View/ Direction	Measurement Type	Variant (Image)	*n*	Mean (mm)	Standard Deviation (mm)	Standard Error of mean (mm)
Left/ Horizontal	Shortest	Base grid Image 1 A	40	80.62	0.86	0.14
	Surface		40	81.16	0.86	0.14
	Tape Measure		40	80.92	0.85	0.13
Left/ Vertical	Shortest	Base grid Image 1 A	42	80.06	0.69	0.11
	Surface		42	80.95	0.96	0.15
	Tape Measure		42	80.69	0.88	0.14
Right/ Horizontal	Shortest	Base grid Image 1 B	40	78.85	0.85	0.13
	Surface		40	79.36	0.88	0.14
	Tape Measure		40	79.14	0.87	0.14
Right/ Vertical	Shortest	Base grid Image 1 B	42	79.93	0.63	0.10
	Surface		42	80.72	0.63	0.10
	Tape Measure		42	80.52	0.65	0.10
N/A	Shortest	Live stitch Image 2	40	79.68	1.01	0.16
		Live stitch Image 3	40	79.60	1.26	0.20
		Live stitch Image 4	40	80.02	0.97	0.15
		Live stitch Image 5	40	80.13	0.71	0.11
		Auto align Image 6	40	79.34	1.43	0.23
		Auto align Image 7	40	80.23	1.26	0.20
N/A	Surface	Live stitch Image 2	40	80.09	1.04	0.16
		Live stitch Image 3	40	79.99	1.23	0.19
		Live stitch Image 4	40	80.52	1.00	0.16
		Live stitch Image 5	40	80.66	0.73	0.12
		Auto align Image 6	40	79.78	1.36	0.22
		Auto align Image 7	40	80.79	1.37	0.22
N/A	Tape Measure	Live stitch Image 2	40	79.89	1.00	0.16
		Live stitch Image 3	40	79.83	1.22	0.19
		Live stitch Image 4	40	80.32	0.98	0.15
		Live stitch Image 5	40	80.49	0.72	0.11
		Auto align Image 6	40	79.57	1.39	0.22
		Auto align Image 7	40	80.58	1.33	0.21

n = the total number of measurements taken per grid.

Table D10. Calibration Settings Test: Basic Statistics

View/ Direction	Measurement Type	Variant (Calibration settings)	*n*	Mean (mm)	Standard Deviation (mm)	Standard Error of mean (mm)
Right/ Horizontal	Shortest	Base Grid (no change in any settings)	40	78.91	0.76	0.12
		Fr Sp-Fld View Image 1	40	80.10	0.99	0.16
		Fr Sp-Fld View Image 2	40	77.80	0.73	0.12
		Cam to Prj Ht-Fr Sp Image 1	40	78.88	0.72	0.11
		Cam to Prj Ht-Fr Sp Image 2	40	79.01	0.84	0.13
		Cam to Prj Dp-Fr Sp Image 1	40	79.01	1.59	0.25
		Cam to Prj Dp-Fr Sp Image 2	40	79.02	0.86	0.14
		Cam to Prj Dp-K1 Image 1	40	78.83	0.82	0.13
		Cam to Prj Dp-K1 Image 2	40	78.88	0.76	0.12
		Cam to Prj Dp-K2 Image 1	40	78.62	0.95	0.15
		Cam to Prj Dp-K2 Image 2	40	79.17	0.77	0.12
		Cam to Sys C-K1 Image 1	40	79.41	0.75	0.12
		Cam to Sys C-K1 Image 2	40	78.66	0.70	0.11
		Cam to Sys C-K2 Image 1	40	79.68	0.62	0.10
		Cam to Sys C-K2 Image 2	40	78.72	0.85	0.13

n = the total number of measurements taken per grid.

Table D10. Calibration Settings Test: Basic Statistics (cont.)

View/ Direction	Measurement Type	Variant (Calibration settings)	*n*	Mean (mm)	Standard Deviation (mm)	Standard Error of mean (mm)
Right/ Horizontal	Surface	Base Grid (no change in any settings)	40	79.36	0.79	0.12
		Fr Sp-Fld View Image 1	40	80.49	0.97	0.15
		Fr Sp-Fld View Image 2	40	78.20	0.75	0.12
		Cam to Prj Ht-Fr Sp Image 1	40	79.32	0.79	0.12
		Cam to Prj Ht-Fr Sp Image 2	40	79.41	0.88	0.14
		Cam to Prj Dp-Fr Sp Image 1	40	79.37	1.60	0.25
		Cam to Prj Dp-Fr Sp Image 2	40	79.45	0.84	0.13
		Cam to Prj Dp-K1 Image 1	40	79.28	0.87	0.14
		Cam to Prj Dp-K1 Image 2	40	79.26	0.77	0.12
		Cam to Prj Dp-K2 Image 1	40	79.04	0.91	0.14
		Cam to Prj Dp-K2 Image 2	40	79.60	0.75	0.12
		Cam to Sys C-K1 Image 1	40	79.86	0.74	0.12
		Cam to Sys C-K1 Image 2	40	79.05	0.72	0.11
		Cam to Sys C-K2 Image 1	40	80.04	0.65	0.10
		Cam to Sys C-K2 Image 2	40	79.22	0.83	0.13

n = the total number of measurements taken per grid.

Table D10. Calibration Settings Test: Basic Statistics (cont.)

View/ Direction	Measurement Type	Variant (Calibration settings)	*n*	Mean (mm)	Standard Deviation (mm)	Standard Error of mean (mm)
Right/ Horizontal	Tape Measure	Base Grid (no change in any settings)	40	79.16	0.77	0.12
		Fr Sp-Fld View Image 1	40	80.32	0.96	0.15
		Fr Sp-Fld View Image 2	40	78.01	0.74	0.12
		Cam to Prj Ht-Fr Sp Image 1	40	79.14	0.76	0.12
		Cam to Prj Ht-Fr Sp Image 2	40	79.21	0.86	0.14
		Cam to Prj Dp-Fr Sp Image 1	40	79.21	1.58	0.25
		Cam to Prj Dp-Fr Sp Image 2	40	79.30	0.86	0.14
		Cam to Prj Dp-K1 Image 1	40	79.12	0.83	0.13
		Cam to Prj Dp-K1 Image 2	40	79.07	0.75	0.12
		Cam to Prj Dp-K2 Image 1	40	78.89	0.92	0.15
		Cam to Prj Dp-K2 Image 2	40	79.40	0.75	0.12
		Cam to Sys C-K1 Image 1	40	79.71	0.75	0.12
		Cam to Sys C-K1 Image 2	40	78.85	0.69	0.11
		Cam to Sys C-K2 Image 1	40	79.86	0.62	0.10
		Cam to Sys C-K2 Image 2	40	79.05	0.83	0.13

n = the total number of measurements taken per grid.

Table D10. Calibration Settings Test: Basic Statistics (cont.)

View/ Direction	Measurement Type	Variant (Calibration settings)	*n*	Mean (mm)	Standard Deviation (mm)	Standard Error of mean (mm)
Right/ Vertical	Shortest	Base Grid (no change in any settings)	42	79.84	0.83	0.13
		Fr Sp-Fld View Image 1	42	80.87	1.07	0.17
		Fr Sp-Fld View Image 2	42	78.89	0.54	0.08
		Cam to Prj Ht-Fr Sp Image 1	42	80.41	0.75	0.12
		Cam to Prj Ht-Fr Sp Image 2	42	79.41	0.59	0.09
		Cam to Prj Dp-Fr Sp Image 1	42	83.53	3.15	0.49
		Cam to Prj Dp-Fr Sp Image 2	42	80.10	1.16	0.18
		Cam to Prj Dp-K1 Image 1	42	80.20	0.80	0.12
		Cam to Prj Dp-K1 Image 2	42	79.81	1.01	0.16
		Cam to Prj Dp-K2 Image 1	42	79.98	0.84	0.13
		Cam to Prj Dp-K2 Image 2	42	80.32	1.24	0.19
		Cam to Sys C-K1 Image 1	42	80.16	0.62	0.10
		Cam to Sys C-K1 Image 2	42	79.96	0.67	0.10
		Cam to Sys C-K2 Image 1	42	80.24	0.52	0.08
		Cam to Sys C-K2 Image 2	42	80.04	0.73	0.11

n = the total number of measurements taken per grid.

Table D10. Calibration Settings Test: Basic Statistics (cont.)

View/ Direction	Measurement Type	Variant (Calibration settings)	*n*	Mean (mm)	Standard Deviation (mm)	Standard Error of mean (mm)
Right/ Vertical	Surface	Base Grid (no change in any settings)	42	80.66	0.93	0.14
		Fr Sp-Fld View Image 1	42	81.54	1.12	0.17
		Fr Sp-Fld View Image 2	42	79.57	0.72	0.11
		Cam to Prj Ht-Fr Sp Image 1	42	81.23	0.90	0.14
		Cam to Prj Ht-Fr Sp Image 2	42	80.10	0.75	0.12
		Cam to Prj Dp-Fr Sp Image 1	42	84.14	3.04	0.47
		Cam to Prj Dp-Fr Sp Image 2	42	80.71	1.20	0.19
		Cam to Prj Dp-K1 Image 1	42	80.98	0.95	0.15
		Cam to Prj Dp-K1 Image 2	42	80.47	1.07	0.17
		Cam to Prj Dp-K2 Image 1	42	80.76	0.98	0.15
		Cam to Prj Dp-K2 Image 2	42	81.33	1.28	0.20
		Cam to Sys C-K1 Image 1	42	80.85	0.70	0.11
		Cam to Sys C-K1 Image 2	42	80.55	0.74	0.11
		Cam to Sys C-K2 Image 1	42	80.83	0.57	0.09
		Cam to Sys C-K2 Image 2	42	80.87	0.78	0.12

n = the total number of measurements taken per grid.

Table D10. Calibration Settings Test: Basic Statistics (cont.)

View/ Direction	Measurement Type	Variant (Calibration settings)	*n*	Mean (mm)	Standard Deviation (mm)	Standard Error of mean (mm)
Right/ Vertical	Tape Measure	Base Grid (no change in any settings)	42	80.44	0.87	0.13
		Fr Sp-Fld View Image 1	42	81.41	1.12	0.17
		Fr Sp-Fld View Image 2	42	79.46	0.69	0.11
		Cam to Prj Ht-Fr Sp Image 1	42	81.01	0.86	0.13
		Cam to Prj Ht-Fr Sp Image 2	42	79.95	0.72	0.11
		Cam to Prj Dp-Fr Sp Image 1	42	83.98	3.05	0.47
		Cam to Prj Dp-Fr Sp Image 2	42	80.55	1.18	0.18
		Cam to Prj Dp-K1 Image 1	42	80.81	0.91	0.14
		Cam to Prj Dp-K1 Image 2	42	80.31	1.03	0.16
		Cam to Prj Dp-K2 Image 1	42	80.50	0.93	0.14
		Cam to Prj Dp-K2 Image 2	42	81.05	1.32	0.20
		Cam to Sys C-K1 Image 1	42	80.67	0.65	0.10
		Cam to Sys C-K1 Image 2	42	80.41	0.73	0.11
		Cam to Sys C-K2 Image 1	42	80.72	0.57	0.09
		Cam to Sys C-K2 Image 2	42	80.67	0.76	0.12

n = the total number of measurements taken per grid.

Table D11. Vertical Grid Angle Position Test: Basic Statistics

View/ Direction	Measurement Type	Variant (Target object angle, degrees)	*n*	Mean (mm)	Standard Deviation (mm)	Standard Error of mean (mm)
Left/ Vertical	Shortest	0° (base grid)	42	79.80	0.82	0.13
		10° backwards	42	79.68	0.54	0.08
		20° backwards	42	79.80	0.56	0.09
		30° backwards	42	79.61	0.58	0.09
		10° forwards	42	79.42	0.65	0.10
		20° forwards	42	79.31	0.55	0.08
	Surface	0° (base grid)	42	80.75	0.95	0.15
		10° backwards	42	80.62	0.55	0.08
		20° backwards	42	80.60	0.61	0.09
		30° backwards	42	80.23	0.59	0.09
		10° forwards	42	81.05	0.93	0.14
		20° forwards	42	80.35	0.62	0.10
	Tape Measure	0° (base grid)	42	80.47	0.96	0.15
		10° backwards	42	80.44	0.53	0.08
		20° backwards	42	80.40	0.60	0.09
		30° backwards	42	80.03	0.54	0.08
		10° forwards	42	80.66	0.86	0.13
		20° forwards	42	80.08	0.68	0.10
Right/ Vertical	Shortest	0° (base grid)	42	79.85	0.82	0.13
		10° backwards	42	79.43	0.58	0.09
		20° backwards	42	79.83	0.56	0.09
		30° backwards	42	79.48	0.80	0.12
		10° forwards	42	79.43	0.63	0.10
		20° forwards	42	79.27	0.67	0.10
	Surface	0° (base grid)	42	80.56	0.88	0.14
		10° backwards	42	80.27	0.56	0.09
		20° backwards	42	80.62	0.59	0.09
		30° backwards	42	80.00	0.82	0.13
		10° forwards	42	80.85	0.78	0.12
		20° forwards	42	80.16	0.78	0.12
	Tape Measure	0° (base grid)	42	80.36	0.88	0.14
		10° backwards	42	80.04	0.62	0.10
		20° backwards	42	80.37	0.60	0.09
		30° backwards	42	79.86	0.81	0.12
		10° forwards	42	80.49	0.74	0.11
		20° forwards	42	79.95	0.79	0.12

n = the total number of measurements taken per grid.

Table D12. Horizontal Grid Angle Position Test: Basic Statistics

View/ Direction	Measurement Type	Variant (Target object angle, degrees)	*n*	Mean (mm)	Standard Deviation (mm)	Standard Error of mean(mm)
Left/ Horizontal	Shortest	0° (base grid)	40	80.23	0.86	0.14
		10° anti-clockwise	40	80.30	0.71	0.11
		20° anti-clockwise	40	80.27	0.84	0.13
		30° anti-clockwise	40	79.88	0.72	0.11
		10° clockwise	40	80.35	0.92	0.15
		20° clockwise	40	80.47	0.64	0.10
		30° clockwise	40	80.39	0.61	0.10
	Surface	0° (base grid)	40	80.73	0.90	0.14
		10° anti-clockwise	40	80.68	0.72	0.11
		20° anti-clockwise	40	80.64	0.85	0.13
		30° anti-clockwise	40	80.24	0.70	0.11
		10° clockwise	40	80.89	0.98	0.15
		20° clockwise	40	80.91	0.66	0.10
		30° clockwise	40	80.91	0.72	0.11
	Tape Measure	0° (base grid)	40	80.54	0.87	0.14
		10° anti-clockwise	40	80.52	0.73	0.12
		20° anti-clockwise	40	80.50	0.85	0.13
		30° anti-clockwise	40	80.10	0.70	0.11
		10° clockwise	40	80.71	0.95	0.15
		20° clockwise	40	80.76	0.66	0.10
		30° clockwise	40	80.74	0.66	0.10
Right/ Horizontal	Shortest	0° (base grid)	40	78.64	1.02	0.16
		5° anti-clockwise	40	78.77	0.73	0.12
		10° anti-clockwise	40	79.40	0.66	0.10
		20° anti-clockwise	40	80.00	0.62	0.10
		30° anti-clockwise	40	80.57	0.51	0.08
		40° anti-clockwise	40	80.73	0.57	0.09
		50° anti-clockwise	40	80.91	0.66	0.10
		5° clockwise	40	77.66	0.78	0.12
		10° clockwise	40	77.77	0.66	0.10
		20° clockwise	40	77.04	0.88	0.14
		30° clockwise	40	76.47	0.89	0.14
	Surface	0° (base grid)	40	79.01	0.99	0.16
		5° anti-clockwise	40	79.13	0.75	0.12
		10° anti-clockwise	40	79.72	0.69	0.11
		20° anti-clockwise	40	80.34	0.66	0.10
		30° anti-clockwise	40	80.91	0.50	0.08
		40° anti-clockwise	40	81.18	0.64	0.10
		50° anti-clockwise	40	81.44	0.71	0.11
		5° clockwise	40	78.02	0.79	0.12
		10° clockwise	40	78.21	0.60	0.09
		20° clockwise	40	77.45	0.89	0.14
		30° clockwise	40	76.78	0.91	0.14

Table D12. Horizontal Grid Angle Position Test: Basic Statistics (cont.)

View/ Direction	Measurement Type	Variant	*n*	Mean (mm)	Standard Deviation (mm)	Standard Error of mean(mm)
Right/ Horizontal	Tape Measure	0° (base grid)	40	78.83	1.01	0.16
		5° anti-clockwise	40	78.96	0.74	0.12
		10° anti-clockwise	40	79.56	0.68	0.11
		20° anti-clockwise	40	80.18	0.63	0.10
		30° anti-clockwise	40	80.77	0.50	0.08
		40° anti-clockwise	40	81.06	0.63	0.10
		50° anti-clockwise	40	81.25	0.68	0.11
		5° clockwise	40	77.86	0.78	0.12
		10° clockwise	40	78.02	0.60	0.09
		20° clockwise	40	77.24	0.87	0.14
		30° clockwise	40	76.62	0.89	0.14

n = the total number of measurements taken per grid.

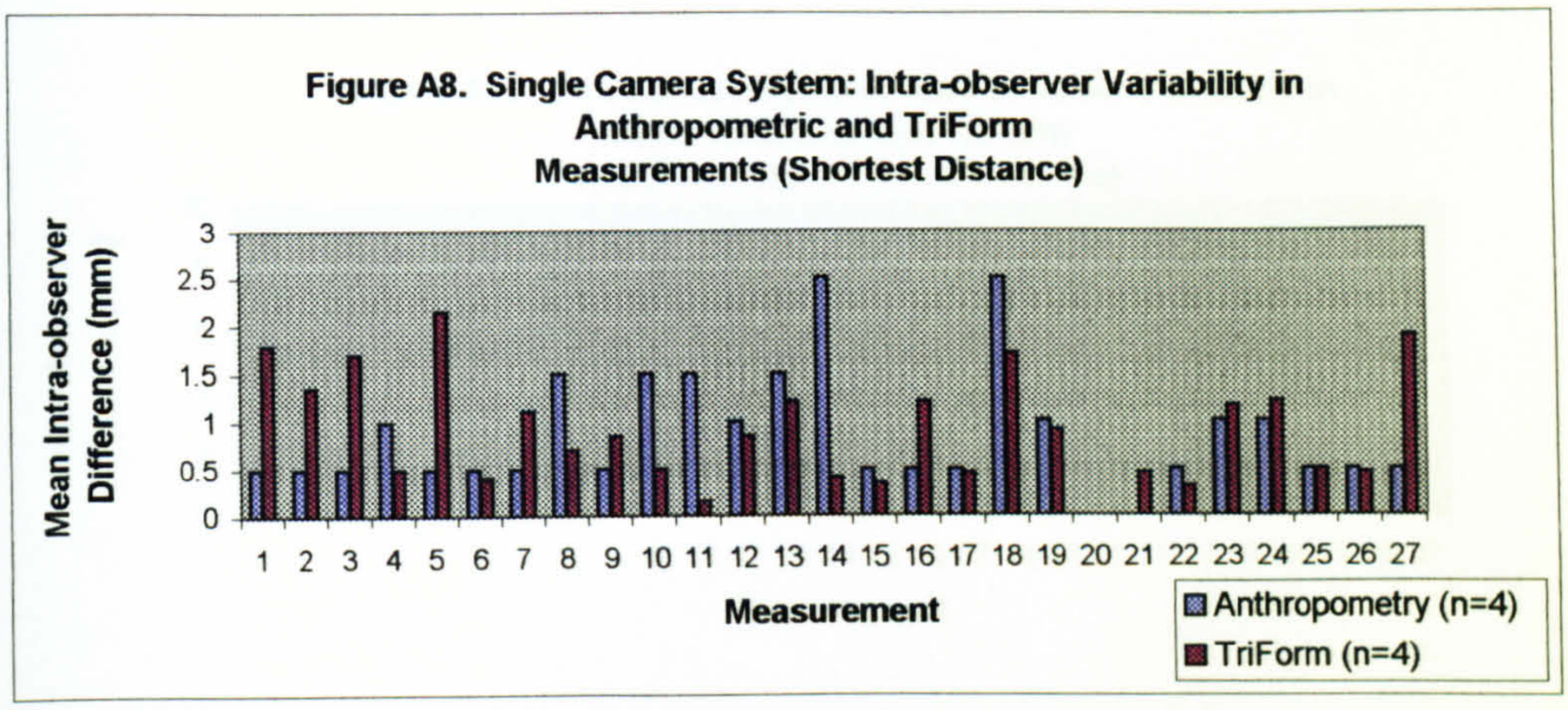

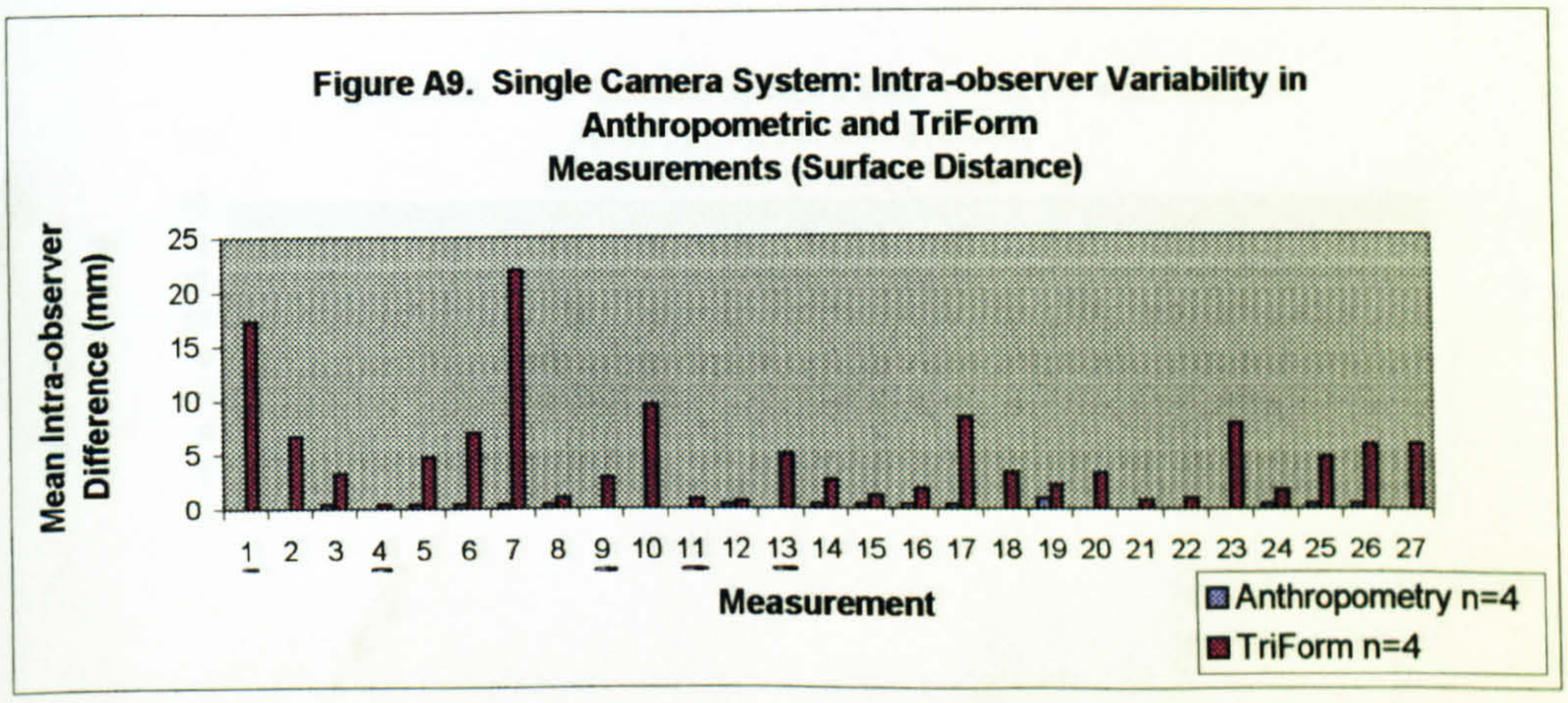

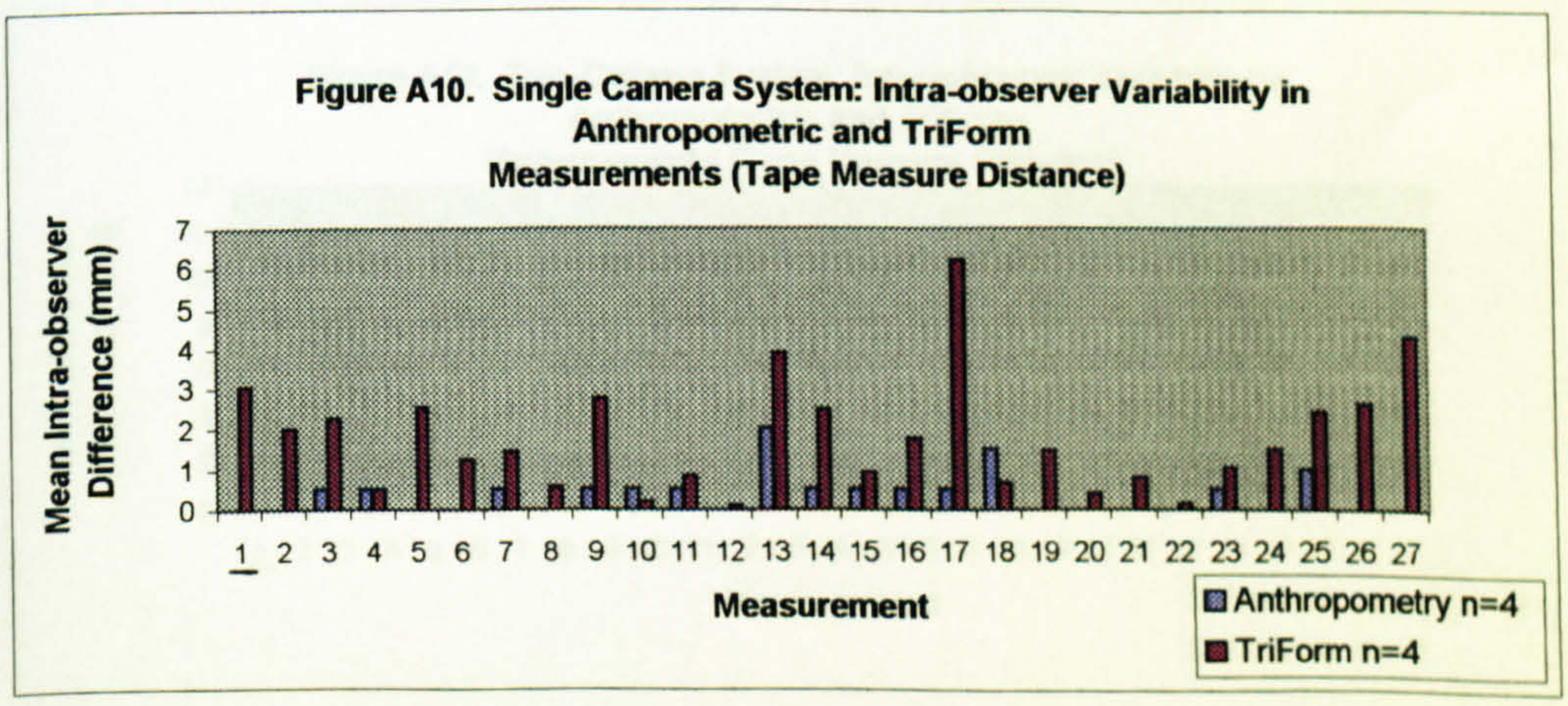

Key: _____ Manual measurements omitted
n = Number of repeat measurements